Analysis of the function of *Drosophila* Cyclin E isoforms and identification of interactors

A thesis submitted for the degree of Doctor of Philosophy

Donna Crack, B.Sc. (Hons.)

Department of Molecular Biosciences

The University of Adelaide

August 2002

Table of Contents

Table of Figures

Table of Tables

Abstract

Regulation of proliferation acts primarily during G1 phase of the cell cycle. The G1 to S phase transition is regulated by the activity of Cdk2(cyclin dependent kinase)/Cyclin E. As in mammals, *Drosophila cyclin E* (*DmcycE*) is essential and rate limiting for entry into S phase. *DmcycE* gives rise to alternative transcripts encoding two proteins that differ at their N termini. Both proteins are nuclear localised during interphase, and become distributed throughout the cytoplasm during mitosis. During embryogenesis DmcycEII is maternally supplied, while DmcycEI is zygotically expressed. In this study, analysis of the expression of DmcycEII throughout development showed that DmcycEII was present during larval development and oogenesis. This implicates a role for DmcycEII outside of early embryogenesis.

Drosophila eye development requires the synchronisation of cells in G1 phase within the morphogenetic furrow (MF) of the eye imaginal disc. Ectopic expression of DmcycEI in the eye imaginal disc has been previously shown to drive the anterior, but not the posterior, G1 phase cells within the MF into S phase. In this study, ectopic expression analyses using full-length DmcycE proteins as well as N- and C-terminal deletions of DmcycEI, revealed that DmcycEII and N-terminal deletions were able to drive all G1 cells within the MF into S phase, while a C-terminal deletion of DmcycEI could not. Taken together, these results show that DmcycEII is more potent than DmcycEI in driving cells into S phase and that the N-terminal region of DmcycEI contains a negative regulatory domain. A model for this, is that an inhibitor is present in the posterior MF that binds to DmcycEI N-terminus and inhibits DmcycEI function.

Two possible candidates for this inhibition, the Cdk inhibitors Dacapo and Roughex, were examined. Both Dacapo and Roughex were shown by yeast 2-hybrid, co-immunolocalization and *in vivo* functional studies not to be the mediator of the DmcycEI inhibition in the posterior MF cells, suggesting that an unknown inhibitory mechanism exists.

To identify the DmcycEI specific inhibitor, genetic interaction and yeast 2-hybrid screens were undertaken. The genetic interaction screen made use of overexpression of DmcycEI in the eye imaginal disc to produce a dose-sensitive rough eye phenotype. This phenotype was then used to screen a collection of *P*-element alleles, and identified dominant enhancers. One of the enhancers, *CG7394*, encoding a DnaJ homologue, appears to be specific for DmcycEI. The yeast 2-hybrid screen isolated proteins that bind the N-terminal region of DmcycEI that were then examined for their ability to inhibit DmcycE/DmCdk2 function and for an *in vivo* interaction with DmcycE. This analysis revealed that *CG9326,* encoding a MAGUK homologue, may be specific for DmcycEI *in vivo*. Further analysis of these and other interactors identified in both the genetic interaction and yeast 2-hybrid screens, will reveal novel mechanisms for the control of cell proliferation during development.

Declaration

This work contains no material which has been accepted for the award of any other degree or diploma in any university or tertiary institution and, to the best of my knowledge and belief, contains no material previously published or written by another person, except where due reference has been made in the text.

I consent to this copy of my thesis, when deposited in the University library, being available for loan and photocopying.

Donna Crack

1st August 2002

Acknowledgments

There are many people I would like to thank for their help and support throughout the period of my PhD: the members of the Genetics Discipline, Centre for the Molecular Genetics of Development, and Molecular Biosciences Department for technical and support services. Thanks particularly to members of the Saint and Richardson lab, past and present, a great group of colleagues that provided a support network in which to work and learn, for their friendship and all their help enabling me to juggle parenthood and research. I would also like to acknowledge a few people in particular whose influence and impact cannot go unmentioned.

Firstly, my supervisor, Helena Richardson, whose depth of knowledge extends well beyond all things cell cycle, and my co-supervisor, Robert Saint, together for providing an exciting and stimulating lab environment, ever changing over the years.

Thanks to Michelle Coulson, for reading drafts and holding it together when it could have come unstuck. I am glad that you survived your dip in the Torrens and other assorted skilled moments of late, at least it has kept me entertained.

My inspiration Zoe, and my life support Jason, thank you. And to the "little baby", for giving me this deadline, I can't wait to meet you.

"Today is gone. Today was fun. Tomorrow is another one. Every day, from here to there, funny things are everywhere", Dr. Seuss.

Chapter 1 : Introduction

1-1 The cell cycle

Precise regulation of the eukaryotic cell division cycle is crucial to enable the correct pattern of proliferation and differentiation during development. If correct regulation of the cell cycle is not maintained, the result is cell death or cancer, emphasising the importance in understanding the molecular basis of cell cycle regulation. The molecules and mechanisms involved in cell cycle regulation have been highly conserved throughout evolution from yeast to human, including *Drosophila melanogaster*, which is used as an animal model system for genetic analysis of cell cycle control during development (reviewed by Nurse, 1990; Edgar and Lehner, 1996).

For faithful propagation of the genetic material, a cell must replicate its DNA and segregate the replicated chromosomes into two daughter cells. In addition to this, the cell also requires a doubling of its biomass. The cell division cycle can be divided into four fundamental phases, S phase (DNA synthesis), M phase (mitosis), and two gap phases, G1 and G2. During S phase, replication of DNA takes place, while during M phase the replicated chromosomes segregate and cell division (cytokinesis) occurs resulting in two genetically identical daughter cells. The gap phases separate M phase and S phase and allow for cellular requirements, such as cell growth and protein synthesis, to occur. To maintain cell integrity there are several control points that ensure the correct order of cell cycle events, such that entry into S phase and entry into M phase occur correctly, and that S and M phases are coordinated (Elledge, 1996; Wuarin and Nurse, 1996).

There are also modifications to this basic cell cycle program that can occur during development to bypass these control points. Examples of this include the endoreplication cycle, which consists of alternating S and G phases with no intervening M phase, giving rise to polytene cells, and the meiotic cycle, where cells undergo a single S phase followed by two successive M phases producing haploid cells. The switch from one type of cell cycle to another requires specific regulation (reviewed by Vidwans and Su, 2001). Thus, not only does cell cycle progression require tight control, but the switching of one cell cycle type to another that occurs during development must also be regulated.

1-1.1 Cell cycle regulation

The correct order of cell cycle transitions, G1 to S phase and G2 to M phase, requires the regulated activity of a family of Cyclin dependent serine/threonine protein kinases (Cdks) (reviewed by Reed, 1996). Cdk proteins are found at constant levels through the cell cycle and

their activity is tightly regulated. As monomers, Cdks have no kinase activity and activation of kinase function occurs by association with regulatory Cyclin proteins (reviewed by Pines, 1992). The Cyclin family of proteins contain a conserved motif of approximately 150 amino acids, termed the cyclin box, that is essential for Cyclin/Cdk interactions (Lees and Harlow, 1993). Unlike Cdk protein levels, Cyclin levels vary dramatically during the cell cycle such that they are only available to associate with a particular Cdk partner at a specific cell cycle stage. The variation in abundance of Cyclins is due to the presence of destruction signals that target the Cyclin for ubiquitin-dependent degradation at specific stages of the cell cycle (reviewed by King *et al.*, 1996).

The variation in Cyclin abundance enables different Cyclin/Cdk complexes to be present at different stages of the cell cycle. In mammalian cells, progression from G2 to M phase requires Cyclin A/Cdk1 and Cyclin B/Cdk1 kinase complexes, whereas progression from G1 to S phase requires Cyclin D/Cdk4(Cdk6), Cyclin E/Cdk2 and Cyclin A/Cdk2 (reviewed by Reed, 1996).

Following the initial activation of a Cyclin/Cdk complexes, kinase function is also regulated by both activating and inhibiting phosphorylation of the Cdk subunit, and by association with Cdk inhibitory proteins (CKIs) (Sherr and Roberts, 1999; Elledge, 1996). Together these provide a complex regulatory system resulting in the active kinase complex phosphorylating substrates necessary for progression through the cell cycle (reviewed by Lew and Kornbluth, 1996).

1-2 The G1 to S phase transition

Of particular importance to cell cycle progression is regulation of the G1 to S phase transition. In mammalian cells, commitment to enter into and complete an entire cell cycle occurs late in G1 at the "restriction point" (Pardee, 1974). This point was defined by examining the requirement for mitogens in cell cycle progression. This work also showed that the G1 phase of the cell cycle is the period in which the cell is responsive to external signals (reviewed by Zhu and Skoultchi, 2001).

1-2.1 G1 Cyclins

Regulation of the transition through the restriction point is controlled by the G1 cyclins, D-type Cyclins (D1, D2 or D3) and Cyclin E (Reed, 1996). Of these two types of cyclins, Cyclin E shows the most dramatic cell cycle variation in mRNA, protein and associated Cdk kinase activity, peaking in late G1 phase just prior to S phase (Lew *et al.*, 1991; Matsushime *et al.*, 1991; Motokura *et al.*, 1991). Immunodepletion studies have shown that Cyclin D is required in mid-G1 phase while Cyclin E is required at the G1/S boundary (Baldin *et al.*, 1993;

Ohtsubo *et al.*, 1995), while over-expression of either Cyclin D or E shortens G1 phase and decreases the requirement for growth factors for the G1 to S phase transition (Baldin *et al.*, 1993; Ohtsubo and Roberts, 1993; Resnitzky *et al.*, 1994). Although Cyclin D functions upstream of Cyclin E, expression of Cyclin E under control of the *cyclin D1* promoter in knock-in mice rescues a *cyclin D1* deficiency, suggesting that Cyclin E can perform all essential Cyclin D1 functions (Geng *et al.*, 1999). Thus, Cyclin D and Cyclin E are essential and rate-limiting for the G1 to S phase transition (Figure 1.1).

Another cyclin, Cyclin A, appears to have a separate role later during G1 or S phase than Cyclins D and E. Although the role of Cyclin A in association with Cdk1 during the G2 to M phase transition for regulation of Mitosis has been well documented, Cyclin A also associates with Cdk2 (reviewed by Desdouets *et al.*, 1995). Cyclin A/Cdk2 activity appears towards the end of G1 phase reaching a peak during S phase and can activate DNA replication in extracts from G1 cells (D'urso *et al.*, 1990). As with other G1 cyclins, overexpression of Cyclin A in cultured cells shortens G1 (Girard, 1991; Pagano *et al.*, 1992) whilst immunodepletion can prevent entry into and progression through S phase (Resnitzky *et al.*, 1995). Thus, in mammalian cells Cyclin D, Cyclin E and Cyclin A appear to have different essential roles in entry into or progression through S phase.

1-3 Regulation of G1 Cyclin/Cdk activity

During G1 phase, positive or negative external signals are integrated to influence whether the cell will enter the cell cycle (Pardee, 1989). In response to positive growth factors, the cell commits to enter and complete the cell cycle, while negative growth factors lead to G1 arrest (Alevizopoulos and Mermod, 1997; Bottazzi and Assoin, 1997). The response to external signals during G1 phase is important to enable processes such as repair of DNA damage, differentiation, senescence and cell growth to occur. As the level of Cyclin/Cdk kinase activity determines whether a cell will enter into a new round of cell division, decrease in activity of the complex by decrease in cyclin abundance, inhibitory phosphorylation and the action of CKIs result in cell cycle exit. These growth factors may act to influence the abundance of G1 cyclins by affecting their transcription and degradation rates, or the activity of Cyclin/Cdk complexes by both activating and inhibiting phosphorylation of the Cdk subunit, and by association with Cyclin-dependent kinase inhibitory proteins (CKIs) (reviewed by Sherr and Roberts, 1999; Elledge, 1996; King *et al.*, 1996; Lew and Kornbluth, 1996).

1-3.1 Cyclin abundance

The levels of Cyclins are not only determined by their rate of synthesis, but also their rate of degradation. Examination of the transcriptional regulation of Cyclins in a variety of organisms from yeast to mammalian cells indicates that regulated transcription is essential

Figure 1.1 : Regulation of the G1 to S phase transition.

A schematic representation of the molecular events that occur during the G1 to S phase transition in mammalian cells. During G1 phase, positive or negative signals are integrated into regulating the cell cycle. In response to negative factors, the INK4 and p21 families of CDKs bind to and inhibit G1 Cyclin/Cdk complexes, whereas the response to positive growth factors results in the formation of active G1 Cyclin/Cdk complexes. Active Cyclin D/Cdk4(6) complex mediates the initial phosphorylation of the retinoblastoma protein, pRb. Active Cyclin E/Cdk2 complexes act in a number of processes at the G1 to S phase transition. Among these is the full inactivation of pRb, thereby modifying the E2F transcriptional program, histone biosynthesis, pre-mRNA splicing, centrosome biosynthesis and initiation of DNA replication.

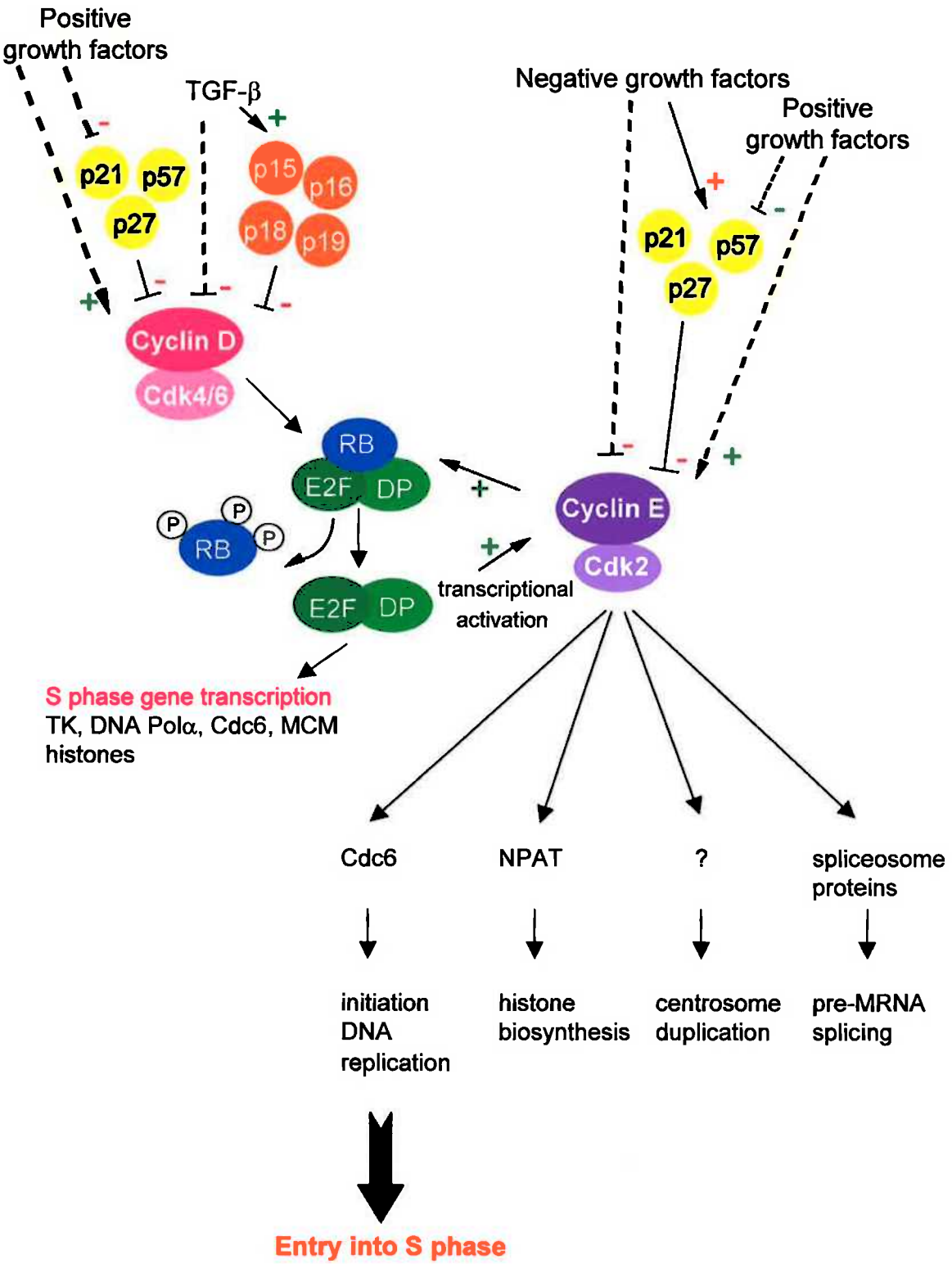
Positive
growth factors
TGF-β
p21
p57
p27
p15
p16
p18
p19
Cyclin D
Cdk4/6
RB
E2F
DP
P
RB
E2F
DP
Negative growth factors
Positive
growth factors
p21
p57
p27
Cyclin E
Cdk2
transcriptional
activation
S phase gene transcription
TK, DNA Polα, Cdc6, MCM
histones
Cdc6
NPAT
?
spliceosome
proteins
initiation
DNA
replication
histone
biosynthesis
centrosome
duplication
pre-MRNA
splicing
Entry into S phase

for cell cycle progression. Protein degradation has also been shown to be important in progression through the cell cycle (reviewed by Krek, 1998). The degradation of M phase cyclins, Cyclin A and B, requires a conserved N-terminal motif, the destruction box, that is essential for these proteins to be degraded by ubiquitin-mediated proteolysis, allowing the completion of M phase (Glotzer, 1995). Ubiquitin-mediated proteolysis is also important for the targeted degradation of G1 cyclins, however their destruction motif differs to that of mitotic cyclins. In budding yeast, G1 cyclins contain multiple PEST (refers to amino acid code) sequences. The importance of these motifs on G1 cyclin instability has been revealed by deletion of these sequences from the budding yeast G1 cyclins Cln2 and Cln3, which results in increased protein stability (Hadwiger *et al.*, 1989; Tyers *et al.*, 1992). PEST sequences have been identified in human Cyclins D and E, with a single PEST sequence located at the C-terminus (Lew *et al.*, 1991). It is not known if these PEST sequences affect protein stability, however degradation of human Cyclin E requires a C-terminal sequence, LTPP (destruction sequence), whereby phosphorylation of the threonine by Cdk2 plays a crucial regulatory function to target Cyclin E to ubiquitin-mediated degradation (Clurman *et al.*, 1996; Won and Reed, 1996). This sequence is highly conserved, being present in *Xenopus*, mouse and *Drosophila*, however it has not yet been shown to be functionally conserved.

1-3.2 Phosphorylation

Not only is the availability of the Cyclin subunit essential for Cyclin/Cdk complex formation, but post-translational modification also plays a crucial role in activation of the complex. Phosphorylation of a conserved Threonine residue (T160) of Cdk2 by Cdk activating kinase, CAK, is essential for Cyclin/Cdk kinase activity (Poon *et al.*, 1993; Solomon *et al.*, 1993). The removal of inhibitory phosphorylation is also important. Analogous to the role of mammalian Cdc25C for entry into mitosis by dephosphorylating tyr15 and thr14 on Cdk1 thereby activating the kinase complex, Cdc25A is involved in dephosphorylating and activating G1 cyclin/Cdk complexes (Hoffman *et al.*, 1994; Jinno *et al.*, 1994). Thus regulated activity of the Cyclin/Cdk complex requires both activating and inhibiting phosphorylation of the Cdk subunit.

1-3.3 Cyclin-dependent kinase inhibitors

CKIs have an important role in regulating the activity of Cyclin/Cdk complexes during the G1 to S phase transition (reviewed by Sherr and Roberts, 1999). There are two major families of CKIs, the INK4 family and the p21 family. The INK4 family of consists of $p15^{INK4b}$, $p16^{INK4a}$, $p18^{INK4c}$ and $p19^{INK4d}$, each contain four ankyrin-like repeats (Carnero and Hannon, 1998). These proteins induce G1 arrest by binding specifically to Cdk4/6 (via ankyrin-like

repeats), preventing the association with Cyclin D and formation of an active kinase complex (Figure 1.1) (Parry *et al.*, 1995).

The p21 family consists of $p21^{Cip1/Waf1}$, $p27^{Kip1}$and $p57^{Kip2}$ (reviewed by Hengat and Reed, 1998). These proteins share conserved N-terminal regions important for Cyclin binding and Cdk inhibition. Unlike INK4 family proteins, p21 family members act by binding to Cyclin D/Cdk4(6), Cyclin E/Cdk2 and Cyclin A/Cdk2 complexes inhibiting kinase activity and resulting in G1 arrest (Figure 1.1) (reviewed by Sherr and Roberts, 1999).

In both tissue culture cells and *in vivo,* the accumulation of CKIs in response to extracellular signals correlates with exit from the cell cycle. In mammalian epithelial cells, the negative growth factor TGF-β acts to arrest cells in late G1 phase by inhibition of Cyclin E/Cdk2. This G1 arrest is mediated by $p27^{Kip1}$, which binds to Cyclin E/Cdk2 inhibiting kinase activity (Koff *et al.*, 1993; Polyak *et al.*, 1994; Slingerland *et al.*, 1994). However, TGF-β does not lead to a direct increase in $p27^{Kip1}$, but rather to an increase in a member of the INK4 family, $p15^{INK4b}$. The presence of increased $p15^{INK4b}$ protein, which binds to Cdk4(6), results in dissociation of Cyclin D/Cdk4(6) complexes containing $p27^{Kip1}$, leaving $p27^{Kip1}$ free to associate with Cyclin E/Cdk2, inhibiting kinase activity (Hannon and Beach, 1994). However to overcome this inhibition, nuclear accumulation of Cyclin E/Cdk2 has also been shown to be important in the concentration-dependent destruction of $p27^{Kip1}$ (Swanson *et al.*, 2000). The role of $p27^{Kip1}$ is highlighted by studies in knockout mice that show abnormalities in cell numbers and organ size, suggesting that cell proliferation continues inappropriately and cell differentiation is delayed, and that $p27^{Kip1}$ may not be crucial for cell cycle exit but rather to the timing of the onset of differentiation (Fero *et al.,* 1996; Kiyokawa *et al.,* 1996; Nakayama *et al.,* 1996; Durand *et al.,* 1998). The role of $p57^{Kip2}$ has also been examined in knockout mice, which display abnormalities including large organ size with a higher number of cells, a phenotype similar to that of $p27^{Kip1}$ knockout mice, indicating that $p57^{Kip2}$ also plays a role in the timing of cell cycle exit prior to differentiation (Yan *et al.,* 1997; Zhang *et al.,* 1997).

Another example of induction of CKI by external signals occurs after irradiation: in response to DNA damage, the transcriptional activity of the tumour suppressor protein p53 is activated resulting in induction of $p21^{Cip1}$ causing a G1 arrest by inhibition of Cyclin E/Cdk2 complexes, in order for DNA repair to occur (El-Deiry *et al.*, 1993; Dulic *et al.*, 1994). Also, $p21^{Cip1}$ is induced by the myogenic transcription factor, MyoD, during muscle cell differentiation in culture and results in inactivation of Cyclin/Cdk, preventing cell division and promoting differentiation (Halevy *et al.*, 1995; Parker *et al.*, 1995). However, the importance of this *in vivo* is unclear as $p21^{Cip1}$ knockout mice show no developmental defects. Rather, it appears that $p21^{Cip1}$ is involved in G1 arrest in response to DNA damage (Deng *et al.,* 1995).

These examples highlight the importance of CKI proteins in negatively regulating Cyclin/Cdk complexes to maintain a G1 arrest, to allow DNA repair and terminal differentiation. In mammalian cells, each of these CKI's is regulated differently in response to negative growth signals, differentiation signals or DNA damage to allow G1 arrest (Figure 1.1).

1-4 Targets of G1 Cyclin/Cdk activity

To promote cell cycle transition from G1 into S phase, active G1 Cyclin/Cdk complexes must phosphorylate key regulatory proteins required for entry into S phase. The major target for Cyclin D/Cdk4(6) complexes appears to be the pRb family of pocket proteins (reviewed by Dyson, 1998). The phosphorylation of pRb, and related proteins p107 and p130, varies through the cell cycle. In the active hypophosphorylated form, pRb acts as a negative cell cycle regulator, as it binds to members of the E2F/DP transcription family forming an inactive complex at S phase gene promoters (reviewed by Dyson, 1998). The E2F transcription complex consists of two subunits, an E2F and DP protein. In mammals, there are 6 members of the E2F family and 3 members of the DP family. E2F/DP binding sites have been found in the promoters of genes required for DNA synthesis (e.g. *DNA polymerase α)*, for synthesis of DNA precursors (e.g. *thymidine kinase)*, for formation of the pre-replication complex (e.g. *cdc6*), for the formation of chromatin (e.g. *H2A)*, and for cell cycle control (e.g. *cyclin E*) (Figure 1.1).

Phosphorylation of pRb by Cyclin D/Cdk4(6) inactivates pRb, resulting in the release of E2F and allowing transcription of S phase genes (reviewed by Tam *et al.*, 1994; Lukas *et al.*, 1995; Planas-Silva and Weinberg, 1997). The inactivation of pRb appears to require multiple modifications. Following the initial phosphorylation by Cyclin D/Cdk4(6), active Cyclin E/Cdk2 kinase complexes further phosphorylate pRb (Resnitzky and Reed, 1995; Lundberg and Weinberg, 1998).

Recent studies in many model organisms have elucidated a role for Cyclin D/Cdk4(6) in the regulation of growth, linking cell growth and cell-cycle progression (reviewed by Prober and Edgar, 2001). The observation that Cyclin D expression is induced by growth-factors has led to the proposal that Cyclin D acts as a growth-factor sensor, linking extracellular cues to the cell cycle machinery. Mice lacking Cyclin D1 are small and have tissue-specific hypoplastic phenotypes (Fantl *et al.*, 1995; Sicinski *et al.*, 1995), whereas overexpression of Cyclin D1 can promote tissue-specific hyperplasia (Wang *et al.*, 1994; Robles *et al.*, 1996; Rodriguez-Puebla *et al.*, 1999). The requirement for Cyclin D/Cdk4 activity in normal growth, along with its ability to promote overgrowth, suggests that it not only acts as a growth-factor sensor, but also as a growth inducer (reviewed by Prober and Edgar, 2001). Therefore, the induction of Cyclin D in response to growth factors ultimately results in S phase progression by leading to downstream events that result in active Cyclin E/Cdk2 complexes.

Whilst the only essential target of Cyclin D/Cdk4(6) appears to be pRb, the role of Cyclin E/Cdk2 appears to be more wide-spread, having other essential functions in S phase entry by controlling pathways downstream of, or parallel to, phosphorylation of pRb and independent of E2F activation (Figure 1.1) (Lukas *et al.*, 1997). Recently, Cyclin E/Cdk2 has been shown to have a direct role in the initiation of DNA replication that depends upon its recruitment to replication origins by the pre-replication complex protein Cdc6 (Furstenthal *et al.*, 2001). Furthermore, a role for Cyclin E/Cdk2 in transcriptional regulation of *histone* genes has been demonstrated by the finding that NPAT, which is required for cell cycle dependent transcription of histone *H2B, H4 and H3,* is regulated by Cyclin E/Cdk2 phosphorylation (Ma *et al.*, 2000; Zhao *et al.*, 2000). Cyclin E/Cdk2 also plays an important role in centrosome duplication (Hinchcliffe *et al.*, 1999; Matsumoto *et al.*, 1999; Okuda *et al.*, 2000; Tokuyama *et al.*, 2001). The finding that the spliceosome associated protein SAP155 is a target of Cyclin E/Cdk2 kinase activity *in vitro* indicates a link between mRNA processing and progression of the cell cycle (Seghezzi *et al.*, 1998).

Thus, the main target of Cyclin D/Cdk4(6) kinase activity appears to be pRb, whereas Cyclin E/Cdk2 functions in multiple pathways in the G1 to S phase transition. Elucidation of these targets has revealed a role for Cyclin E/Cdk2 in the initiation of DNA synthesis, but a role in other processes required for cellular duplication have also been discovered (Figure 1.1).

The above examples highlight the importance of integrating information from extracellular and intracellular signals to regulate Cyclin E/Cdk2 activity and thus the G1 to S phase transition. Although regulation of the G1 to S phase transition has been well studied in mammalian tissue culture cells, relatively few studies have addressed G1 to S phase regulation in a whole animal. *Drosophila melanogaster* provides an excellent model organism to study regulation of the cell cycle during development, since the pattern of cell divisions during development are well characterised and homologues of mammalian cell cycle regulators have been identified (reviewed by Edgar and Lehner, 1996; Vidwans and Su, 2001).

1-5 Cell cycle regulation during *Drosophila* development

The cellular basis of *Drosophila* development, including the patterns of proliferation, is well documented. In addition, a number of different types of cell cycles have been characterised, including the synchronous cleavage cycles following fertilisation, endoreplicative cycles and meiotic cycles. *Drosophila* embryonic and eye development are summarised below and the remainder of this chapter will focus on the role of *Drosophila* Cyclin E in regulation of the G1 to S phase transition during development.

1-5.1 Embryonic Development

Embryonic development initiates following fertilisation, and the first 13 nuclear divisions, consisting of alternating S and M phases with no G phases, occur synchronously in a syncytium (Foe and Alberts, 1983). These cycles are rapid and their regulation relies on maternal gene products, deposited into the oocyte during oogenesis, as no zygotic transcription occurs during these cleavage cycles. Cellularisation occurs during G2 of cycle 14 and marks a change in the cell cycle with the addition of a regulated G2 phase (Edgar and O'Farrell, 1990). As the stores of various maternal products are depleted by cycle 14, continued cell division relies on zygotic transcription. The first zygotically controlled cell cycles, the post-blastoderm cycles (14, 15 and 16), require the product of the *string* gene, the cyclin dependent kinase and mitotic activator Cdc25 phosphatase (Edgar and O'Farrell, 1990). Expression of *string* occurs in specific spatial and temporal domains that results in asynchronous mitoses (Foe, 1989). Following mitosis 16, most cells arrest in their first G1 phase of cycle 17 and begin to differentiate.

Some cell types continue to cycle, including those of the ectodermal thoracic patch which undergo a mitotic cycle 17 (G1, S, G2 and M phase), the embryonic endoderm as well as larval tissues which undergo endoreplication cycles, consisting of alternating S and G phases with no M phases (Smith and Orr-Weaver, 1991). Also during embryogenesis and larval development the neuroblasts continue to proliferate in a S, G2 and M phase cycle, similar to cycles 14-16, while the imaginal cells, which will give rise to the adult structures, recommence cell division during larval development and proceed with mitotic cell cycles consisting of G1, S, G2, and M phases (Figure 1.2) (reviewed by Edgar, 1995).

1-5.2 Eye Development

The larval eye imaginal disc provides an excellent example of a tissue with a developmentally regulated G1 to S phase transition. The eye imaginal disc, set aside during embryogenesis, proliferates and differentiates during larval development resulting in the formation of the adult compound eye. This highly regular eye structure is comprised of about 750 identical units, called ommatidia. Each individual ommatidium is composed of several cell types, eight photoreceptor cells arranged in a precise pattern, and 12 accessory cells, comprising cone cells, pigment cells and a mechanosensory bristle (Wolff and Ready, 1993).

Differentiation of the eye imaginal disc initiates during the third larval instar, at the posterior edge of the eye disc. Differentiation proceeds anteriorly across the disc, with cells that are about to differentiate associated with an indentation referred to as the morphogenetic furrow (MF) (reviewed by Wolff and Ready, 1993). Prior to differentiation, cells arrest in G1 phase within and anterior to the MF (Wolff and Ready, 1993; Thomas *et al.*, 1994). For the purpose of

Figure 1.2 : Various cell cycles occur during *Drosophila* development.

A schematic representation of cell cycles. Following fertilisation the first 13 syncytial divisions consist of alternating S and M phases. After cellularisation a regulated G2 phase is present. Most cells of the embryo arrest in G1 of cycle 17, although the cells of neural lineage continue to proliferate. Later during development, a regulated G1 phase is introduced in the imaginal disc cells. Finally, the endoreplication cycles required for polytenisation, consist of alternating S and G phases.

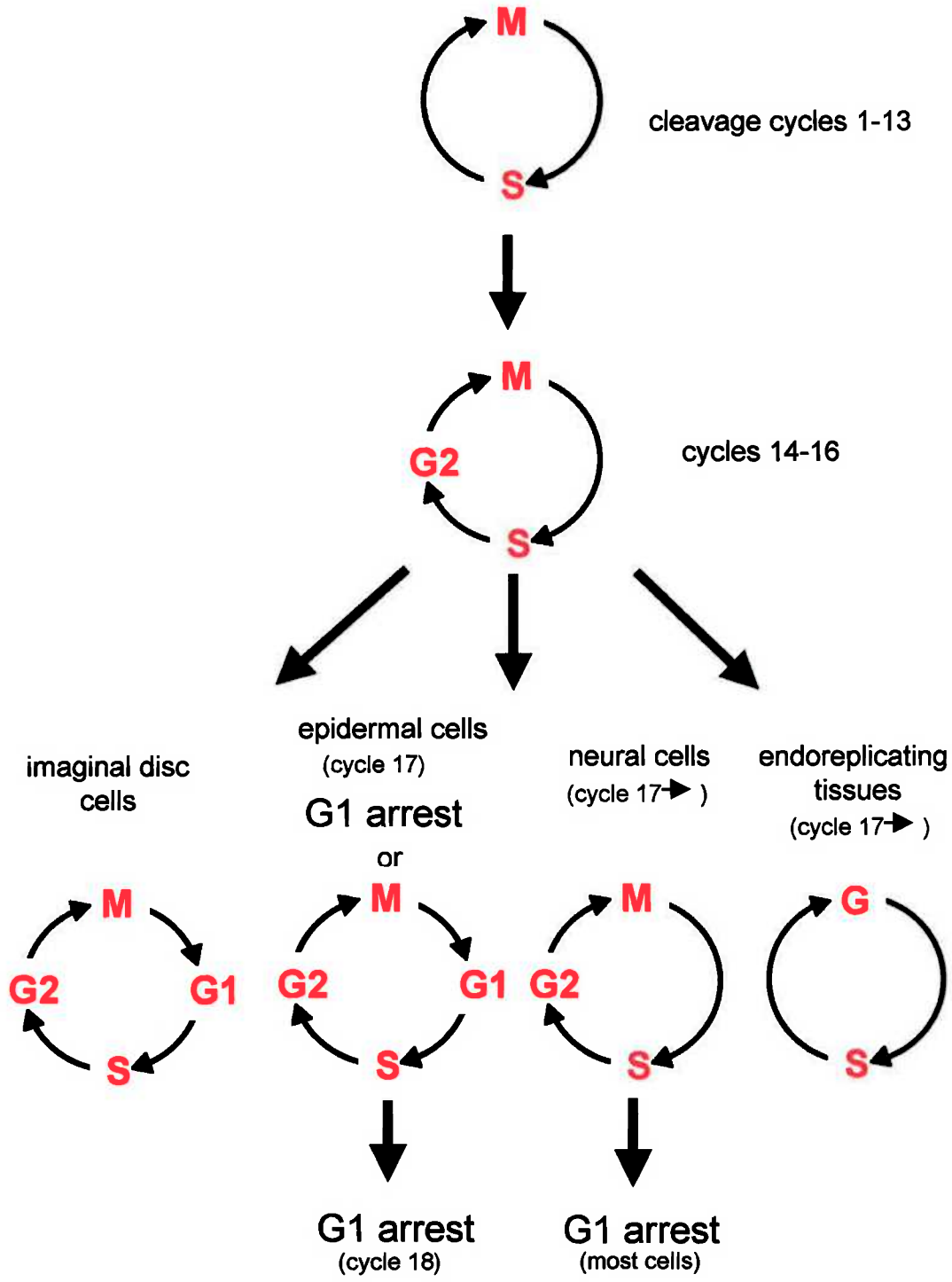
M
S
cleavage cycles 1-13
M
G2
S
cycles 14-16
imaginal disc cells
epidermal cells
(cycle 17)
G1 arrest
or
neural cells
(cycle 17→)
endoreplicating tissues
(cycle 17→)
M
G2
G1
S
M
G2
G1
S
M
G2
S
G
S
G1 arrest
(cycle 18)
G1 arrest
(most cells)

this study, the MF will be defined to include all of these G1 arrested cells. Posterior to the MF, a subset of cells undergo a synchronous S phase before differentiating. In the remainder of the eye disc, cells in the posterior region are differentiating, the more posterior cells being the most differentiated, whilst anterior cells are undifferentiated and cycle asynchronously. Thus, the eye imaginal disc is characterised by a spatial arrangement of cell division phases and differentiating cells (Figure 1.3).

1-6 *Drosophila DmcycE*

In *Drosophila*, Cyclin E appears to be the most important cyclin in regulation of the G1 to S phase transition, since recent studies have shown that Cyclin D/Cdk4(6) acts primarily as a cell growth regulator (Datar *et al.*, 2000; Meyer *et al.*, 2000). As in mammalian cells, *Drosophila cyclin E (DmcycE)* is essential and rate-limiting for the G1 to S phase transition (Richardson *et al.*, 1993; Knoblich *et al.*, 1994; Secombe *et al.*, 1998). *DmcycE* was identified by homology to human cyclin E and interacts with the *Drosophila* homologue of Cdk2, Cdc2c (referred to as DmCdk2) (Knoblich *et al.*, 1994). *DmcycE* encodes two proteins with common C-terminal and unique N-terminal regions that arise from alternative transcripts and are differentially expressed during development (Richardson *et al.*, 1993). The *DmcycEII* transcript encodes a 709 amino acid protein with a unique 119 amino acid N-terminal region, while the DmcycEI protein has 12 unique amino acids at the N terminus (Richardson *et al.*, 1993). The cyclin box, essential for Cdk interaction, is located in the central region of both DmcycE proteins. At the N- and C-termini, both proteins contain several PEST sequences, with additional sequences located in the unique N-terminus of DmcycEII. The destruction sequence identified in human Cyclin E, LTPP, is conserved in DmcycE and is located in the C-terminus.

The unique N-terminal regions of these proteins also contain different potential nuclear localisation sequences (NLS). The putative NLS of DmcycEII is similar to the canonical SV40 T antigen NLS, whereas DmcycEI has a putative bipartite NLS (Richardson *et al.*, 1993). DmcycEII, but not DmcycEI, has multiple serine and threonine residues flanking the putative NLS, and therefore phosphorylation of these residues may affect nuclear localisation (Garcia-Bustos *et al.*, 1991). Since the unique N-terminal regions of these proteins containing different PEST sequences, potential phosphorylation sites and potential NLS, it is likely that they have different properties.

1-6.1 *DmcycE* expression

During development the type I and type II transcripts have distinct expression patterns (Richardson *et al.*, 1993; Knoblich *et al.*, 1994; Richardson *et al.*, 1995). *DmcycEII* mRNA is supplied maternally, whereas *DmcycEI* is zygotically expressed in all proliferating tissues

Figure 1.3 : Schematic representation of cell cycle progression in the eye imaginal disc.

In the anterior region, cells are dividing asynchronously, with cells in all phases of the cell cycle. As the wave of differentiation (in the direction of the arrow), marked by an indentation referred to as the morphogenetic furrow (MF), proceeds anteriorly, cells become synchronized in G1 phase. Immediately posterior to the MF a subset of cells enter a synchronous S phase followed by mitosis.

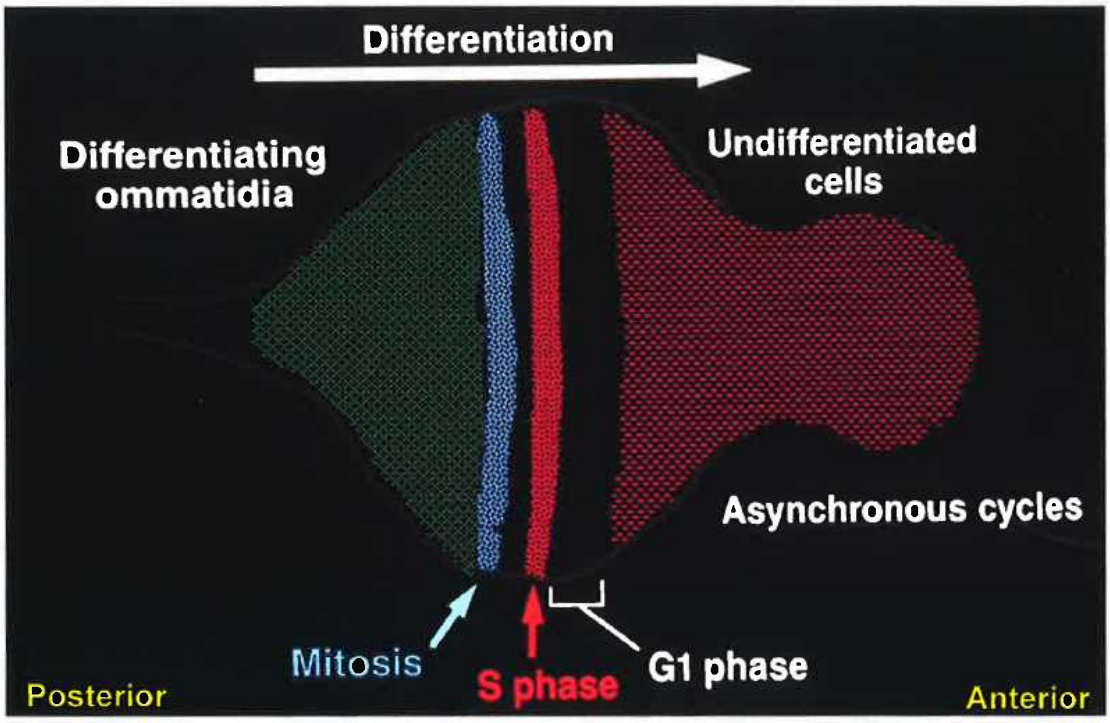
Differentiation
Differentiating ommatidia
Undifferentiated cells
Asynchronous cycles
Mitosis
S phase
G1 phase
Posterior
Anterior

during embryogenesis. During the first 13 cleavage cycles, *DmcycEII* mRNA and protein are present at high levels (Richardson *et al.*, 1993). At the time of pole (presumptive germ) cell formation, *DmcycEII* mRNA is concentrated at the posterior of the embryo where the pole cells are forming. During cellularisation, *DmcycEII* transcripts are excluded from the somatic cells and are rapidly degraded prior to mitosis 14, although transcripts remain in the pole cells. Zygotic expression of *DmcycEI* is first detected after cycle 10 and subsequently in all mitotically proliferating and endoreplicating tissues during embryogenesis. Cells that arrest in G1 of cycle 17 and begin to differentiate have no detectable *DmcycEI* mRNA or protein, suggesting a requirement for down-regulation of *DmcycE* transcription for G1 arrest (Richardson *et al.*, 1993; Knoblich *et al.*, 1994). In addition, the upregulation of other proteins such as the p21 homologue Dacapo, and the Rb homologue Rbf are also required for the initiation or maintenance of this G1 arrest (de Nooij *et al.*, 1996; Lane *et al.*, 1996; Du *et al.*, 1996).

The localisation of DmcycE protein during embryogenesis is consistent with *DmcycE* mRNA expression. To investigate the distribution of DmcycE protein during embryogenesis, DmcycE polyclonal antisera raised to the region of DmcycE present in both the type I and type II proteins was used (Richardson *et al.*, 1995). During the first 16 embryonic cell cycles, maternal DmcycEII protein (prevalent during 0-3 hour AED; see Figure 1.4) and zygotic DmcycEI protein (prevalent after 3 hours AED) are nuclear-localised in interphase cells (Figure 1.4 A-F). At the onset of prophase, DmcycE becomes dispersed throughout the cytoplasm until late in telophase, where it again becomes localised to the nucleus (Figure 1.4 A-F). Although less DmcycE protein appears to be present in mitotic cells, this is due to dispersion or epitope-masking rather than degradation since analysis by immunoblotting has shown that DmcycE protein levels do not decrease during mitosis (Sauer *et al.*, 1995).

Throughout embryogenesis, DmcycE protein is present in proliferating cells, but is down-regulated as cells stop dividing. After the 16th mitosis, most cells in the embryo enter their first G1 phase and begin to differentiate. At this time, DmcycE is no longer detected in differentiating epidermal cells but is present in patches of epidermal cells in the thoracic segments (Figure 1.4 G), which go through one further cycle (Knoblich *et al.*, 1994). When proliferation of cells in the thoracic patches ceases, DmcycE is no longer detected in these cells (Figure 1.4 H) but is still present in the dividing cells of the central and peripheral nervous system (Figure 1.4 G-L). As the nervous system cells cease division, expression of DmcycE protein also ceases. This is evident in peripheral nervous system cells, where DmcycE protein is no longer present once these cells cease proliferation (compare Figure 1.4 I with K,L). In addition, DmcycE protein can be detected at low levels in endoreplicating tissues when S phases are occurring (Figure 1.4 J,L). Thus the pattern of DmcycE protein distribution during

Figure 1.4 : DmcycE localization during embryogenesis.

DmcycE protein distribution during embryogenesis. Embryos were incubated with DmcycE mouse polyclonal antisera followed by HRP detection (Crack *et al.*, 2002).

A. A syncytial embryo in interphase (~1 hour AED) showing nuclear localisation of DmcycE.

B. An embryo undergoing the parasynchronous syncytial divisions (~1 hour AED) co-stained with Hoechst 33258 (bright blue), showing nuclear localisation of DmcycE in interphase nuclei and loss from the nuclei as they enter prophase.

C. An embryo undergoing the parasynchronous syncytial divisions (~1 hour AED).

D. The same embryo as in (**C**) co-stained with Hoechst 33258 showing re-accumulation of DmcycE in telophase nuclei.

In **B** and **D** the stages of mitosis are marked, P = prophase, M = metaphase, A = anaphase, T = telophase and I = interphase.

E. An embryo undergoing the G2-regulated cycle 14 (~3.5 hour AED) showing an apparent decrease in DmcycE protein abundance in mitotic domains.

F. The same embryo as in (**E**) co-stained with Hoechst 33258 showing mitotic nuclei.

Note in **B**, **D** and **F**, nuclear DmcycE staining has quenched the Hoechst 33258 staining.

G. An embryo after the completion of cycle 16 (~6-7 hour AED) showing DmcycE in the epidermis of the thoracic segments T1 and T2 that undergo a 17th cycle (arrowheads). Expression in the underlying peripheral nervous system (PNS) and central nervous system (CNS) can also be seen.

H. An embryo a short time later (~7 hour AED) showing DmcycE in PNS cells.

I. A germ band retracted embryo (~10 hour AED) showing DmcycE in the PNS and CNS.

J. An embryo at the same stage as (**I**) showing DmcycE in the pole (germ) cells (pc) and in the endo-replicating tissue of the midgut (mg).

K. A ventral view of an embryo at ~13 hour AED showing DmcycE in the CNS.

L. An embryo at the end of head involution (~16 hour AED) showing expression of DmcycE in the CNS and regions in the endo-replicating tissues of the midgut (mg).

Embryos are orientated anterior to the left and ventral side down.

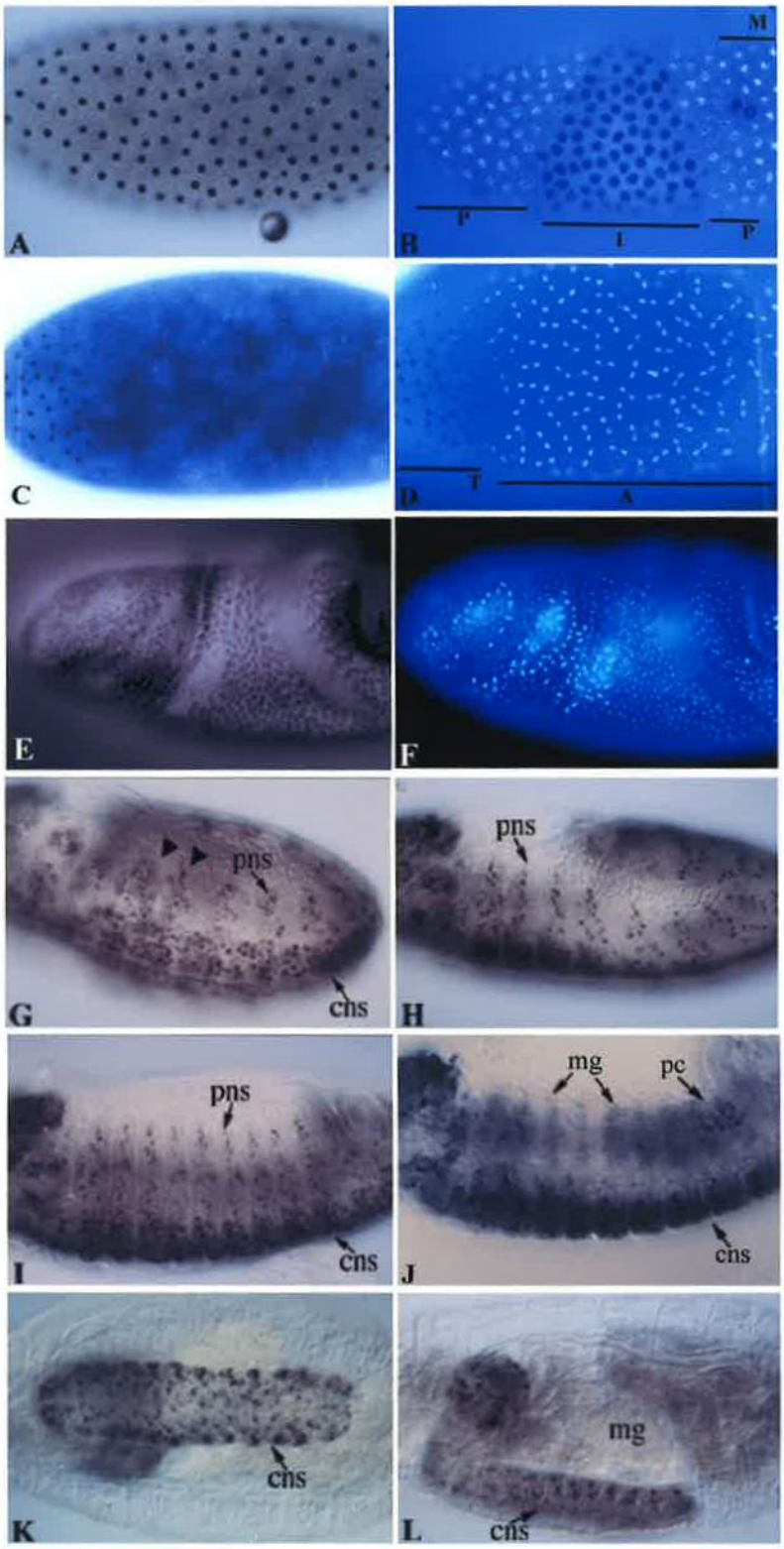
A
B
M
P
I
P
C
D
T
A
E
F
G
pns
cns
H
pns
I
pns
cns
J
mg
pc
cns
K
cns
L
mg
cns

embryogenesis generally correlates with the pattern of *DmcycE* mRNA, being expressed in mitotically proliferating and endoreplicating cells and down-regulated when these cells cease replication (Richardson *et al.*, 1993; Knoblich *et al.*, 1994).

Expression of *DmcycE* in the third larval instar eye imaginal disc has been characterised, and as expected correlates with proliferation. *DmcycE* is expressed in a subset of the asynchronously dividing cells, and in a band corresponding to the synchronous S phases immediately posterior to the MF in the eye disc (Figure 1.5). Expression of *DmcycE* is not detected in the band of G1-arrested cells immediately anterior to the MF or within the MF (Richardson *et al.*, 1995). Thus in the larval eye imaginal disc, *DmcycE* is undetectable in G1-arrested cells, but is strongly expressed in a pattern correlating with S phases. These studies have shown that the expression pattern of DmcycE is consistent with its role in regulating entry into S phase during *Drosophila* development.

1-6.2 DmcycE is rate-limiting for the G1 to S phase transition

The importance of *DmcycE* in regulating the G1 to S phase transition is highlighted by examination of mutant phenotypes. Null alleles of *DmcycE* are homozygous lethal, with embryonic cells arresting at G1 of cycle 17 due to an absence of DmcycEI, revealing that it is an essential gene (Knoblich *et al.*, 1994). A hypomorphic *DmcycE* mutation, $DmcycE^{JP}$, is homozygous viable with a mutant phenotype appearing later in development. Homozygous larvae have a reduction in the number of S phase cells in the eye imaginal disc, due to a decrease of *DmcycE* expression in this tissue, with the most dramatic reduction seen in the band of S phase cells posterior to the MF. This results in adult flies with small and disorganised (or rough) eyes (Secombe *et al.*, 1998).

Previous studies have shown that ectopic expression of *DmcycEI* in terminally-arrested G1 cells of cycle 17 of embryogenesis is sufficient to induce entry into S phase (Knoblich *et al.*, 1994). Similarly, ectopic expression of *DmcycEI* in the eye imaginal disc can drive many, but not all, G1-arrested cells within the MF into S phase (Richardson *et al.*, 1995). Cells in the posterior part of the MF are refractory to ectopic expression of DmcycEI, while the anterior-most cells are induced into S phase. A similar effect is observed when *DmcycEII* is ectopically expressed in the eye imaginal disc, resulting in induction of G1-arrested cells into S phase. However, unlike DmcycEI, DmcycEII was able to induce the G1-arrested cells within the posterior part of the MF into S phase. These results suggest that cells in the posterior region of the MF are more resistant than anterior cells to being induced into S phase by DmcycE, and that DmcycEII is more potent than DmcycEI in overcoming this resistance.

Figure 1.5 : DmcycE localisation during eye imaginal disc differentiation.

Wild-type third instar larval eye-antennal imaginal discs.

A. Distribution of DmcycE protein. DmcycE is detected in asynchronously dividing cells anterior to the MF, and in the band of S phase cells immediately posterior to the MF. No DmcycE is detectable in the G1 arrested cells within the MF.

B. S phase cells, labelled by BrdU incorporation. The pattern of S phases seen correlates with expression of DmcycE.

Anterior is to the right, the MF is indicated by the arrow.

Figure from Richardson *et al.,* 1995.

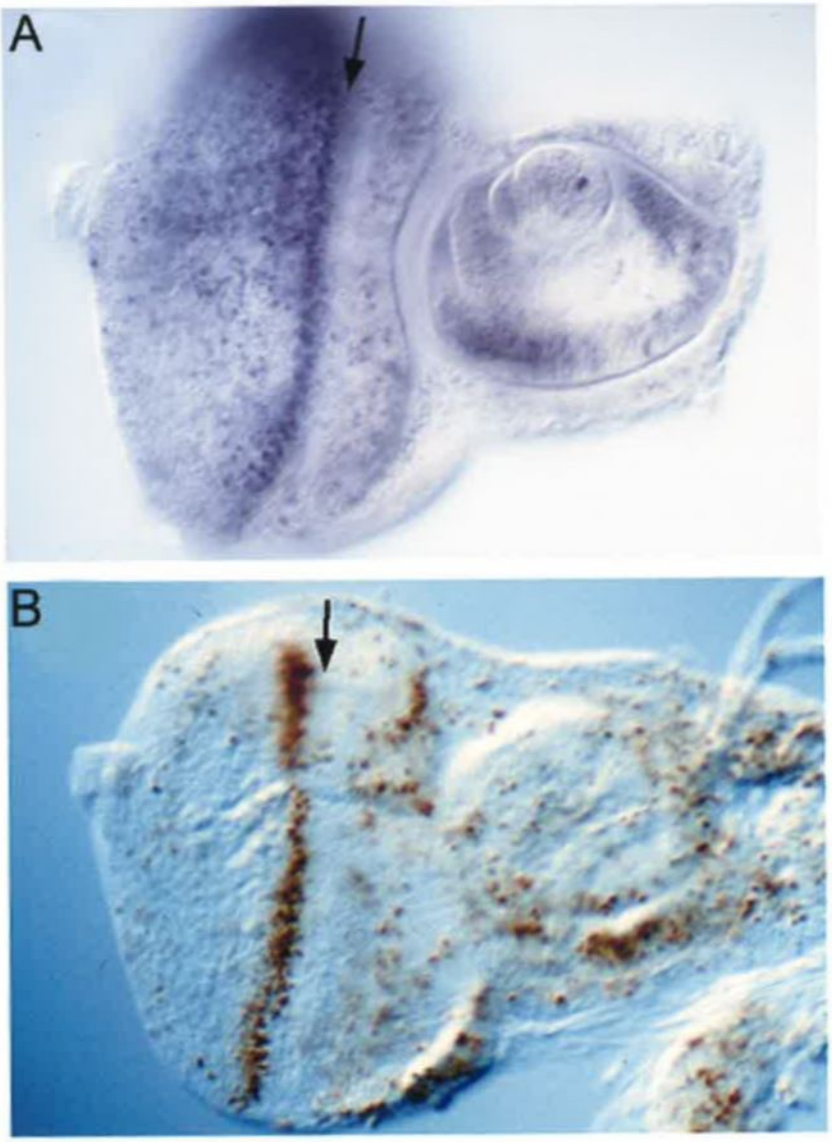
A
B

1-7 Regulation of the G1 to S phase transition in the MF

The maintenance of the G1 arrest, prior to differentiation, is important. The *Drosophila* TGF-β homologue, *decapentapligic (dpp),* is expressed in the G1-arrested cells within the MF and has been shown to have a role in regulation of the G1 arrest (Masucci *et al.*, 1990; Penton *et al.*, 1997; Horsfield *et al.*, 1998). Clones of cells mutant for *thickveins (tkv)*, the *dpp* receptor, spaning the MF are unable to respond to Dpp. They fail to arrest in G1 phase in the anterior region of the MF, express cell cycle genes and continue to cycle asynchronously. However, cells in *tkv* clones in the posterior region of the MF are still able to arrest in G1 phase (Horsfield *et al.*, 1998). Therefore the anterior MF cells require Dpp signalling to arrest in G1, whilst a *dpp*-independent mechanism is required for the G1 arrest in the posterior part of the MF. Conversely, ectopic expression of *dpp* in the eye imaginal disc leads to a rapid G1 arrest, suggesting that the Dpp pathway may act post-transcriptionally on DmcycE (Horsfield *et al.*, 1998). Thus although there are undetectable levels of DmcycE in the MF there may be low levels that need to be inhibited by either a Dpp-dependent or Dpp-independent pathway in order to establish and maintain the G1 arrest in the MF.

The role of Dpp in inducing G1 arrest may occur in a similar way to that of TGF-β in mammalian cells, where G1 arrest is mediated by the induction of CKIs. However, the *Drosophila p21* homologue, *dacapo (dap)*, is not expressed in the G1-arrested cells in the anterior region of the MF (de Nooij *et al.*, 1996; Lane *et al.*, 1996). Therefore, the Dpp-mediated G1 arrest is likely to occur by the induction of a novel inhibitor. In addition, there appears to be a Dpp-independent mechanism that acts to induce G1 arrest in the posterior part of the MF, and this may require *dap* (Figure 1.6) (Horsfield *et al.*, 1998).

1-7.1 The role of Dacapo, a negative regulator of DmcycE in development

Dacapo (Dap), the *Drosophila* homologue of the p21 family of mammalian CKIs, associates specifically with Cyclin E/DmCdk2 complexes and inhibits kinase activity (de Nooij *et al.*, 1996; Lane *et al.*, 1996). During embryogenesis, *dap* is highly expressed in cells that are exiting the cell cycle, and in homozygous mutant *dap* embryos, epidermal cells fail to arrest in G1 and undergo an additional S phase (de Nooij *et al.*, 1996; Lane *et al.*, 1996). Conversely, ectopic *dap* expression in embryos results in a premature G1 arrest (Lane *et al.*, 1996). During eye development, *dap* is expressed in a band of cells initiating differentiation posterior to the MF, whilst it is not expressed in the anterior region in G1-arrested cells (de Nooij *et al.*, 1996; Lane *et al.*, 1996). Thus, during development, *dap* may function similarly to the vertebrate p21 inhibitors in that it is required for a precisely timed exit from the cell cycle.

Figure 1.6 : Regulation of the G1 arrest that occurs in the MF of the eye imaginal disc.

Schematic representation of the MF region of an eye imaginal disc during third larval instar development. Within the MF, mechanisms exist to prevent the inappropriate expression and/or activation of DmcycE and DmcycA. DmcycA is prevented from accumulating by Rux, which is inactivated by DmcycE/DmCdk2. DmcycE is kept inactive in the anterior half of the MF by a Dpp-dependent mechanism, and in the posterior half of the MF by a Dpp-independent mechanism.

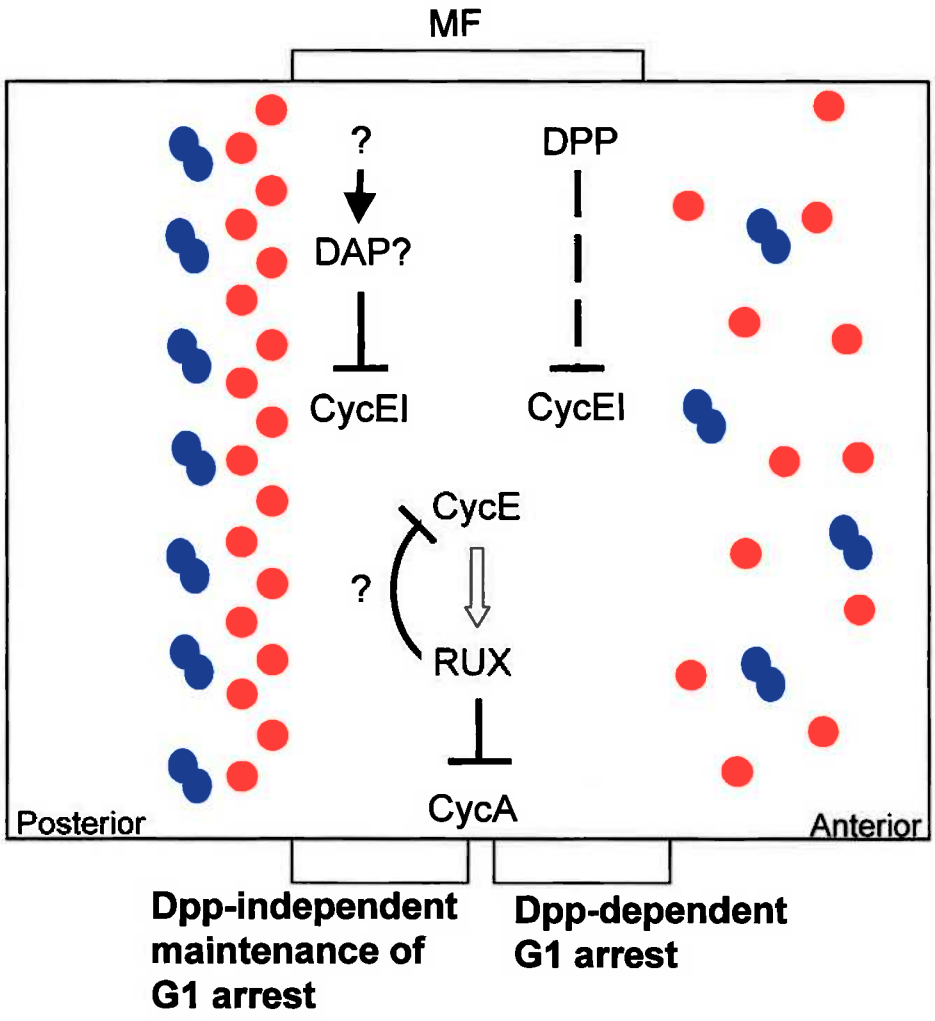
MF
?
DAP?
CycEI
DPP
CycEI
CycE
?
RUX
CycA
Posterior
Anterior
Dpp-independent maintenance of G1 arrest
Dpp-dependent G1 arrest
Mitotic cell
S phase nucleus

1-7.2 The role of Roughex, a negative regulator of Cyclin A during development

An important regulator of the G1 arrest in the MF during eye development is the *roughex (rux)* gene, which encodes a novel CKI protein required to down-regulate DmcycA activity (Thomas *et al.*, 1994). Rux is expressed predominantly in the G1-arrested cells in the anterior region of the MF and in differentiating cells in the posterior region of the eye imaginal disc. In *rux* mutant eye discs, ectopic DmcycA accumulates in cells anterior to the MF, preventing them from arresting in G1. Rather, these cells enter S phase precociously, resulting in adults with rough eyes (Thomas *et al.*, 1994; 1997). In addition, ectopic expression of DmcycA during eye development induces the G1-arrested cells into S phase, and this is suppressed by co-expression of Rux (Thomas *et al.*, 1997). During both embryonic and eye development, Rux acts to negatively regulate DmcycA by affecting the protein localisation, resulting in targeted degradation (Sprenger *et al.*, 1997; Thomas *et al.*, 1997). Inactivation of Rux is required to allow accumulation of DmcycA during S phase and this is accomplished by DmcycE/DmCdk2, which phosphorylates and inactivates Rux (Sprenger *et al.*, 1997; Thomas *et al.*, 1997). These results suggest that Rux controls DmcycA stability in G1-arrested cells, which is maintained until DmcycE/DmCdk2 accumulates, to induce S phase. This results in inhibition of Rux, allowing accumulation of DmcycA during S phase. Thus, DmcycA can act to induce entry of G1-arrested cells into S phase, but is normally inhibited by Rux until DmcycE/DmCdk2 accumulates and initiation of S phase occurs.

Studies of Rux have shown the importance of controlling DmcycA to prevent precocious S phases. It is unknown, however, what is involved in controlling DmcycE activity in the G1-arrested cells in the MF. While Dpp signalling plays a role in DmcycE inhibition in the anterior MF cells, a negative regulator of DmcycE/DmCdk2 activity in the posterior part of the G1-arrested MF cells has yet to be identified.

1-8 Aims and approaches of this thesis

The broad aim of this thesis is to understand the regulation of DmcycE in a developing animal. The specific aims include: 1) to examine the function of DmcycEII during development and 2) to investigate a mechanism by which DmcycEI is inhibited, resulting in a G1 arrest during eye development.

To assess the properties and roles of DmcycEI and II proteins, the distribution of DmcycEI and II during development was examined (as described in Chapter 3). In addition, a functional analysis was undertaken whereby the effects of ectopically expressing full-length and truncated forms of DmcycE proteins in the eye imaginal disc was examined (as described in Chapter 4). This revealed a model whereby the unique N terminal region of DmcycEI may be

the target region for an inhibitor, present within the MF, which would bind and prevent function of DmcycEI. Approaches undertaken to identify this inhibitor included the examination of candidate inhibitors, Dap and Rux (as described in Chapter 4), revealing that they were not DmcycEI specific inhibitors.

To identify negative regulators of DmcycE, two different approaches that would hopefully reveal DmcycEI specific inhibitors were undertaken (Chapters 5 and 6). Chapter 5 describes a genetic interaction screen making use of overexpression of DmcycEI in the eye to produce a dose-sensitive rough eye phenotype as a result of an increase in S phases in the posterior of the eye disc. This phenotype was then used to screen a collection of *P*-element mutations to identify dominant enhancers. The interactors identified were then further characterised to validate their role in regulating DmcycE.

Chapter 6 describes the use of the yeast 2-hybrid screen to isolate proteins that can bind to the N-terminal region of DmcycEI. Interactors isolated were then examined for their ability to inhibit DmcycE/DmCdk2 function, and for an *in vivo* interaction with DmcycE.

Further analysis of the interactors identified in these screens may reveal novel mechanisms for the control of the G1 to S phase transition. Together, the results from the two major aims of this study will increase our knowledge of DmcycE regulation in different developmental contexts, in an animal model system.

Chapter 2 : Materials and Methods

2-1 Abbreviations

Abbreviations used are as described in "Instructions to authors", Biochem. J (1978) 169, 1-27.

In addition;

A600	absorbance at 600nm	IPTG	Isopropyl ß-D-thiogalactopyranoside
AED	After egg deposition	kb	kilobase pairs
Ade	Adenine	kDa	kilo daltons
BCIG	5-Bromo-4-chloro-3-indolyl ß-D-galactopyranoside (X-gal)	Leu	Leucine
		Met	Methionine
BCIP	5 Bromo-4-chloro-3-indolyl phosphate	MQ	MilliQ
Blotto	5% skim milk powder in PBT	NBT	4-Nitro blue tetrozolium chloride
bp	base pairs	NP-40	nonidet P-40
BrdU	5 Bromo 2' deoxyuridine	OD	optical density
BSA	bovine serum albumin	ONPG	o-Nitrophenyl-D-galactopyranoside
CIP	alkaline calf intestinal phosphatase	PAGE	polyacylamide gel electrophoresis
DAB	3, 3' Diaminobenzidine	PBS	phosphate buffered saline
DIC	differential interferance contrast	PBT	PBS + 0.1% Tween 20 or TritonX-100
DMF	dimethyl formamide	PEG	polyethylene glycol
DNA	deoxyribonucleic acid	Raff	Raffinose
dNTP	deoxyribonucleoside triphosphate	RNA	ribonucleic acid
DTE	dithioerythritol	rpm	revolutions per minute
DTT	dithiothreitol	RT	room temperature
EDTA	ethylenediaminetetraacetic acid	SDS	sodium dodecyl sulphate
Gal	Galactose	SEM	scanning electron micrograph
Glu	Glucose	Trp	Tryptophan
His	Histidine	Ura	Uracil
HRP	Horseradish peroxidase	X-gal	BCIG

2-2 Materials

2-2.1 Chemical reagents

All reagents were of analytical grade, or the highest grade obtainable.

2-2.2 Enzymes

Enzymes were obtained from the following sources:

Restriction endonucleases — Boehringer Mannheim, New England Biolabs, Pharmacia

T4 DNA ligase — Boehringer Mannheim, New England Biolabs

CIP — Boehringer Mannheim

RNase A and Lysozyme — Sigma

Pfu DNA polymerase — Stratagene

2-2.3 Kits

QIAquick gel extraction kit — Qiagen

QIAprep spin miniprep kit — Qiagen

Vectastain ABC kit — Vector Laboratories Inc.

Enhanced Chemiluminescence (ECL) kit — Amersham

BRESAspin plasmid mini kit — Geneworks

Western blot recycling kit — Alpha Diagnostics

2-2.4 Molecular weight standards

DNA

λDNA was digested with *Bst* EII and *Sal* I to produce fragments of the following sizes (in kb) 14.14, 8.45, 7.24, 5.70, 4.82, 4.32, 3.68, 3.13, 2.74, 2.32, 1.93, 1.37, 1.26, 0.70, 0.50, 0.22 and 0.12.

Protein

High molecular weight markers (GIBCO BRL) in kDa — 205, 116, 97, 66, 45 and 29.

Prestained molecular weight markers (NEB) in kDa — 175, 83, 62, 47.5, 32.5, 25, 16.5 and 6.5.

Kaleidoscope prestained standards (Bio-Rad) in kDa — 216, 132, 78, 45.7, 32.5, 18.4 and 7.6.

2-2.5 Antibodies

Primary Antibody	Dilution	Source
α-BrdU (mouse monoclonal)	1/50 in PBT + 2% goat serum	Becton Dickinson
α-cyclin E (rat polyclonal)	1/500 in PBT + BSA	H. Richardson
α-cyclin E 8B10 (mouse monoclonal)	1/10 in Blotto	H. Richardson
α-cyclin E II (rat polyclonal)	1/500 in PBT + BSA 1/1000 in Blotto	This study
α-Dap (mouse monoclonal)	1/25 in PBT + BSA	I. Hariharan
α-GAL DBD (rabbit polyclonal)	1/500 in Blotto	Santa cruz
α-LexA (rabbit polyclonal)	1/500 in Blotto	R. Brent (Harvard, USA)
α-LexA (mouse monoclonal)	1/1500 in Blotto	Clontech
α-DmcycA (rabbit polyclonal)	1/200	D. Glover
α-Myc-Tag 9B11 (monoclonal)	1/1500	Cell Signalling
α-DIG-Alkaline Phosphatase (sheep Fab fragment)	1/2000 in PBT	Boehringer Mannheim

All secondary and tertiary antibodies were reconstituted according to the manufacturers instructions.

Secondary Antibody	Dilution	Source
α-mouse-biotin	1/200 in Blotto	Amersham
α-rat-biotin	1/200 in Blotto	Jackson Laboratories
α-mouse-HRP	1/3000 in Blotto	Jackson Laboratories
α-rabbit-HRP	1/3000 in Blotto	Jackson Laboratories
α-rat-HRP	1/3000 in Blotto	Jackson Laboratories
α-rat-Rhodamine	1/200 in PBT + BSA	Jackson Laboratories
Tertiary Complex	**Dilution**	**Source**
streptavidin-Alexa 488SA	1/200 in PBT	Quantum
streptavidin-FITC	1/200 in PBT	Jackson Laboratories
streptavidin-HRP (Vectastain ABC)	1/200 in PBT	Amersham
streptavidin-texas red	1/200 in PBT	Jackson Laboratories

2-2.6 Bacterial strains

E. coli DH5α — F', f80, *lacZ*ΔM15, *rec*A1, *end*A1, *gyr*A96, *thi*-1, *hsd*R17, (r_K-, m_K+), *sup*E44, *rel*A1, *deo*R, Δ(*lac*ZYA-*arg*F) U169

E. coli KC8 — *hsdR, leuB600, trpC9830, pyrF, hisB463, lacDX74, strA, galU, K*

2-2.7 Yeast strains

EGY48 — *MATα, trp1, his3, ura3,* 6lexAops-*LEU2* (obtained from R. Brent Harvard, USA)

PJ69-4A — MAT**a/α,** trp1-901, leu2-3,112, ura3-52, his3-200, gal4Δ, gal80Δ, LYS2::GAL1-HIS3, GAL2-ADE2, met2::GAL7-lacZ (James et al., 1996)

For DmcycE/Cdk2 inhibition analysis in yeast the following Cyclin E lethal yeast strains were used:

DmcycEI#70 — *pGAL-DmcycEI ADE1, pGAL-cdk2* (obtained from T. Brumby)

DmcycEII#22 — *pGAL DmcycEII ADE1, pGAL-cdk2*

DmcycEI or *DmcycEII* were cloned into the *Bam*HI site of *pGAL ADE1* which was constructed from YCpG2 (Mendenhall et al., 1988) by removal of the *URA3* and *LEU2* genes and replacement with the *ADE1* gene into the *Eco*RI and *Sma*I sites. Plasmids were transformed into the yeast strain 15D *ura3 leu2 his2 ade1 trp1* containing *Dmcdk2* under control of the *pGAL* promoter (constructed from YCpG2 *Dmcdk2;* Lehner and O'Farrell, 1990) integrated into the *his2* gene. Co-expression of DmcycE and Cdk2 was achieved by growth on galactose media.

2-2.8 *Drosophila* strains

Unless otherwise indicated, deficiency and *P*-element stocks (Spadling *P*-element stocks were available in the lab) were obtained from Bloomington Stock centre, Bloomington, Indiana. All fly stocks are as described in either FlyBase (www://flybase.bio.indiana.edu/) or Lindsay and Zimm (1992).

Strain	Obtained from
w ; DmcycE^{JP}	H. Richardson
b DmcycE^{JP} bw	H. Richardson
GMR-GAL4, UAS-gcycEI (2nd)	H. Richardson
GMR-GAL4, UAS-DmcycEII	D. Crack
hsp70-DmcycEI 3rd	H. Richardson *et al.*, 1995
hsp70-DmcycEII (Z4) X	D. Crack
hsp70-12ΔN-DmcycE (H23A) 2nd	this study
hsp70-195ΔN-DmcycE (1.2) 2nd	J. Secombe
hsp70-519ΔC-DmcycEI (C1) 2nd	J. Secombe
hsp70-195ΔN519ΔC-DmcycE (B3) 2nd	J. Secombe
dap^{4} (intragenic deletion generated by imprecise excision of the *dap^{1} P*-element)	de Nooij *et al.*, 1996; Lane *et al.*, 1996
*dap^{2X10}/Cy*O (null)	de Nooij *et al.*, 1996; Lane *et al.*, 1996
GMR-p21 3rd (human p21^{CIP})	de Nooij and Hariharan 1995
GMR-dE2F dDP p35	N. Dyson
rux^{3}/FM7	B. Thomas
caz^{1}/FM7	S. Hanes
caz^{2}/FM7	S. Hanes
S(DmcycE^{JP}) alleles	H. Richardson
E(Esev-cycE) alleles	C. Lehner
E(E2F,Dp) alleles	N. Dyson
S(GMR-p21) alleles	I. Hariharan

2-2.9 Buffers and solutions

Specific buffers and solutions of interest are listed, all others used in this work can be found in Sambrook *et al.*, (1989).

Agarose gel loading buffer (10x) — 50% (v/v) glycerol, 1mM EDTA, 0.1% (w/v) bromophenol blue

Buffer B — 100mM KH_2PO_4/K_2HPO_4 (pH 6.8), 450mM KCl, 150mM NaCl and 20mM $MgCl_2$.

Devitellinizing Buffer — 150 µl Buffer B, 200 µl 20% paraformaldehyde and 650 µl H_20.

Embryo injecting buffer (1x) — 5mM KCl, 0.1mM $NaPO_4$ pH 6.8

HEN buffer (10X) — 1M HEPES, O.5M EGTA, 0.1% NP-40, pH to 6.9 and filter sterilised.

PBS (1x) —7.5mM Na_2HPO_4, 2.5mM NaH_2PO_4, 145mM NaCl

PBT — 1 x PBS, 0.1% Tween 20 or Triton X-100

Protein gel running buffer (5x) — 1.5% Tris-base, 7.2% Glycine, 0.5% SDS

Protein gel transfer buffer — 50mM Tris-base, 0.3% Glycine, 0.04% SDS, 20% methanol

Protein sample buffer (3x) — 62.5mM Tris-HCl, 10% glycerol, 2% SDS, 0.00125% bromophenol blue, 5% β-mercaptoethanol added fresh, pH 6.8

SD buffer (10x) — 30mM Tris-HCL pH7.8, 625mM KAc, 100mM MgAc, 40mM spermadine, 5mM DTE

STET — 50mM Tris-HCl pH8.0, 50mM EDTA, 8%(w/v) sucrose and 5% Triton X-100

TAE — 40mM Tris-acetate, 20mM sodium acetate, 1mM EDTA, pH 8.2

Z-buffer — 60mM Na_2HPO_4, 40mM NaH_2PO_4, 10mMKCl, 1mM $MgSO_4$, 0.27% β-mercaptoethanol, pH7.0, with 1mg/ml X-gal.

2-2.10 Bacterial Media

All media were prepared with MQ water and sterilised by autoclaving, excepts heat labile reagents, which were filter sterilised. Where appropriate the media was supplemented with ampicillin (50μg/ml) from sterile stock solutions after the media had been autoclaved.

L-Broth: 1% (w/v) bactotyptone, 0.5% yeast extract, 1% NaCl, pH 7.0

SOC: 2% bactotyptone, 0.5% yeast extract, 10mM NaCl, 2.5mM KCl, 10mM $MgCl_2$, 10mM $MgSO_4$, 0.4% glucose

L-agar plates: L-Broth with 1.5% (w/v) bactoagar

Minimal A media plates: 0.1% $(NH_4)_2SO_4$, 0.45% KH_2PO_4, 1.05% K_2HPO_4, 0.005%NaCitrate, 1mM $MgSO_4$, 0.2% glucose, 0.5μg/ml vitamin B1, 40μg/ml each amino acid (Ura, His, and Leu or Trp), 1.5% (w/v) bactoagar

2-2.11 Yeast media

All media were prepared with MQ water and sterilised by autoclaving, except heat labile reagents, which were filter sterilised. Media was supplemented with appropriate amino acids (1x) and carbon source (2% Glu, or 2% Gal + 2% Raff) from sterile stock solutions after the media had been autoclaved.

Minimal media: 0.17% yeast nitrogen base, 0.5% ammonium sulphate, 2% carbon source

YPD: 1% yeast extract, 2% bactopeptone, 0.05% K_2HPO_4, 0.05% KH_2PO_4, and 2% glucose

MM plates: Minimal media liquid broth with 2% bactoagar

X-gal plates: Minimal media liquid broth, 70mM potassium phosphate pH 7.0, 40μg X-gal (20mg/ml in DMF), 2% bactoagar

100x Amino acid stocks:

Ade 0.3%, His 0.4%, Leu 0.4%, Met 0.4%, Try 0.4%, Ura 0.1%.

2-2.12 *Drosophila* media

Fortified (F1) *Drosophila* medium — 1%(w/v) agar, 18.75% compressed yeast, 10% treacle, 10% polenta, 1.5% acid mix (47% propionic acid, 4.7% orthophosphoric acid), 2.5% tegosept (10% *para*-hydroxybenzoate in ethanol)

Grape juice agar plates — 3% agar, 25% grape juice, 0.3% sucrose, 0.03% tegosept mix

2-2.13 Plasmids

Cloning and expression vectors:

pBluescript KS+ (Statagene)

pEG202 — *ADH* promoter expresses LexA(1-202aa) DNA binding domain (Gyuris *et al.,* 1993)

pGilda — *GAL1* promoter expresses LexA(1-202aa) DNA binding domain (Origene Technologies)

pJG4-5 — *GAL1* promoter expresses activation domain (Gyuris *et al.*, 1993)

pAS1 — *ADH* promoter expresses Gal4(1-147aa) DNA binding domain (S. Elledge)

pACT — *ADH* promoter expresses activation domain (S. Elledge)

pGEX3X — generate GST fusion protein (Smith and Johnson, 1988)

Drosophila transformation vectors:

pCaSpeR-hs — hsp70 promoter (obtained from H. Richardson)

pUAST — UAS promoter (obtained from H. Richardson)

Drosophila melanogaster libraries:

Library	Stage	Vector	Complexity	Obtained from
RFLY1	0-12hr embryonic cDNA	pJG4-5	$4.2x10^6$	R. Finley
SE L3	3rd instar larval cDNA	pACT	$1x10^7$-$1x10^8$	S. Elledge

Constructs generated by others and used in this work:

pSH18-34 — Eight *LexA* operators direct transcription of *lacZ* (Gyuris *et al.*, 1993)

pSE1111 — Snf4 fused to the activation domain in pACT (obtained from S. Elledge)

pSE1112 — Snf1fused to the Gal4 DNA binding domain in pAS1 (obtained from S. Elledge)

pπ25.7wc — *P*-element helper plasmid, encoding Δ2-3 transposase (from H. Richardson)

E4-3 — *DmcycEI* cDNA clone in pT7T319U (Richardson *et al.*, 1993)

NB23 — *DmcycEII* cDNA clone in pNB40 (Richardson *et al.,* 1993)

pT3T718U-DmcycEII — (obtained fromH. Richardson)

pJGDAP — *dap cdi4* clone in pJG4-5 (obtained from R. Finley)

pRF+Rux — *rux* cDNA clone in pJG4-5 (obtained from R. Finley)

pRF4-5-DmEI — *DmcycEI* cDNA clone in pJG4-5 (obtained from R. Finley)

pRF4-5-DmEII — *DmcycEII* cDNA clone in pJG4-5 (obtained from R. Finley)

UAS-GFP — obtained from Barry Dickson

Ub-GAL4 — obtained from Thomas Kornberg

UAS-DmcycEI — *DmcycEI* cDNA under control of the UAS promoter (H. Richardson)

Constructs generated for this work:

- *pGildaDmEI* was generated by subcloning *DmcycEI* as *Eco*RI/*Xho*I from pRF4-5-DmEI into pGilda.
- *pGildaDmEII* was generated by subcloning *DmcycEII* as *Eco*RI/*Xho*I from pRF4-5-DmEII into pGilda.
- *pEG-46N* was generated using 5' N term *Bam*HI primer and 3' 46N *Bam*HI primers with E41 as the template and inserted into pEG202.
- *pEG-195N* was generated using 5' N term *Bam*HI and 3' 195N *Bam*HI primers with E41 as the template and inserted into pEG202.
- *pEG-Cterm* was generated using 5' C term *Bam*HI and 3' C term *Bam*HI primers with E41 as the template and inserted into pEG202.
- *pAS-46N* was generated using 5' N term *Bam*HI and 3' 46N *Bam*HI primers with E41 as the template and insertied into pAS1.
- *hsp70-12ΔN-DmcycE* was generated using 5' 12del N *Bam*HI primer and the 3' C term *Bam*HI primer with E41 as a template and inserted into pCaSpeR-hs.
- *pGEX3X-119N DmcycEII* was generated using 5' ty II *Bam*H1 and 3' ty II *Bam*H1 primers with pT3T718U-DmcycEII as the template and inserted into pGEX-3X.
- *pBS-mt* was generated by subcloning 6 myc epitope tag as a *Cla*I -*Eco*RI fragment from pCS2 (obtained from S. Prokopenko).
- *pBS-mt-dcmaguk* was generated using 5' maguk *Spe*I and 3' pACT-R primers with pACT-DC14 (SEL3 library clone) as the template. The PCR product was digested with *Spe*I and inserted into pBS-mt.
- *UAS-mt-dcmaguk* was generated by subcloning *mt-dcmaguk* from *pBS-mt-dcmaguk* as *Xho*I-*Xba*I fragment into pUAST.

2-2.14 Oligonucleotides

DmcycE oligonucleotides:

5' N term *Bam*HI	5'-CGG GAT CCT TAT GAA GTT GGA AC	Geneworks
3' 195N *Bam*HI	5'-CGG GAT CCG TTA ATC ATC AGG TCA C	Geneworks
3' 46N *Bam*HI	5'-CGG GAT CCG AGG AGG CAA CCG ATG ACA GAT TG	Geneworks
5' C term *Bam*HI	5'-CGG GAT CCT TAT GGC TCA GGA TG	Geneworks
3' C term *Bam*HI	5'-CGG GAT CCT CAG GGA TTG CTT CTA C	Geneworks
5' ty II *Bam*HI	5'-CGG GAT CCT TAT GGG TTT AAA TGC CAA GAG	H. Richardson
3' ty II *Bam*HI	5'-CGG GAT CCC GTT TGA ATC GCT GCT TAA ACG	H. Richardson
5' 12ΔN *Bam*HI	5'-CGG GAT CCA AAA TGG ACC CTG AAC TCG G	Pacific oligos

dcmaguk oligonucleotide:

5' maguk *SpeI*	5'-GGA CTA GTC CAT GAT GAG ATA GGA GC	Geneworks
3' pACT-R	5'-TGC GGG GTT TTT CAG TAT CTA	K. Mills

Sequencing oligonucleotides:

5' pEG202	5'-CGT CAG CAG AGC TTC ACC ATT	S. O'Connell
5' pJG4-5	5'-CTG AGT GGA GAT GCC TCC	S. O'Connell
5' pACT-F	5'-CTA TTC GAT GAT GAA GAT ACC	K. Mills
3' pACT-R	5'-TGC GGG GTT TTT CAG TAT CTA	K. Mills

2-3 Methods

Standard molecular genetic techniques were performed as described in Sambrook *et al.* (1989) or Ausubel *et al.* (1994).

2-3.1 Generation of recombinant plasmids

Dephosphorylation of vector DNA:

After the vector DNA was linearized by restriction enzyme digestion, 1-2 U of CIP was added to the reaction and incubated at 37°C for at least 1 hour.

Purification of DNA from agarose gels:

QAIquick gel extraction kit was used to purify DNA bands from agarose gels, applying the protocol provided.

Ligation:

DNA fragments to be ligated were placed in a mix (total volume 20μl) containing 1U of T4 DNA ligase, and 1x ligation buffer and incubated at 18°C overnight. For transformation by electroporation, the ligation was phenol/chloroform extracted, precipitated by adding 1 μl glycogen, 1/10 volume 3 M NaAcetate pH 5.2 and 2.5 volumes ethanol, then washed in 70% ethanol prior to resuspension in 10μl MQ water.

2-3.2 Transformation of Bacteria

500ml of L-broth was innoculated with 5ml of an overnight culture of *E. coli* (*DH5α* or KC8) cells and grown to an OD_{A600} of 0.5-1.0. The culture was then chilled in an ice slurry for 15 to 30 minutes and the cells harvested by centrifugation at 4000g for 15 minutes. The cells were then resuspended in 500ml of ice-cold MQH_2O, pelleted at 5000g, resuspended in 250ml of ice-cold MQH_2O, pelleted at 4000g, resuspended in 10ml of ice-cold 10% glycerol, repelleted at 3000g and finally resuspended in 1ml of ice-cold 10% glycerol. The competent cells were then snap frozen in liquid nitrogen and stored as 45µl aliquots at -80°C.

For transformation, cells were thawed at RT, added to ligation reaction mixture and incubated on ice for at least 30 seconds. Cells were then transferred to an ice-cold 2mm electroporation cuvette and electroporated in a Bio-Rad Gene Pulser set to 2500V, 25 µFD capacitance and Capacitance Extender set to 500 µFD. The cuvette was immediately washed out with 1ml of SOC, and the suspension incubated at 37°C for 30 minutes. Cells were then pelleted for 8 seconds at 14 000rpm, then 800µl of the supernatant was removed, and the cells gently resuspended in the remaining SOC. The cell suspension was plated onto L-agar plates supplemented with 50µg/ml ampicillin and incubated at 37°C overnight. If selection for β-galactosidase activity (blue/white colour selection) was required, 10µl of 10% IPTG and 10µl of 20% BCIG were added prior to plating.

2-3.3 Isolation of plasmid DNA

Small scale preparation- Rapid boiling lysis method:

A 2ml culture supplemented with the appropriate antibiotics, was incubated overnight at 37°C, with shaking. Cells were harvested by centrifugation at 14 000 rpm in a microcentifuge for 15 seconds. The bacterial pellet was resuspended in 200µl of STET, followed by addition of 10µl of lysozyme (10mg/ml). The suspension was heated at 100°C for 45 seconds and centrifuged at 14 000 rpm for 15 min. The pellet was removed with a toothpick. Plasmid DNA was then precipitated with 240µl of isopropanol, centrifuged, and washed with 70% ethanol. The pellet was then dried and resuspended in 20µl MQ H_2O.

Large scale preparation:

Alkaline lysis midi-preps were prepared from 25-50 ml cultures following standard protocols (Sambrook *et al.*, 1989).

High quality plasmid DNA for microinjection of *Drosophila* embryos was prepared using Qiagen midi columns, according to manufacturer's instructions.

Mini columns from Bresatec were used to prepare DNA, following manufacturer's instructions, for dye terminator sequencing reactions and yeast transformation.

2-3.4 PCR amplification of DNA

Pfu polymerase was used in all of the reactions according to the manufacturers instructions. PCR conditions were using 0.5 U *Pfu* polymerase, 1 ng template DNA, 0.1 ng primers and 0.2 mM dNTPs in *Pfu* PCR buffer (20mM Tris-HCl, 10mM KCl, 10mM $(NH_4)_2SO_4$, 20mM $MgSO_4$, 0.1% Triton X-100, 0.1 mg/ml BSA, pH 8.75). Reactions were performed on a Corbett Research FTS-1S Capillary Thermal Sequencer, with the following conditions: 35 cycles of 95°C for 30 sec, 55°C for 1 min and 72°C for 1 min 30.

2-3.5 Automated sequencing

DNA was sequenced using the ABI Prism™ Dye Terminator Cycle Sequencing Ready Reaction Kit (Perkin-Elmer), essentially as described in the manufacturer's protocol with the modification of using half the described amount of reaction mix. Double-stranded DNA was used as a template and, in general, primers were de-salted. Reactions were performed on a Corbett Research FTS-1S Capillary Thermal Sequencer, with the following conditions: 25 cycles of 96°C for 10 seconds, 50°C for 5 seconds and 60°C for 4 minutes with a temperature ramp setting of 2. Running and analysis of Dye Terminator gels was conducted by the Sequencing Centre at IMVS Molecular Pathology, Adelaide, SA.

2-3.6 Protein gel electrophoresis

A Bio-Rad mini-Protean II gel electrophoresis system was used with 0.8mm analytical gels prepared according to manufacturer's instructions. Protein samples were electrophoresed at 180-200V for 45 min.

2-3.7 Protein purification for antibody production

A 1/50 ditution of an overnight culture of DH5α transfromed with pGEX3X-119 *DmcycEII* was used to inoculate 50 ml of L broth. The culture was then grown to OD=0.8 then GST-119 DmcycEII fusion protein induced by addition of 0.1mM IPTG. Total protein extracts from induced bacteria culture were separated on 1.5mm 12% SDS-PAGE. The gel was stained in Coomassie Blue (1%) in water to visualise the protein bands, and the induced fusion protein, GST-119 DmcycEII was sliced out. The gel containing the protein was homogenised by sequentially passing through different gauge needles, 19G, 21G, 23G and 26G and injected into rats, by A. Bartlet, Laboratory Animal Services, University of Adelaide. After the initial inoculation the rats were given three boosts of gel purified fusion protein, three weeks apart. Seven days after the final boost the total sera was harvested.

2-3.8 Western blotting

Western blotting of proteins onto nitrocellulose membrane was performed using a Bio-Rad Transblot SD Semi-dry transfer cell according to manufacturer's guidelines. In general, a current of 3 mA per cm^2 of gel was applied for 30 min. After transfer, the filter was soaked in 2% Ponceau's stain (Sigma) for 20 min to visualise the amount of protein. Nitrocellulose blots were washed thoroughly with PBT and then blocked for 1 hour in 5% Blotto. Primary antibody incubations were carried out overnight at 4°C and secondary antibody incubations for 2hr at RT, with the appropriate dilutions of antibody in Blotto. The secondary antibodies were HRP conjugated and detected by ECL.

2-3.9 Transfection of S2 cells

The S2 cell line (Schneider, 1972) was grown in S2 media (Gibco BRL) supplemented with 10% v/v foetal calf serum (FCS; Gibco BRL) and 100U/ml penicillin. S2 cells were grown until log phase and approximately 1 x 10^6/ml were transfected with a 19:1 ratio calcium phosphate DNA precipitate of *UAS-mt-dcmaguk*: *Ub-GAL4* plasmid respectively, in 1ml per 5ml of culture, as described by (Fehon *et. al.*, 1990). Typically, transfection efficiencies of 5% were obtained. Following transfection cells were allowed to recover for 16hrs in S2 media + 10% v/v FCS.

2-3.10 Co-immunoprecipitation

Preparation of S2 cell lysate:

Transfer cells to 1.5ml microcentrifuge tube and pellet cells at 2 500rpm for 2-3 min then remove the supernatant. Resuspend the cell pellet in 50µl of cell lysis buffer (50mM Tris, pH7.8, 150mM NaCl, 1% NP-40 and protease inhibitor cocktail tablet) and vortex. The cell suspension was incubated at 37°C for 10 min then vortexed and the cell debri was pelleted by centrifugation at 14 000rpm for 10 min at 4°C. The cell lysate (supernatant) was then transferred to a new tube and stored at -80°C.

Immunoprecipitation:

200µl of cell lysate was thawed on ice, an appropriate dilution of primary antibody added and incubated with gentle rocking overnight at 4°C. The Protein A agarose beads were prepared to a slurry of 50% in cell lysis buffer, with 20µl added to the cell lysate/antibody mix and incubated with gentle rocking for 3hr at 4°C. The mix was then centrifuged for 30 sec at 4°C and the pellet was washed 5x with 500µl of cell lysis buffer, keeping the samples on ice during the washes. The pellet was resuspended in 20µl of 3x Protein Sample Buffer. Prior to analysis by western blotting the sample was vortexed for 30 sec, heated at 100°C for 2 min then loaded on a SDS-PAGE gel.

2-3.11 Transformation of yeast

Small scale: 5 ml of media was inoculated to an OD_{A600} of 0.2, from an overnight culture, and allowed to grow for 3 hours if in YPD and for 5 hours if in dropout media at 30°C with shaking. The yeast were then pelleted for 5 min at 2 800rpm in a bench top centrifuge and the pellet was resuspended in 1ml of 0.9M LiOAc/TE and transferred to a microfuge tube. The yeast were then spun at 8 000rpm for 30 seconds and the supernatant was removed and the yeast were resuspended in 100µl of 0.9M LiOAc/TE for every 0.2 OD units/5ml. For each transformation 8µl of DNA from a rapid boiling prep (or 1µl of DNA from a Bresaspin prep with 1µl carrier DNA (10mg/ml salmon sperm) in a total volume of 8µl), was added to a microfuge tube along with 12µl of competent yeast and 45µl of sterile 50% PEG 3350. The tubes were then placed in a 30°C shaking incubator for 1 hour and heat shocked for 5 minutes in a water bath at 42°C. The yeast were then plated out onto selective media and placed at 30°C for 3-4 days to allow growth of transformants.

Large scale high efficiency transformation:

High efficiency yeast transformation was achieved using the TRAFO method (Gietz and Schiestl, 1996).

2-3.12 Interaction mating

Preparation of "bait" and "prey" strains:

The "bait" strain is prepared by transformation of the "bait" into the MAT***a*** yeast strain. The library "prey" strain is prepared by high efficiency transformation of the library into MATα yeast strain. The primary "prey" transformants are collected by scraping plates, washing yeast, resuspending in 1 pellet vol glycerol solution (65% glycerol, 0.1M $MgSO_4$, 25mM Tris, pH8) and then stored as 0.5ml aliquots at -80°C.

Mating the "bait" and "prey" strains:

30ml of dropout medium was inoculated to an OD_{A600} of 0.2, from an overnight "bait" culture, and allowed to grow to mid-late log at 30°C with shaking. The yeast were then pelleted for 5 min at 2 800rpm in a bench top centrifuge and the pellet was resuspended in 1ml. The mating is set up by mixing 200µl of this "bait" strain with 200µl of a thawed aliquot of the "prey" strain. In parallel a control mating is set up with the "bait" strain and the empty library vector. The cell mix is centrifuged at 2 500rpm for 5 min, the yeast pellet then resuspended in 200µl of YPD medium and the cell suspension is plated on a 9cm plate which is incubated overnight at 30°C. The diploid yeast are collected by scraping the plate, washing yeast, and resuspending in 5ml MQ water. The diploid yeast are then plated on selection plates to identify interactors and incubated at 30°C for 3-5 days.

2-3.13 Yeast plasmid DNA extraction protocol

A large toothpick-scrape of yeast was resuspended in 200µl of Back Extraction buffer (0.1M Tris pH 9.0, 0.1M NaCl, 0.5% SDS, 1mM EDTA) and 425-625µm sterile glass beads added to just below the surface level. 200µl of phenol/chloroform was added and the mix vortexed vigorously for 3 min followed by centrifugation at 14 000rpm for 5 min. The aqueous layer was transfered to a new microfuge tube and phenol/chloroform 3 times before ethanol precipitation in 1/10 volume 3 M NaAcetate pH 5.2 and 2 volumes 95% ethanol. The pellet was then washed in 80% ethanol, air dryed and resuspended in 20µl MQ water, with 10µl of the plasmid prep used to transform into bacteria.

2-3.14 Yeast protein extraction protocol

A 50 ml culture of yeast was set up in the appropriate selective media and allowed to grow overnight at 30°C with shaking to an OD_{A600} of approximately 0.8. The yeast were then pelleted in a sterile falcon tube at 2 800 rpm for 5 minutes and the supernatant was removed. The yeast were then resuspended in between 200-400µl of ice cold lysis RIPA buffer (50mM Tris-HCl pH 7.4, 150mM NaCl, 5mM EDTA, 0.1% NP-40, 50mM DTT and 5mM PMSF) depending on the amount of yeast. The yeast were then transferred to a cold screw cap microfuge tube and half the volume of 425-625µm glass beads were added. The tubes were then placed into a "bead beater" and beat 3x 20sec, with a 20 sec incubation on ice in between. The tubes were then spun at 14 000 rpm for 15 minutes at 4°C. The supernatant was then transferred to a clean cold tube and stored at -20°C.

2-3.15 Yeast interaction screening procedure

Three individual transformants were streaked onto selective plates and grown at 30°C for 2-3 days. Using a toothpick, yeast cells were then scraped from the plate and resuspended in 100µl minimal media and a 1:10 dilution made (in liquid media). 10µl of each was aliquoted onto interaction screening selective plates and grown at 30°C for 3 days.

2-3.16 Assay for β-galactosidase in liquid cultures

Yeast were diluted from an overnight culture, into selective media to an OD_{A600} of 0.5, and allowed to grow for 5 hours at 30°C with shaking. The cells were pelleted and resuspended in 4ml Z buffer. The OD_{A600} was determined and reactions set up with 0.5 ml sample and 0.5 ml Z buffer. Cells were lysed by adding SDS and chloroform and LacZ activity was assayed after addition of 0.2 ml of 4mg/ml ONPG, at 30°C. The reaction was terminated by addition of 0.4 ml of 1M Sodium Carbonate, cell debris was pelleted and OD_{A420} was measured.

Miller LacZ units $=1000x\ OD_{420}/[time(min) \times vol(ml) \times OD_{600}]$.

2-3.17 Heat shock induction of *DmcycE* contructs

Heat-shock induction of *DmcycE* in wandering third instar larvae was carried out by collecting larvae in a microfuge tube and incubating at 37°C for 1hr. The larvae were left to recover for a specified time, after which they were then dissected in PBT. The eye-antennal discs, brain lobes and salivary glands were stained using α-cycE antibodies, or protein extracts were analysed by western blot. For analysing the effect of ectopic expression of *DmcycE* constructs on eye development, the heat-shocked larvae were returned to 18°C and left to develop into adults.

2-3.18 *Drosophila* protein extracts

For western analysis of DmcycE protein, *Drosophila* larval protein extracts were prepared by homogenisation of three larvae, or tissue of interest was dissected in PBT from 20 larvae, and transferred directly to 50 µl of protein sample buffer and stored at -20°C. The proteins samples were placed at 100°C for 5 minutes, then vortexed thoroughly and centrifuged before being loaded onto a SDS-polyacrylamide gel and Western blots carried out.

2-3.19 Collection and fixation of *Drosophila* embryos

Embryos were collected on grape juice agar plates smeared with yeast. They were then harvested and washed thoroughly in a basket using 0.7%NaCl, 0.15%Triton X-100. The basket was then transferred into a container with 50% commercially available bleach (2% sodium hypochlorite) for 3 minutes to de-chorionate the embryos. The embryos were once again washed thoroughly in the basket using 0.7%NaCl, 0.15%Triton X-100. They were then transferred to a glass scintillation vial containing a two-phase mix of 4 ml of 4% formaldehyde in 1 x HEN and 4 ml of heptane. The vial was then shaken on an orbiting platform such that the interface between the liquid phases was disrupted and the embryos were bathing in an emulsion, for 20 minutes to 'fix' the embryos. The bottom phase (aqueous) was drawn off and replaced with 4 ml of methanol and the vial was shaken vigorously for 30 seconds to de-vitellinise the embryos. De-vitellinised embryos sink from the interface and were collected from the bottom phase (methanol). Embryos were rinsed thoroughly in methanol at which point they were stored at -20°C in methanol.

2-3.20 *In situ* hybridisation of *Drosophila* embryos

Generation of DIG labelled RNA probes:

Antisense RNA probes were generated from plasmids containing the gene of interest, linearised using an enzyme that cuts at the 5' end of the clone. RNA was transcribed *in vitro*, incorporating DIG-11-UTP using T7 or T3 RNA polymerase using the promoter at the 3' end of the clone. The labelling reaction was done using a Boehringer Mannheim DIG RNA labelling kit according to the suppliers instructions.

Hybridisation and colour detection:

Fixed embryos were rehydrated in PBT for at least 30 minutes. Embryos were then rinsed in a 50:50 mix of PBT and hybridisation mix (50% formamide, 5 x SSC, 50mg/ml heparin, 0.1% Tween-20, 100mg/ml sonicated boiled salmon sperm DNA), then rinsed once in hybridisation mix and then put at 55°C for at least 2 hours. The RNA DIG probe then added to the embryos (50µl total volume) and incubated at 55°C overnight. The next day, embryos were washed once with pre-hybe mix (55°C), once with a 50:50 mix of PBT and pre-hybe (55°C), and 5 times (20 minutes each) in PBT (55°C). The embryos were then incubated with 1/2000 dilution anti-DIG-AP for 1 hour at room temperature, followed by four 20 minute washes in PBT. Embryos were then rinsed in AP buffer, then the AP detected by incubating embryos in a solution of (per 1ml) 3.5µl BCIP (50mg/ml in DMF) and 4.8µl NBT solution (100mg/ml in 70% DMF) in darkness. Embryos were then rinsed several times in PBT and mounted in 80%.

2-3.21 Whole mount immunolocalisation of *Drosophila* embryos

The methanol was removed from fixed embryos in a microfuge tube and replaced with 50% Methanol/1 x PBT. Several rinses were then done using 1 x PBT followed by a single wash for 30 minutes. The embryos were then 'blocked' in 200µl of 1 x PBT containing 0.1% BSA and 5% normal goat serum (NGS) for at least 1 hour. The blocking solution was removed and primary antibody diluted in fresh blocking solution was added (usually 50-200µl). The embryos were routinely incubated with gentle rocking at 4°C overnight. The next day, the antibody solution was removed and the embryos were washed extensively in 1 x PBT (several changes of buffer over a 2 hour time period). The embryos were then incubated with secondary antibody diluted in fresh blocking solution for at least 2 hours at room temperature with gentle rocking. Following a period of washing, as for the primary antibody, the embryos were incubated with a tertiary complex for two hours and then washed extensively for two hours in 1 x PBT. Embryos were then stained for 2 mins with Hoechst and washed in 1 x PBT on the nutator overnight. The embryos were mounted in PBS/80% glycerol onto a slide under a coverslip supported by two pieces of double sided tape and coverslips were sealed to the glass using commercially available clear nail varnish.

2-3.22 Immunolocalisation of *Drosophila* larval tissues

Discs were dissected in 1 x PBS and fixed in a mixture of 3 parts 1.5 x Brower fix (1.5 Brower fix: 0.15M PIPES, 3mM $MgSO_4$, 1.5mM EGTA, 1.5% NP-40 pH6.9), 0.5 part 16% Formaldehyde and 0.5 parts water for 30 minutes on ice. Discs were washed in PBT-BSA (1 x PBS, 0.3% triton-X100, 1mg/ml BSA) and blocked with a solution of 1 x PBS, 0.3% triton-X100, 5mg/ml BSA for at least 1 hour on ice. The primary antibody was added directly to the blocking solution and incubated at 4°C overnight. The next day, discs were washed extensively

in PBT-BSA before adding the secondary antibody conjugated to biotin diluted in PBT-BSA. After several washes at 4°C, the tertiary antibody was added and incubated with the discs at 4°C for at least 2 hours. After further washes, the discs were stored in a solution of 30% glycerol, 50mM Tris pH8.8, 150mM NaCl, 0.02% sodium azide until ready to be mounted. To prevent photobleaching, discs were mounted in a solution of 30% glycerol, 50mM Tris pH8.8, 150mM NaCl, 0.02% sodium azide, 0.5mg/ml p-Phenylenediamine p1519 and photographed.

2-3.23 Immunolocalisation of *Drosphila* ovaries

Ovaries were dissected in Ringers and fixed in devitellinizing buffer for 10 minutes rocking at room temperature. The ovaries were then washed 3 times in PST for 10 minutes each. Background peroxidase activity was removed by treatment in 0.3% H_2O_2 in methanol for 30 minutes then gradually rehydrated by washing sequentially in 70% methanol in PBS, 50% methanol in PBS, 30% methanol in PBS and twice in PBT. The ovaries were incubated in 5% goat serum in PBT (PBTG) for 30 minutes before the addition of diluted primary antibody incubated at 4°C overnight. The antibody was removed prior to washes in PBT, these were 3 washes for 5 minutes and 3 washes for 30 minutes. The ovaries were then incubated in PBTG for 30 minutes and the diluted secondary antibody was added, and incubated for 2 hours at room temperature. The antibody was removed prior to washes in PBT, these were 3 washes for 5 minutes and 3 washes for 30 minutes. The peroxidase reaction requires adding 1/10 DAB(5mg/ml) in 200µl of PBT, intensified by addition of 8% NiCl, to ovaries and catalysing the reaction by the addition of 3µl of 3% H_2O_2. The colour reaction was allowed to develop in the dark (5-20 minutes), and then stopped by rinsing several times in PBT plus NaOAc. The ovaries were then dissected into individual ovarioles and mounted onto a microscope slide in 80% glycerol in PBT.

2-3.24 BrdU incorporation into *Drosophila* eye discs

For BrdU-labelling of eye-antennal discs, larvae were dissected in PBT and incubated with 60µg/ml BrdU in Schneider's tissue culture media for 1hr at 25°C. Tissues were fixed in 60% ethanol, 30% chloroform, 10% acetic acid for 30 minutes and rehydrated in PBT. Samples were hydrolysed in 2N HCl for 30 min at RT and washed extensively with PBT. BrdU labelled cells were detected after blocking with 2% goat serum in PBT for 1hour, with a monoclonal primary antibody at 4°C overnight, followed by an α-mouse biotinylated secondary antibody for 2 hours at RT. BrdU incorporation was then detected using HRP detection system (Vectastain ABC kit) and colour detection using 0.08% $NiCl_2$, DAB (0.5 µg/ml) and H_2O_2 (0.045 µg/ml).

2-3.25 Scanning electron microscopy

Drosophila eyes were prepared for scanning electron microscopy by dehydration in serial acetone dilutions (25%, 50%, 75% and 100% acetone). Flies were then air dryed, mounted onto EM studs and viewed with out coating at 1mV accelerating voltage by field emission scanning electron microscopy (Phillips, at CEMMSA, Adelaide University). Digital images were collected and analysed in Adobe Photoshop 6.0.

2-3.26 *Drosophila* cultures

Flies were raised at 18°C or 25°C, with 70% humidity, on F1 medium.

2-3.27 *P*-element mediated transformation of *Drosophila*

Micro-injection:

DNA for injection was prepared using the Qiagen kit according to the suppliers protocol. An injection mix was prepared to a concentration of 0.5-1μg/μl transformation vector plasmid DNA and 0.3μg/μl of pπ25.7wc (Δ2-3 transposase) plasmid in 1x Embryo injecting buffer. The injection needle was back filled using a drawn out capillary containing 2μl of the injection mix which had been centrifuged briefly to remove any particulate matter. w^{1118} embryos to be injected were collected from 30 min lays on grape juice agar plates at 25°C, dechorionated in 50% bleach for 3 min, and rinsed thoroughly in MQH_20. Embryos were then aligned along a strip of non-toxic rubber glue such that their posterior ends would then face the needle. A drop of liquid parafin was placed over the embyros and the slide placed on the stage of an inverted microscope. A micromanipulator was used to position the needle and injection was carried out by moving the microscope stage to bring the embryos to the needle, such that a very small amount of DNA was injected into the posterior cytoplasm.

Identification of transformants:

The slides of microinjected embryos were then placed in a petri dish containing moist tissue paper with a small amount of yeast paste surrounding the embryos and kept at 18°C to allow the embryos to hatch. Larvae were collected after 2 days using strips of Whatman paper and placed in a fly food vial where they developed into adult flies. The flies were then crossed to w^{1118} flies to identify transformants on the basis of the *mini-white*$^+$ eye pigmentation phenotype. Numerous independent transformants were mapped to determine the chromosome of insertion, using the dominantly-marked balancer chromosomes CyO and TM6B in the stocks *w ; Sco / CyO* and *w ; Df(3R)ro*^{XB3} */ TM6B Hu,* and homozygous lines generated using these balancers.

2-3.28 Microscopy and photography

Photography was done with either Kodak Ektachrome 160T film or images were collected digitally with Photograb after viewing on a Zeiss Axiophot light microscope using 10X eyepiece lenses and Plan-Neofluar 20X/0.5 or 40X/0.75 objectives with DIC optics. Slides were scanned in with a Kodak RFS 2035 film scanner at >500dpi. Fluorescence microscopy was performed on an Olympus AX70 and digital images were collected with a cooled CCD camera. For Confocal analysis, a Biorad MRC1000 Confocal microscope was used. Adobe photoshop 6.0 was used for image preparation.

2-3.29 Regulatory considerations

All manipulations involving recombinant DNA were carried out in accordance with the regulations and approval of the Genetic Manipulation Advisory Committee and the University Council of Adelaide University. All manipulations involving animals were carried out in accordance with the regulations and approval of the Animal Ethics Committee and the University Council of Adelaide University.

2-4 Glossary

Markers:

Black cells (Bc) — A dominant mutation on the 2nd chromosome that results in third instar larvae having black spots throughout their body. Homozygous lethal.

Curly (Cy) — Dominant wing marker on the 2nd chromosome that results in flies with curled wings. Homozygous lethal.

Scutoid (Sco) — A dominant mutation on the 2nd chromosome that results in reduced number of scuttelar bristles. Homozygous lethal.

Tubby (Tb) — Dominant larval phenotype that results in third instar larvae being shorter and fatter than wild-type. Homozygous lethal.

white (w)— A recessive eye colour marker on the X chromosome, homozygous *w* flies have white eyes.

wild type (+) — The normal appearance of a fly, as seen in the absence of any genetic markers. w^{1118} is used as "wild type" in this work.

Balancer chromosomes:

*Cy*O — Second chromosome balancer. Carries the dominant marker *Curly*. Homozygous lethal.

Cy-Tb — Second chromosome balancer that has part of *TM6B* translocated onto the second. Has both *Curly* and *Tubby* dominant markers. Homozygous lethal.

TM6B — Third chromosome balancer. Carries the dominant marker *Tubby*. Homozygous lethal.

3-1 Introduction

During *Drosophila* embryogenesis, *DmcycEII* transcript is present throughout the embryo during the first 13 rapid and synchronous syncytial divisions. Following cellularisation, however it is only detected in the pole cells (Richardson *et al.,* 1993) (Chapter 1). This expression corresponds to maternally-supplied mRNA, as these transcripts are still present in embryos homozygous for a *DmcycE* deficiency. Unlike *DmcycEII* expression, zygotic transcription of *DmcycEI* is first detected in cycle 10, with high levels present following cellularisation. Subsequently, *DmcycEI* is expressed in all mitotically-proliferating and endocycling embryonic cells and then down-regulated when cells exit into G1 phase (Richardson *et al.,* 1993). The pattern of DmcycE protein distribution, as detected by an antibody raised to the common region of DmcycEI and DmcycEII, mostly correlates with the pattern of *DmcycE* mRNA during embryogenesis.

With respect to later developmental stages, *DmcycE* expression has been characterised during eye imaginal disc development (using a probe common to *DmcycEI* and *DmcycEII*) (Richardson *et al.,* 1995). As expected, *DmcycE* expression correlates with proliferating cells, and is detected in the anterior cells of the eye disc which are undergoing asynchronous cell cycles and in a band of cells immediately posterior to the MF that are undergoing a synchronous S phase.

An important developmental question is whether or not the two isoforms of DmcycE have different properties. One approach used to investigate this was to analyse the distribution of DmcycEI and II proteins during development. This required a way of distinguishing between the localisation of DmcycEII and DmcycEI. This chapter describes the generation of an antibody to the unique N-terminal region of DmcycEII and determining the localisation of DmcycEII during development.

3-2 Distribution and localisation of DmcycEII protein

3-2.1 Generation of a DmcycEII-specific antibody

Detection of the DmcycEII protein required the generation of a type II-specific antibody. A protein expression construct was generated containing the unique N-terminal 119 amino acids of DmcycEII fused to the *Schistosoma japonicum* glutathione S-transferase protein (GST). This was achieved by PCR amplification using TyII5' and TyII3' primers and *pT3T718U-DmcycEII*, generating a 0.36 kb *DmcycEII* fragment encoding to amino acids 1-119. This fragment was cloned into the protein expression vector *pGEX-3X*, generating a GST-119N DmcycEII fusion

protein. Expression of the GST-119N DmcycEII fusion protein was induced in bacterial cells and the harvested proteins analysed by SDS-PAGE. A band of approximately 40.5 kDa was detected, the size of the predicted weight of GST (27.5 kDa) plus the 119 amino acids of type II (~13.1 kDa), which was absent in non-induced cells (Figure 3.1 A). The SDS-PAGE purified GST-119N DmcycEII fusion protein was then used to inoculate rats. Following the initial inoculation, three boosts were given three weeks apart using SDS-PAGE purified fusion protein, and following the final boost the serum was harvested.

To examine the specificity of the antiserum, western analysis was performed on third larval instar total protein extracts from transgenic lines containing heat shock-inducible *DmcycE*. Western analysis showed that the anti-DmcycEII antiserum detected protein bands at ~97 kDa after heat shock induction of the *DmcycEII* transgene, but not in extracts from larvae after expression of a heat shock-inducible *DmcycEI* transgene (Figure 3.1 B upper panel). The protein samples were also analysed using the mouse anti-DmcycE monoclonal antisera, which detects both DmcycEI and DmcycEII (Figure 3.1 B lower panel). These results demonstrate that the DmcycEII antisera was specific for the DmcycEII protein.

3-2.2 Distribution of DmcycEII during embryonic development

To investigate the tissue distribution of DmcycEII protein during development, immunolocalisation using anti-DmcycEII was carried out on embryos. In early syncytial embryos, DmcycEII protein was detected at high levels in interphase nuclei but upon entry into mitosis became distributed throughout the cytoplasm (Figure 3.2 A). In cellularised cycle 14 embryos, DmcycEII was also detected at high levels in the nuclei of interphase cells (Figure 3.2 B). However, at later developmental times, in embryos undergoing cycle 15 or 16, low levels of the DmcycEII protein were detected throughout most of the embryo, although higher levels were present in the amnioserosa (Figure 3.2 C and data not shown). At slightly later times when most epidermal cells have arrested in G1, no DmcycEII protein was detectable in the epidermis or in proliferating cells of the central and peripheral nervous system (Figure 3.2 D). The persistence of DmcycEII protein during cycles 15 and 16 is consistent with the observation that *DmcycE* zygotic null mutants complete cycles 15 and 16 and arrest in G1 of cycle 17 (Knoblich *et al.*, 1994). DmcycEII protein persisted in the pole cells until late in embryogenesis (Figure 3.2 E), consistent with the expression of the *DmcycEII* transcript in these cells (as discussed in Section 3-1).

3-2.3 Distribution of DmcycEII in the eye-antennal and wing imaginal discs

The localisation of DmcycEII during embryogenesis was mostly coincident with the analysis of the mRNA expression and from what was predicted by the phenotype of *DmcycE* mutant embryos. However, it was unknown whether DmcycEII is expressed at later

developmental stages. The localisation of DmcycE has previously been examined during third instar larval eye imaginal disc development using an antibody that detects both DmcycE proteins (anti-DmcycE) and therefore it was unclear whether this represents DmcycEI or II. Furthermore, *DmcycEII* transcripts have been detected by RT-PCR from third larval instar wing imaginal discs (Prober and Edgar, 2000). Therefore, to specifically determine if DmcycEII was present, the type II specific antibody was used to analyse eye-antennal and wing imaginal disc tissue.

To determine if DmcycEII protein was present in the wing disc and also in the eye-antennal imaginal disc, western analysis was performed on dissected disc extracts using anti-DmcycEII. As a control, extracts from heat shock-induced *hsp70-DmcycEI* or *hsp70-DmcycEII* third instar larval eye-antennal discs were immunoblotted with anti-DmcycEII. High intensity bands at ~97 kDa were detected with heat shock-induced DmcycEII. Low intensity bands at 97 kDa were also detected in wild type and heat shock-induced DmcycEI, showing that DmcycEII protein is present in both wing and eye-antennal discs (Figure 3.3 A).

To investigate the distribution of DmcycEII protein in the third instar larval eye-antennal imaginal disc, immunolocalisation was carried out using anti-DmcycEII. The DmcycEII protein was detected in cells in the anterior of the eye disc corresponding to those undergoing asynchronous cell cycles, but was absent from the band of cells undergoing synchronous S phases posterior to the MF (Figure 3.3 B). Weak staining was detected in the differentiating photoreceptor cells in the posterior region of the eye disc, which may represent background staining since it was not detected using the common DmcycE antibody (Richardson *et al.*, 1995), or this may represent an alternative form not recognised by the common antibody. To investigate the distribution of DmcycEII protein in the third instar larval wing imaginal disc, immunolocalisation was carried out using anti-DmcycEII. The DmcycEII protein was detected in cells surrounding the zone of non-proliferation, corresponding to asynchronous cell cycles, and not within the zone of non-proliferation where cells are arrested in either G1 or G2 (Johnston and Edgar, 1998) (Figure 3.3 C). However, the localisation of DmcycEII in these tissues is preliminary and requires further characterisation by co-labelling of DmcycEII distribution and S phases or with mitotic markers. The detection of DmcycEII during larval development suggests that DmcycEII may have a specific role at this stage.

3-2.4 Distribution of DmcycEII during oogenesis

During *Drosophila* oogenesis, formation of the egg occurs within a 16 cell germ-line cyst within the germarium (Figure 3.4 A). New cysts are formed by asymmetric divisions of the stem cell, following this the daughter cell then undergoes four successive mitotic divisions, without complete cytokinesis, resulting in 16 cells linked by ring canals, the cystoblast.

Figure 3.1 : Generation and characterisation of anti-DmcycEII antisera.

A. Induction of GST-119N DmcycEII fusion protein in bacterial cells. Total bacterially-expressed protein was separated by 10% SDS-PAGE and stained with Coomassie to visualise proteins. Lane 1, protein extract from un-induced *pGEX3X-DmcycEII*; Lane 2, protein extract from induced *pGEX3X-DmcycEII*, detecting a band of approximately 40.5 kDa (arrow), the size of the predicted weight of GST (27.5 kDa) plus the 119 amino acids of DmcycEII (13 kDa), which was absent in non-induced cells. The sizes of the molecular weight markers (in kDa) are indicated on the left.

B. Western analysis of DmcycE proteins using rat polyclonal antiserum raised to the unique N-terminal region of DmcycEII (anti-DmcycEII) and mouse monoclonal antibody raised to full-length DmcycEI (8B10). Lanes 1 and 4, protein extract from heat-shocked control larvae; Lanes 2 and 5, protein extract from heat-shocked *hsp70-DmcycEI* larvae; Lane 3 and 6, protein extract from heat-shocked *hsp70-DmcycEII* larvae, taken immediately after a 60 minute heat shock. Lanes 1, 2 and 3 were detected using the rat anti-DmcycEII polyclonal antiserum followed by HRP conjugated anti-rat secondary antibody and detected by enhanced chemiluminescence. A DmcycEII specific band is observed in lane 3 (arrow head, size 97kDa), and is absent from lanes 1 and 2. Lanes 4, 5 and 6 were detected using the mouse anti-DmcycE monoclonal antiserum, which detects both DmcycEI and DmcycEII, followed by HRP conjugated anti-mouse secondary antibody detected by enhanced chemiluminescence. The bands corresponding to DmcycEI protein (lane 5 arrow, size 75 kDa) are distinguishable from the higher molecular weight bands from the DmcycEII protein (lane 6 arrow head, size 97 kDa). Under these conditions, endogenous DmcycE protein is not detectable.

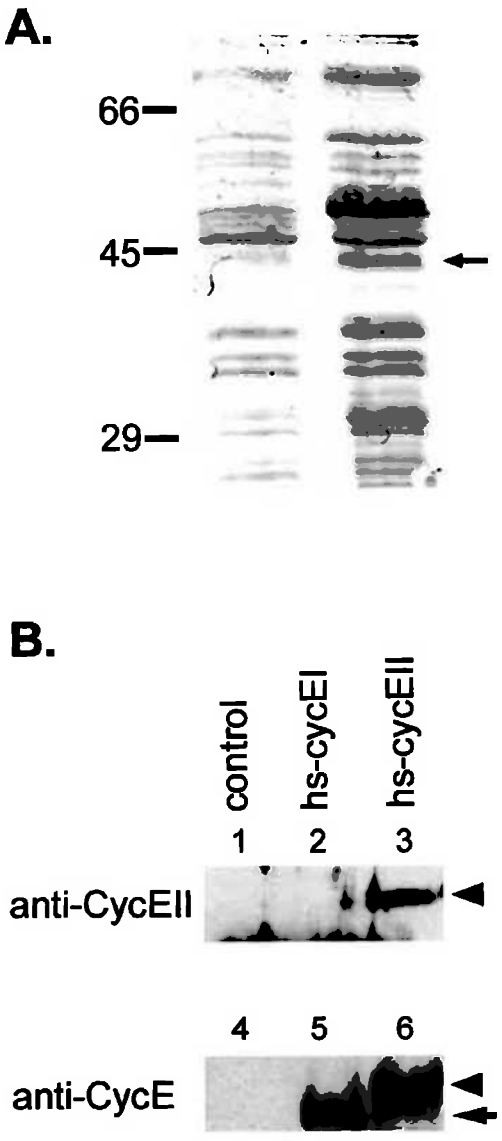
A.
66
45
29
B.
control
hs-cycEI
hs-cycEII
1
2
3
anti-CycEII
4
5
6
anti-CycE

Figure 3.2 : Distribution of DmcycEII during embryonic development.

Embryos were stained with anti-DmcycEII rat polyclonal antisera followed by HRP detection.

A. A syncytial embryo (~1 hour AED) showing nuclear localisation of DmcycEII.

B. Cellularised embryo in G2 phase of cycle 14 (~3.5 hour AED), showing nuclear localisation of DmcycEII.

C. An embryo undergoing cycle 15 (~5 hour AED) showing generally weak expression of DmcycEII, but higher levels in the amnioserosa (am).

D. A germ band retracted embryo (~10 hour AED) showing staining of the pole cells (pc).

E. An embryo undergoing head involution (~13 hour AED) showing staining of the pole cells.

Embryos are orientated anterior to the left.

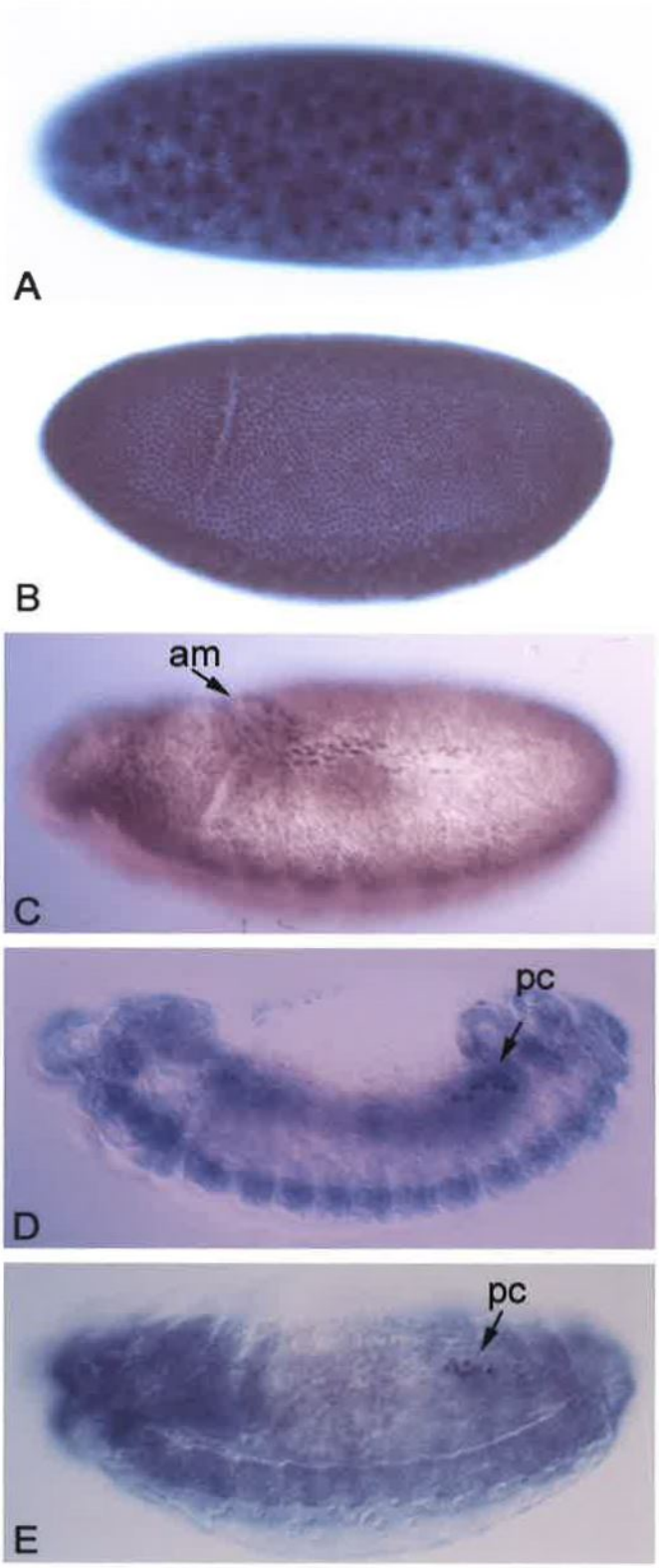
A
B
am
C
pc
D
pc
E

Figure 3.3 : Distribution of DmcycEII in the eye-antennal and wing imaginal discs.

A. Western analysis of DmcycEII protein from eye-antennal and wing imaginal discs. Lanes 1 and 2, protein extract from 20 heat shocked *hsp70-DmcycEI* and *hsp70-DmcycEII* third instar larvae eye-antennal imaginal discs taken immediately after a 60 minute heat shock. Lane 3 protein extract from 20 wild type eye-antennal imaginal discs and Lane 4 protein extract from 20 wild type wing imaginal discs. Samples were detected using the rat anti-DmcycEII polyclonal antisera followed by HRP conjugated anti-rat secondary antibody and detected by enhanced chemiluminescence. A DmcycEII specific band is observed in all lanes (arrow), with an increase in intensity in lane 2, corresponding to a greater abundance of DmcycEII protein from the heat shock-induced *hsp70-DmcycEII.*

B. Third instar larval eye discs were stained with anti-DmcycEII rat polyclonal antisera followed by HRP detection, showing localisation of DmcycEII in asynchronously-dividing cells in the anterior region of the eye disc, and not detected in the band of S phase cells posterior to the MF. Anterior is to the right and the bar spans the MF.

C. Third instar larval wing discs were stained with anti-DmcycEII rat polyclonal antisera followed by HRP detection, showing localisation of DmcycEII in asynchronously-dividing cells outside of the zone of non-proliferation (ZNP).

The ZNP is represented by a box.

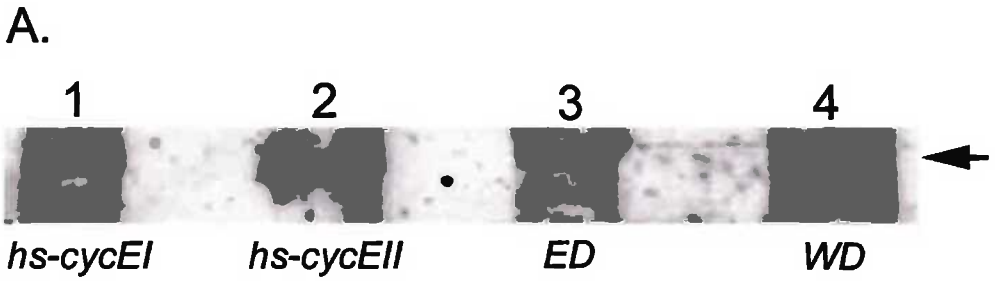
A.
1
2
3
4
hs-cycEI
hs-cycEII
ED
WD

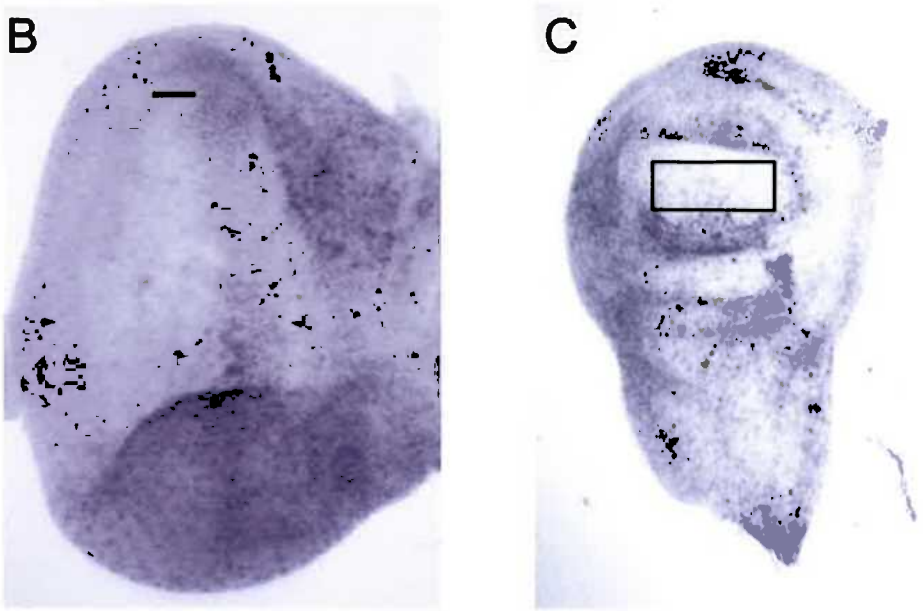
B
C

Figure 3.4 : Distribution of DmcycEII during oogenesis.

A. Schematic representation of the different stages of oogenesis, ON refers to oocyte nucleus (from de Nooij *et al.,* 2000).

B. Egg chambers were stained with anti-DmcycE 8B10 mouse monoclonal antisera followed by HRP detection. DmcycE protein levels vary between individual nurse cell nuclei, with some nuclei staining dark and others light or absent.

C. Egg chambers were stained with anti-DmcycEII rat polyclonal antisera followed by HRP detection. DmcycEII protein is detected during early oogenesis and in the oocyte nucleus.

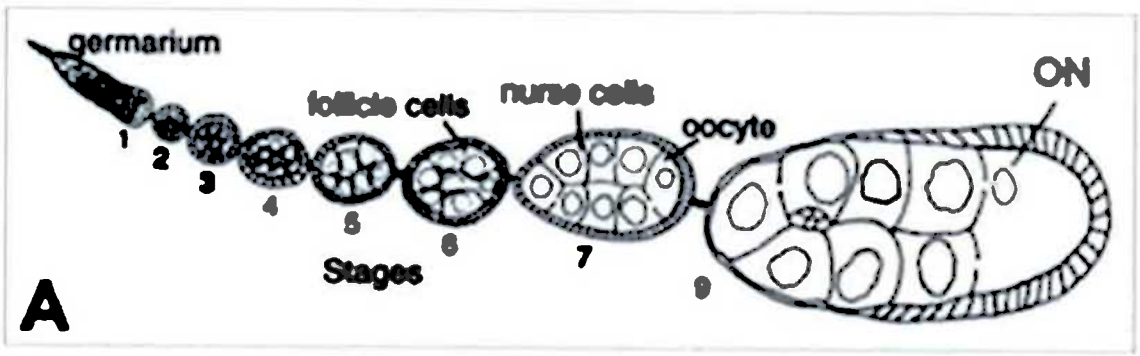
germarium
follicle cells
nurse cells
oocyte
ON
1
2
3
4
5
6
7
9
Stages
A

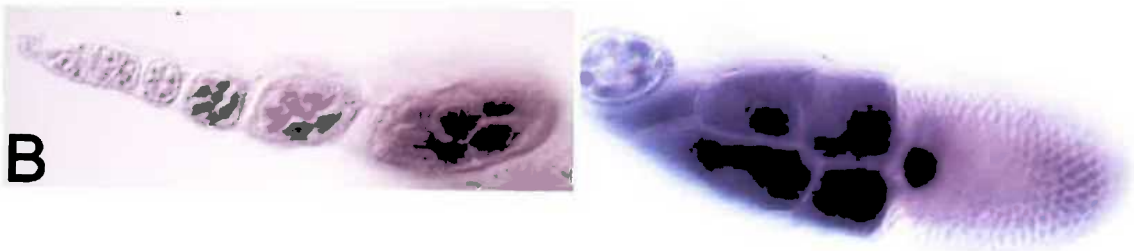
B


C

Following cyst formation, one of the two cells joined by 4 ring canals accumulates specific mRNAs that are transported from the other 15 cells. This individual cell undergoes meiosis and differentiates as the oocyte, with the remaining cells undergoing endocycles and becoming polyploid nurse cells (Spradling, 1993). Each germ-line cyst is enveloped by somatic follicle cells, which arise by mitotic division, and form a monolayer surrounding the cyst. Thus, oogenesis consists of various cell cycles, meiotic, mitotic and endocycles, that may require alternative forms of DmcycE for their regulation. In mitotically-proliferating cells, feedback controls ensure that M phase does not commence before completion of S phase. However, these controls must be modified to allow meiosis I and II to be coupled without an intervening S phase, and for the alternating S and G phases of the endocycles.

Previous studies using anti-DmcycE have shown that DmcycE is present in the early stages of oogenesis, corresponding to a requirement for DmcycE in regulation of the enodreplication cycles in the nurse cells (Figure 3.4 B) (Crack, 1996; Lilly and Spradling, 1996). DmcycE expression is detected at varying levels within the nurse cell nuclei of each egg chamber, with nuclei containing high, intermediate, low or undetectable levels, and at high levels in the oocyte nucleus (germinal vesicle) (Crack, 1996; Lilly and Spradling, 1996).

DmcycEII message is maternally deposited, with transcripts present at high levels in the nurse cells, prior to their deposition into the oocyte (Crack, 1996). However, whether DmcycEII has a role in regulation of meiosis, endocycles or proliferation of the somatic follicle cells is not known. The regulation of the early divisions required for formation of the 16 cell cyst may also require *DmcycE*, so either DmcycEI or II or both may be required for these early cycles.

To investigate the distribution of DmcycEII protein during oogenesis, immunolocalisation was carried out using anti-DmcycEII. The DmcycEII protein was detected in the germarium corresponding to the early divisions required for formation of the 16 cell cyst (Figure 3.4 C) (de Nooij *et al.*, 2000). During later stages of oogenesis, strong staining was detected in the oocyte nucleus, whereas, the nurse cell nuclear staining decreased and cytoplasmic staining increased. This may represent DmcycEII protein ready for deposition into the oocyte, or may be due to background staining, however the latter is unlikely as it is also detected with the common antibody. Therefore, the staining detected at varying levels in the nurse cell nuclei at these stages using the common antibody represents DmcycEI. Thus it appears that both DmcycE proteins are present during oogenesis and their respective localisations suggest distinct roles, with DmcycEII required early for cyst formation and in the oocyte nucleus, and DmcycEI is required for the nurse cell endocycles.

3-3 Discussion

This chapter has analysed the distribution of DmcycEII during development. DmcycEII is nuclear localised during interphase, as is DmcycEI, and becomes distributed in the cytoplasm during mitosis. DmcycEII protein, which is maternally-deposited, is most abundant during the early rapid nuclear divisions of embryogenesis, whilst DmcycEI protein is more abundant during later stages of development, during the more regulated cell cycles.

The distribution of DmcycE proteins during development mostly correlates with proliferating cells, with a few exceptions; there are two cases during embryonic development in which DmcycE is not down-regulated in cells that have ceased proliferating. Firstly, the amnioserosa cells, which exit from the cell cycle in G2 phase of cycle 14, maintain high levels of DmcycE for at least 1-2 hours after they cease division. DmcycE in the amnioserosa persists without the presence of detectable DmcycE transcript (Richardson *et al.,* 1993), implying that DmcycE protein is stabilized in these cells. Secondly, DmcycE is maintained at high levels throughout embryogenesis in the non-proliferating G2-arrested pole cells, even though these cells remain dormant for at least 14 hours and do not recommence division until the end of embryogenesis (Su *et al.,* 1998). The presence of high levels of DmcycE protein in the pole cells correlates with high levels of maternally-derived transcript localised to these cells during early embryogenesis, and represents maternally-derived DmcycEII protein, since it is present in *DmcycE* deficient embryos that have no zygotic expression of DmcycE (Richardson *et al.,* 1993; 1995) and is detected with the DmcycEII-specific antibody. For the same reasons, DmcycE protein persisting in the amnioserosa is DmcycEII. The role of DmcycEII (if any) in the amnioserosa and pole cells, which are arrested in G2 phase, is unclear. However, these G2 phase arrested cells do not enter S phase even though DmcycEII is present, suggesting that DmcycEII does not play a role in S phase induction in these cells.

The function of DmcycEII during development was examined by characterisation of the expression pattern during embryogenesis, larval development and oogenesis. DmcycEII is present at high levels in the early embryo where cell cycles are very rapid and essentially have no G1 or G2 phases. It is possible that DmcycEII has a role in allowing the very rapid S phases to occur in these early embryonic cycles. The observation that DmcycEII is present during third larval instar eye-antennal and wing imaginal disc development is intriguing, as this and previous studies have described DmcycEII as maternally-derived and perhaps having a specific role during the rapid early embryonic cell cycles. It is striking that DmcycEII is not detected in the post MF S phase cells, suggesting that a specific function may be fulfilled by expression of DmcycEI in these cells. It remains unclear as to the precise role of DmcycEII versus DmcycEI,

however, DmcycEII may play an important role in specific cells, for example in overcoming an inhibitor or to drive entry into S phase.

During oogenesis, DmcycEII is present at varying levels in the nurse cells. These cells are undergoing cycles consisting of alternating S and G phases, and it has been proposed that varying levels of DmcycE present in individual nuclei of these egg chambers is due to cycling of DmcycE protein levels. This would occur such that DmcycE accumulates during the G phase until a threshold level is reached and S phase initiated, at which time DmcycE is rapidly degraded (Lilly and Spradling, 1996). The presence of high levels of DmcycEII in the oocyte nucleus is surprising, as the oocyte nucleus arises in the germarium and, as it has completed S phase, there is no apparent role in the oocyte for a G1-specific cyclin. However, in *Xenopus* and sea urchin, cyclin E has been shown to be present during both meiotic and early embryonic cell cycles (Rempel *et al.,* 1995; Sumerel *et al.,* 2001).

An important developmental question is whether the two isoforms of DmcycE, which are present at different developmental stages, have different functions. The following chapter describes functional studies to examine the role of DmcycEII versus DmcycEI.

Chapter 4 : Analysis of DmcycEI and DmcycEII Function

4-1 Introduction

As described in Chapter 1, in the third larval instar eye imaginal disc, DmcycEI and DmcycEII differ in their abilities to induce the G1 arrested cells within the MF into S phase. Ectopic expression of DmcycEI is able to induce the anterior, but not posterior, G1 cells within the MF into S phase, whilst ectopic expression of DmcycEII results in induction of all of the G1 arrested cells within the MF into S phase. Importantly, these cells included those in the posterior part of the MF that were refractory to ectopic DmcycEI expression. These results suggest that cells in the posterior region of the MF are more resistant than the anterior cells to S phase induction by DmcycE, and that DmcycEII is more potent than DmcycEI in overcoming this resistance.

This chapter describes the analysis of DmcycE deletion constructs to determine if the difference in activity between DmcycEI and DmcycEII is due to their unique N-terminal regions, and the analysis of a potential inhibitory mechanism specific for DmcycEI. The results of some of the analysis described below have been published (Crack *et al.*, 2002).

4-2 Analysis of truncated forms of DmcycE

4-2.1 Ectopic expression of N- and C-terminal DmcycE truncations

The differential effect of DmcycEI relative to DmcycEII in driving G1 cells within the MF into S phase was shown to be time dependent. At 60 min after heat shock induction, ectopic S phases were observed in the anterior region of the MF, not in the posterior region, for both DmcycEI and DmcycEII (Figure 4.1) (Crack, 1996). However, 120 min after induction, DmcycEII induced the posterior MF cells into S phase, whilst in DmcycEI these cells remained arrested in G1 (Figure 4.2 B and C). Furthermore, at 180 min DmcycEI is still unable to induce the posterior G1 MF cells into S phase (Figure 4.2 D). Western analysis and immunostaining after heat shock induction indicated that these effects were not due to differences in the levels or localisation of DmcycEI and DmcycEII and thus represent functional differences (Figure 4.2 E-H). Since the only difference between these proteins is their unique N-terminal regions, it is possible that this region could be responsible for the differential effect observed. To test this, the relative abilities of N- and C -terminal truncated versions of DmcycE in transgenic flies to induce S phase in the eye imaginal disc were examined (Figure 4.3).

Like full-length DmcycE, N-terminal (Δ195N-DmcycE), C-terminal (Δ519C-DmcycEI) or both N- and C-terminal (Δ195NΔ519C-DmcycE) truncations of DmcycE have been shown to

Figure 4.1 : Ectopic DmcycEI and DmcycEII induce cells into S phase.

Cells undergoing S phase, as detected by BrdU labelling, of eye imaginal discs 60 min after heat shock induction of *DmcycE* transgenes. **A.** *hsp70-DmcycEI* and **B.** *hsp70-DmcycEII* eye discs showing an increase in S phase cells in the anterior part of the MF and in cells immediately posterior to the MF, but not in the posterior region within the MF (Crack, 1996).

Anterior is to the right and the MF is indicated by the bar.

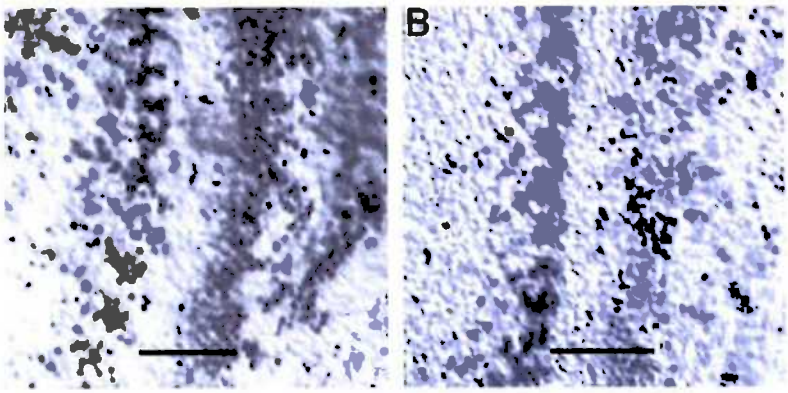
B
hs-cycEI
hs-cycEII

Figure 4.2 : Ectopic expression of *DmcycEII* induces all MF cells into S phase.

(**A-D**) Cells undergoing S phase, as detected by BrdU labelling, in eye imaginal discs. At 120 min after induction by heat shock **A.** Control eye disc, **B.** *hsp70-DmcycEII* eye disc showing that all cells within the MF are driven into S phase, and **C.** *hsp70-DmcycEI* eye disc showing an increase in S phase cells in the anterior part of the MF and in cells immediately posterior to the MF but not in the posterior MF cells. **D.** *hsp70-DmcycEI* eye disc 180 min after induction by heat shock, still showing an absence of S phases within the posterior part of the MF.

(**E-G**) Immunolocalisation of DmcycE in eye imaginal discs 120 min after heat shock induction of *DmcycE* transgenes. **E.** Control heat shocked eye disc. **F.** *hsp70-DmcycEII* eye disc. **G.** *hsp70-DmcycEI* eye disc. DmcycE proteins were detected using anti-DmcycE rat polyclonal antibody and visualised using a FITC-conjugate. DmcycEI and DmcycEII show similar protein localisation, and importantly both DmcycEI and DmcycEII are present within the MF.

(**H**) Western analysis of DmcycE protein levels in eye-antennal imaginal discs from heat shocked wild type control (lane 1), heat shocked *hsp70-DmcycEI* (lane 2), and heat shocked *hsp70-DmcycEII* (lane 3). Third instar larvae were heat shocked and allowed to recover for 120 min before dissection of the eye-antennal disc. Protein samples were prepared and analysed by immunoblotting using anti-DmcycE mouse monoclonal serum, 8B10, and detected by enhanced chemiluminescence. The DmcycE antiserum detected an abundant protein band at ~75 kDa, corresponding to DmcycEI in lane 2, and a higher molecular weight band at ~97 kDa in lane 3, corresponding to DmcycEII protein. At this exposure the endogenous DmcycE protein bands are not visible in the heat-shocked wild type control (lane 1).

Published in Crack *et al.,* (2002).

Anterior is to the right and the MF is indicated by the bar.

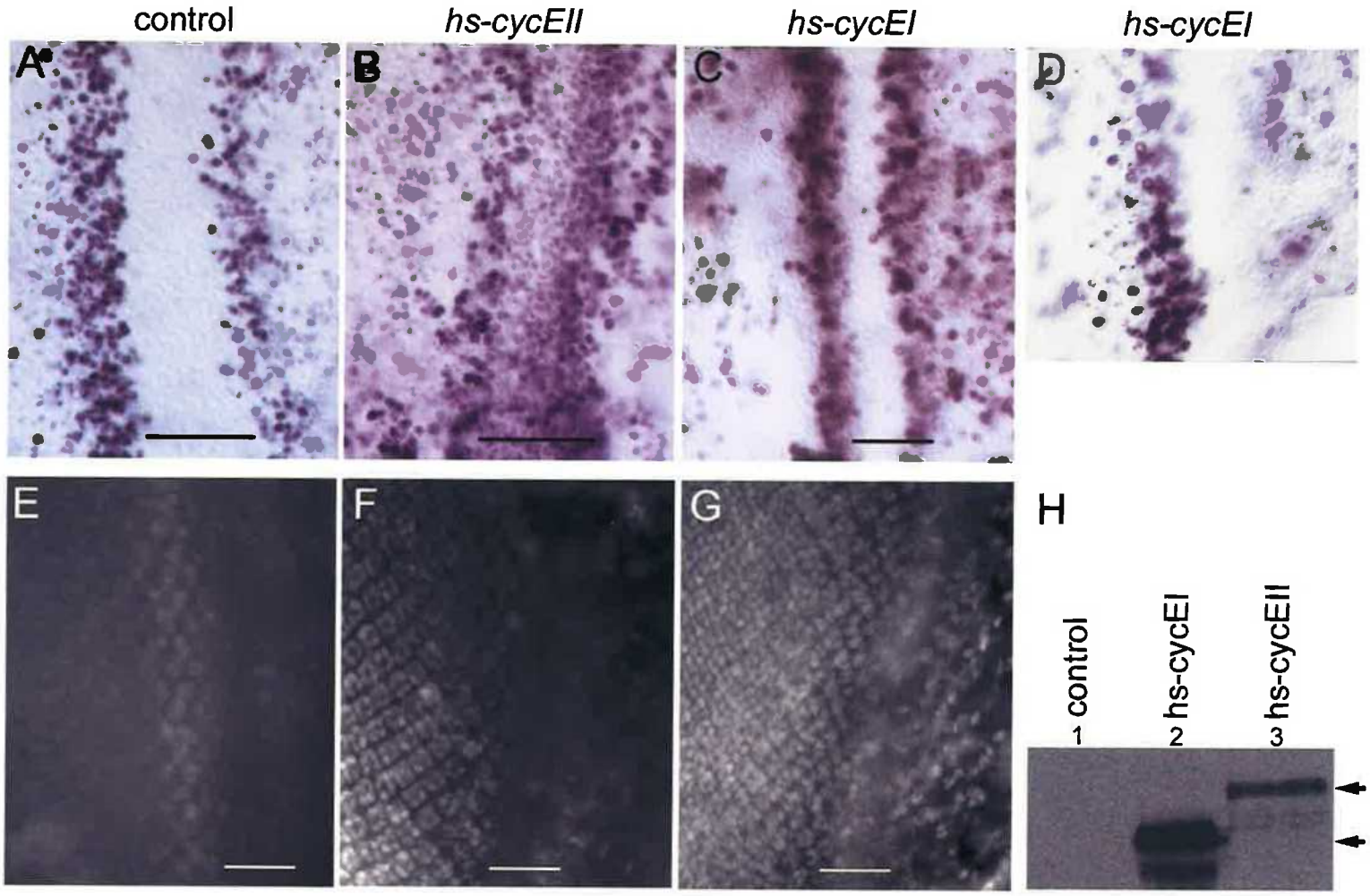
control
hs-cycEII
hs-cycEI
hs-cycEI
A
B
C
D
E
F
G
H
1 control
2 hs-cycEI
3 hs-cycEII

Figure 4.3 : Schematic diagram of DmcycEI and II proteins and truncations.

The unique regions of DmcycEI and DmcycEII are shown by the different coloured N-terminal regions, and the cyclin box is represented by the blue box. Arrows indicate the position of potential nuclear localisation sequences. The numbers correspond to the amino acid, with the truncated constructs corresponding to DmcycEI amino acid number.

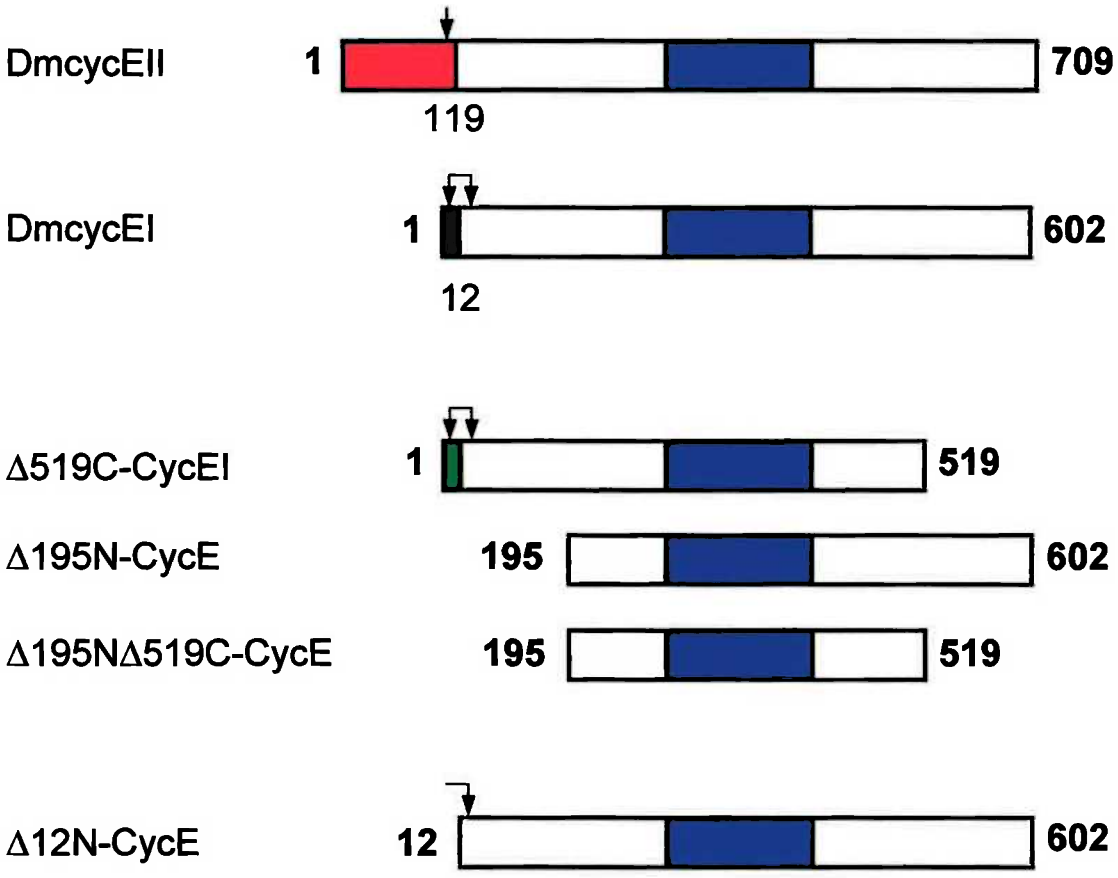
DmcycEII
1
709
119
DmcycEI
1
602
12
Δ519C-CycEI
1
519
Δ195N-CycE
195
602
Δ195NΔ519C-CycE
195
519
Δ12N-CycE
12
602

be capable of inducing the anterior-most G1 arrested cells within the MF into S phase when assayed at 60 min after heat shock induction (Secombe, 1995). Thus, it was concluded that all the truncated forms of DmcycE are functional.

To determine whether these DmcycEI truncations were more potent than full-length DmcycEI in driving G1-arrested cells within the MF into S phase, BrdU labelling was carried out at 120 min after heat shock induction of the *Δ195N-DmcycE, Δ519C-DmcycEI* or *Δ195NΔ519C-DmcycE* transgenes (Figure 4.4). Ectopic expression of Δ519C-DmcycEI, like full-length DmcycEI, was only able to drive the anterior MF cells into S phase. In contrast, both of the DmcycE 195N-terminal truncation constructs (Δ195N-DmcycEI and Δ195NΔ519C-DmcycE) resulted in ectopic S phases in all G1-arrested cells at 120 minutes after heat shock induction. Thus it appears that the N-terminal 195 amino acid region prevents DmcycEI from triggering S phase in the posterior part of the MF. As the available antisera did not recognise Δ195N-DmcycE, the relative levels of the induced proteins was unable to be determined. Therefore, it was not possible to confirm that this effect was not due to higher levels of Δ195N-DmcycE or Δ195NΔ519C-DmcycE relative to Δ519C-DmcycEI or full-length DmcycEI. However, given the results obtained for DmcycEII, and results described below, this is unlikely to be the case.

4-2.2 Generation and analysis of a 12 amino acid N-terminal DmcycEI truncation

The only region unique to DmcycEI that may be responsible for the apparent inhibition of DmcycEI function in the posterior part of the MF is the first 12 amino acids. To examine the role of this region, transgenic flies containing a deletion of the first 12 amino acids of DmcycEI were generated (Figure 4.3). A PCR product corresponding to 12 amino acid N-terminal deleted DmcycEI was inserted into *pCaSpeR-hs* transformation vector and used for *P*-element mediated transformation of *Drosophila* (Section 2-3).

Heat shock-induced ectopic expression of Δ12N-DmcycEI resulted in induction of all G1 arrested cells within the MF into S phase (Figure 4.5 B). Western analysis showed that similar amounts of Δ12N-DmcycEI and DmcycEI were present at 120 min following heat-shock induction, showing that this effect was not a result of more Δ12N-DmcycEI protein being produced (Figure 4.5 C). Furthermore, immunostaining of eye imaginal discs showed Δ12N-DmcycEI and DmcycEI proteins are present throughout the eye imaginal discs after heat shock induction, including all cells within MF (H. Richardson, Crack *et al.,* 2002) (Figure 4.5 D-I).

Interestingly, Δ12N-DmcycEI protein was not specifically nuclear localised as was DmcycEI, but rather was present in both cytoplasmic and nuclear compartments in eye imaginal disc and salivary gland cells (Figure 4.5 and data not shown) (Crack *et al.,* 2002).

Figure 4.4 : DmcycEI N-terminal deletions can induce all G1 MF cells into S phase.

Cell undergoing S phase, as detected by BrdU labelling, of eye imaginal discs from third instar larvae at 120 min after heat shock induction of *DmcycE* transgenes. **A.** *hsp70-Δ195N-DmcycE* eye disc showing that all cells within the MF are driven into S phase. **B.** *hsp70-Δ519C-DmcycEI* eye disc showing that cells in the anterior and not posterior part of the MF are induced into S phase. **C.** *hsp70-Δ195NΔ519C-DmcycE* eye disc showing that all cells within the MF are driven into S phase.

Published in Crack *et al.*, (2002).

Anterior is to the right and the MF is indicated by the bar.

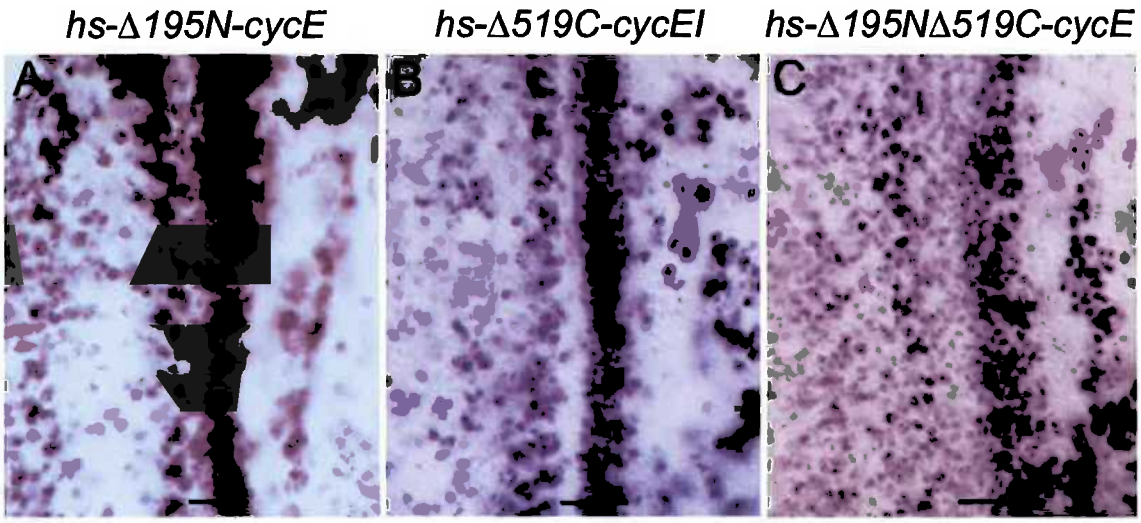
hs-Δ195N-cycE
hs-Δ519C-cycEI
hs-Δ195NΔ519C-cycE
A
B
C

Figure 4.5 : Ectopic expression of Δ12N-DmcycEI can induce all of the MF cells into S phase.

(**A-B**) Cells undergoing S phase, as detected by BrdU labelling, of eye imaginal discs from third instar larvae at 120 min after heat shock. **A.** Control eye disc. **B.** *hsp70-Δ12N-DmcycE* eye disc showing that all cells within the MF are driven into S phase.

(**C**) Western analysis of DmcycEI and Δ12N-DmcycE protein levels from third larval instar eye-antennal discs dissected immediately (lanes 1,3) and at 120 mins (lanes 2,4) after induction by heat shock. Protein samples were analysed by immunoblotting using anti-DmcycE mouse monoclonal sera, 8B10, and detected by enhanced chemiluminescence. The DmcycE antisera detected an abundant protein band at ~75 kDa corresponding to DmcycEI in lanes 1 and 2, and a very slightly lower molecular weight protein band in lane 3 and 4 corresponding to Δ12N-DmcycE protein, showing similar levels across all lanes.

(**D-I**) Immunolocalisation of DmcycE spanning the MF cells of eye imaginal discs from third larval instar 120 min after heat shock induction of *DmcycE* transgenes. DmcycE proteins were detected using anti-DmcycE rat polyclonal antibody and visualised using a FITC-conjugate (red). DNA was visualised by staining with Hoechst 33258 (blue). (**D-F**) *hsp70-DmcycEI*: **D.** Anti-DmcycE, **E.** Hoechst 33258, and **F.** Merge. (**G-I**) *hsp70-Δ12N-DmcycE*: **G.** Anti-DmcycE, **H.** Hoechst 33258, and **I.** Merge. DmcycEI and Δ12N-DmcycE proteins are present within the MF, however the majority of Δ12N-DmcycE protein is cytoplasmic whereas DmcycEI is nuclear-localised (H. Richardson, Crack *et al.*, 2002).

Anterior is to the right and the MF is indicated by the bar.

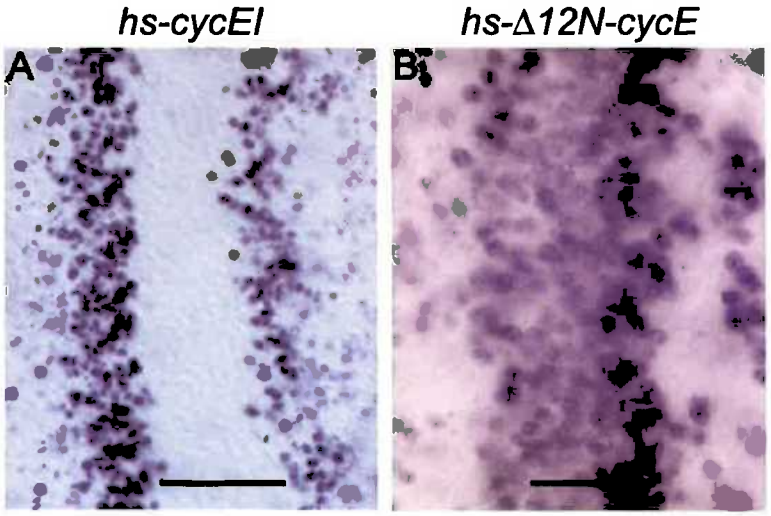
hs-cycEI
hs-Δ12N-cycE
A
B

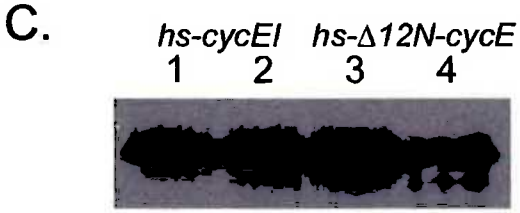
C.
hs-cycEI
hs-Δ12N-cycE
1
2
3
4

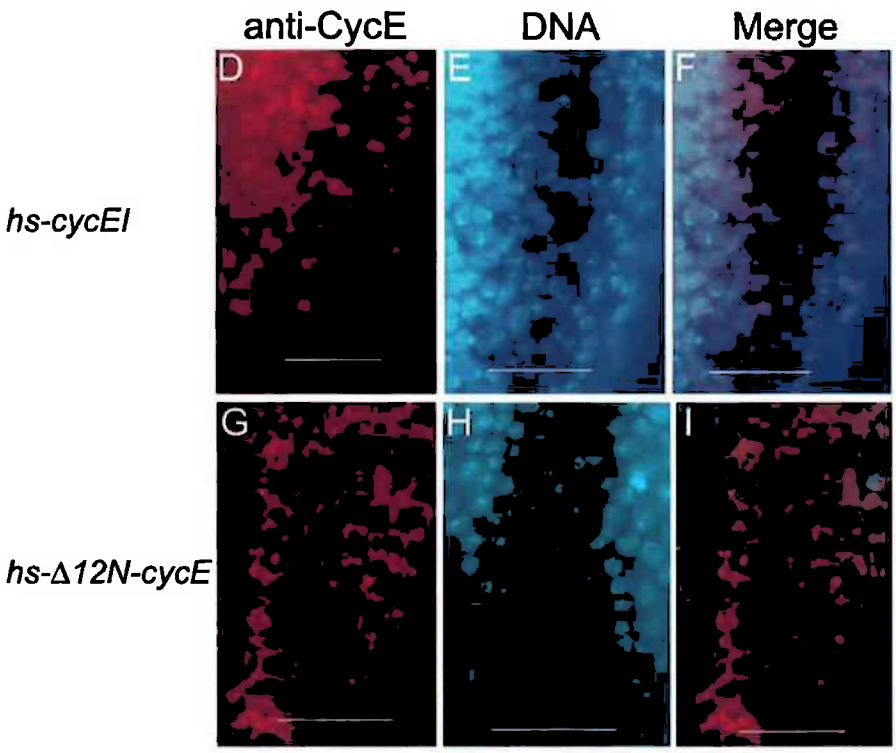
anti-CycE
DNA
Merge
hs-cycEI
hs-Δ12N-cycE
D
E
F
G
H
I

The deletion of the first 12 amino acids of DmcycEI is expected to remove part of the potential bipartite nuclear localisation signal (NLS), QKRKF(X_{13})AKRQQR at amino acid positions 5-28. The loss of nuclear targeting of Δ12N-DmcycEI suggests that the putative NLS functions as a nuclear targeting signal. Since low levels of Δ12N-DmcycEI were observed in the nucleus this suggests that an alternative less efficient mechanism must exist. Furthermore, the fact that Δ12N-DmcycEI and the larger N-terminal deletion constructs are able to affectively trigger S phase, suggests that DmcycE, when over-expressed at least, is able to function regardless of specific targeting to the nucleus.

Thus, the ability of Δ12N-DmcycEI to induce all of the G1 arrested MF cells into S phase suggests that the 12 unique amino acids of DmcycEI may act as an inhibitory domain in the posterior of the MF. A potential mechanism for this effect may be that the 12 amino acid N-terminal region functions as an inhibitor binding domain, whereby an inhibitor present in the posterior MF cells can bind to and inhibit DmcycEI function specifically, without significantly effecting DmcycEII. Although there is a delay with DmcycEII induction of posterior MF cells into S phase and this occurs after the anterior cells have been induced into S phase. The remainder of this chapter describes the analysis of candidate DmcycEI-specific inhibitors.

4-3 Examination of potential DmcycEI specific inhibitors

4-3.1 Is Dacapo the DmcycEI specific inhibitor?

As described in Chapter 1, a model for G1 arrest in the MF cells requires a Dpp-dependent mechanism in the anterior MF cells and a Dpp-independent mechanism in the posterior MF cells. A possible candidate inhibitor of DmcycE in the posterior MF cells is the *Drosophila* CKI, Dacapo (Dap), a p27/p21 homologue, which has been demonstrated to be required to inhibit DmcycE/DmCdk2 activity during embryogenesis (de Nooij *et al.*, 1996; Lane *et al.*, 1996).

Dap is expressed in the posterior region of the eye disc (de Nooij *et al.*, 1996; Lane *et al.*, 1996). To examine more precisely where Dap is expressed in relation to the MF, co-immunolocalisation of Dap and DmcycE was performed in eye imaginal discs (Figure 4.6). DmcycE is normally present at high levels the subset of cells undergoing S phase posterior to the MF (Richardson et. al., 1995), but not within the MF. Dap localisation was observed to partially overlap with the band of DmcycE posterior to the MF, but was not detectable in cells within the MF (Figure 4.6). The localisation of Dap posterior to the MF was confirmed by co-localisation with a MF specific marker, *dpp*-lacZ (Crack *et al.*, 2002).

To rule out Dap as the possible DmcycEI specific inhibitor, the interaction of Dap with DmcycEI or DmcycEII was examined. Dap has been shown to bind to the cyclin box region of

Figure 4.6 : Localisation of Dacapo and DmcycE in eye imaginal discs.

Dacapo and DmcycE immunolocalisation relative to the MF in the eye imaginal disc. **A.** DmcycE protein was detected using anti-DmcycE rat polyclonal antibody and visualised using a rhodamine-conjugate (red), **B.** Dap protein was detected using anti-Dap mouse monoclonal antibody and visualised using an Alexa488-conjugate (green) and **C.** Merge. Dap is present in cells posterior to, but not within, the MF where it co-localises with a subset of DmcycE cells.

Published in Crack *et al.,* (2002).

Anterior is to the right and the MF is indicated by the bar.

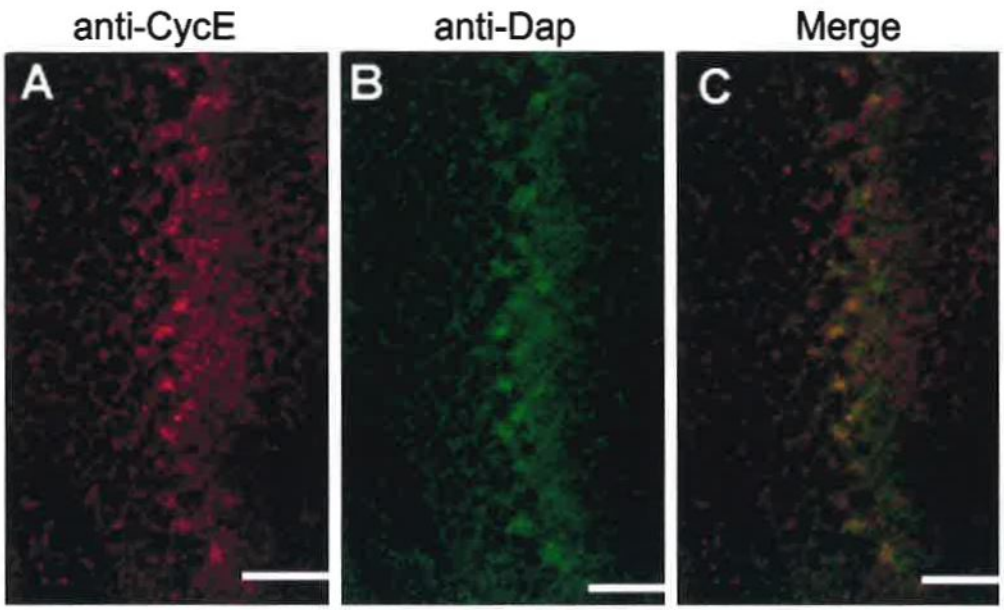
anti-CycE
anti-Dap
Merge
A
B
C

DmcycE (Thomas *et al.*, 1997), however it is possible that the different N-terminal regions may influence this binding. First, the yeast 2-hybrid system was used to determine whether Dap could interact with the N-terminal region of DmcycEI. To test for interaction, *Dap* and *DmcycE* constructs were transformed into yeast strain *EGY48*, which contains a *lacZ* reporter plasmid, *pHS18-34*. An interaction could then be assayed in terms of the level of expression of the *lacZ* reporter, quantified using Miller LacZ units. It was found that Dap (*pJG-Dap*) did not interact with either the N-terminal 46 amino acids of DmcycEI (*pEG-46N*) or with the C-terminal 86 amino acids of DmcycEI (*pEG-Cterm*) (Table 4.1, Appendix 4.A). Dap was then tested for relative binding to full-length DmcycEI and DmcycEII, with the result that Dap (*pJG-Dap*) interacted with both DmcycEI (*pGilda-DmEI*) and DmcycEII (*pGilda-DmEII*) to a similar level in the yeast 2-hybrid system (Table 4.1, Appendix 4.A). Finally, a functional assay in yeast was used to test the relative inhibition of the DmcycEI/DmCdk2 complex or the DmcycEII/DmCdk2 complex by Dap. Expression of DmcycE and DmCdk2 in yeast is lethal, as is expression of mammalian Cdk2 and Cyclin E (K.-A. Won and S. Reed, personal communication). However, this lethality can be rescued by co-expression of human p21 or Dap. The lethality of yeast expressing DmcycEI/DmCdk2 or DmcycEII/DmCdk2 was rescued to similar levels by co-expression of Dap (Figure 4.7).

Table 4.1: Dap interactions in the yeast 2-hybrid system

	pJG-Dap	*pJG*	Max-Min increase*
pEG-46N	0.71 ± 0.59	1.10 ± 0.76	
pEG-Cterm	0.57 ± 0.53	1.07 ± 0.29	
pGilda-DmEI	19.1 ± 4.1	1.21 ± 0.56	19.2 - 12.4 x
pGilda-DmEII	30.94 ± 5.6	1.32 ± 0.28	27.7 – 19.2 x

* Maximum and minimum increase was determined by division of the max and min lacZ units by the average vector alone (pJG) value.

Although immunolocalisation of Dap and DmcycE does not seem to support Dap as a DmcycEI-specific inhibitor in the posterior MF, a final experiment was carried out to determine whether ectopic expression of *DmcycEI* in *dap* mutant eye discs could induce all cells within the MF into S phase. In order to examine eye imaginal discs that lacked Dap expression, flies were generated containing a dap^{2X10} null allele balanced over *Cy*O-*Tb,* allowing homozygous *dap* to be identified by the absence of the dominant larval marker *Tubby*. The eye imaginal discs from dap^{2X10} homozygous larvae were examined for the pattern of S phases, and found to show no significant difference to the pattern of wild type S phases (Figure 4.8). The effect of ectopic

Figure 4.7 : Dacapo inhibits both DmcycEI and DmcycEII lethality in yeast.

Analysis of inhibition of DmcycE/DmCdk2 function in yeast. Co-expression of *pGAL-DmcycEI*, or *pGAL-DmcycEII*, with *pGAL-Dmcdk2* was induced by growth on galactose media, resulting in lethality. Rescue of the lethality was observed with co-expression of Dap (*pJG-Dap)*, but not *pJG* (without insert). A similar level of rescue was observed for the DmcycE/DmCdk2 and DmcycEII/DmCdk2 strains. Three individual transformants for each assay are plated in a 10-fold serial dilution.

Published in Crack *et al.*, (2002).

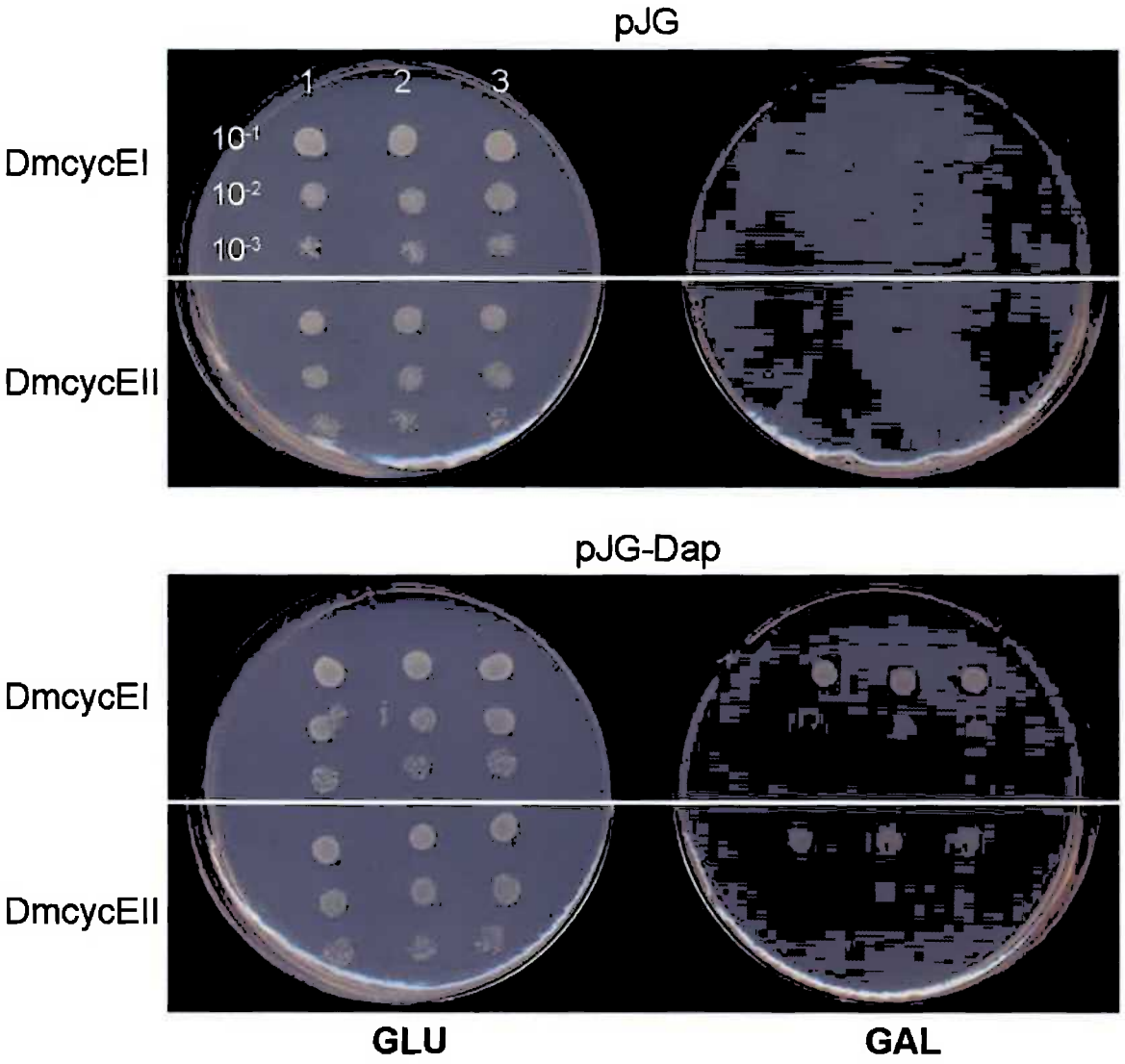
pJG
1
2
3
10-1
10-2
10-3
DmcycEI
DmcycEII
pJG-Dap
DmcycEI
DmcycEII
GLU
GAL

Figure 4.8 : *dap* mutant eye disc do not show a disruption to S phases.

(A,B) Cells undergoing S phase, as detected by BrdU labelling, in eye imaginal discs from third instar larvae. **A.** Control w^{1118} eye disc. **B.** Homozygous dap^{2X10} eye disc does not show any significant difference in the pattern of S phases compared to wild type.

Anterior is to the right and the MF is indicated by the bar.

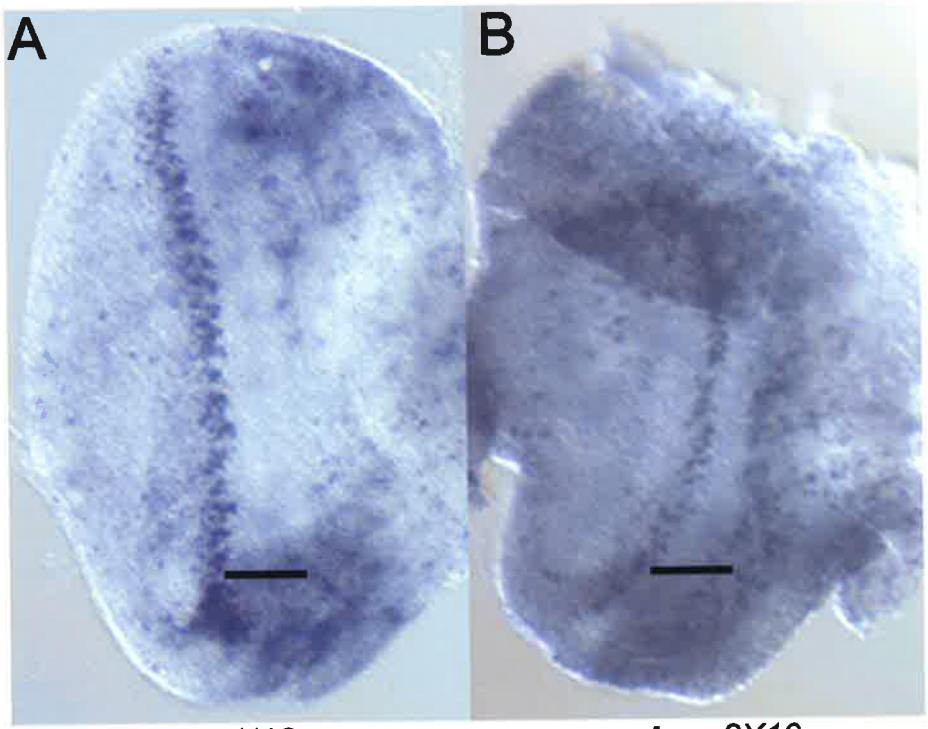
A
B
w1118
dap2X10

expression of *DmcycEI* in homozygous *dap* mutant eye discs was then examined. This required the generation of the line *dap*^{4454}*/Gla Bc; hsp70-DmcycEI,* containing both *dap* mutant allele and the *hsp70-DmcycEI* transgene (Figure 4.9). *dap*^{4454}*/Gla Bc; hsp70-DmcycEI* flies were crossed to *dap*^{2X10}*/Gla Bc* and homozygous *dacapo* mutant larvae were picked by the absence of the dominant marker, *Bc* (*Black cells*). Heat shock-induced ectopic expression of *DmcycEI* in homozygous *dap* mutant eye discs showed an increase in S phase cells posterior to the MF, and in the anterior region of the MF as expected, but not in the posterior region of the MF (M. Coombe, Crack *et al.,* 2002) (Figure 4.10).

Together these results show that, Dap was not detectable in the posterior part of the MF, could not bind specifically to the N-terminus of DmcycEI, and did not show higher binding efficiency or inhibition of DmcycEI/DmCdk2 compared with DmcycEII/DmCdk2. Therefore, Dap is not the mediator of the DmcycEI specific inhibition in the posterior region of the MF.

4-3.2 Is Roughex the DmcycEI specific inhibitor?

An important regulator of the G1 arrest in the MF is *roughex (rux)*, which encodes a novel Cdk inhibitor protein required to down-regulate DmcycA activity (Chapter 1). In *rux* mutant eye discs, cells fail to arrest in G1 prior to the MF (Thomas *et al.,* 1994). During both embryonic and eye development, Rux acts to negatively regulate DmcycA by affecting the protein localisation, resulting in targeted degradation (Sprenger *et al.,* 1997; Thomas *et al.,* 1997). Rux has been shown to inhibit DmcycA/DmCdk1/2 activity *in vitro* (Avedisov *et al.,* 2000) and inhibit induction of S phase by DmcycA in both embryonic and eye imaginal disc cells (Thomas *et al.*, 1994; 1997). DmcycE/DmCdk2 has been shown to phosphorylate and inactivate Rux, leading to activation of DmcycA/DmCdk1 (Thomas *et al.*, 1997; Avedisov *et al.,* 2000). However, the studies of Thomas *et al.,* (1997) did not specifically examine whether Rux could act as an inhibitor of DmcycE function in the MF. A possible model for DmcycEI-specific inhibition in the posterior MF, is that Rux acts as a substrate inhibitor of DmcycEI kinase function in S phase induction but does not affect DmcycEII function.

Rux is expressed in the anterior region of the MF and in differentiating cells in the posterior region of the eye imaginal disc (Thomas *et al.*, 1994). If Rux is involved in inhibition of DmcycEI specifically, then reducing the dose of *rux* may result in an increase in active DmcycEI kinase complex and thus increased induction into S phase, including those cells in the posterior region of the MF. To examine the effect of reducing the dose of *rux* in heat shock-induced *DmcycEI* and *DmcycEII* eye discs required crossing *rux*^{8}*/FM7* to homozygous *hsp70-DmcycEI* and *hsp70-DmcycEII.* The eye imaginal discs from third instar larvae heterozygous for *rux*^{8} and either *hsp70-DmcycEI* or *hsp70-DmcycEII* were identified by the absence of *Bar*, which is carried on the *FM7* chromosome. No effect on the pattern of S phases was observed when the

Figure 4.9 : Generation of a stock for expression of DmcycEI in *dap* mutant eye discs.

A. Generation of a stock containing both a *dap* mutant allele and the *hsp70-DmcycEI* transgene. dap^{4454}*/CyO* flies were crossed to the *DmcycEI* transgenic stock *(hsp70-DmcycEI)* containing a 2nd chromosome dominant marker (*Sco*) and flies carrying both dap^{4454} and *hsp70-DmcycEI* (Pw^{+}) were selected. These flies were then crossed to the 2nd chromosome dominant larval marker, *Bc (Black cells)*, to generate the stock required for part B.

B. To analyse S phase induction by *hsp70-DmcycEI* in a *dacapo* mutant background, dap^{4454}*/Gla Bc;hsp70-DmcycEI* flies were crossed to dap^{2X10}*/Gla Bc*. dap^{4454}/dap^{2X10}; *hsp70-DmcycEI/+* mutant larvae were picked by the absence of the *Bc* marker.

A.

$$w^{1118}; \frac{dap^{4454}}{CyO} \quad \text{X} \quad w^{1118}; \frac{Sco}{CyO}; [Pw^{+}\ hsp70\text{-}DmcycEI]$$

$$\downarrow$$

$$w^{1118}; \frac{dap^{4454}}{CyO}; \frac{hsp70\text{-}DmcycEI}{+} \quad \text{X} \quad w^{1118}; \frac{Gla\ Bc}{CyO}$$

$$\downarrow$$

generate stock $\quad w^{1118}; \frac{dap^{4454}}{Gla\ Bc}; \frac{hsp70\text{-}DmcycEI}{+}$

B.

$$w^{1118}; \frac{dap^{4454}}{Gla\ Bc}; hsp70\text{-}DmcycEI \quad \text{X} \quad \frac{dap^{2X10}}{Gla\ Bc}$$

$$\downarrow$$

select larvae $\quad \frac{dap^{4454}}{dap^{2X10}}; \frac{hsp70\text{-}DmcycEI}{+}$

Figure 4.10 : Expression of DmcycE1 in *dap* mutant eye discs can not drive posterior MF cells into S phase.

Cells undergoing S phase, as detected by BrdU labelling, in eye imaginal discs from third instar larvae. **A.** Control eye disc. **B.** Homozygous *dap* mutant *hsp70-DmcycEI* (1 copy) eye discs at 120 min after heat shock induction showing an increase in S phases, but not within the posterior region of the MF. **A', B'** show higher magnification, highlighting the MF (M. Coombe, Crack *et al.*, 2002).

Anterior is to the right and the MF is indicated by the bar.

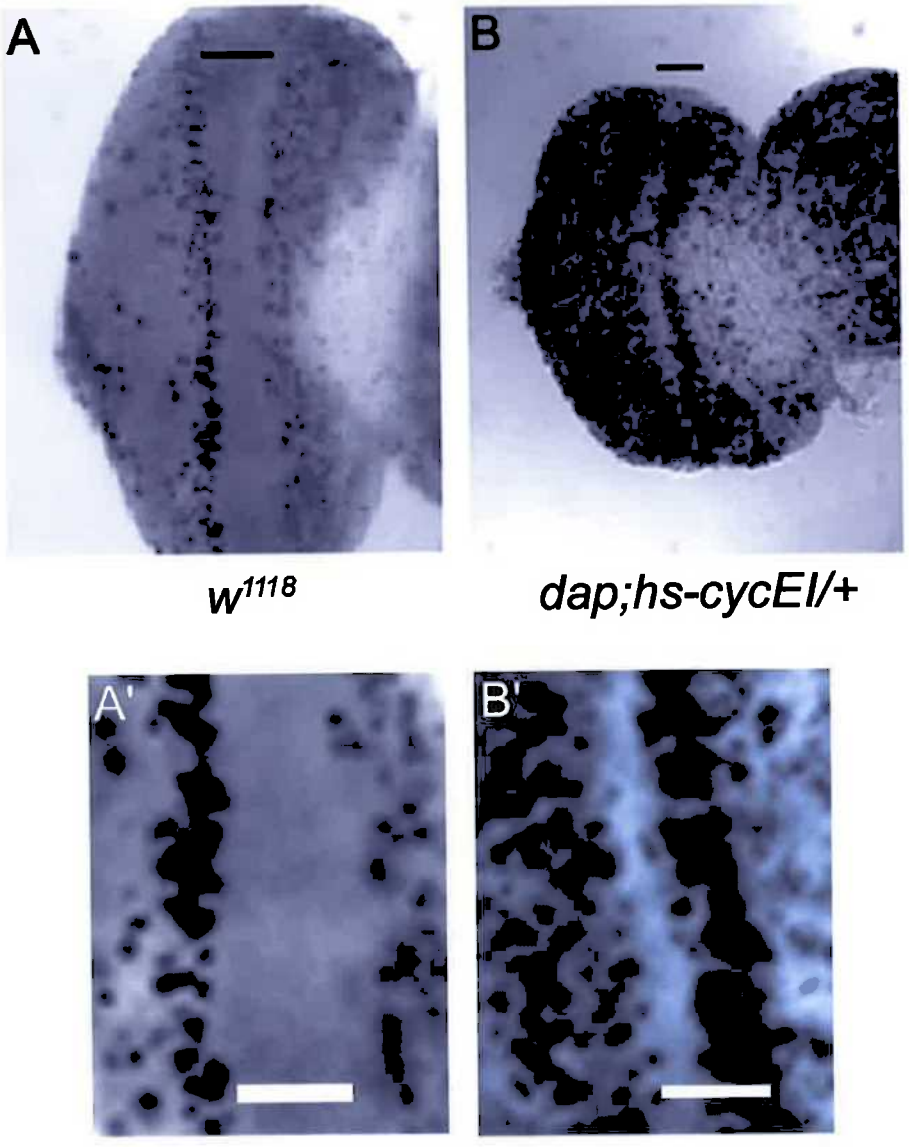

w^{1118} *dap;hs-cycEI/+*

dose of *rux*^{8} was reduced in *hsp70-DmcycEI* or *hsp70-DmcycEII,* compared with *hsp70-DmcycEI* or *hsp70-DmcycEII* alone, at either 60 min or 120 min after heat shock induction (Figure 4.11 and data not shown). This suggests that Rux is not a rate-limiting regulator of DmcycEI activity. Another possibility is that DmcycEII is more potent in inactivating Rux than DmcycEI. In this case, DmcycEII, but not DmcycEI, may be expected to lead to an increase in DmcycA in the posterior MF cells. To investigate this, the localisation of DmcycA was examined following heat shock-induced ectopic expression of *DmcycEI* and *DmcycEII* in third instar larval eye imaginal discs. DmcycA was not ectopically expressed within the posterior MF cells by ectopically expressed DmcycEII, suggesting DmcycEII does not lead to ectopic S phases in the posterior MF cells by inactivating Rux and leading to increased DmcycA (Figure 4.12).

To further rule out Rux as the possible DmcycEI-specific inhibitor, the interaction of Rux with DmcycEI or DmcycEII was examined. Although Rux has been shown to bind to the cyclin box region of DmcycE, it is possible that the different N-terminal regions may influence this binding (Thomas *et al.,* 1997). Again, the yeast 2-hybrid system was used to determine whether Rux could interact with the N-terminal region of DmcycEI. Rux *(pJG-Rux)* was unable to interact with either the N-terminal 46 amino acids of DmcycEI *(pEG-46N)* or with the C-terminal 86 amino acids of DmcycEI *(pEG-Cterm)* (Table 4.2, Appendix 4.A). Furthermore, Rux interacted with both DmcycEI *(pGilda-DmEI)* and DmcycEII *(pGilda-DmEII)* to a similar degree in the yeast 2-hybrid system (Table 4.2, Appendix 4.A). The functional yeast assay (as described above) was used to test the relative inhibition of DmcycEI/DmCdk2 or DmcycEII/DmCdk2 by Rux. Yeast expressing DmcycEI/DmCdk2 or DmcycEII/DmCdk2 were not rescued by co-expression of Rux, suggesting that Rux does not inhibit DmcycEI or II at least not to the level of Dap (data not shown).

Table 4.2 : Rux interactions in the yeast 2-hybrid system

	pJG-Rux	*pJG*	Max- Min increase*
pEG-46N	0.53 ± 0.11	1.61 ± 0.45	
pEG-Cterm	0.64 ± 0.13	1.07 ± 0.35	
pGilda-DmEI	22.81 ± 10.5	1.21 ± 0.69	27.5 – 10.2 x
pGilda-DmEII	29.24 ± 2.19	1.51 ± 0.08	20.8 – 17.9 x

* Maximum and minimum increase was determined by division of the max and min lacZ units by the average vector alone (pJG) value.

Taken together, these data do not provide any evidence for Rux inhibiting DmcycEI, suggesting that an unknown inhibitory mechanism acts in the posterior part of the MF to inhibit DmcycEI activity.

Figure 4.11 : Expression of DmcycEI in *rux* mutant eye disc cannot drive posterior MF cells into S phase.

Cells undergoing S phase, as detected by BrdU labelling, in eye imaginal discs from heterozygous *rux* third instar larvae at 120 min after heat shock induction of *DmcycE* transgenes. **A.** *rux*^{8}*/+; hsp70-DmcycEI/+* eye disc showing that cells in the anterior and not posterior part of the MF are induced into S phase and **B.** *rux*^{8}*/hsp70-DmcycEII* eye disc showing that all cells within the MF are driven into S phase.

Anterior is to the right and the MF is indicated by the bar.

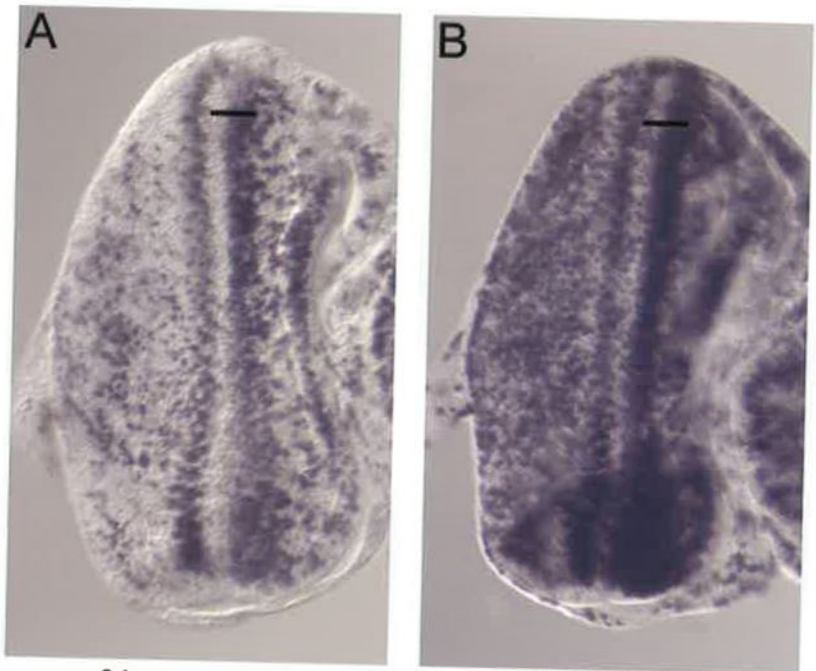

rux^{8}/+ ; hs-cycEI/+

rux^{8}/+ ; hs-cycEII/+

Figure 4.12 : Expression of DmcycEI or DmcycEII does not affect DmcycA localisation.

Immunolocalisation of DmcycA in eye imaginal discs from third instar larvae at 120 min after heat shock induction of *DmcycE* transgenes. DmcycA protein was detected using Cyclin A rabbit polyclonal antibody, followed by HRP detection. **A.** Control heat shock eye disc showing the localisation of DmcycA. **B.** *hsp70-DmcycEI* and **C.** *hsp70-DmcycEII* eye discs, showing that DmcycA protein is not ectopically expressed within the MF.

Anterior is to the right and the MF is indicated by the bar.

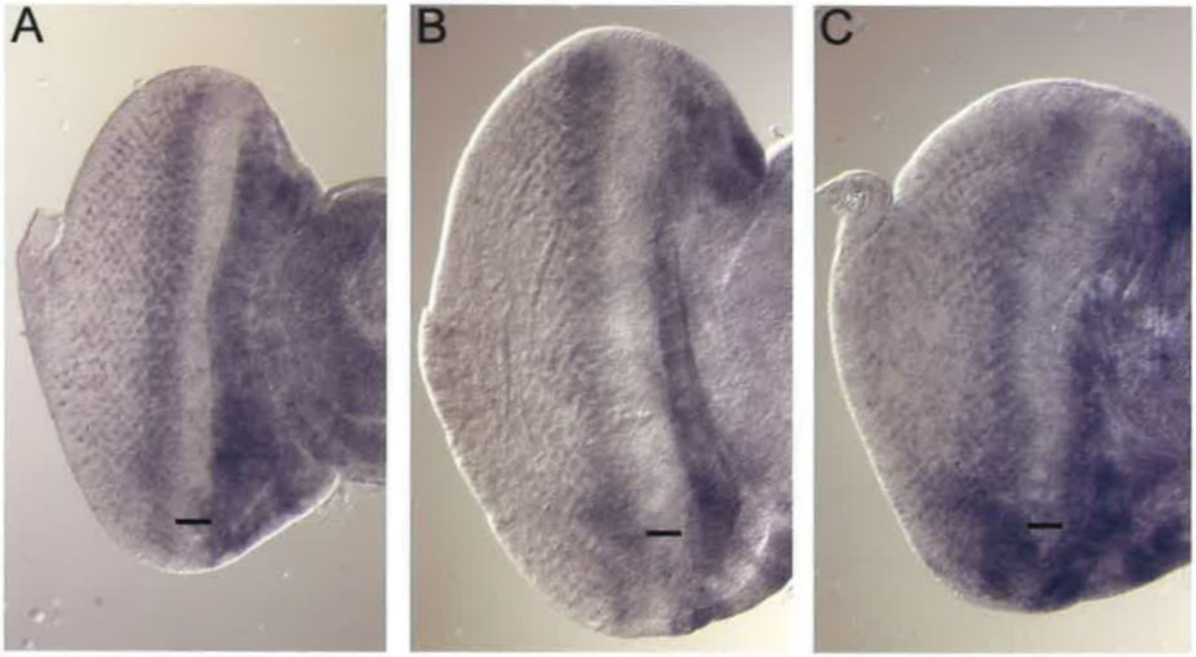

w^{1118} *hs-cycEI* *hs-cycEII*

4-4 Discussion

In this chapter, the ability of DmcycE truncations to induce G1 cells within the MF into S phase was examined. Ectopic expression of Δ195N-DmcycE, Δ195NΔ519C-DmcycE or Δ12N-DmcycE in the eye imaginal disc was able to induce all of the G1-arrested cells within the MF into S phase. These data suggest that the unique 12 N-terminal amino acids of DmcycEI may act as an inhibitory domain. This agrees with the previous observation that DmcycEII, which lacks these 12 amino acids, can also induce all G1 cells with in the MF into S phase. The inhibitory domain may be a target for an inhibitor that is present within the posterior part of the MF.

It is intriguing that the DmcycEII protein, which differs from DmcycEI only by a replacement of the 12 N-terminal amino acids of DmcycEI with a novel 119 residue sequence, is able to overcome inhibition in the posterior region of the MF. It should be noted, however, that induction of these posterior MF cells into S phase by DmcycEII occurs after S phase induction of the anterior MF cells. This suggests that DmcycEII may be partially sensitive to inhibition within the posterior region of the MF. Likewise, the N-terminal truncations of DmcycEI also showed a delay in inducing the posterior MF cells into S phase, suggesting that this inhibitory mechanism may act upon a region of DmcycE shared by DmcycEI and DmcycEII, or on the kinase partner of DmcycE, DmCdk2. Interestingly, DmcycA, which functions with Cdc2, appears to be resistant to inhibition within the posterior region of the MF, as ectopic expression of DmcycA can induce all cells within the MF into S phase with equal efficacy (Dong *et al.*, 1997). Similarly, in the complete absence of Rux function DmcycA is stabilised and accumulates in the MF, and this is sufficient to induce all the MF cells into S phase (Thomas *et al.*, 1994; 1997).

During differentiation of the eye imaginal disc, cells arrest in G1 within the MF and *DmcycE* is not expressed (Richardson *et al.*, 1995). The *Drosophila* TGF-β homologue, Dpp, is expressed in these G1 arrested cells (Masucci *et al.*, 1990) and appears to be required to establish G1 arrest in the anterior MF cells (Penton *et al.*, 1997; Horsfield *et al.*, 1998). This mechanism of G1 arrest appears to act downstream of DmcycE protein accumulation, possibly by inhibiting DmcycE/DmCdk2 activity. Analogous to the mechanism of G1 arrest by mammalian TGF-β, expression of Dpp may also lead to the induction of a Cdk inhibitor. However, the *Drosophila* p21/p27 homologue, Dap, is not expressed in the G1-arrested cells in the anterior of the MF, but only in the differentiating cells posterior to the MF (de Nooij *et al.*, 1996; Lane *et al.*, 1996), including a subset of cells overlapping DmcycE expression. Thus, the Dpp-mediated G1 arrest is unlikely to involve Dap, suggesting that it occurs by the induction of an alternative inhibitor.

In addition to the Dpp-dependent mechanism, there is a Dpp-independent mechanism that acts to induce G1 arrest in the posterior part of the MF (Horsfield *et al.*, 1998). It is possible that this Dpp-independent mechanism is equivalent to the mechanism that has been observed in this study, which acts upon the N-terminus of DmcycEI. If the Dpp-independent mechanism occurs by the induction of an inhibitor, it was possible that this inhibitor was Dap. However, results presented here showed that Dap was not detectable in the posterior part of the MF, could not bind to the N-terminus of DmcycEI, and did not show higher binding efficiency or inhibition of DmcycEI/DmCdk2 compared with DmcycEII/DmCdk2. Therefore, these data rule out the possibility that Dap is the inhibitor that acts upon the N-terminal region of DmcycEI in the posterior part of the MF.

The novel CKI, Rux, has been shown to be an important regulator of the G1 arrest in the MF and was examined for a role in regulating DmcycEI in the posterior MF cells. Although it has previously been shown that Rux interacts directly with DmcycE, there was no evidence that this was a negative interaction. Thus a possible model for DmcycEI inhibition may occur by inhibition of DmcycEI/DmCdk2 function where Rux acts as a substrate inhibitor of DmcycEI kinase function in S phase induction. However, the data described here showed that Rux could not bind to the N-terminus of DmcycEI and showed neither higher binding efficiency nor inhibition of DmcycEI/DmCdk2 compared with DmcycEII/DmCdk2. Furthermore, the levels of S phases induced by ectopic DmcycEI or II expression were not affected by reducing the dose of *rux,* and no alteration in the levels of DmcycA were detected following ectopic expression of *DmcycEI* or *DmcycEII.* It is possible that Rux may affect the localisation of DmcycEI resulting in its degradation, however no effect of DmcycEI levels were observed (see Figure 4.2). Therefore, Rux is not the mediator of the DmcycEI specific inhibition in the posterior of the MF. The absence of a role for *rux* in S phase induction is consistent with the observation that although *rux* genetically interacts with a hypomorphic allele of *DmcycE, DmcycE*^{JP}, this does not occur by increasing S phase cells (Secombe *et al.,* 1998).

Taken together, these data do not provide any evidence for Dap or Rux inhibiting DmcycEI in the posterior MF cells, suggesting that an unknown inhibitory mechanism acts in these posterior MF cells to inhibit DmcycEI. The remainder of this thesis addresses approaches undertaken in an attempt to identify a DmcycEI specific inhibitor.

Chapter 5 : A Genetic Screen for *DmcycE* Interactors

5-1 Introduction

As described in Chapter 4, analysis of ectopic *DmcycE* expression in the eye imaginal disc identified an inhibitory zone in the posterior MF that is refractory to induction of S phase by DmcycEI. The inhibition of DmcycEI was shown to be due to the unique N-terminal region of DmcycEI. A possible model to explain these results is that there is an inhibitor present in the posterior region of the MF that binds to the DmcycEI N-terminus and inhibits DmcycEI function. Two possible candidates, Dacapo and Roughex, were ruled out, suggesting that a novel inhibitor is involved.

One approach to identify the proposed DmcycEI inhibitor is to undertake a genetic interaction screen. Dose-sensitive genetic screens using rough eye phenotypes have been used successfully in *Drosophila* to identify components of regulatory pathways (for example Simon *et al.*, 1991; Raftery *et al.*, 1995; Dong *et al.*, 1997; Staehling-Hampton *et al.*, 1999). Several approaches to generate dose-sensitive systems for use in genetic interactor screens are available for *Drosophila*, including the use of hypomorphic alleles, of activated alleles, of overexpression of genes, or of dominant-negative alleles. A *DmcycE* hypomorphic allele, $DmcycE^{JP}$, has previously been used in a genetic screen (Secombe, 1999). The $DmcycE^{JP}$ allele is homozygous viable, giving rise to adults with a rough eye phenotype that is due to a decrease in DmcycE levels, resulting in fewer S phases during eye imaginal disc development (Secombe *et al.*, 1998). A $DmcycE^{JP}$ genetic interactor screen was undertaken to identify genes involved in both the upstream signals required for *DmcycE* transcription as well as genes that act upon DmcycE/DmCdk2 kinase activity and the downstream targets that lead to entry into S phase. In this screen EMS and X-ray mutagenesis was used and dominant suppressors and enhancers of the $DmcycE^{JP}$ rough eye phenotype were isolated (Secombe, 1999).

The $DmcycE^{JP}$ screen did not uncover all DmcycE interactors, as it focused only on the 2nd and 3rd chromosome and was not saturating. Therefore, to specifically identify negative DmcycEI interactors that act downstream of DmcycE transcription, overexpression of DmcycEI from a heterologous promoter was used to generate a phenotype that could be used to identify interacting genes. This system could then be used to test candidates identified in the $DmcycE^{JP}$ screen as well as screening for novel negative regulators of DmcycEI.

This chapter describes the characterisation of an ectopic expression system in the eye imaginal disc to generate a scoreable phenotype by overexpression of DmcycE, and its use in a genetic screen. A collection of *P*-element mutations was screened in an attempt to identify the putative DmcycEI inhibitor present in the posterior MF cells and to identify novel negative regulators of DmcycE and downstream negative regulators of entry into S phase.

5-2 Analysis of *GMR>gcycEI* as a system to identify *DmcycE* interactors

5-2.1 The *GMR>gcycEI* phenotype

To determine if ectopic expression of DmcycEI produced a sufficiently sensitive phenotype for use in a genetic screen, the effect of tissue-specific ectopic expression of DmcycEI was analysed. As described in Chapter 4, heat shock-induced ectopic expression of *DmcycE* transgenes results in an increase in S phases in the eye imaginal disc, which results in a rough eye phenotype (Richardson *et al.,* 1995). To determine if tissue-specific ectopic expression resulted in a similar rough eye phenotype that was sensitive to levels, a *DmcycEI* transgene (a genomic *DmcycEI* mini-gene under *UAS* control (*UAS-gcycEI*), a gift from C. Lehner) was used for ectopic expression analysis.

Tissue-specific expression of *UAS-gcycEI* was driven in the eye imaginal disc under control of various promoters using the *GAL4/UAS* system. The *GAL4/UAS* system is a useful tool in *Drosophila* for driving expression of a gene of interest by specific promoters (Brand and Perrimon, 1993). It is a two component system where *GAL4* expression is driven by tissue-specific enhancers, and the presence of GAL4 then results in transcriptional activation from the GAL4 binding sites, *UAS*, driving a gene of interest. Several drivers were examined, including *dpp-GAL4, hairy-GAL4* and *eyeless-GAL4*. However, ectopic expression of *UAS-gcycEI* from these drivers did not produce a usable rough eye phenotype (H. Richardson pers. com.).

Ectopic expression of *UAS-gcycEI* using the *GMR* (glass multimer reporter) promoter, *GMR-GAL4, UAS-gcycEI (GMR>gcycEI)* resulted in a mild rough eye phenotype (Figure 5.1). In the third instar larval eye imaginal disc the *GMR* promoter drives expression of *GAL4* (*GMR-GAL4)* in the posterior region of the disc (Hay *et al., 1994*). However, as this is a two component system, a delay in DmcycEI expression is expected. The rough eye phenotype of *GMR>gcycEI* was found to be due to an increase in S phases posterior to the MF in the eye imaginal disc, which is consistent with the pattern of expression from the *GMR* promoter (Figure 5.1). Even though this will not result in increased expression of DmcycEI in the MF, it was considered possible that the proposed MF inhibitor may also be expressed in the posterior region of the eye imaginal disc or may lead to ectopic S phases in the MF when halved in dosage, resulting in enhancement of the *GMR>gcycEI* rough eye phenotype.

The *GMR>gcycEI* rough eye phenotype was more severe when the transgene was present in 2 copies than in a single copy, indicating that this eye phenotype was sensitive to the level of DmcycE (data not shown). Also, when flies were maintained at 18°C, rather that at 25°C, the rough eye phenotype was milder due to the decrease in expression of *GAL4* at lower temperature (data not shown).

5-2.2 Sensitivity of the *GMR>gcycEI* phenotype in identifying dominant enhancers

To assess the sensitivity of the *GMR>gcycEI* rough eye phenotype for use in a genetic screen, previously identified negative regulators of DmcycE were tested for modification of the phenotype. Two such negative regulators, *dap* and *Rbf,* have been shown to interact with $DmcycE^{JP}$, whereby reducing the dose of either *dap* or *Rbf* resulted in an increase in S phases and suppression of the $DmcycE^{JP}$ rough eye phenotype (Secombe *et al.,* 1998). The role of Rb in mammalian cells has been characterised as a transcriptional repressor of Cyclin E, and in *Drosophila* Rbf has been shown to function downstream of DmcycE, being phosphorylated and inactivated by DmcycE/DmCdk2 (Du and Dyson, 1999). As expected, reducing the dose of either *dap* or *Rbf* by half resulted in a more severe, or enhanced, *GMR>gcycEI* rough eye phenotype, and this was due to a further increase in S phases in the eye imaginal disc (Figure 5.2). Therefore, the *GMR>gcycEI* phenotype is sensitive to a reduction in the dosage of known negative regulators of the G1 to S phase transition, thus providing the basis for a sensitised genetic screening system.

5-3 Identification of *DmcycE* interactors by screening for enhancement of the *GMR>gycycEI* rough eye phenotype

5-3.1 Testing candidates from similar screens

The $DmcycE^{JP}$ screen identified novel dominant suppressor alleles that are candidate inhibitors of DmcycE. Suppression of the $DmcycE^{JP}$ phenotype could occur as the result of reducing the dose of a DmcycE inhibitor, such that there is an increase in DmcycE activity and S phases. Such suppressors were then candidates for enhancers of the *GMR>gcycEI* rough eye phenotype. Table 5.2 summarises the results of examination of $DmcycE^{JP}$ suppressors for enhancement *GMR>gcycEI* (see Appendix 5.A).

In addition the $DmcycE^{JP}$ screen was also used to test a collection of third chromosome deficiencies for genetic interactions (Secombe, 1999). This identified 10 regions on the third chromosome that suppressed the $DmcycE^{JP}$ rough eye phenotype and therefore removed potential genes involved in *DmcycE* regulation. Candidate genes could not be assigned to 7 of the chromosomal regions (Secombe, 1999). Therefore these deficiency regions were tested for enhancement of *GMR>gcycEI* (Appendix 5.B). A summary of the 3rd chromosome regions that enhanced *GMR>gcycEI* rough eye phenotype is listed in Table 5.1.

Together this revealed, as enhancers of *GMR>gcycEI,* five 3rd chromosome deficiency regions (Table 5.1) and five $DmcycE^{JP}$ suppressors, as candidates for DmcycEI inhibitors.

Figure 5.1 : The *GMR>gcycEI* rough eye is caused by an increase in S phases.

(A,B) Scanning electron micrographs of adult eyes from **A.** wild-type w^{1118} and **B.** *GMR>gcycEI/+*. Ectopic expression of DmcycEI indirectly from the *GMR-GAL4* driver results in a disruption to the ordered array of ommatidia and bristles.

(C,D) S phase cells, labelled with BrdU, in eye imaginal discs from third instar larvae. **C.** wild-type and **D.** *GMR>gcycEI/+* eye discs showing that the number of S phases is significantly increased in *GMR>gcycEI/+*.

Anterior is to the right and the MF is indicated by the bar.

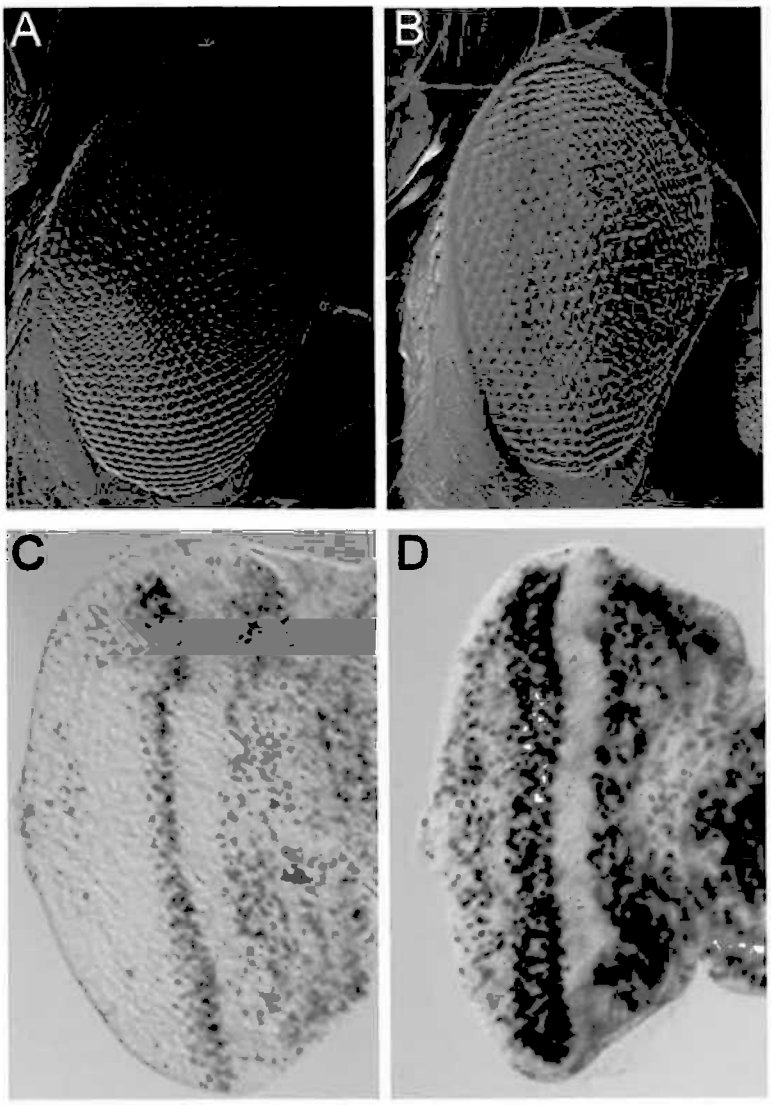

wild type

GMR>gcycEI/+

Figure 5.2 : The *GMR>gcycEI* rough eye phenotype is enhanced by *dacapo* and *Rbf*.

(A-C) Scanning electron micrographs of adult eyes.

A. *GMR>gcycEI/+*, **B.** *GMR>gcycEI/dap*^{4454} and **C.** *Rbf*^{14}*/+;GMR>gcycEI/+* showing an enhancement of the *GMR>gcycEI/+* rough eye phenotype.

(D-F) S phase cells as detected by BrdU labelling in eye imaginal disc from third instar larvae.

D. *GMR>gcycEI/+*, **E.** *GMR>gcycEI/dap*^{4454} and **F.** *Rbf*^{14}*/+;GMR>gcycEI/+* eye discs showing an increase in the number of S phases posterior to the MF.

Anterior is to the right and the MF is indicated by the bar.

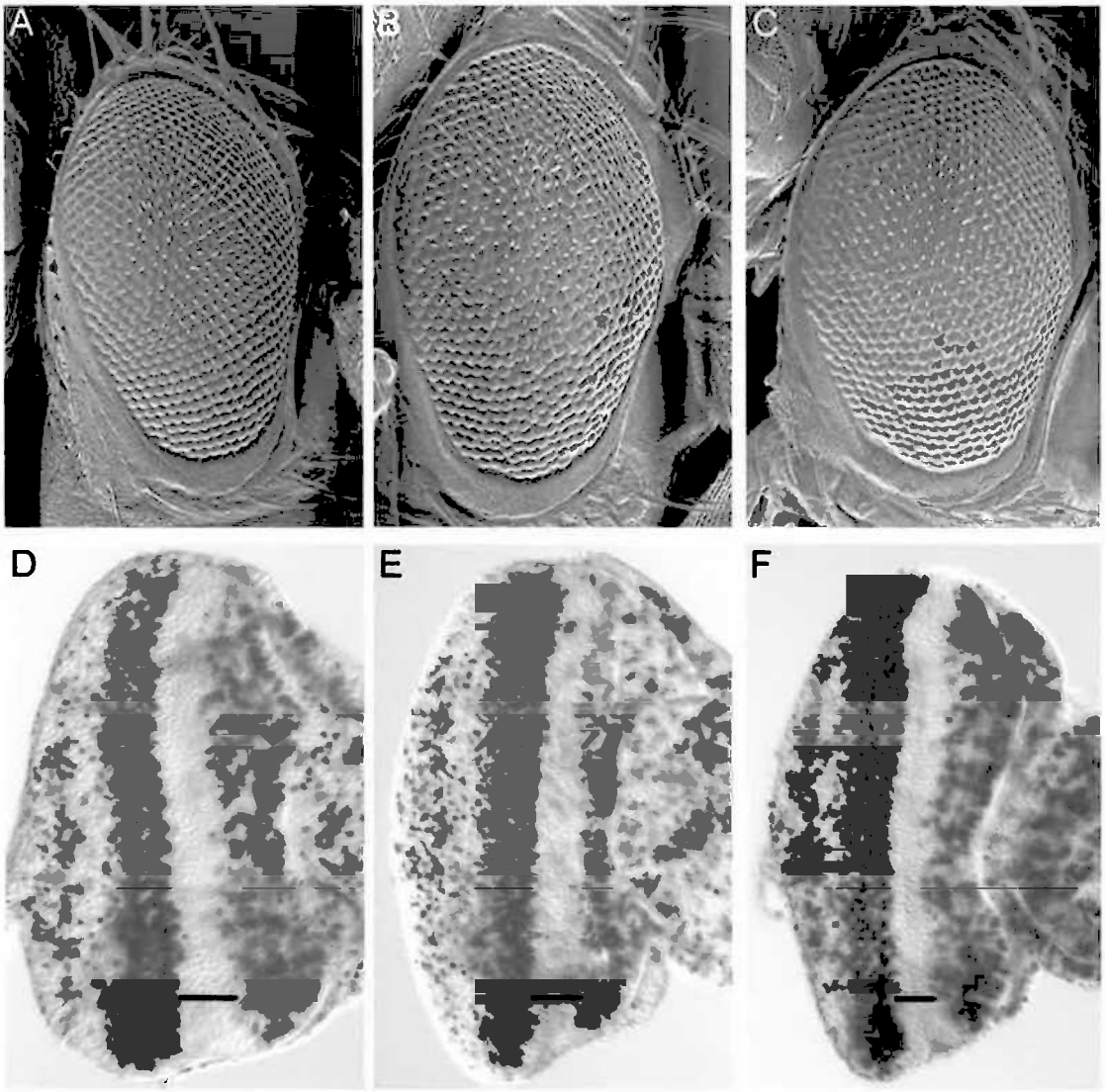

GMR>gcycEI/+ *GMR>gcycEI/dap^{4454}* *Rbf^{14}/+;GMR>gcycEI/+*

Table 5.1: Summary of 3rd chromosome deficiencies that enhanced *GMR>gcycEI*

Deficiency	Cytology	*GMR>gcycEI*
Df(3L)M21	62F; 63D	Enhanced
Df(3L)HR119	63C2; 63F7	Enhanced
Df(3L)vin5	68A2-3; 69A1-3	Mild enhancement
Df(3R)p712	84D4-6; 85B6	Enhanced
Df(3R)by10	85D8-12; 85E7-F1	Not tested
Df(3R)ChaM7	90F1-F4; 91F5	No effect
Df(3R)slo^{8}	96A2-7; 96D2-4	No effect
Df(3R)B81	99C8; 100F5	Mild enhancement

During the period of this study a genetic interactor screen was undertaken by another group, using the *sevenless* enhancer *(Esev)* to ectopically express *DmcycEI* (Lane *et al.,* 2000). Transgenic flies containing E*sev-cycE*, a *DmcycEI* cDNA downstream of two copies of *sev* enhancer, drives expression of *DmcycEI* in cells posterior to the MF in the eye imaginal disc which results in a rough eye phenotype due to an increase in S phases in these cells (Lane *et al.,* 2000). This phenotype was used to screen for EMS mutations that dominantly modified *Esev-cycE*. This screen identified as enhancers 8 single hit mutations (including *scab*) as well as 3 complementation groups corresponding to *split ends/polycephalon*, *dacapo,* and *dE2F1*. The mutations identified in this screen were considered likely to also dominantly enhance *GMR>gcycEI*. Interestingly, not all of the *Esev-cycE* enhancers tested interacted with *GMR>gcycEI* (Appendix 5.C). The results of this are summarised in Table 5.2. This may be due to the differences in expression pattern of *DmcycEI* in eye disc from the different promoters, as *sev* is expressed in a subset of *GMR* expressing cells, and/or because *Esev-cycE* results in direct expression of *DmcycEI* as opposed to the delayed expression of *DmcycEI* by the two step system of *GMR-GAL4, UAS-gcycEI.*

The human Cyclin E inhibitor, p21^{Cip1}, blocks S phases when expressed in *Drosophila* (de Nooij and Hariharan, 1995). This was used as the basis of a genetic screen whereby expression of *p21*^{Cip1} directly from the *GMR* promoter (*GMR-p21)* results in a rough eye phenotype due to a reduction in S phases in the posterior eye imaginal disc (de Nooij, 1998). Since the phenotype produced by overexpression of p21 results in a decrease in S phases, it is expected that suppressors of this phenotype would act as enhancers of *GMR>gcycEI.* Single suppressor alleles identified in the *GMR-p21* screen were examined for their ability to enhance the *GMR>gcycEI* rough eye phenotype (Appendix 5.D). However, none of these suppressors of *GMR-p21* affected the *GMR>gcycEI* phenotype.

A genetic interactor screen for negative regulators of E2F/DP was undertaken by Staehling-Hampton *et al.* (1999). This screen made use of a rough eye phenotype produced in transgenic flies expressing *dE2F, dDP,* and the baculovirus cell death inhibitor protein p35 all under direct control of the *GMR* promoter (*GMR-dE2F, dDP, p35*). The phenotype results from an increase in S phases in the posterior part of the eye imaginal disc which is intensified by preventing cell death (Staehling-Hampton *et al.*, 1999). Dominant enhancers identified include *brahma, moira,* and *osa* (all *trithorax* group genes), *pointed* (an ETS family TF) and *split ends/ polycephalon* (a regulator of Deformed homeotic function) as well as novel interactors. As this screen made use of an increase in S phases in the posterior part of the eye imaginal disc, a similar consequence as occurs with *GMR>gcycEI* expression, enhancers identified in this screen were candidates for enhancers of *GMR>gcycEI* (Appendix 5.E). Table 5.2 summarises the results of screening these *GMR-dE2F, dDP, p35* interactors against *GMR>gcycEI.*

Table 5.2: Enhancers of *GMR>gcycEI* identified from alternative screens

DmcycE^{JP}	***Esev-cycE***	***GMR-dE2F dDP p35***
II.127S3 (l(2)gl)	*E(Esev-CycE)^{e93} (scab)*	*E(E2F/DP) rpd^{16}*
II.11 62S9 (scab)		*E(E2F/DP) 2^{B}*
II.10 65S13		*point^{kirk}*
brahma		
moira		

The finding that *brahma* and *moira* enhanced the *GMR>gcycEI* rough eye phenotype is consistent with the biochemical evidence that they act downstream of DmcycE (Brumby *et al.*, 2002). A role for how the other genes identified act to enhance *GMR>gcycEI* remains to be determined.

Since a subset of interactors identified in other screens enhanced *GMR>gcycEI,* it therefore appears that *GMR>gcycEI* is a useful system to screen for novel interactors and the putative DmcycEI inhibitor.

5-3.2 Identification of novel negative regulators of DmcycEI

The identification of novel genes involved in DmcycEI regulation relies on the generation of random mutations in single genes throughout the genome. Three common approaches used to generate such mutations in *Drosophila* are chemical (EMS), X-ray and *P*-element insertional mutagenesis. Rather than generate additional EMS or X-ray mutations,

existing *P*-element mutations were screened. The main advantage of *P*-element mutations is that the *P*-element acts as a tag to identify the genomic localisation of the insertion, thus allowing for rapid identification of a nearby gene likely to be disrupted. At the commencement of the screen approximately 25% of the estimated 3600 essential *Drosophila* genes are likely to be affected in a collection of *P*-element mutations available (Spradling *et al.,* 1999). To asses the value of this screen, a moderate scale approach focusing on third chromosome *P*-elements mutations was carried out. This pilot screen would clearly not be exhaustive.

A primary collection of *P*-elements, of which approximately 65% of the *P* insertions have been shown to be the cause the recessive lethality, has been generated from seven separate *P*-element mutagenesis screens and was available from the public stock centre (Spradling *et al.*, 1999). Third chromosome *P* insertions from this collection as well as additional *P*-element alleles from Spradling *et al.* (1995), totalling 552 lines, were obtained (Appendix 5.F), and screened for enhancement of the *GMR>gcycEI* rough eye phenotype. The progeny from a cross between flies homozygous for *GMR>gcycEI* on the 2nd chromosome and heterozygous 3rd chromosome *P*-element mutants were examined for enhancement of the rough eye phenotype. An enhanced rough eye phenotype was scored by examination under a dissection microscope and comparison to the control rough eye of heterozygous *GMR>gcycEI.* Adults with an enhanced rough eye were then examined more closely by scanning electron microscopy. A summary of enhancers identified is listed in Table 5.3, and described in detail in Section 5-4.

Table 5.3: Summary of *P*-element enhancers of *GMR>gcycEI*

***P*-element**	**Cytology**
l(3)05408	68C12-13
orb^{dec}	94E1-94E10
l(3)rk344	97D1-2
l(3)06734	99B8-10
l(3)j2D5	99F1-2
l(3)00720	100B5-7

This screen identified 6 *P*-elements as enhancers of *GMR>gcycEI* (Table 5.3). The genes affected in these *P*-element lines are candidates for DmcycEI inhibitors. The characterisation of the *P*-element interactors is described below.

5-4 Analysis of *P*-element enhancers

Initial characterisation of the *GMR>gcycEI* interacting *P*-elements (listed in Table 5.3) included examination of whether the enhancement was occurring at the level of S phases in the eye imaginal disc. To determine if an enhancer was acting at the level of S phase, *P*-element insertion chromosomes balanced over *TM6B* third chromosome balancer, which carries the *Tubby* dominant larval marker, were crossed to homozygous *GMR>gcycEI*. *GMR>gcycEI/+; P-element/+* larvae were then examined for the pattern of S phases in the eye imaginal disc.

To further characterise the *P*-element interactor a number of genetic crosses were carried out as described below. It is expected that enhancers of *GMR>gcycEI* would act as suppressors of $DmcycE^{JP}$, as their respective rough eye phenotypes are due to opposite effects on S phase induction. To determine whether the identified *P*-elements also modified $DmcycE^{JP}$ required examining the effect of the *P*-element mutation in a $DmcycE^{JP}$ homozygous background. This required several crosses (Figure 5.3). Flies and larvae of the genotype $DmcycE^{JP}$; *P-element/+* were then examined for the effect on the rough eye phenotype and on the pattern of S phases in the eye imaginal disc.

As the *GMR>gcycEI* screen was initiated in an attempt to identify a DmcycEI-specific inhibitor, the effect of the identified *P*-elements upon the rough eye phenotype of ectopic expression of *DmcycEII* (driven by *GMR*, using the GAL4/UAS system: *UAS-cycEII (X); GMR-GAL4*, referred to as *GMR>cycEII)* was examined. As ectopic expression of DmcycEI and DmcycEII in the eye imaginal disc differ in their abilities to induce G1 phase cells within the MF into S phase, a DmcycEI-specific inhibitor would be expected not to enhance the rough eye phenotype of *GMR>cycEII*. The progeny from a cross between homozygous *GMR>cycEII* and heterozygous 3rd chromosome *P*-element mutants were examined for enhancement of the *GMR>cycEII* rough eye phenotype.

The effect of the *P*-element mutations on the rough eye phenotype caused by overexpression of *p21* was also tested. Overexpression of *p21* directly from the *GMR* promoter results in a rough eye phenotype due to a reduction in S phases in the posterior eye imaginal disc (de Nooij and Hariharan, 1995). Therefore, enhancers of *GMR>gcycEI* would be expected to suppress the *GMR-p21* rough eye phenotype. Likewise, effect of the *P*-elements on the rough eye phenotype caused by overexpression of *dE2F, dDP* and *p35* under *GMR* control (*GMR-dE2F, dDP, p35)* was also tested. This phenotype results from an increase in S phases in the posterior region of the eye imaginal disc, so enhancers of *GMR>gcycEI* would be expected to enhance the *GMR-dE2F, dDP, p35* rough eye phenotype.

In addition to G1 regulators, the regulators of DmcycA, *rux* and *rca1* were also identified as modifiers of $DmcycE^{JP}$. Therefore, the *P*-elements identified as modifiers of *GMR>gcycEI*

were examined for their ability to modify the *rux* rough eye phenotype. Hypomorphic *rux* mutants, *rux*^{3}, have a rough eye phenotype due to inappropriate expression of DmcycA protein in the MF, which results in ectopic S phases. It was therefore expected that if an enhancer of *GMR>gcycEI* acts as a modifier of *rux*^{3}, then the gene may also be involved in DmcycA regulation.

To further validate the interaction, to show that it was due to the mutation of the gene into which the *P*-element was inserted, rather than an independent mutation on the chromosome, other alleles of the gene were tested where available. If independent alleles were not available, deficiency stocks covering the point of insertion of the *P*-element were used. In the case where the site of insertion of the *P*-element was not verified, genetic interactions could not easily be confirmed or discounted. Therefore, in the absence of independent null alleles, validation of the interaction required the generation of *P*-element revertants that could then be tested for reversion of the genetic interaction.

The characterisation of each of the interacting *P*-elements is discussed below.

5-4.1 *l(3)06734*

The *P*-element *l(3)06734* was identified as a strong enhancer of *GMR>gcycEI*, and also suppressed the *DmcycE*^{JP} rough eye phenotype (Figure 5.4). To examine if the modifications of the rough eye phenotypes were due to an increase in S phases, BrdU labelling was carried out on third larval instar eye imaginal discs. Unexpectedly, it was found that in *GMR>gcycEI* eye imaginal discs, reducing the dose of *l(3)06734* appears to actually decrease the number of S phases in the posterior region (Figure 5.4). When the dose of *l(3)06734* was reduced in a homozygous *DmcycE*^{JP} eye imaginal disc there was no obvious increase in S phases observed, which would have been expected if suppression of the *DmcycE*^{JP} rough eye phenotype was at the level of S phases (Figure 5.4). These results suggested that the enhancement of the *GMR>gcycEI* phenotype by *l(3)06734* was not due to an effect on S phases.

As the interactions between *l(3)06734* and *DmcycE* did not seem to be acting at the level of S phases, other genetic interactions were examined in order to determine how this effect may be occurring. Reducing the dose of *l(3)06734* also acted to enhance the *GMR>cycEII* rough eye phenotype and again this did not occur at the level of S phase (data not shown). The effect of reducing the dose of *l(3)06734* on the *rux*^{3} phenotype was examined, and showed no interaction, indicating that *l(3)06734* acts independently of Rux. Further genetic analysis with other cell cycle regulators indicates that *l(3)06734* appears to act inconsistently, suppressing the *GMR-p21* rough eye phenotype as expected, but also suppressing *GMR-dE2F, dDP, p35*, which is opposite to what was expected. *l(3)06734* has also been identified in a genetic screen for suppressors of the Ras1 signalling pathway (Maixner *et al.*, 1998).

Figure 5.3 : Generation of a stock for analysis of *P*-element effect on *DmcycE^{JP}*.

A. Generation of a stock homozygous for *DmcycE^{JP}* and heterozygous for *P*-element interactor. *P*-element mutations, balanced using *TM6B* and also the second chromosome balancer, *Cy*O, carrying the dominant marker *Curly*, were crossed to *DmcycE^{JP}* homozygotes, carrying *TM6B*. The *DmcycE^{JP}*/*Cy*O; *P-element*/*TM6B* progeny were selected and crossed again to *DmcycE^{JP}*; +/*TM6B*. This cross gave rise to the stock *DmcycE^{JP}*; *P-element*/*TM6B*.

B. This stock was then used to cross to homozygous *DmcycE^{JP}* enabling the rough eye phenotype to be examined without the presence of the *TM6B* balancer. Larvae of the genotype *DmcycE^{JP}*; *P-element*/+ were distinguished by the absence of *Tubby* and examined for the pattern of S phases in the eye imaginal disc.

A.

$$DmcycE^{JP}\,;\frac{+}{TM6B} \quad \text{X} \quad \frac{+}{CyO}\,;\frac{[P]}{TM6B}$$

$$\downarrow$$

$$DmcycE^{JP}\,;\frac{+}{TM6B} \quad \text{X} \quad \frac{DmcycE^{JP}}{CyO}\,;\frac{[P]}{TM6B}$$

$$\downarrow$$

Stock : $DmcycE^{JP}\,;\frac{[P]}{TM6B}$

B.

Interaction cross: $DmcycE^{JP}\,;+ \quad \text{X} \quad DmcycE^{JP}\,;\frac{[P]}{TM6B}$

$$\downarrow$$

Select larvae : $DmcycE^{JP}\,;\frac{[P]}{+}$

Figure 5.4 : *l(3)06734* enhances *GMR>gcycEI* and suppresses *DmcycE^{JP}*.

(A-D) Scanning electron micrographs of adult eyes. **A.** *GMR>gcycEI/+;+* and **B.** *GMR>gcycEI/+; l(3)06734/+* rough eye phenotypes showing enhancement of the *GMR>gcycEI* rough eye phenotype. **C.** *DmcycE^{JP}*; + and **D.** *DmcycE^{JP}; l(3)06734/+* rough eye phenotypes showing suppression of the *DmcycE^{JP}* rough eye phenotype.

(E-H) S phases cells as detected by BrdU labelling of eye discs from third instar larvae. **E.** *GMR>gcycEI/+;+* and **F.** *GMR>gcycEI/+; l(3)06734/+* eye discs showing that enhancement of the *GMR>gcycEI* rough eye phenotype does not result from an increase in the number of S phases posterior to the MF. **G.** *DmcycE^{JP}*;+ and **H.** *DmcycE^{JP}; l(3)06734/+* eye discs showing that suppression of the *DmcycE^{JP}* rough eye phenotype does not result from an increase in the number of S phases posterior to the MF.

Anterior is to the right and the MF is indicated by the bar.

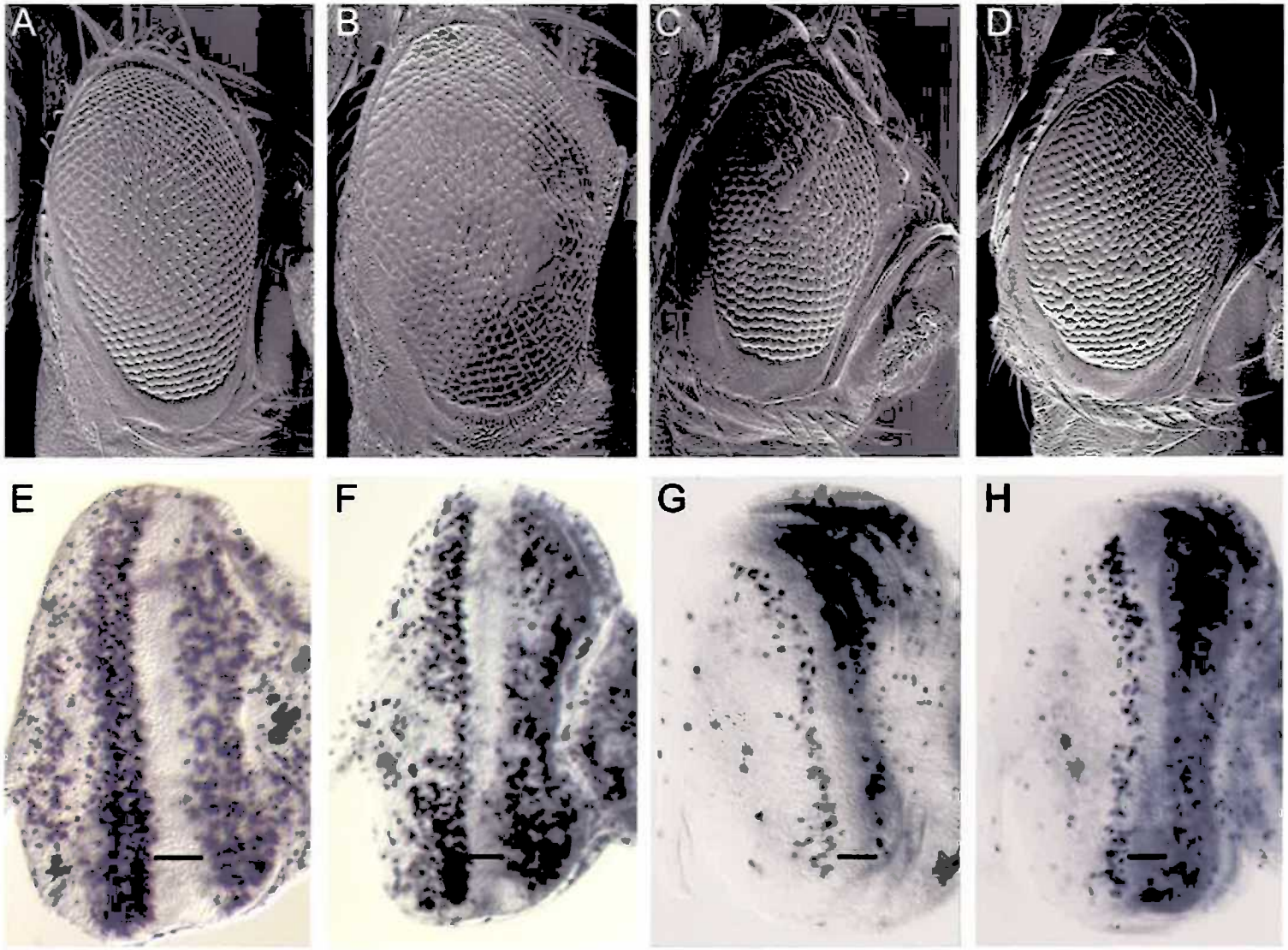
A
B
C
D
E
F
G
H
GMR>gcycE/+
GMR>gcycEI/+; l(3)06734/+
DmcycE^JP
DmcycE^JP; l(3)06734/+

Since the characterisation of the *l(3)06734* interaction indicated that it does not appear to act at the level of S phases and behaved inconsistently in genetic analyses, this suggests that *l(3)06734* is unlikely to encode a DmcycEI inhibitor. Therefore, no further characterisation of this *P*-element was undertaken.

5-4.2 *l(3)05408*

The *P*-element enhancer of *GMR>gcycEI*, *l(3)05408*, also suppressed the $DmcycE^{JP}$ rough eye phenotype (Figure 5.5). To test if the modifications on the rough eye phenotypes were due to an increase in S phases, BrdU labelling was carried out on third instar larval eye imaginal discs. Reducing the dose of *l(3)05408* resulted in an increase in the number of S phases in the posterior region of the eye imaginal disc in both *GMR>gcycEI* and homozygous $DmcycE^{JP}$ eye imaginal discs (Figure 5.5).

Further analysis of genetic interactions with *l(3)05408* indicated that it appears to act consistently as a downstream modifier of *DmcycE,* as it mildly enhanced *GMR-dE2F, dDP, p35*, mildly suppressed *GMR-p21*, and acts independently of Rux, as there was no effect on the *rux* phenotype (Table 5.4). Importantly, reducing the dose of *l(3)05408* appeared to have no effect on the *GMR>DmcycEII* rough eye phenotype, indicating that it may interact specifically with DmcycEI.

Table 5.4: Genetic interactions of *l(3)05408*

	Affect on S phases	***l(3)05408***
$DmcycE^{JP}$	decrease	Suppressed
GMR-p21	decrease	Mild suppression
GMR>DmcycEII	increase	No effect
GMR-dE2F, dDP, p35	increase	Mild enhancement
rux^{3}	increase	No effect

The location of *l(3)05408*, as determined by *in situ* hybridisation to polytene chromosomes, is 68C12-13 (FlyBase). The interaction between *GMR>gcycEI* and *l(3)05408* was verified by examining a deficiency in the region, as no other alleles were available to test. To verify that the recessive lethality was due to the *P*-element insertion, a deficiency uncovering 68C12-13, *Df(3L)vin5* (68A2-3; 69A1-3), was tested for complementation to *l(3)05408*. This deficiency failed to complement the *P*-element, indicating that the *P* insertion is lethal. This deficiency was tested for a genetic interaction with *GMR>gcycEI*, and showed a mild enhancement of the rough eye phenotype, consistent with a gene in the deficiency enhancing the *GMR>gcycEI* rough eye phenotype. *Df(3L)vin5* has also been shown to suppress the $DmcycE^{JP}$

Figure 5.5 : *l(3)05408* enhances *GMR>gcycEI* and suppresses *DmcycE^{JP}*.

(A-D) Scanning electron micrographs of adult eyes. **A.** *GMR>gcycEI/+;+* and **B.** *GMR>gcycEI/+; l(3)05408/+* eye phenotypes showing enhancement of the *GMR>gcycEI* rough eye phenotype. **C.** *DmcycE^{JP};+* and **D.** *DmcycE^{JP}; l(3)05408/+* eye phenotypes showing suppression of the *DmcycE^{JP}* rough eye phenotype.

(E-H) S phases as detected by BrdU labelling of eye discs from third instar larvae. **E.** *GMR>gcycEI/+;+* and **F.** *GMR>gcycEI/+; l(3)05408/+* eye discs showing enhancement of the *GMR>gcycEI* rough eye phenotype results from an increase in the number of S phases posterior to the MF. **G.** *DmcycE^{JP};+* and **H.** *DmcycE^{JP}; l(3)05408/+* eye discs showing suppression of the *DmcycE^{JP}* rough eye phenotype results from an increase in the number of S phases posterior to the MF.

Anterior is to the right and the MF is indicated by the bar.

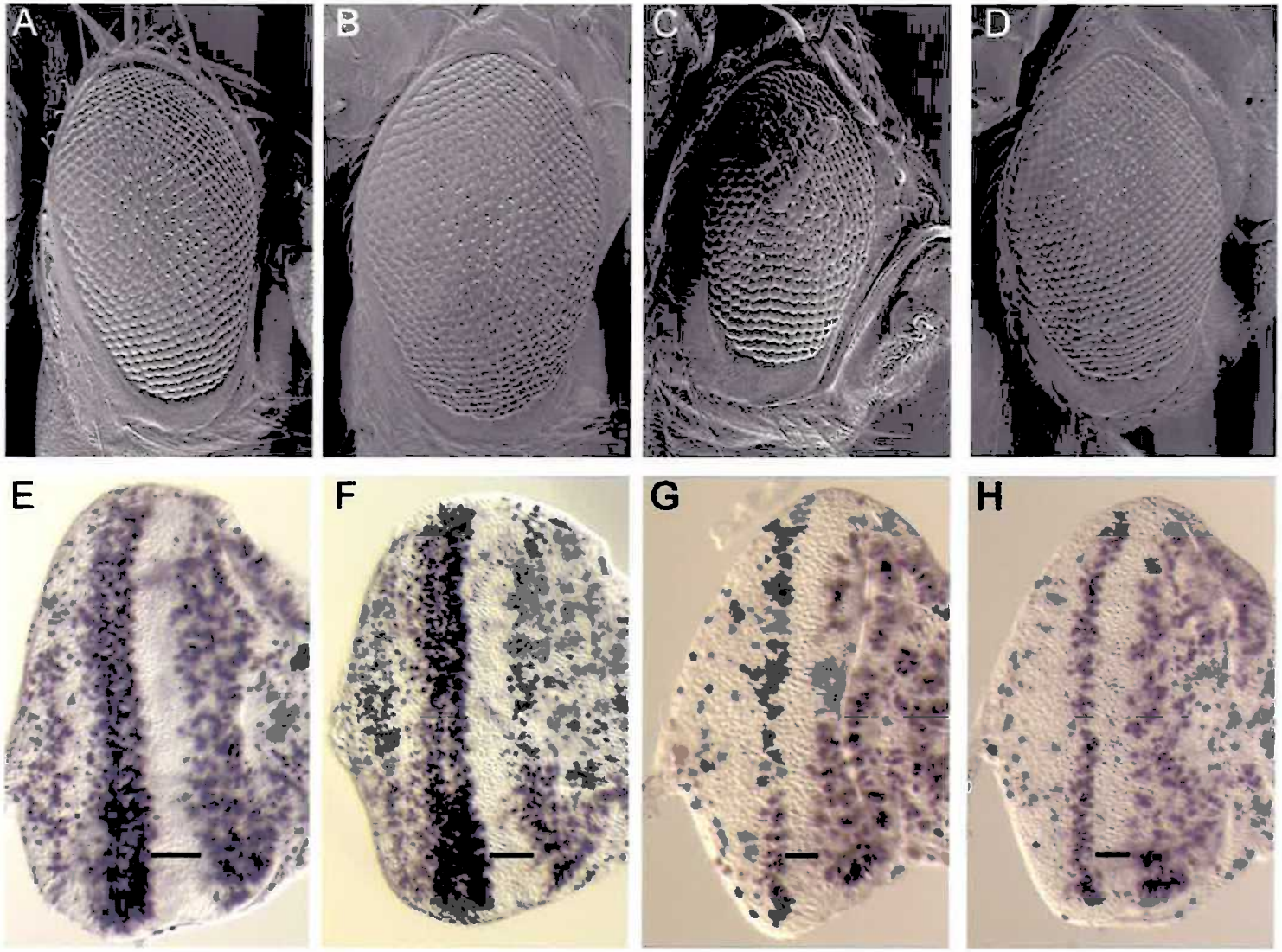
A
B
C
D
E
F
G
H
GMR>gcycEI/+
GMR>gcycEI/+; I(3)05408/+
DmcycE^JP
DmcycE^JP; I(3)05408/+

rough eye phenotype, but no obvious candidates were identified in the region (Secombe, 1999). Therefore, the *P*-element *l(3)05408* is a candidate for this interaction. To further verify this interaction, *P*-element reversions need to be generated.

The genomic sequence recovered from the 5' end of the *l(3)05408* *P*-element was available (FlyBase). To analyse the adjacent genes a BLAST search with this sequence was carried out, localising the *P*-element insertion to 68C7, indicating that there are inaccuracies in the cytological mapping. Further database searches against the *P* sequence identified the predicted gene, *CG7394*, as a candidate for the *P*-element mutation. *CG7394* putatively encodes a protein with homology to DnaJ domain-containing protein (see Discussion).

5-4.3 *l(3)00720*

The *P*-element enhancer of *GMR>gcycEI*, *l(3)00720*, also suppressed the $DmcycE^{JP}$ rough eye phenotype (Figure 5.6). To examine if the modifications on the rough eye phenotypes were due to an increase in S phases, BrdU labelling was carried out on third instar larval eye imaginal discs. Reducing the dose of *l(3)00720* resulted in an increase in the number of S phases in the posterior region of the eye imaginal disc in both *GMR>gcycEI* and homozygous $DmcycE^{JP}$ eye imaginal discs (Figure 5.6).

Further analysis of genetic interactions with *l(3)00720* indicates that it appears to act consistently as a downstream modifier of *DmcycE,* as it also enhanced *GMR-dE2F, dDP, p35*, suppressed *GMR-p21*, and acts independently of Rux, as there was no effect on the *rux* phenotype (Table 5.5). *l(3)00720* requires examination against *GMR>cycEII* to determine whether the interaction is specific to *DmcycEI.*

Table 5.5: Genetic interactions of *l(3)00720*

l(3)00720	Affect on S phases	Modification
$DmcycE^{JP}$	decrease	Suppressed
GMR-p21	decrease	Mild Suppression
GMR>DmcycEII	increase	Not tested
GMR-dE2F, dDP, p35	increase	Mild enhancement
rux^{3}	increase	No effect

The location of *l(3)00720*, as determined by *in situ* hybridisation to polytene chromosomes was placed at 100B5-7 (FlyBase). To verify the interaction between *GMR>gcycEI* and *l(3)00720,* a deficiency in the region was examined, as no other alleles were available. *Df(3R)tll-e* (100A2; 100C2-3) has been verified as failing to complement *l(3)00720* (Spradling *et al.,* 1999). Therefore, this deficiency was obtained to confirm the localisation and

Figure 5.6 : *l(3)00720* enhances *GMR>gcycEI* and suppresses *DmcycE^{JP}*.

(A-D) Scanning electron micrographs of adult eyes. **A.** *GMR>gcycEI/+;+* and **B.** *GMR>gcycEI/+; l(3)00720/+* eye phenotypes showing enhancement of the *GMR>gcycEI* rough eye phenotype. **C.** *DmcycE^{JP};+* and **D.** *DmcycE^{JP}; l(3)00720/+* eye phenotypes showing suppression of the *DmcycE^{JP}* rough eye phenotype.

(E-H) S phases as detected by BrdU labelling of eye discs from third instar larvae. **E.** *GMR>gcycEI/+;+* and **F.** *GMR>gcycEI/+; l(3)00720/+* eye discs showing enhancement of the *GMR>gcycEI* rough eye phenotype results from an increase in the number of S phases posterior to the MF. **G.** *DmcycE^{JP};+* and **H.** *DmcycE^{JP}; l(3)00720/+* eye discs showing suppression of the *DmcycE^{JP}* rough eye phenotype results from an increase in the number of S phases posterior to the MF.

Anterior is to the right and the MF is indicated by the bar.

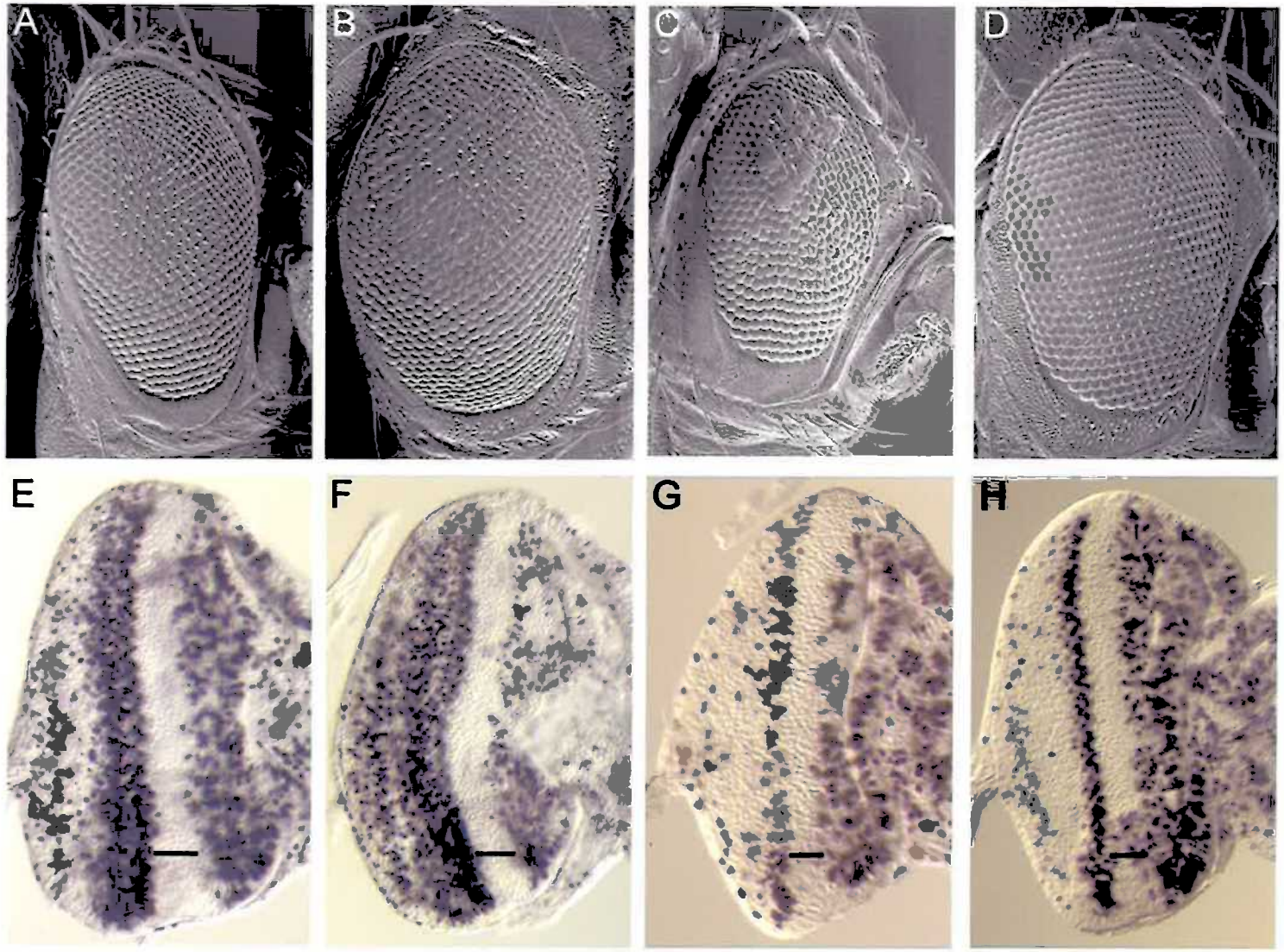
A
B
C
D
E
F
G
H
GMR>gcycEI/+
GMR>gcycEI/+; l(3)00720/+
DmcycE^JP
DmcycE^JP; l(3)00720/+

used to verify the genetic interaction. However, it was found that *Df(3R)tll-e* complemented *l(3)00720* (19/70), indicating that this *P*-element is either not lethal, or is incorrectly localised. To investigate this, *Df(3R)tll-e,* was tested for a genetic interaction with *GMR>gcycEI,* and showed mild enhancement of the rough eye phenotype, indicating there is a gene in the deficiency enhancing the *GMR>gcycEI* rough eye phenotype. However, as the *P*-element *l(3)00720* complements *Df(3R)tll-e* it may not be a candidate for this interaction, or alternatively may be a non-lethal interactor.

To determine the localisation of the *P*-element, analysis of the genomic sequence derived from the 5' end of *l(3)00720* (STS Dm0496, FlyBase) by BLAST search revealed that this sequenced localised to chromosome 2L region 40A-40C (BAC clone BACR42E05). This finding was surprising, as 3rd chromosome *P*-elements were screened, and the *P* insertion localised to the 2nd chromosome at 40A-C. These data suggest that there is a *P*-element on the 2nd chromosome as well as the 3rd and, if mapped correctly, the 3rd chromosome *P* does not appear to be associated with the lethal. Verification of the interaction would require determining the localisation of the lethal, as well as the generation of *P*-element reversions to determine whether the enhancement is due to the *P* allele.

5-4.4 *orb^{dec}*

The *P*-element enhancer of *GMR>gcycEI*, *orb^{dec}*, also suppressed the *DmcycE^{JP}* rough eye phenotype (Figure 5.7). To examine if the modifications of the rough eye phenotypes were due to an increase in S phases, BrdU labelling was carried out on third instar larval eye imaginal discs. Reducing the dose of *orb^{dec}* resulted in an increase in the number of S phases in the posterior region of the eye imaginal disc in both *GMR>gcycEI* and homozygous *DmcycE^{JP}* eye imaginal discs (Figure 5.7).

Analysis of genetic interactions between *orb^{dec}* and *GMR-p21* indicated that it appears to act consistently as a downstream modifier of *DmcycE,* as it suppressed the *GMR-p21* rough eye phenotype (data not shown). *orb^{dec}* needs to be analysed for its effect on the *GMR>cycEII* rough eye phenotype to determine whether it is specific for *DmcycEI.*

orb encodes a protein of the cytoplasmic polyadenylation element binding (CPEB) family and is required for egg formation (see Discussion). Several alleles of *orb* are present in private collections, and these have been requested to enable verification of the genetic interaction. Upon acquisition of the *orb* alleles and verification of the interaction, further genetic analysis can be undertaken.

Figure 5.7 : *orb*^{dec} enhances *GMR>gcycEI* and suppresses *DmcycE*^{JP}.

(A-D) Scanning electron micrographs of adult eyes. **A.** *GMR>gcycEI/+;+* and **B.** *GMR>gcycEI/+; orb*^{dec}*/+* eye phenotypes showing that enhancement of the *GMR>gcycEI* rough eye phenotype. **C.** *DmcycE*^{JP}*;+* and **D.** *DmcycE*^{JP}*; orb*^{dec}*/+* eye phenotypes showing suppression of the *DmcycE*^{JP} rough eye phenotype.

(E-H) S phases as detected by BrdU labelling of eye discs from third instar larvae. **E.** *GMR>gcycEI/+;+* and **F.** *GMR>gcycEI/+; orb*^{dec}*/+* eye discs showing that enhancement of the *GMR>gcycEI* rough eye phenotype results from an increase in the number of S phases posterior to the MF. **G.** *DmcycE*^{JP}*;+* and **H.** *DmcycE*^{JP}*; orb*^{dec}*/+* eye discs showing suppression of the *DmcycE*^{JP} rough eye phenotype results from an increase in the number of S phases posterior to the MF.

Anterior is to the right and the MF is indicated by the bar.

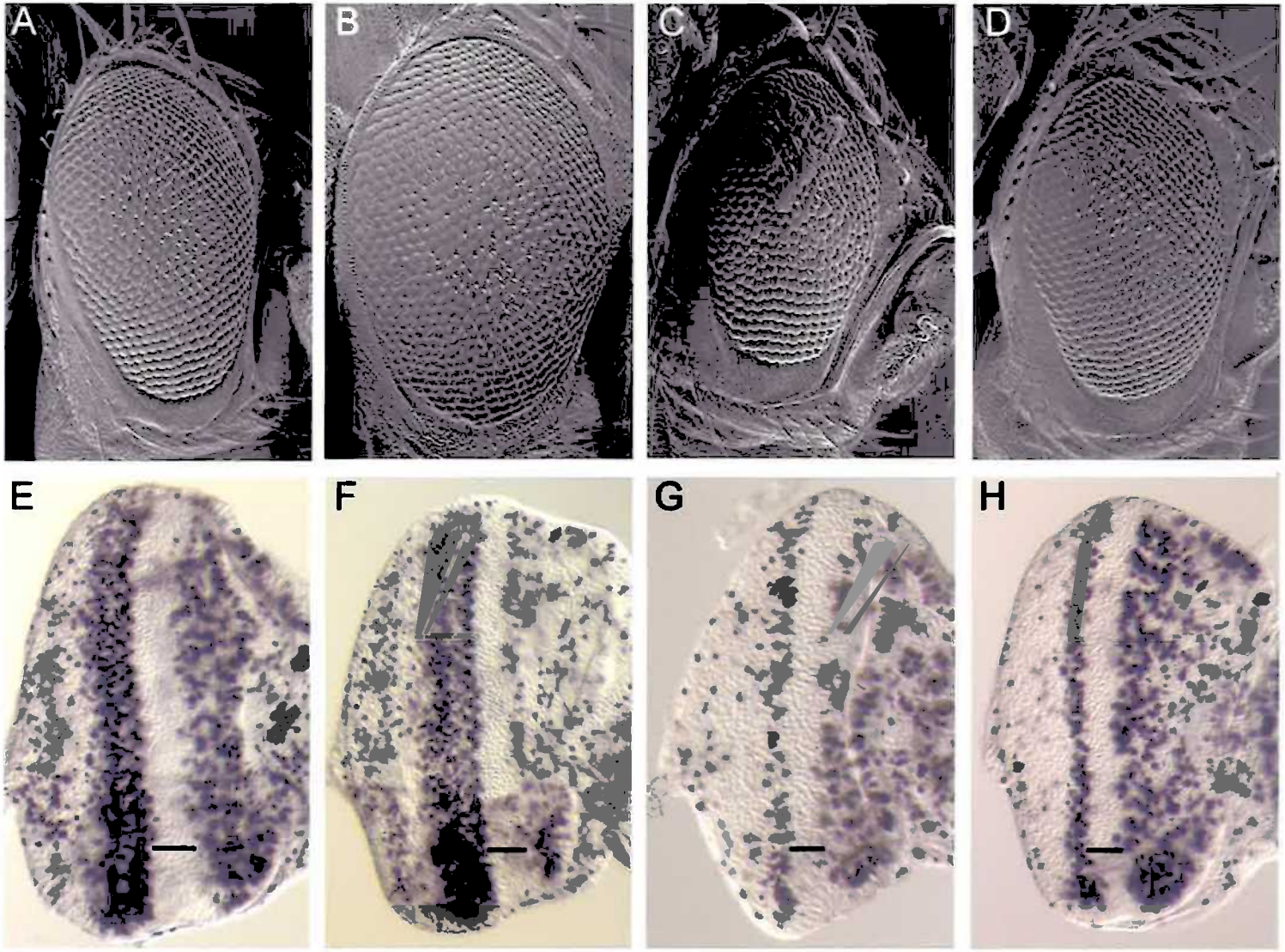
A
B
C
D
E
F
G
H
GMR>gcycEI/+
GMR>gcycEI/+; orb^dec/+
DmcycE^JP
DmcycE^JP; orb^dec/+

5-4.5 *l(3)rK344*

The *P*-element *l(3)*rK344 showed mild enhancement of *GMR>gcycEI*, but showed good suppression of the $DmcycE^{JP}$ rough eye phenotype (Figure 5.8). To examine if the modifications of the rough eye phenotypes were due to an increase in S phases, BrdU labelling was carried out on third instar larval eye imaginal discs. Reducing the dose of *l(3)rK344* resulted in a small increase in the number of S phases in the posterior region of the eye imaginal disc in both *GMR>gcycEI* and homozygous $DmcycE^{JP}$ eye imaginal discs (Figure 5.8).

This *P*-element was localised to 97D1-2 and does not appear to result in a lethal insertion (FlyBase), however, the stock is homozygous lethal, indicating the presence of a lethal mutation elsewhere on the chromosome. Therefore, further analysis of this *P*-element will require identification of the lethal and determining if the interaction is due to the *P*-element or the lethal mutation.

5-4.6 *l(3)j2D5*

The *P*-element *l(3)j2D5* enhanced *GMR>gcycEI*, but only mildly suppressed the $DmcycE^{JP}$ rough eye phenotype (Figure 5.9). To examine if the modifications of the rough eye phenotypes were due to an increase in S phases, BrdU labelling was carried out on third instar larval eye imaginal discs. Reducing the dose of *l(3)j2D5* resulted in a small increase in the number of S phases in the posterior region of the eye imaginal disc in both *GMR>gcycEI* and homozygous $DmcycE^{JP}$ eye imaginal discs (Figure 5.9).

This *P*-element was found to be inserted in a *yoyo* element (FlyBase). Thus as a result the flanking genomic sequence did not yield information about its genomic position or genes affected. Given this and since the effect at the level of S phases on the *GMR*>gcycEI and $DmcycE^{JP}$ phenotypes was subtle no further analysis of this gene was undertaken.

5-5 Discussion

Genetic interaction screens have previously been useful in dissecting numerous regulatory pathways. This chapter describes the *GMR>gcycEI* rough eye phenotype and its use in a screen to identify negative DmcycEI interactors. Upon undertaking this screen, it was expected that examination of *P*-element mutations would make elucidation of the gene of interest straightforward compared to other types of mutations. However, in some cases this strategy has been complicated due to the *P* allele not being lethal, potential mapping problems or the insertion of the *P* into repetitive sequences.

The *P*-element mutations identified as enhancers of *GMR>gcycEI* should disrupt genes that act downstream of *DmcycEI* transcription to negatively regulating entry into S phase. These

Figure 5.8 : *l(3)rK344* enhances *GMR>gcycEI* and suppresses *DmcycE^{JP}*.

(A-D) Scanning electron micrographs of adult eyes. **A.** *GMR>gcycEI/+;+* and **B.** *GMR>gcycEI/+; l(3)rK344/+* eye phenotypes showing mild enhancement of the *GMR>gcycEI* rough eye phenotype. **C.** *DmcycE^{JP};+* and **D.** *DmcycE^{JP}; l(3)rK344/+* eye phenotypes showing good suppression of the *DmcycE^{JP}* rough eye phenotype.

(E-H) S phases as detected by BrdU labelling of eye discs from third instar larvae. **E.** *GMR>gcycEI/+;+* and **F.** *GMR>gcycEI/+; l(3)rK344/+* eye discs showing that enhancement of the *GMR>gcycEI* rough eye phenotype results from a small increase in the number of S phases posterior to the MF. **G.** *DmcycE^{JP};+* and **H.** *DmcycE^{JP}; l(3)rK344/+* eye discs showing that suppression of the *DmcycE^{JP}* rough eye phenotype results from a small increase in the number of S phases posterior to the MF.

Anterior is to the right and the MF is indicated by the bar.

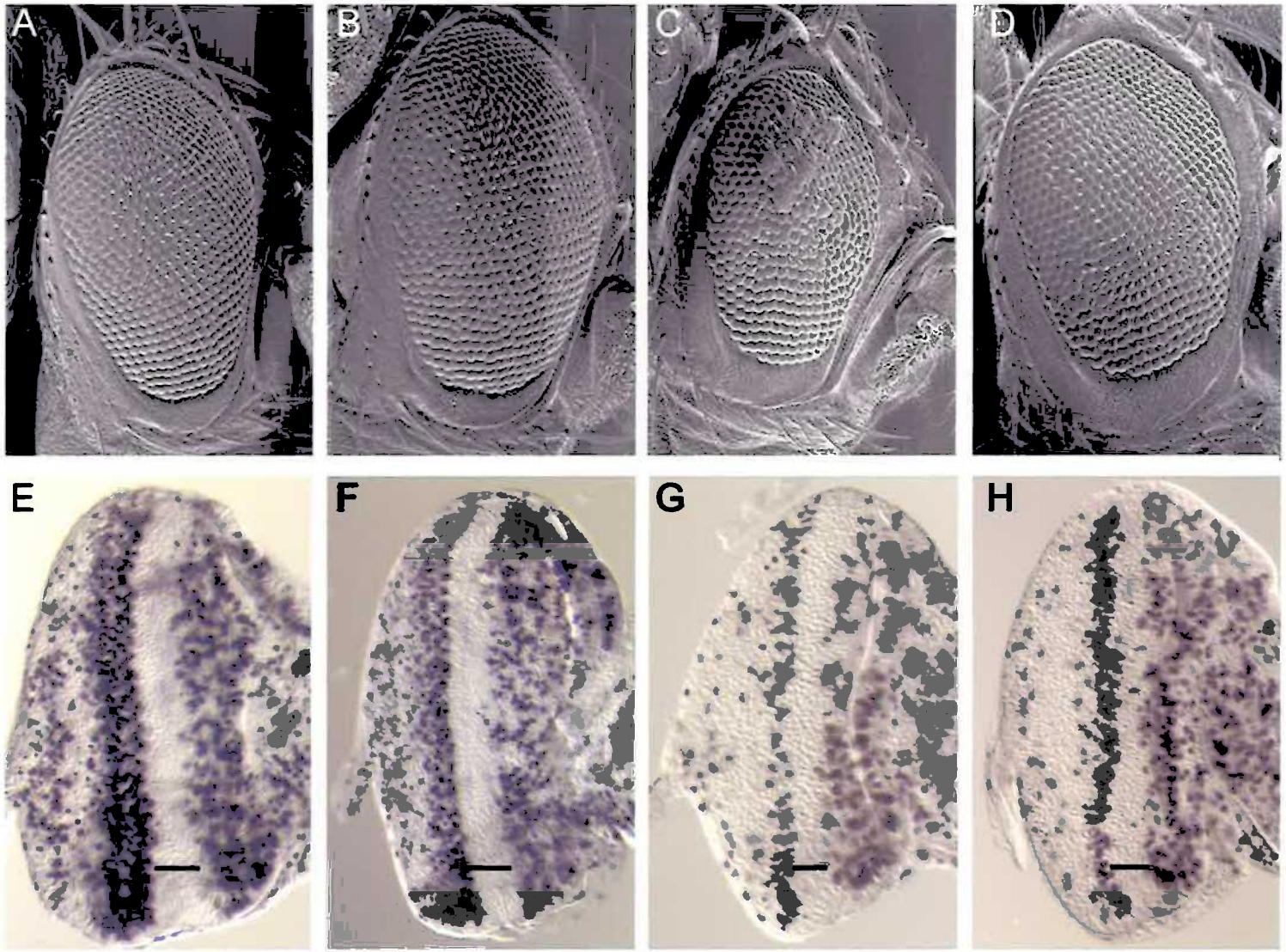
A
B
C
D
E
F
G
H
GMR>gcycEI/+
GMR>gcycEI/+; l(3)rK344/+
DmcycE^JP
DmcycE^JP; l(3)rK344/+

Figure 5.9 : *l(3)j2D5* enhances *GMR>gcycEI* and suppresses *DmcycE^{JP}*.

(A-D) Scanning electron micrographs of adult eyes. **A.** *GMR>gcycEI/+;+* and **B.** *GMR>gcycEI/+; l(3)j2D5/+* eye phenotypes showing enhancement of the *GMR>gcycEI* rough eye phenotype. **C.** *DmcycE^{JP};+* and **D.** *DmcycE^{JP}; l(3)j2D5/+* eye phenotypes showing mild suppression of the *DmcycE^{JP}* rough eye phenotype.

(E-H) S phases as detected by BrdU labelling of eye discs from third instar larvae. **E.** *GMR>gcycEI/+;+* and **F.** *GMR>gcycEI/+; l(3)j2D5/+* eye discs showing that enhancement of the *GMR>gcycEI* rough eye phenotype results from a small increase in the number of S phases posterior to the MF. **G.** *DmcycE^{JP};+* and **H.** *DmcycE^{JP}; l(3)j2D5/+* eye discs showing that suppression of the *DmcycE^{JP}* rough eye phenotype results from a small increase in the number of S phases posterior to the MF.

Anterior is to the right and the MF is indicated by the bar.

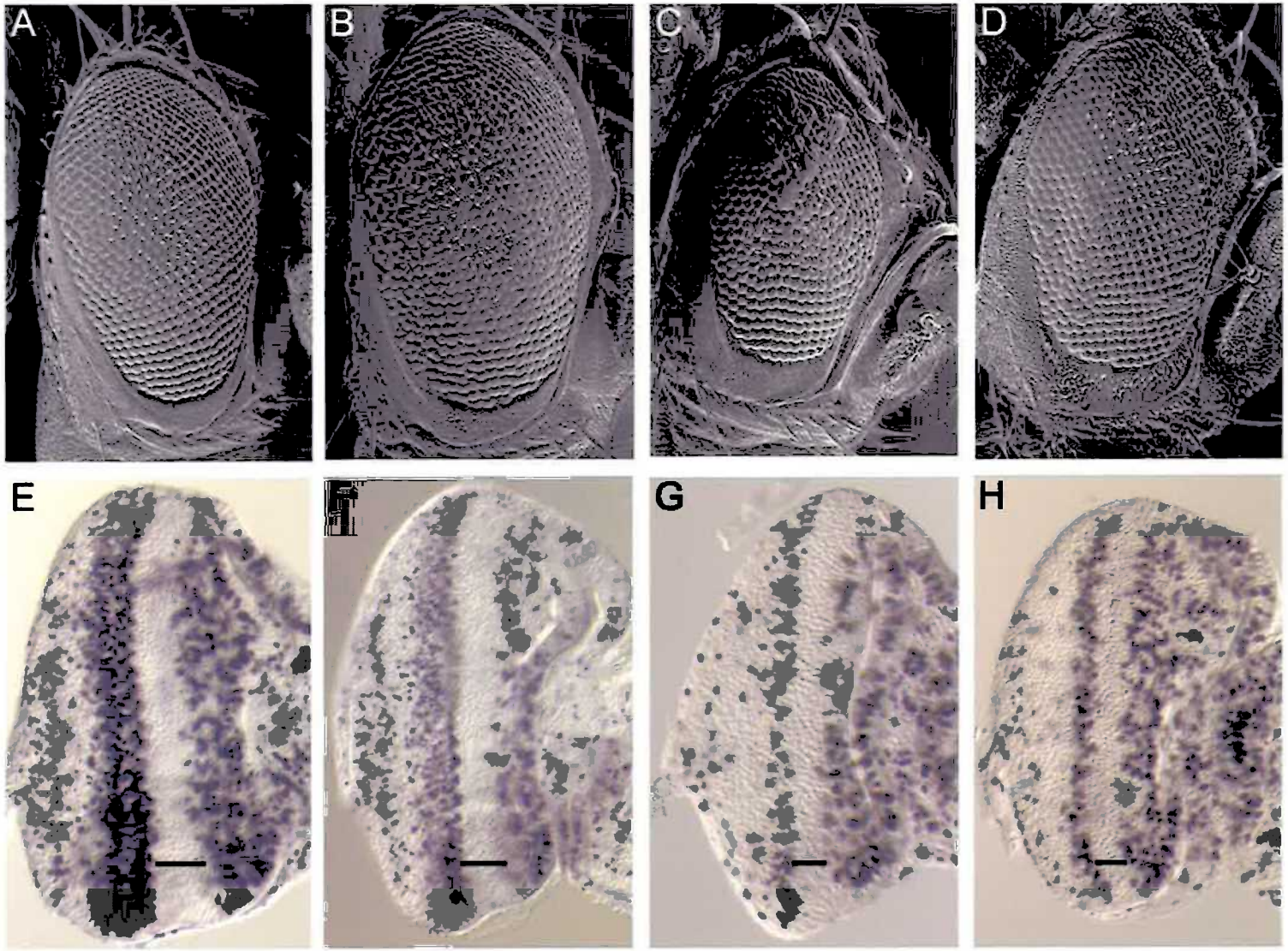
A
B
C
D
E
G
H
GMR>gcycEI/+
GMR>gcycEI/+; I(3)j2D5/+
DmcycE^JP
DmcycE^JP; I(3)j2D5/+

may include DmcycEI-specific inhibitors. In order to verify the genetic interaction with *GMR>gcycEI,* the interacting *P*-element lines were examined for their interaction with $DmcycE^{JP}$. In all cases interaction was observed with both systems, indicating a direct or indirect effect on *DmcycE* activity. To determine if the interactions were occurring at the level of S phase, BrdU labelling was carried out. This revealed that *l(3)06734* was in fact not acting at the level of S phases, but that the remaining interactors were. However none of the interactors resulted in an increase in S phases within the MF, as is expected for the putative DmcycEI-specific inhibitor.

Confirmation of a cell cycle regulatory role for the genes affected in the *P*-element lines was achieved by analysis of the affect of reducing the dose of the *P* interactors in both the *GMR-dE2F, dDP, p35* and *GMR-p21* genetic interaction systems. As overexpression of *p21* results in a rough eye phenotype due to a reduction in S phases in the posterior eye imaginal disc, *GMR>gcycEI* enhancer *P*-element alleles identified would be expected to suppress the *GMR-p21* rough eye phenotype and this was shown to be the case for those alleles examined. Likewise, the *P*-element lines were was also tested for an effect on the rough eye phenotype caused by overexpression of *dE2F, dDP, p35,* which results from an increase in S phases in the posterior region of the eye imaginal disc. Enhancers of *GMR>gcycEI* would be expected to enhance this phenotype. This was shown to be the case for the *P*-element lines examined.

Halving the dose of the *P*-elements had no effect on the rux^3 rough eye phenotype. *rux* mutants result in ectopic DmcycA in the MF, which is sufficient to induce these cells into S phase. The increase in S phases seen in the *GMR>gcycEI* eye discs when the dose of the *P* alleles was halved could be due to increases in levels of DmcycA, bypassing the requirement for DmcycE. This appeared not to be the case as none of the *P*-element alleles tested interacted with the rux^3 phenotype, suggesting that these genes do not act through the Rux pathway.

To determine if any of the interactions were specific for DmcycEI, the *P*-element alleles were examined for their affect on ectopic expression of *DmcycEII*, using *GMR>cycEII.* This identified *l(3)05408* as a likely candidate, however further verification will require other assays including the yeast 2-hybrid analysis and the effect on the DmcycE/DmCdk2 lethal yeast strain.

The cytological location of the *P*-elements had been determined and verified by identification of genomic DNA flanking the *P*-element. This enabled the identification of candidate genes disrupted by the *P*-element insertion, which need to be confirmed by testing specific mutants. In the cases of the *P*-elements *l(3)rk344, l(3)j2D5* and *l(3)00720,* this analysis did not reveal a candidate, and in the case of *l(3)rk344* and *l(3)00720* at least two aberrations were present in the stock. However, two candidates were identified: *orb,* encoding an RNA binding protein, and a novel gene *CG7394,* encoding DnaJ homologue gene, discussed below.

5-5.1 Role of *l(3)05408*

The *P*-element *l(3)05408* is inserted in gene *CG7394*, which encodes a protein containing a DnaJ domain. The canonical DnaJ protein (Hsp40) in *E. coli,* functions together with the Hsp70 chaperone. The Hsp70 family of chaperones is highly conserved throughout evolution, and performs many functions, including facilitation of protein folding (reviewed by Mayer and Bukau, 1998). Not only do Hsp70 chaperones interact with denatured substrates, they also mediate cellular functions such as translocation of proteins across membranes, and assembly of multimeric protein complexes. The Hsp70 chaperones cycle between an ATP-bound form, which has unstable protein substrate interactions, and an ADP-bound form, which has stable interactions (reviewed by Mayer and Bukau, 1998). The regulation of the cycling between the two forms is fundamental to chaperone function, whereby the hydrolysis of ATP requires a Hsp40 family protein. Like Hsp70 chaperones, the Hsp40 family is highly conserved. The Hsp40 family of proteins contain four distinct domains, including a DnaJ domain. The DnaJ domain consists of a highly conserved 70-amino acid region, that includes the tripeptide HPD, which is critical for the function of the J domain (Kelley, 1998). A subclass of the Hsp40 family proteins contain only the J domain, and represent diverse proteins that participate in a variety of complex biological processes such as protein folding and translocation (Hendrick *et al.,* 1993), cell cycle control by DNA tumour viruses (e.g. Schilling *et al.,* 1998; Zalvide *et al.,* 1998), and regulation of protein kinases (Calpan *et al.,* 1995).

The prototypical DnaJ domain protein in *Drosophila* is Tid56, encoded by the *lethal(2) tumorous imaginal discs (l(2)tid)* gene. Homozygous *l(2)tid* mutants develop lethal tumours, during pupariation, that are derived from imaginal discs that fail to differentiate. This hyperproliferation phenotype of *l(2)tid* mutants suggests that it may be involved in regulation of cell proliferation and death (Kuriz *et al.,* 1995). The human homologue, *TID1*, has be shown to modulate interferon-γ-mediated signalling by interacting with JAK2 and Hsp70, suggesting that hTid-1 is a modulator of the JAK-STAT pathway (Sarkar *et. al.,* 2001). TID1 has also been isolated as an interactor of E7 protein from human papillomavirus type 16 (Schilling *et al.,* 1998).

BLAST searches using the gene *CG7394*, potentially disrupted by the *P* insertion *l(3)05408,* have identified mammalian homologues as well as a *C. elegans* homologue (Figure 5.10). The human homologue, *methylation-controlled J protein* (*MCJ*), has been implicated in ovarian cancer, as loss of *MCJ* expression by deletion of one allele and methylation of the other was found in several ovarian tumours (Shridhar *et al., 2001).* This suggests that MCJ, a DnaJ domain protein, may be acting as a tumour suppressor. The role of the murine and *C. elegans* homologues is uncharacterised.

A role for DnaJ proteins interacting with Cyclins has not been described in metazoans, however Yaglom *et al.* (1996) have shown that in budding yeast, the phosphorylation dependent degradation of Cln3 (G1 cyclin) by CDC28 (Cdk2) requires the DnaJ domain protein, Ydj1. By analogy to this, *CG7394* (DnaJ) may regulate the Cdk2 phosphorylation of Cyclin E that signals its degradation, whereby reduction in CG7394 (DnaJ) would results in an increase in DmcycE stability. Given this analogy it is likely that CG7394 acts at the level of DmcycE protein stability, although it should be noted that the p21 inhibitor can also play a role as a chaperone for Cyclin D/Cdk4(6) complex assembly (Hannon and Beach, 1994). Further analysis is required to investigate the mechanism of CG7394's action. Examination of the levels of DmcycE protein in *GMR>gcycEI/+; l(3)05408/+* eye imaginal discs would determine if CG7394 (DnaJ) acts to mediate depletion of DmcycE consistent with this possibility.

5-5.2 Role of *orb*

The *orb* gene encodes an RNA recognition motif (RRM)-type RNA-binding protein that is a member of the cytoplasmic polyadenylation element binding (CPEB) protein family (reviewed by Mendez and Richter, 2001). The regulated translation of mRNA is crucial for many developmental processes including oocyte maturation and establishment of the embryonic axes. One of the mechanisms of translational regulation occurs by cytoplasmic polyadenylation. This process is driven by the cytoplasmic polyadenylation element binding (CPEB) protein, a highly conserved, sequence-specific RNA-binding protein that binds to the cytoplasmic polyadenylation element to regulate translation and mRNA localisation (reviewed by Mendez and Richter, 2001).

Analysis of *orb* mutant ovaries indicates that the gene is required early in oogenesis for the formation of the 16-cell cyst, and plays a role in restriction of meiosis to one cell of the cyst by regulating translation (Lantz *et al.*, 1994). *orb* is also required later in oogenesis in the determination of the dorsoventral and anteroposterior axes of the embryo by targeted localisation and translational regulation of specific mRNAs (Lantz *et al.*, 1994; Chang *et al.*, 1999; Chang *et al.*, 2001).

A role for CPEBs in *Xenopus* oogenesis has also been characterized. In *Xenopus* embryos, progression into M phase requires the polyadenylation-induced translation of cyclin B1 mRNA, mediated by CPEB. Following this, exit from M phase appears to require deadenylation and translational silencing of *cyclin B1* mRNA by another CPEB, Maskin, an eIF4E binding factor. These observations have suggested a role for CPEBs in regulating *cyclin B1* mRNA translation and silencing, which are essential for progression through M phase (Groisman *et al.*, 2002).

Figure 5.10 : *CG7394* encodes a DnaJ domain protein.

CG7394 encodes a protein that has homology to DnaJ domain containing proteins. The alignment shown compares human methylation-controlled J protein (MCJ) (Shridhar *et al.*, 2001), murine and *C. elegans* homologues. The HPD (marked by ***) tripeptide essential for function of the J domain is conserved. Conserved amino acids between all 4 sequences represented by the black boxes, conservation across 3 sequences in grey box white text and conservation across 2 in grey box black text.

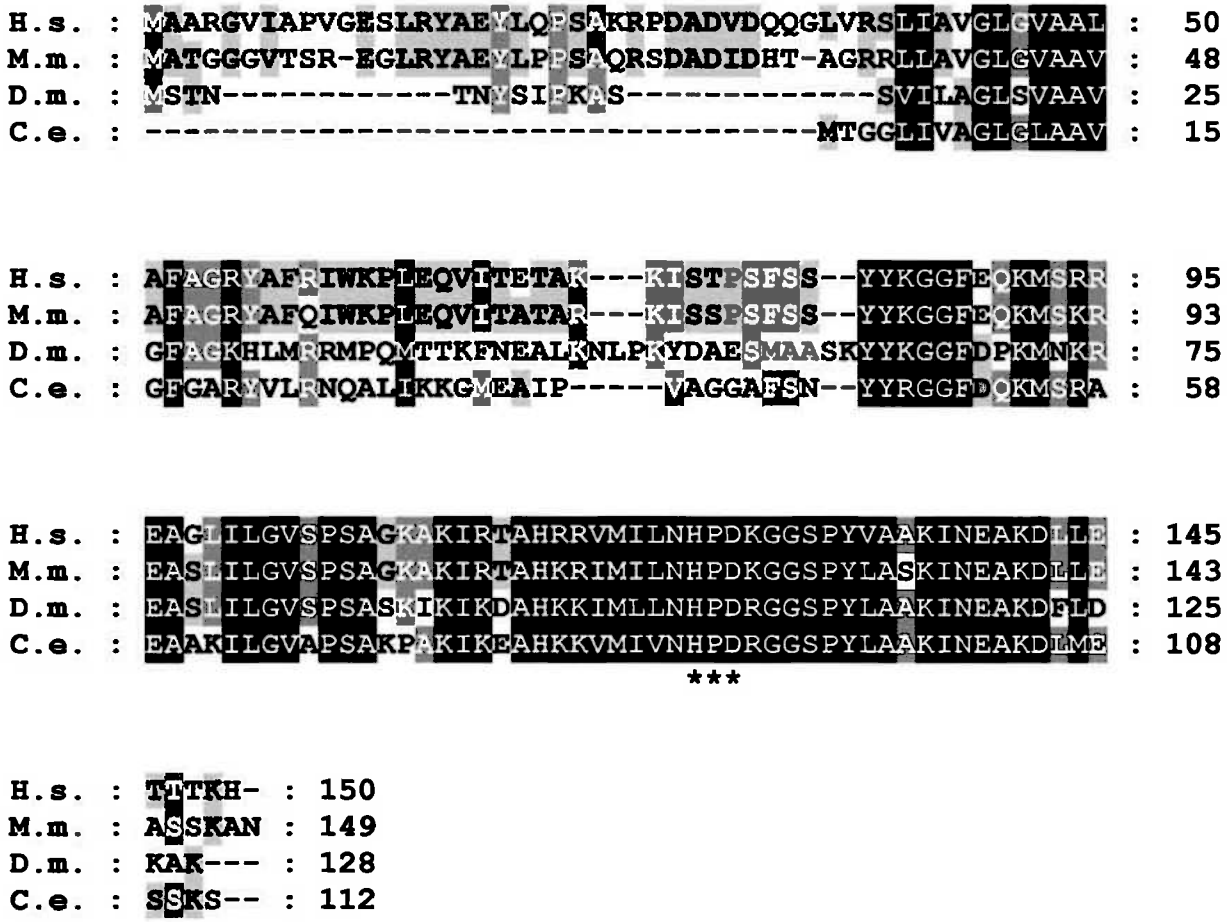
H.s. : MAARGVIAPVGESLRYAEYLQPSAKRPDADVDQQGLVRSLIAVGLGVAAL : 50
M.m. : MATGGGVTSR-EGLRYAEYLPPSAQRSDADIDHT-AGRRLLAVGLGVAAV : 48
D.m. : MSTN----------TNYSIPKAS----------SVILAGLSVAAV : 25
C.e. : ----------MTGGLIVAGLGLAAV : 15
H.s. : AFAGRYAFRIWKPLEQVITETAK---KISTPSFSS--YYKGGFEQKMSRR : 95
M.m. : AFAGRYAFQIWKPLEQVITATAR---KISSPSFSS--YYKGGFEQKMSKR : 93
D.m. : GFAGKHLMRRMPQMTTKFNEALKNLPKYDAESMAASKYYKGGFDPKMNKR : 75
C.e. : GFGARYVLRNQALIKKGMEAIP-----VAGGAFSN--YYRGGFDQKMSRA : 58
H.s. : EAGLILGVSPSAGKAKIRTAHRRVMILNHPDKGGSPYVAAKINEAKDLLE : 145
M.m. : EASLILGVSPSAGKAKIRTAHKRIMILNHPDKGGSPYLASKINEAKDLLE : 143
D.m. : EASLILGVSPSASKIKIKDAHKKIMLLNHPDRGGSPYLAAKINEAKDFLD : 125
C.e. : EAAKILGVAPSAKPAKIKEAHKKVMIVNHPDRGGSPYLAAKINEAKDLME : 108
***
H.s. : TTTKH- : 150
M.m. : ASSKAN : 149
D.m. : KAK--- : 128
C.e. : SSKS-- : 112

A role for *orb* outside of oogenesis has not been established. However, insights from *Xenopus* indicate that it may play a role in cell cycle dependent regulation of translation. It is possible that *orb* may act to translationally regulate DmcycE, such that reducing the dose of Orb could result in the unregulated translation of DmcycE. It would be interesting to examine the levels of DmcycE in *GMR>gcycEI* eye imaginal discs when the dose of Orb is reduced, to determine if there is an increase in DmcycE protein levels.

5-5.3 Conclusion

This chapter describes the characterisation of tissue-specific ectopic expression of DmcycEI and its use in a genetic interaction screen of a collection of *P*-element alleles. The screen was successful in the identification of novel DmcycEI interactors and further characterization of DnaJ CG739 and Orb interactions may elucidate a role for these proteins as novel negative regulators of DmcycE or downstream negative regulators of entry into S phase. This genetic interaction screen was limited to the 3rd chromosome, however from the success of this, the screening of *P*-elements on other chromosomes for enhancement of the *GMR>gcycEI* rough eye phenotype should be expected to reveal other potential candidates of the DmcycEI specific inhibitor.

Chapter 6 : Yeast Screen for DmcycE Interactors

6-1 Introduction

To complement and extend the genetic search for the proposed inhibitor that acts on the N-terminus of DmcycEI (Chapter 5), a screen to identify direct protein interactors of the DmcycEI N-terminus was carried out.

The yeast two-hybrid system has been widely used to identify interacting proteins and has been successful in identifying cell cycle regulators (Gyuris *et al.*, 1993). The yeast two-hybrid system relies on the separable domains of transcription activators (e.g. GAL4 and LexA) where the DNA binding domain can be separated from, and act in *trans* to, the transactivating domain. Specifically, one construct contains a sequence specific DNA binding domain fused to a protein of interest (the "bait") and the other contains a transcription activation domain fusion protein (the "prey"). If the two proteins interact (bait and prey), the resulting complex can bind to DNA binding sites upstream of a reporter gene, and this tethering of the activation domain fusion to the DNA binding domain results in activation of reporter gene expression.

This chapter describes the use of the yeast two-hybrid system to identify proteins that interact directly with the N-terminus of DmcycE.

6-2 Yeast 2-hybrid analysis to identify DmcycE interactors

6-2.1 LexA fusion system to identify N-terminal DmcycEI interactors

An initial yeast two-hybrid analysis was undertaken using the *E. coli* LexA repressor as the DNA binding domain (*pEG202*) and two different reporter genes, *LEU2* and *lacZ*, each containing upstream LexA operator binding sites. A 0-12hr *Drosophila* embryonic cDNA library, fused to an activation domain and conditionally expressed under the control of the *GAL1* promoter (in *pJG4-5*), was used (*RFLY1)* (Gyuris *et al.*, 1993). To examine interacting proteins, the LexA-fusion (bait) and library (prey) were transformed into *S. cerevisiae* strain EGY48 containing a chromosomal *LEU2* gene with 6 upstream LexA binding sites (*6lexAops-LEU2),* as well as a *lacZ* reporter plasmid containing *lacZ* gene with 8 LexA operator binding sites (*pSH18-34*). In this system, induction of expression of the library (prey) by growth on galactose and selection in the absence of Leu (-Leu) on X-gal plates, to assay for *LEU2* and *lacZ* reporter gene expression, allows the identification of "prey" that interact with the "bait".

To identify proteins that interact directly with the N-terminus of DmcycEI, based on the *in vivo* constructs (Chapter 4), two DmcycEI N-terminal LexA-fusion constructs were generated in *pEG202*, for use as "bait" in a yeast two-hybrid. One construct included amino acids 1-195 of DmcycEI, corresponding to the region deleted in the 195NΔDmcycE transgenic fly construct (*pEG-195N*). A smaller DmcycEI N-terminal-LexA fusion was also generated using amino acids 1-46 DmcycEI (*pEG-46N*). This construct retained the unique 12 amino acids of DmcycEI and included a further 34 amino acids to aid in the maintenance of appropriate protein structure of the N-terminal region. The constructs were generated using high fidelity PCR and sequenced to ensure that the correct reading frame was maintained from *lexA* into *DmcycE* sequence.

To determine if the fusion proteins were suitable to use in a yeast 2-hybrid screen, their ability not to auto-activate reporter gene expression was examined. Following transformation of *pEG-195N* into yeast strain EGY48 containing *pSH18-34* (*lacZ* reporter vector) the LexA-195N fusion protein activated both the chromosomal *LEU2* reporter and the *lacZ* reporter and therefore was unsuitable for use in the yeast 2-hybrid screen (data not shown). Transformation of *pEG-46N* into EGY48 containing *pSH18-34*, showed that the presence of the LexA-46N fusion protein did not activate the *LEU2* or *lacZ* reporter genes and therefore was suitable for use in a screen (data not shown). The expression of the *pEG-46N*, once transformed into the yeast strain EGY48 + *pSH18-34*, was examined by western analysis performed using α-LexA antisera. This confirmed that LexA-46N was being expressed (data not shown).

LexA-46N was used as a bait to screen a 0-12hr *Drosophila* embryonic cDNA library (*RFLY1*). Initially, interacting transformants were screened by growth on Gal -Leu + X-gal media, to induce the activation domain library and to assay for both *LEU2* and *lacZ* reporter gene expression. From 1.66x 10^6 transformants, this approach identified 27 positives. The library clone was isolated and restriction digests carried out to determine how many distinct clones the 27 positives represented (data not shown). Two positives could be discarded immediately as they had lost their insert, leaving 2 remaining classes, one with 24 members and a single clone (Table 6.1). To confirm the interaction, single clones from these two classes were retransformed back into the "bait" strain and again tested for growth on Gal -Leu + X-gal media. The single clone did not interact upon re-testing. The large class of 24 members still showed reporter gene expression, however, sequence analysis revealed that the insert was *lacZ*. The source of the *lacZ* clone in the library was unknown, however, its presence made the approach based on screening for *lacZ* expression unfeasible.

Table 6.1: Summary of yeast 2-hybrid screen #1

Bait	Prey	Transform.	Screening	# clones	gene
LexA-46N	RFLY1	1.66 x 10^6	Gal–leu+Xgal	1	NR*
				2	No insert
				24	*lacZ*

*NR=not relevant, since did not retest

An alternative approach was undertaken to screen the *RFLY1* library for interactors of LexA-46N on Gal -Leu media, to induce the library and to assay for activation of *LEU2* reporter gene expression. From 7.2x 10^5 transformants, 1x 10^3 colonies were able to grow on the Gal -Leu media. The identification of true positives required re-screening of these transformants onto Gal -Leu and Glu -Leu media to compare the growth. Following re-screening of 1x 10^2 colonies, 13 positives were identified. To determine how many unique interactors this represented, the library clones were then isolated and restriction digests carried out to determine how many distinct clones the 13 positives represented (data not shown). This identified 8 classes of which one class, containing 3 clones, could be discarded immediately as it no longer contained an insert. A single clone from each of the remaining classes was then retransformed back into the "bait" strain and tested for growth on Gal -Leu media with the addition of X-gal to confirm the interaction (summary Table 6.2). 46N101 and 46N63 did not interact upon re-testing. The remaining classes maintained an interaction, so sequence analysis of the inserts was undertaken (Table 6.2). This identified several ribosomal proteins, but as they are frequently identified as false positives in yeast 2-hybrid screens, they were not studied any further. Two other genes, *eIF5A* and *caz* were further analysed. Once transformed back into the "bait" strain, *eIF-5A* and *caz* were assayed for *lacZ* reporter gene expression to quantitate the interaction (Table 6.3, Appendix 6.A). As a control a C-terminal DmcycE construct (86 most C terminal amino acids in *pEG202*, *pEG-Cterm*) was used to determine the specificity of the interaction. The results from this assay confirmed Caz as an interactor with 46N specifically, however eIF-5A did not show any interaction.

This method of screening on Gal -Leu media, without X-gal, proved extremely difficult due to a high level of background transformants that were initially able to grow on the Leu deficient plates but when rescreened did not interact. The greater sensitivity of the chromosomal *LEU2* over the *pSH18-43* reporter has been previously demonstrated and can result in an unworkably high background for some "baits" (Estojak *et al.*, 1995). Given this and the contamination of a *lacZ* clone in the library, an alternative screening approach was undertaken.

Table 6.2: Summary of yeast 2-hybrid screen #2

Bait	Prey	Transform.	Screening	# clones	gene
LexA-46N	RFLY1	7 x 10^5	Gal -leu	46N16, 103	eIF-5A
				46N27	RpL7
				46N59	cabeza
				46N63	NR
				46N101	NR
				46N62, 82, 104	RpL19
				46N107	RpS6
				46N105, + 2	No insert

*NR=not relevant, since did not retest

Table 6.3 : LacZ assay for interaction with N- and C-terminal regions

Interactor	LexA-46N	LexA-C term
pJG4-5	1.619 ± 0.317	1.074 ± 0.354
eIF-5A	0.349 ± 0.157	0.718 ± 0.115
cabeza	3.197 ± 2.57	0.113 ± 0.031

An alternative library was obtained to screen for interactors of LexA-46N in EGY48 + *pSH18-34*. This library was a *Drosophila* 3rd instar larval cDNA library fused to the GAL4 activation domain under the control of a constitutive *ADH* promoter, constructed in the *pACT* vector (referred to as *SEL3*; from S. Elledge). This required screening for interactors by assaying for *lacZ* reporter gene expression only as the library vector contains the *LEU2* gene for selection of yeast transformants making it incompatible with screening of *LEU2* reporter in EGY48. 1.4 x 10^7 transformants were screened for interactors on X-gal media and 9 candidates were obtained. The library clones were then isolated and restriction digests carried out (data not shown) to reveal that all 9 were distinct. To eliminate false positives each clone was retransformed into EGY48 + *pSH18-34* + "bait" and assayed for *lacZ* reporter gene expression, whereby 2 maintained an interaction (Table 6.4). The positive clones were sequenced and correspond to *Bip2* and *Su(var)2-10* (see Discussion). The interaction between *Bip2* and *Su(var)2-10* and the "bait" was quantitated using lacZ liquid assay, showing *Bip2* as a strong interactor, but *Su(var)2-10* showed a weaker interaction with LexA-46N (Table 6.5, Appendix 6.A).

Table 6.4: Summary of yeast 2-hybrid screen #3

Bait	Prey	Transform.	Screening	# clone	gene
LexA-46N	SEL3	1.4 x 10^7	Glu + X-gal	DC2	*Bip2*
				DC3	*Su(var)2-10*
				7	false +

Table 6.5: LacZ assay for interaction with N-terminal

Interactor	LexA-46N
pACT	0.396 ± 0.027
Bip2	157.8 ± 4.033
Su(var)2-10	8.475 ± 1.521

It was a concern that this system was also giving many false positives so a new yeast strain PJ69-4A was obtained to screen the *SEL3* library. This required cloning into *pAS1* vector, containing the GAL4 DNA binding domain, rather than LexA.

6-2.2 Gal fusion system to identify N-terminal DmcycEI interactors

Due to the presence of the *lacZ* clone in the *RFLY1* library and the difficulties with background growth, an alternative approach was undertaken. This alternative approach was to screen the *Drosophila* 3rd instar larval cDNA library (*SEL3*) using the DmcycEI N-terminus fused to the GAL4 DNA binding domain (in *pAS1* which is *TRP1* selectable) and three different chromosomal reporter genes, *ADE2, HIS3* and *lacZ* each with a distinct Gal DNA binding site present in yeast strain PJ69-4A (James *et al.,* 1996). This strain was chosen to minimise the number of false positives, as each of the reporters is driven by a distinct Gal4 promoter (Gal1p-*ADE2,* Gal2p-*HIS3* and Gal7p-*lacZ*) that are induced to high levels in response to GAL4. This enables identification of "prey" that interact with the "bait" by assaying for growth in the absence of Ade and His (-Ade -His) due to activation of the *ADE2* and *HIS3* reporters and blue colonies on X-gal due to activation of the *lacZ* reporter.

Screening of the *SEL3* library in yeast strain PJ69-4A, required the construction of a DmcycEI N-terminal 46 amino acid-GAL4 fusion in *pAS1* vector (*pAS-46N*). The construct was generated using high fidelity PCR and sequenced to ensure that the correct reading frame was maintained from *GAL4* to *DmcycE 46N.* Following transformation of *pAS-46N* alone into the yeast strain PJ69-4A, the GAL4-46N fusion protein did not activate the chromosomal *ADE2, HIS3* and *lacZ* reporter genes and was therefore suitable for the screen (data not shown). The

expression of the *pAS-46N*, in PJ69-4A, was examined by western analysis performed using α-GAL4(DBD) antisera, which demonstrated that GAL4-46N was being expressed (data not shown).

The *pAS-46N* construct was used as a "bait" to screen the *SEL3* library. Interacting transformants were selected by growth on Glu -Ade -His media, to assay for both *ADE2* and *HIS3* reporter gene expression. However, the generation of sufficient transformants in yeast strain PJ69-4A containing pAS-46N proved extremely difficult. It appeared that the presence of pAS-46N in this yeast strain greatly reduced the transformation efficiency. Therefore to permit screening of the complete library an interaction hunt was performed by mating (Finley and Brent 1994). Interaction mating makes use of the feature that haploid yeast have two different mating types, *MAT***a** and *MAT*α. When haploid yeast of opposite mating type come together they can fuse to form diploids. For interaction hunt by mating, the "bait" and the "prey" are present in haploid yeast of opposite mating types and come together by mating. The resulting diploids, containing both "bait" and "prey" that are selected on appropriate plates, can then be screened for interaction. The library was transformed into yeast strain PJ69-4Aα (the opposite mating type to the yeast strain containing the "bait"), and 3.7x 10^8 transformants per 100μL were obtained. These library transformants were then harvested and used to mass mate with PJ694A**a** containing pAS-46N, whereby 2x 10^7 diploids were generated and then screened for interaction on Glu -Ade -His media to select for both *ADE2* and *HIS3* reporter gene expression. 22 Ade^+ His^+ colonies were obtained, from which the library clones were isolated and restriction digests carried out (data not shown). The 22 positives represented 2 classes, that when retransformed into the "bait" strain maintained an interaction. The positive clones were sequenced and found to correspond to *Fat body protein 1* (*Fbp1)* and a novel gene *CG9326* referred to as *dcmaguk*, of the membrane associated guanylate kinase class (FlyBase).

Table 6.6: Summary of yeast 2-hybrid screen #4

Bait	Prey	# diploids	Screening	# clones	gene
GAL4-46N	SEL3	2 x 10^7	Glu-Ade-His	6	*dcmaguk*
				16	*Fbp1*

Together, yeast 2-hybrid analyses have screened 3.638 x 10^7 library cDNAs and identified *caz, Bip2, Su(var)2-10, dcmaguk* and *Fbp1* as candidate interactors of DmcycEI. To determine if the interaction was specific for DmcycEI, the interaction between the candidates and full length DmcycEI compared to DmcycEII was examined.

6-3 Interactions with full length DmcycEI and DmcycEII

6-3.1 Yeast 2-hybrid analysis of candidates with DmcycEI and DmcycEII

To verify the interactors identified using the 46N terminal constructs, yeast 2-hybrid analysis was carried out using full length DmcycEI and II. Constitutive expression of full length DmcycE has been shown to be lethal in *S. cerevisiae*, therefore, a galactose-inducible LexA DNA binding domain yeast two hybrid vector, *pGilda*, was used to generate LexA-DmcycEI and LexA-DmcycEII fusion proteins. *pGilda-DmEI* and *pGilda-DmEII* constructs were generated by subcloning full length *DmcycEI* and *DmcycEII* from *pJG4-5* vector (from R. Finley) into *pGilda*. The constructs were transformed into EGY48 containing *pSH18-34* (*lacZ* reporter) and tested for the ability to grow on galactose, overcoming the lethality, and for the ability to autoactivate the *LEU2* and *lacZ* reporter gene. As the DmcycE-LexA fusions alone were able to weakly activate *LEU2* reporter gene expression, analysis of interactions was determined by quantitation of *lacZ* expression. Caz, Bip2, Su(var)2-10, Dcmaguk and Fbp1 were examined for an interaction with full length DmcycEI and DmcycEII and also with an unrelated bait, C-terminal Pcl (Polycomblike, a Polycomb group protein) fused to LexA (Table 6.7, Appendix 6.B).

Table 6.7: LacZ assay of candidates with full length DmcycEI and DmcycEII

Interactor	LexA-DmcycEI	LexA-DmcycEII	LexA-Pcl-C*
pACT	13.26 ± 3.3	10.54 ± 2.3	0
Bip2	228.93 ± 29.55	189.01 ± 35.77	5.2 ± 0.7
Su(var)2-10	36.78 ± 6.91	26.49 ± 6.04	0
pACT	9.47 ± 2.82	8.30 ± 2.01	0
Fbp1	129.72 ± 41.69	90.92 ± 15.52	0
DcMaguk	49.6 ± 11.15	28.43 ± 9.39	0
pJG4-5	3.7 ± 0.4	1.8 ± 0.4	0
caz	7.1 ± 0.7	5.6 ± 0.4	0

* A zero result indicates that no interaction was detected.

As Bip2 interacted with the non-related bait, it was discarded from further analysis (Table 6.7). Even though Fbp1 appears to interact specifically and strongly with both full length proteins, it also interacted with the C-terminal region of DmcycE (*pAS-Cterm*)(Table 6.7 and data not shown). *Fbp1* encodes an insect-specific oxygen transporter (arthropod hemocyanin/ insect LSP domain) and an *in vivo* interaction with DmcycE did not seem likely as it interacted not only with full length proteins but also with both N- and C-terminal regions. Thus, Fbp1 was not analysed further. Caz, Su(var)2-10 and Dcmaguk interacted with both full length DmcycEI

and DmcycEII and not with the unrelated bait (Table 6.7). As Caz, Su(var)2-10 and Dcmaguk bound relatively similarly to both DmcycEI and DmcycEII, they do not appear to be specific to the unique N-terminal 12 amino acids of DmcycEI.

6-3.2 Assay for DmcycEI and DmcycEII inhibition in the lethal yeast assay

A functional assay in yeast was used to determine if the yeast 2-hybrid interactors were able to inhibit DmcycEI/DmCdk2 or DmcycEII/DmCdk2 activity. Expression of DmcycE and DmCdk2 in yeast is lethal, however, this lethality can be rescued by co-expression Dap (Section 4-3.1). Yeast expressing DmcycEI/DmCdk2 or DmcycEII/DmCdk2 were unable to be rescued by expression of either *Su(var)2-10, cabeza* or *dcmaguk* (data not shown). Therefore, the interactions between Su(var)2-10, Caz and Dcmaguk with DmcycEI and DmcycEII does not appear to be inhibitory to DmcycE activity, at least not to the same degree as Dap. To verify and investigate the function of these interactors, *in vivo* studies were required.

6-4 Characterisation of interacting proteins

6-4.1 Interactions between *cabeza* and *DmcycE*

Cabeza encodes a RNA binding protein containing a RNA recognition motif (RRM), and appears to be a component of the RNA polymerase II transcription machinery (see Discussion). The interaction between Caz and DmcycE was verified *in vivo* by examination of genetic interactions. As described in Chapter 5, the rough eye phenotypes generated by *GMR>gcycEI* and $DmcyE^{JP}$ are dose sensitive systems to evaluate dominant genetic interactions. To assess the ability of *caz* alleles (caz^{1} and caz^{2}) to interact with $DmcycE^{JP}$, flies homozygous for $DmcycE^{JP}$ and heterozygous for *caz* were generated. Halving the dose of *caz* was able to suppress the $DmcycE^{JP}$ rough eye phenotype (Figure 6.1 and data not shown). To determine if the suppression was acting at the level of S phase, BrdU incorporation was carried out on eye imaginal discs from third instar larvae homozygous for $DmcycE^{JP}$ and heterozygous for *caz* (Figure 6.1). Halving the dose of *caz* was able to increase S phases in the eye imaginal disc of homozygous $DmcycE^{JP}$ third instar larvae. Furthermore, in a homozygous $DmcycE^{JP}$ background, males hemizygous for *caz* are obtained, indicating that $DmcycE^{JP}$ is suppressing the lethality of *caz*. The ability of *caz* alleles to genetically interact with *GMR>gcycEI* was also examined, but no interaction was observed (data not shown).

To confirm a direct interaction between Caz and DmcycE *in vivo*, co-immunoprecipitation from embryonic extracts were attempted using Caz antibody (a gift from S. Haynes). However, no conclusive results could be obtained since Caz protein levels in the samples used appeared to be too low. To increase Caz levels, ectopic expression of a *caz*

transgene should be performed to facilitate investigation of whether an *in vivo* interaction between DmcycE and Caz can occur.

6-4.2 Interactions between *Su(var)2-10* and *DmcycE*

Su(var)2-10 encodes a protein with homology to PIAS, a regulator of JAK-STAT signalling (see discussion). The interaction between Su(var)2-10 and DmcycE was verified *in vivo* by examining genetic interactions. To assess the ability of *Su(var)2-10* to interact with *GMR>gcycEI*, flies heterozygous for *GMR>gcycEI* and *Su(var)2-10* were generated. Halving the dose of $Su(var)2\text{-}10^2$ showed a mild enhancement of the *GMR>gcycEI* rough eye phenotype (Figure 6.2). To confirm this interaction, an alternative system was used, making use of the rough eye phenotype generated by expression of human p21, a CyclinE/Cdk2 inhibitor, under *GMR* control (de Nooji and Hariharan, 1995). This rough eye phenotype results from a decrease in S phases in the eye imaginal disc and is sensitive to the dose of interactors. To assess the ability of *Su(var)2-10* to interact with *GMR-p21*, flies heterozygous for *GMR-p21* and $Su(var)2\text{-}10^2$ were generated. Halving the dose of $Su(var)2\text{-}10^2$ was able to slightly suppress the *GMR-p21* rough eye phenotype (Figure 6.2). Together, these results indicated that wild type *Su(var)2-10* may interact and negatively regulate DmcycE. To determine if the suppression is acting at the level of S phase, BrdU incorporation needs to be carried out on eye imaginal discs from third instar larvae heterozygous for *Su(var)2-10* and *GMR-p21*.

To confirm a direct interaction between Su(var)2-10 and DmcycE *in vivo*, co-immunoprecipitation from embryonic extracts were attempted using Su(var)2-10 antibody (a gift from P. Huen). However, no conclusive results were obtained, as it seems that the Su(var)2-10 protein levels were too low and therefore ectopic expression of Su(var)2-10 may be needed in order to be able to detect an *in vivo* interaction.

6-4.3 Interactions between Dcmaguk and DmcycE

Dcmaguk (CG9326), is an uncharacterised protein of the membrane-associated guanylate kinase family, containing several protein interaction domains: PDZ, SH3 and GUK (see discussion). To confirm the interaction between Dcmaguk and DmcycE, co-immunoprecipitation from *Drosophila* S2 cell extracts was performed. This required the generation of an epitope-tagged Dcmaguk protein and its expression in S2 cells. The GAL4-UAS system can be used to drive expression of the transgene of interest in S2 cells (Brand and Perrimon, 1993; Phelps and Brand, 1998). To achieve this, Dcmaguk was PCR amplified and cloned into the *pBS+mt* vector to generate a N-terminal 6 *myc* tagged *dcmaguk* (*mt-dcmaguk*) which was subcloned into the *Drosophila* transformation vector, *pUAST* whereby

Figure 6.1 : *cabeza* suppresses the *DmcycE^{JP}* rough eye phenotype.

(A-B) Scanning electron micrographs of adult eyes. **A.** +; *DmcycE^{JP}* and **B.** *caz^{2}*/+; *DmcycE^{JP}* eye phenotypes showing suppression of the *DmcycE^{JP}* rough eye phenotype.

(C-D) S phases cells as detected by BrdU labeling of eye discs from third instar larvae. **C.** +; *DmcycE^{JP}* and **D.** *caz^{2}*/+; *DmcycE^{JP}* eye discs showing suppression of the *DmcycE^{JP}* rough eye phenotype results from an increase in the number of S phases posterior to the MF.

Anterior is to the right.

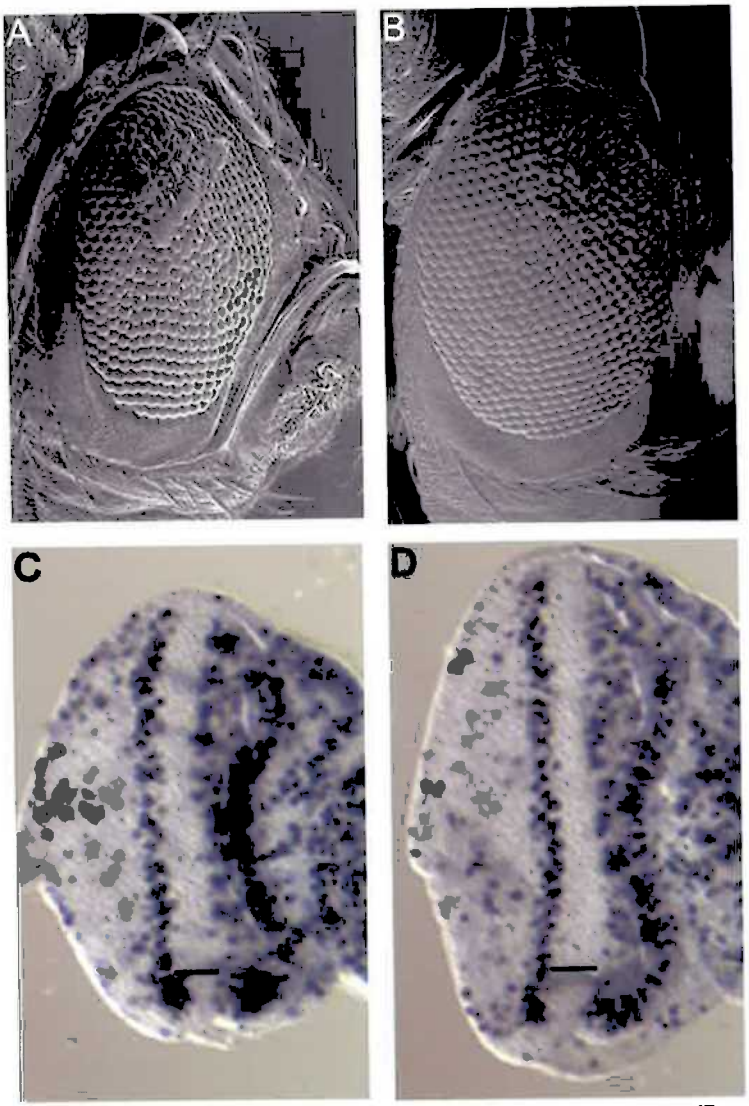

DmcycE^{JP} *caz^{2}/+; DmcycE^{JP}*

Figure 6.2 : *Su(var)2-10*^{2} enhances *GMR>gcycEI* and suppresses the *GMR-p21* rough eye phenotypes.

(A,B) Scanning electron micrographs of adult eyes from **A.** *GMR>gcycEI/+* and **B.** *Su(var)2-10/GMR>gcycEI* showing mild enhancement of the *GMR>gcycEI* rough eye phenotype.

(C,D) Scanning electron micrographs of adult eyes. **C.** +; *GMR-p21/+* and **D.** *Su(var)2-10/+*; *GMR-p21/+* eye phenotypes showing mild suppression of the *GMR-p21* rough eye phenotype.

Anterior is to the right.

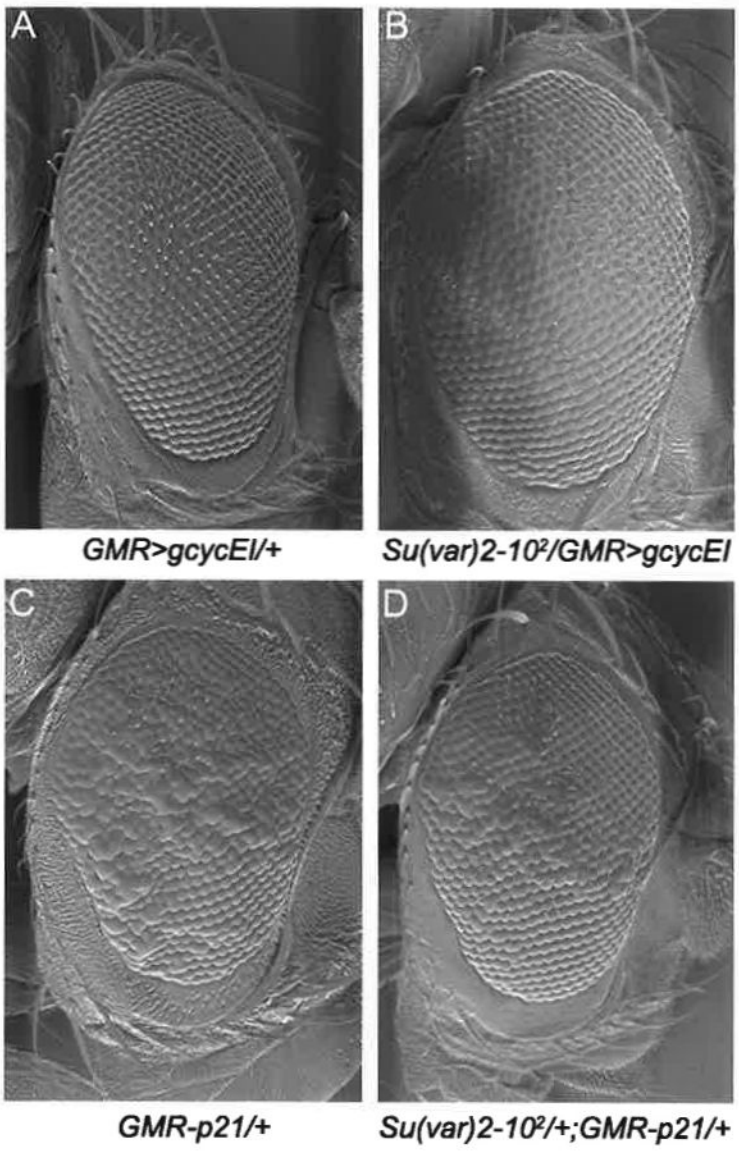
A
B
GMR>gcycEI/+
Su(var)2-10²/GMR>gcycEI
C
D
GMR-p21/+
Su(var)2-10²/+;GMR-p21/+

expression is under the control of Gal4 binding sites, *UAS* (*UAS-mt-dcmaguk).* The ubiquitin promoter can be used to ubiquitously drive expression of GAL4 (*Ub-GAL4*) in S2 cells. Thus whereby co-transfection of the *GAL4* and *UAS* constructs in one cell, results in ubiquitous ectopic expression of the gene of interest from *UAS.* To identify the transfection efficiency S2 cells were co-transfected with *UAS-GFP*, such that the number of transfected cells could be observed by the expression of GFP.

Co-immunoprecipitation experiments were performed on cells co-transfected with either *UAS-GFP*, *UAS-mt-dcmaguk*, and *Ub-GAL4*, or cells co-transfected with *UAS-GFP*, *UAS-mt-dcmaguk*, *UAS-DmcycEI* and *Ub-GAL4.* In addition as a negative control, cells were co-transfected with only *UAS-GFP* and *Ub-GAL4* (without *UAS-mt-dcmaguk).* In extracts from cells transfected with *UAS-mt-dcmaguk* an interaction between MT-Dcmaguk and DmcycE was observed. This was detected by immunoprecipitation with anti-DmcycE antibody and blotting with anti-Myc tag antibody (Figure 6.3 lanes 5 and 6 upper panel) and conversely by immunoprecipitation with anti-Myc tag antibody and blotting with anti-DmcycE antibody (Figure 6.3 lanes 5 and 6 lower panel). Co-immunoprecipitation experiments performed on cells transfected without *UAS-mt-dcmaguk* did not show an interaction (Figure 6.3 lanes 4 upper and lower panels). Interestingly, anti-DmcycE blotting revealed a higher molecular weight band at ~100kDa, corresponding to the size of DmcycEII, in the supernatant (Figure 6.3 lanes 1, 2 and 3 lower panel) that did not co-precipitate with Dcmaguk (Figure 6.3 lanes 4, 5 and 6 lower panel). Although this needs to be confirmed by specific blotting with anti-DmcycEII antibody, this suggests that *in vivo* in S2 cells Dcmaguk interacts specifically with DmcycEI and not DmcycEII. This is inconsistent with the observation that Dcmaguk interacted similarly with DmcycEI and DmcycEII in yeast 2-hybrid analysis, and may be explained by a DmcycEII modification that occurs in S2 cells but not in yeast. These results verify the yeast 2-hybrid interaction between Dcmaguk and DmcycEI and suggest that *in vivo* Dcmaguk may specifically associate with DmcycEI.

To determine the function of *dcmaguk* during *Drosophila* development, the spatial and temporal expression pattern of *dcmaguk* was examined by *in situ* hybridisation of whole mount embryos (Figure 6.4). An anti-sense probe was transcribed using T3 RNA polymerase from *pBS-dcmaguk. dcmaguk* can first be detected during gastrulation where it appears to localise to cells that are undergoing shape change. At germ band extension, *dcmaguk* expression was detected in the hindgut, where it persists throughout embryogenesis, and in the tracheal pits, which are in the dorsal region of each segment. During germ band retraction, expression in the epidermis demarcates the ingressing lateral segmentation boundaries, but these stripes do not

Figure 6.3 : Co-immunoprecipitation of S2 cell extracts showing that DmcycE and Dcmaguk associate.

Anti-cycE monoclonal antibody (8B10) and anti-Myc tag monoclonal antibody were used to immunoprecipitate transfected S2 cell extracts. The immunoprecipitated samples and supernatants were separated using 10% PAGE and subjected to western analysis, using anti-Myc tag antibody (upper panel) and anti-DmcycE antibody (lower panel).

Lanes 1 and 4, extracts from *Ub-GAL4* and *UAS-GFP* co-transfected cells, Lane 2 and 5 extracts from *Ub-GAL4, UAS-GFP* and *UAS-mt-dcmaguk* co-transfected cells and Lane 3 and 6 extracts from *Ub-GAL4, UAS-GFP*, *UAS-mt-dcmaguk* and *UAS-DmcycEI* co-transfected cells. Lanes 1-3: supernatant and Lanes 4-6: immunoprecipitation.

A band corresponding to Dcmaguk (~75kDa) is detected in the *dcmaguk* transfected samples lanes 2,3,5 and 6 (upper panel). The high abundance in the supernatant indicated that it is highly overexpressed. A band corresponding to DmcycEI (~75kDa) is detected in lanes 2,3,5,and 6 (lower panel). Significantly in the absence of MT-Dcmaguk, no DmcycEI can be detected (lane 4).

The higher molecular weigh bands present in the anti-cycE western blot (lower panel) are likely to represent DmcycEII protein.

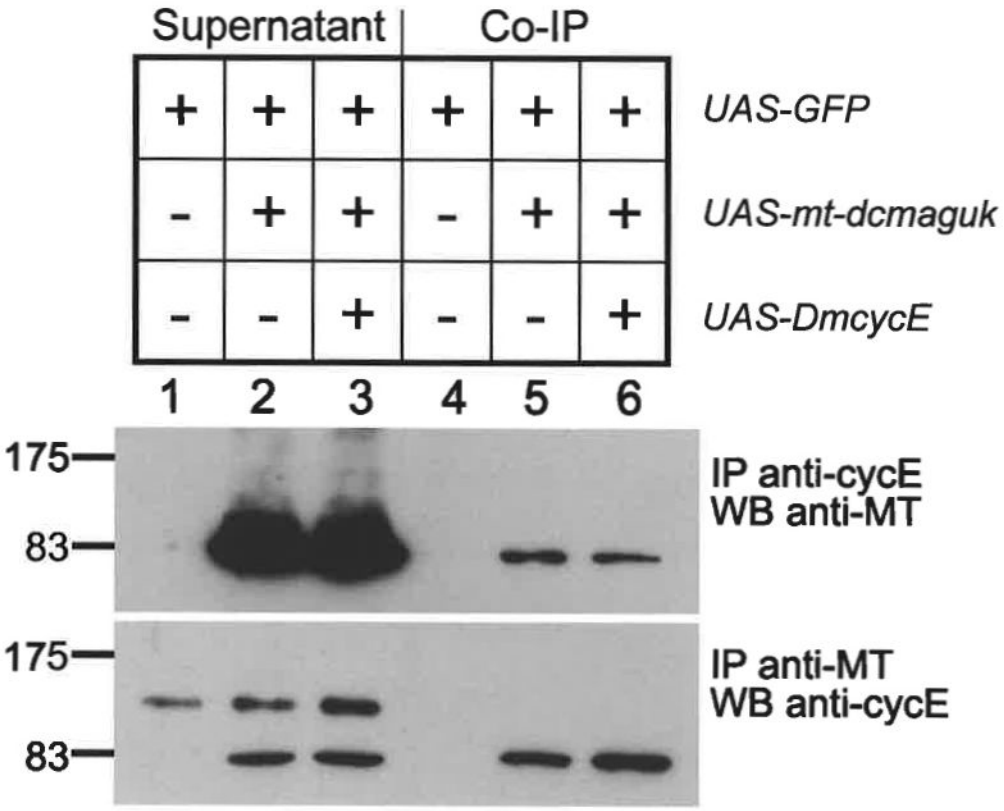
Supernatant
Co-IP
+ + + + + +
UAS-GFP
- + + - + +
UAS-mt-dcmaguk
- - + - - +
UAS-DmcycE
1 2 3 4 5 6
175
83
IP anti-cycE
WB anti-MT
175
83
IP anti-MT
WB anti-cycE

Figure 6.4 : Expression of *dcmaguk* during embryogenesis.

A. Gastrulating embryo showing expression of *dcmaguk* in invaginating cells of the ventral and chephalic furrow.

B. Germ band extension showing staining in the hindgut (hg) and in the tracheal pits (tp).

C. Germ band retraction showing staining in the foregut (fg), hindgut (hg) and segmental stripes.

D. During germ band retraction, expression appears epidermal and demarcates the ingressing lateral segmentation boundaries (*), but these stripes do not extend across the ventral region.

E. Later germ band retraction showing staining in the foregut, salivary glands (sg), pharyngeal muscles (ph), hindgut and in a row of cells running anterioposteriorly along the midgut region (arrowhead).

F. Late embryo showing persistence of staining in the foregut and hindgut.

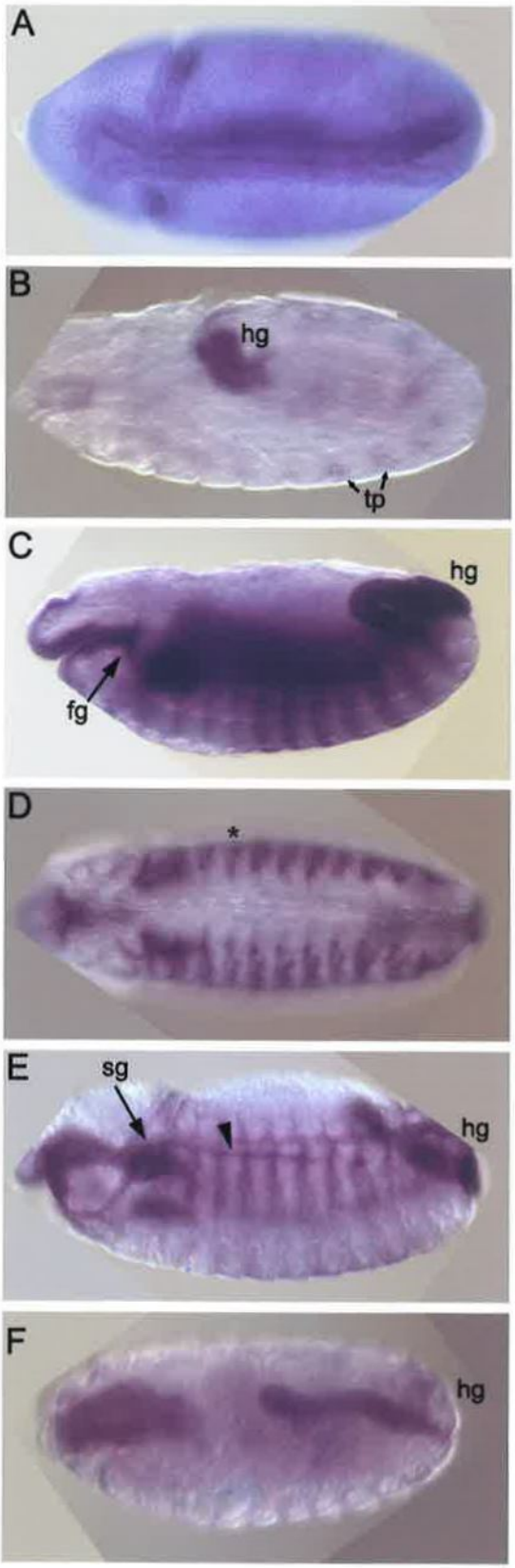
A
B
hg
tp
C
hg
fg
D
*
E
sg
hg
F
hg

cross the ventral region. Staining was also seen in the foregut, salivary glands, pharyngeal muscles, and in a row of cells running anterioposteriorly along the midgut region. This expression pattern may correspond to cells that are undergoing cell shape change. Further stainings with *DmcycE* and other cell cycle markers is required to elucidate how this expression correlates with *DmcycE* and cell proliferation.

To gain an insight into the nature of the interaction between Dcmaguk and DmcycE, whether it is a positive or negative one, genetic interactions were examined. As there is no mutant available, the deficiency *Df(2L)TW161*, which uncovers the region 38A6-B1 to 40A4-B1 removing *dcmaguk,* was used. This deficiency did not affect the *GMR>gcycEI* rough eye phenotype. However, the yeast interaction between Dcmaguk and DmcycE could not be predicted to be a negative one, and as the *GMR>gcycEI* rough eye phenotype is sensitive to the dose of negative interactors, an alternative system was used, making use of the *GMR-p21* rough eye phenotype. It was found that *Df(2L)TW161* strongly enhanced this *GMR-p21* (Figure 6.5), and also enhanced the $DmcycE^{JP}$ rough eye phenotype (H. Richardson pers. com.). This indicates that wild type Dcmaguk may act as a positive regulator of DmcycE. However, this may not represent the true nature of the genetic interaction with DmcycE as the deficiency used also uncovers several other genes involved in cell proliferation, including *E2F2* and a region required for DNA replication (Smith *et al.,* 1994).

As there are no mutations of *dcmaguk* currently available, to determine a function *in vivo* Si RNA can be used to knock out function during embryogenesis. Also the *GAL4-UAS* system can be used to over-express *dcmaguk* during *Drosophila* development. The *GAL4-UAS* system is a powerful tool for misexpressing genes of interest in order to elucidate their biological function. The *UAS-MT-dcmaguk* construct can be used to transform *Drosophila*. Analysis of the effect of Si RNA and ectopic expression of *dcmaguk* during development, will aid in elucidating the role of the interaction of Dcmaguk with DmcycE.

6-5 Discussion

This chapter described the use of the yeast two-hybrid system to identify proteins that interact directly with the N-terminus of DmcycEI. This identified Caz, Su(var)2-10 and Dcmaguk as interactors of DmcycE, with Dcmaguk potentially specifically interacting with DmcycEI. Their identification as interactors with DmcycE is of interest for understanding the regulation of DmcycE.

Figure 6.5 : *Df(2L)TW161* removing *dcmaguk* enhances the *GMR-p21* rough eye phenotype.

(A,B) Scanning electron micrographs of adult eyes. **A.** +; *GMR-p21/+* and **B.** *Df(2L)TW161/+; GMR-p21/+* eye phenotypes showing strong enhancement of the *GMR-p21* rough eye phenotype.

Anterior is to the right.

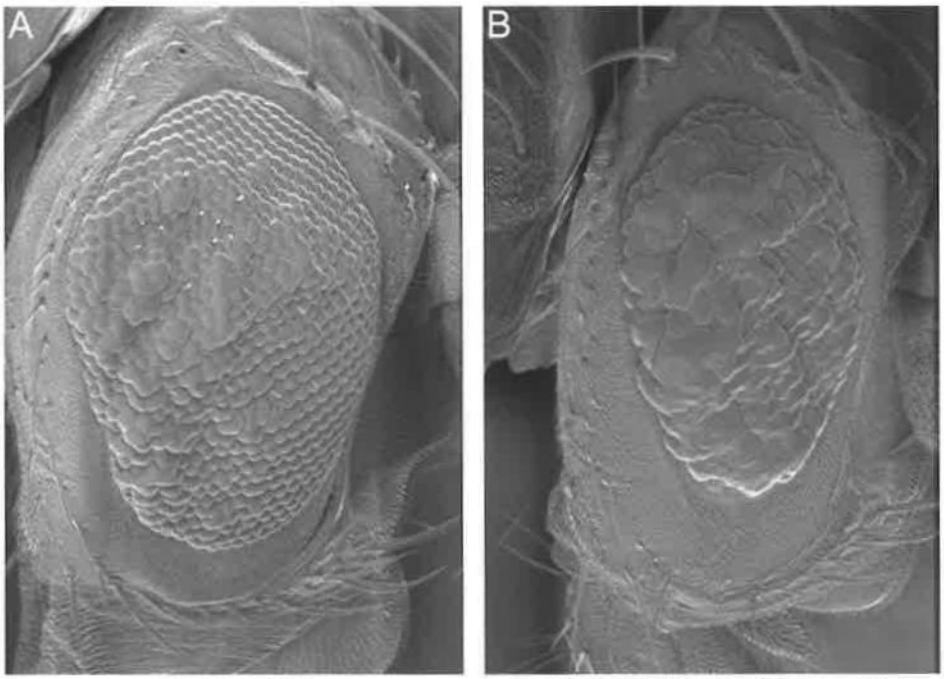

GMR-p21/+ *Df(2L) TW161/+;GMR-p21/+*

6-5.1 Role of Cabeza

The transcription machinery required for expression of eukaryotic structural genes consists of RNA polymerase II associated with general transcription factors. There are at least six general transcription factors (TFIIA, TFIIB, TFIID, TFIIE, TFIIF, and TFIIH) that assemble on the promoter in a sequential order to form a pre-initiation complex (PIC) (reviewed by Burley and Roeder 1996; Green 2000). The binding of TFIID to the TATA box is the initial step in formation of a PIC. TFIID is composed of TATA-binding protein (TBP) and coactivator subunits termed TBP-associated factors (TAF_{II}s). As with other components of the transcription machinery, TAF_{II}s are highly conserved, and analysis of yeast TAF_{II}s has shown that they are essential for viability.

Cabeza was initially isolated by homology to two human genes, EWS (Ewing's sarcoma) and TLS (transcribed in liposarcoma), and was referred to as SARFH (sarcoma-associated RNA-binding fly homologue). Chromosomal translocations resulting in the fusions of EWS and TLS to other cellular genes result in sarcoma formation (Immanuel *et al.* 1995). Expression of Caz in mammalian cells results in nuclear localisation. However, upon treatment with inhibitors of RNA pol II, Caz accumulates in the cytosol, and this relocation is dependent on the presence of the RRM domain. In addition, a functional UV crosslinking assay was used to show that the RRM domain functions as an RNA binding motif (Stolow and Haynes 1995). Furthermore, Caz and activated RNA pol II (phosphorylated form) show co-immunolocalisation on polytene chromosomes. Together, these results suggest that Caz participates in a function common to the expression of most genes transcribed by RNA pol II (Immanuel *et al.* 1995). This appears consistent with the suggestion that Caz is a homologue of human $TAF_{II}68$, and, with no apparent homologue in yeast, may represent a metazoan-specific TAF_{II}.

Caz shows ubiquitous early expression during embryogenesis, followed by later enrichment in the brain, central nervous system and gut. During larval development Caz is not restricted to the nervous system, as it is detected in the nuclei of fat bodies, in the gut, at low levels in salivary glands, and shows uniform nuclear ubiquitous staining in eye-antennal, wing and leg imaginal discs (Stolow and Haynes 1995). Caz expression was undetectable in brain, but was observed in the ventral nerve chord. It will be interesting to further examine this expression with regards to *DmcycE* expression and other cell cycle markers.

Therefore, from the yeast 2-hybrid interaction and genetic interaction with DmcycE, Caz may interact with DmcycE and play a negative role in cell cycle regulation in the eye imaginal disc. By analogy with the role of mammalian Cyclin E in regulating the activity of the transcriptional repressor Rb (Ekholm and Reed 2000), and in regulating the transactivation

activity of the androgen receptor (Yamamoto *et al.,* 2000), DmcycE may have a role in activating gene transcription by binding and inactivating Caz.

6-5.2 Role of Su(var)2-10

In mammals, protein inhibitors of activated STAT (PIAS) were first identified as cofactors that inhibit the transcriptional potential of the JAK-STAT pathway (Liu *et al.*, 1998). Activation of the JAK-STAT pathway occurs following the binding of cytokines to cell surface receptors, the Janus kinase, or JAK, family of tyrosine kinases. Activated JAKs phosphorylate a family of at least seven cytoplasmic transcription factors termed STATs (signal transducer and activator of transcription). STATs mediate specific transcriptional responses. In vertebrates, four PIAS proteins (PIAS1, PIAS3, PIASx, and PIASy) have been identified (Liu *et al.,* 1998). PIAS1 (protein inhibitor of activated STAT1) was first identified as a specific inhibitor of STAT1 signalling, but conversely was shown to enhance the transcriptional activity of nuclear hormone receptors (Liu *et al.*, 1998; Kotaja *et al.*, 2000; Gross *et al.,* 2001). PIAS1 and PIAS3 inhibit DNA binding of the STAT1 and STAT3 factors (Chung *et al.*, 1997; Liu *et al.*, 1998). In contrast, the PIASy protein represses STAT1 and the activity of the androgen receptor without affecting DNA binding (Gross *et al.*, 2001).

The JAK-STAT pathway operates in *Drosophila;* STAT92E is activated by Hopscotch (Hop), the single *Drosophila* non-receptor tyrosine kinase of the JAK family (review by Luo and Dearolf, 2001). Phosphorylated STAT92E then translocates to the nucleus and directly activates transcription. The *Drosophila* JAK-STAT pathway has been shown to regulate the development and/or differentiation of multiple cell types and processes, including germ cell development, embryogenesis, hematopoiesis, and imaginal cell development (review by Luo and Dearolf, 2001). Although, a role for the JAK-STAT pathway in cell proliferation in *Drosophila* has not been well characterized, there appears to be a positive role in proliferation of imaginal discs, but a negative role in the proliferation of blood cells (Harrison *et al.,* 1995).

Su(var)2-10 was originally identified as a suppressor of position effect variegation, and was recently shown by Hari *et al.* (2001) to be required for normal chromosome function. This gene, also described as *zimp* (Mohr and Boswell, 1999) and *dpias* (Betz *et al.,* 2001), has strong homology to the mammalian PIAS (protein inhibitors of activated stats) genes. As described above, PIAS proteins have been well described in the mammalian cell and molecular biology literature as antagonists of STAT proteins. From the recent completion of the genome sequence and annotation of the *Drosophila* genome, there appears to be a single STAT gene, *stat92E*, and a single PIAS homologue, *Su(var)2-10. Drosophila* STAT92E and Su(var)2-10 have been shown to interact functionally to regulate hematopoiesis and eye development (Betz *et al.,* 2001). Ectopic expression of *Su(var)2-10*, using the *eyeless-GAL4* driver, causes a small rough

eye phenotype, having a primary effect on early proliferating eye disc cells, while removal of the *Su(var)2-10* in somatic eye clones blocked cellular differentiation into photoreceptor cells and other cell types. The genetic interaction experiments are consistent with a role for Su(var)2-10 in negative cell cycle regulation and promoting differentiation (Betz *et al.*, 2001).

Hypermorphic alleles of *hop* have been shown to suppress the $DmcycE^{JP}$ rough eye phenotype (Secombe, 1999). The phenotypes of hypermorphic *hop* alleles show over-proliferation of larval hematopoietic tissue, small imaginal discs and give rise to melanotic tumours (Watson *et al.*, 1991). Given this phenotype and the suppression of $DmcycE^{JP}$ by activated *hop,* suggests that Hop acts as a positive cell cycle regulator in eye imaginal discs. As halving the dose of *Su(var)2-10* suppressed the *GMR-p21* rough eye phenotype, implicating wild type Su(var)2-10 a negative cell cycle regulator. This suggests that any direct interaction between Su(var)2-10 and DmcycE may result in the inhibition of DmcycE and result in G1 arrest. Together, with the analysis of the role of Su(var)2-10 during eye development, this suggests that Su(var)2-10 inhibits DmcycE, and that Su(var)2-10 is inactivated by the Hop/Stat92E pathway in promoting cell proliferation.

An additional role for Su(var)2-10 in the regulation of chromosome structure and function has been identified (Hari *et al.*, 2001). Mutations in the *Su(var)2-10* locus cause chromosome transmission defects and abnormal chromosome morphologies, affecting both mitotic chromosome condensation and the organization of interphase chromatin (Hari *et al.*, 2001). The primary targets of Su(var)2-10 that account for this mutant phenotype are unknown, but may involve downstream components of the JAK-STAT pathway. Overexpression of Cyclin E, but not Cyclin D1 or A, in tissue culture cells has been shown to result in chromosome instability (Spruck *et al.*, 1999). These results indicate that downregulation of Cyclin E/Cdk2 kinase activity following the G1/S-phase transition may be necessary for the maintenance of karyotypic stability. Given this data, the chromosome defects of *Su(var)2-10* mutants may be due to misregulated DmcycE activity.

Recent evidence has arisen implicating a mammalian PIAS as a SUMO E3 ligase. SUMO (small ubiquitin-related modifier) is a conserved ubiquitin-like small protein that is covalently attached to other proteins to modulate their functions (reviewed by Melchior, 2000). SUMO has been shown to play critical roles in both nuclear and cytoplasmic processes, including nuclear transport, the regulation of transcriptional processes, the targeting of transcriptional regulators to subnuclear domains, and the regulation of mitosis (review by Jackson, 2001). Enzymes regulating the addition of SUMO to target proteins, called SUMO E3 ligases, have been described in yeast and mammals. The mammalian PIAS protein, PIASy, has been shown to repress the activity and affect the subnuclear localization of LEF1 (a Wnt-

responsive transcription factor) by directing SUMO addition to LEF1, implicating it as a SUMO E3 ligase (Sachdev *et al.,* 2001). A SUMO conjugation system has been identified in *Drosophila*, but the targets of sumolyation and the pathways involved have not been elucidated (Long and Griffith, 2000).

Further characterisation of the role of Su(var)2-10 in the JAK-STAT pathway and in sumolyation will aid in understanding the role of Su(var)2-10 and the significance of the potential interaction with DmcycE. One possiblility is that DmcycE is a direct target of Su(var)2-10 SUMO ligase activity, whereby Su(var)2-10 functions in the JAK-STAT pathway to sumolyate and inactiate DmcycE, inhibiting cell cycle progression. However, further analysis is needed to determine if Su(var)2-10 directly interacts with DmcycE and if DmcycE is in fact sumolyated.

6-5.3 Role of Dcmaguk

Membrane associated guanylate kinases (MAGUK) contain several protein-protein interaction domains: PDZ, Src homology 3 (SH3), and a C-terminal guanylate kinase like domain (GUK) that may act as a protein-binding domain (Figure 6.6) (reviewed by Anderson, 1996). The prototypical MAGUK family member is the *Drosophila* tumour suppressor, Discs-large (Dlg), which is required for apical-basal epithelial cell polarity (reviewed by Bryant and Huwe, 2000). There are several mammalian MAGUKs, with functions including the assembly of ion channels, in cell-adhesion, cytoskeletal scaffolding proteins and components of synapses. Due to their modular structure it has been suggested that they are able to bind several proteins.

The correct maintenance of epithelial structure, is important for restricting cell proliferation, as is evident by mutations in several *Drosophila* genes that lead to loss of apical-basal polarity and proliferation phenotypes characteristic of neoplastic tumour suppressors (Bilder *et al.*, 2000; Bilder and Perrimon 2000). These phenotypes are exhibited by mutants of *discs-large (dlg)*, *lethal giant larvae (lgl),* which encodes a protein with a WD-40 repeat, and *scribble (scrib),* a PDZ domain and leucine rich repeat containing protein. All of these mutants die as over-grown larvae with a similar phenotype there is loss of tissue polarity and epithelial tissues lose structure and continue to proliferate in three dimensions. Furthermore, *dlg, lgl* and *scrib* and have been shown to genetically interact (Bilder et al., 2000; Brumby *et al.,* 2002). Togeather, these data suggests that Dlg, Lgl and Scrib act in a common pathway at septate junctions to control apical-basal cell polarity and cell proliferation. It is presently unknown as to how Dlg/Lgl/Scrib function to prevent uncontrolled proliferation, but it is clearly evident that cell polarity and proliferation are tightly connected. In mammalian cells, Dlg and Scribble have been implicated as tumour suppressor genes, as they are targeted for degradation by human papillomavirus E6 oncoprotein in transformed cells (Kiyono et al., 1997; Lee et al., 1997).

Moreover, transfection of the human Dlg into cells results in G1 arrest (Suzuki et al., 1999; Ishidate et al., 2000).

A role for these genes in regulation of cell proliferation is highlighted by the finding that *dlg, lgl* and *scrib* all interact genetically with $DmcycE^{JP}$, suppressing the rough eye phenotype (Secombe, 1999; Brumby *et al.,* 2002). Furthermore, *scrib* and *lgl* mutant clones of cells ectopically express *DmcycE* (H. Richardson pers.com.). Thus, Dlg, Lgl and Scrib appear to act to negatively regulate *DmcycE* transcription. The role of Dcmaguk could be similar to that of Dlg in negatively regulating cell proliferation. Although a negative role is inconsistent with *Df(2L)TW161* enhancing *GMR-p21* and $DmcycE^{JP}$, this may in fact be due to another gene, since an enhancer of $DmcycE^{JP}$, E2F2 from the genetic screen maps to this region (H. Richardson pers. com.). Further analysis of the function of Dcmaguk is required to elucidate such a role and the significance of the interaction with DmcycE. This will require the generation of transgenic flies and the identification of a *dcmaguk* mutant.

6-5.4 Conclusion

In summary, this chapter has described the use of yeast 2-hybrid analysis to identify direct protein interactors of DmcycE, identifying *cabeza, Su(var)2-10* and *dcmaguk.* Further characterisation of the interactions with DmcycE may demonstrate a role for these proteins, in addition to their previously described roles, as regulators of cell proliferation. The identification of such proteins as interactors of DmcycE, highlights the importance of the use of the yeast 2-hybrid screen to identify novel genes involved in DmcycE-mediated cell cycle regulation.

Figure 6.6 : *dcmaguk* (*CG9326*) encodes a MAGUK family protein.

A. Domain structure of Dcmaguk

L27 domain (yellow): The L27 domain is found in the *C. elegans* receptor targeting proteins Lin-2 and Lin-7. Mutations in these proteins result in mislocalisation of the growth factor receptor, Let23.

PDZ domain (green): Present in PSD-95, Dlg, and ZO-1/2. Some PDZs have been shown to bind C-terminal polypeptides; others appear to bind internal (non-C-terminal) polypeptides. Different PDZs possess different binding specificities.

SH3, Src homology 3 domain (blue): SH3 domains bind to target proteins through sequences containing proline and hydrophobic amino acids. Pro-containing polypeptides may bind to SH3 domains in 2 different binding orientations. SH3 domains are often indicative of a protein involved in signal transduction related to cytoskeletal organization. First described in the Src cytoplasmic tyrosine kinase. The structure is a partly opened beta barrel.

GUK, Guanylate kinase domain (red): Active enzymes catalyze ATP-dependent phosphorylation of GMP to GDP. The structure resembles that of adenylate kinase. The membrane-associated guanylate kinase homologues (MAGUKs) do not possess guanylate kinase activity, rather they posses protein-binding function.

B. The alignment compares Dcmaguk (D.m.) with mammalian homologues, human (H.s.) Dlg2 (Vam-1) (Tseng *et al.*, 1995; Mazoyer *et al.*, 2001) and mouse (M.m.) Pals2 (muguk p55 #6) (Kamberov *et al.*, 2000). Dcmaguk shows 38% identity and 56% similarity with Human Dlg2. Conserved amino acids between all 3 sequences represented by the black boxes and conservation across 3 sequences in grey.

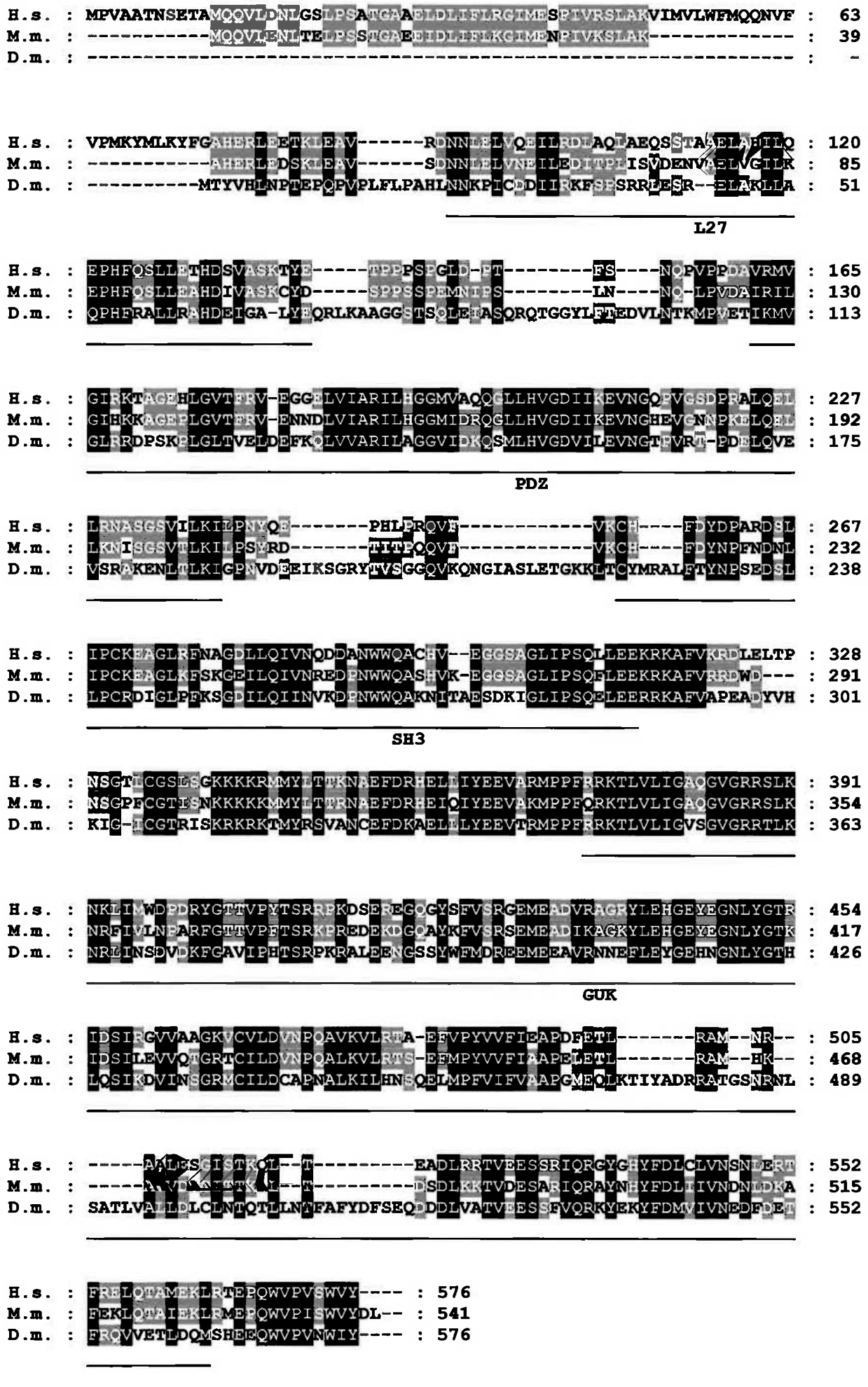
H.s. : MPVAATNSETAMQQVLDNLGSLPSATGAAELDLIFLRGIMESPIVRSLAKVIMVLWFMQQNVF : 63
M.m. : ----------MQQVLENLTELPSSTGAEEIDLIFLKGIMENPIVKSLAK---------- : 39
D.m. : ---------- : -
H.s. : VPMKYMLKYFGAHERLEETKLEAV------RDNNLELVQEILRDLAQLAEQSSTAAELAHILQ : 120
M.m. : ----------AHERLEDSKLEAV------SDNNLELVNEILEDITPLISVDENVAELVGILR : 85
D.m. : ----------MTYVHLNPTEPQPVPLFLPAHLNNKPICDDIIRKFSPSRRLESR--ELAKLLA : 51
L27
H.s. : EPHFQSLLETHDSVASKTYE-----TPPPSPGLD-PT--------FS-----NQPVPPDAVRMV : 165
M.m. : EPHFQSLLEAHDIVASKCYD-----SPPSSPEMNIPS--------LN-----NQ-LPVDAIRIL : 130
D.m. : QPHFRALLRAHDEIGA-LYEQRLKAAGGSTSQLEHASQRQTGGYLETEDVLNTKMPVETIKMV : 113
H.s. : GIRKTAGEHLGVTFRV-EGGELVIARILHGGMVAQQGLLHVGDIIKEVNGQPVGSDPRALQEL : 227
M.m. : GIHKKAGEPLGVTFRV-ENNDLVIARILHGGMIDRQGLLHVGDIIKEVNGHEVGNNPKELQEL : 192
D.m. : GLRRDPSKPLGLTVELDEFKQLVVARILAGGVIDKQSMLHVGDVILEVNGTPVRT-PDELQVE : 175
PDZ
H.s. : LRNASGSVILKILPNYQE--------PHLPRQVF----------VKCH-----FDYDPARDSL : 267
M.m. : LKNISGSVTLKILPSYRD-------TITLQQVF----------VKCH-----FDYNPFNDNL : 232
D.m. : VSRAKENLTLKIGPNVDEEIKSGRYTVSGGQVKQNGIASLETGKKLTCYMRALETYNPSEDSL : 238
H.s. : IPCKEAGLRFNAGDLLQIVNQDDANWWQACHV--EGGSAGLIPSQLLEEKRKAFVKRDLELTP : 328
M.m. : IPCKEAGLKFSKGEILQIVNREDPNWWQASHVK-EGGSAGLIPSQFLEEKRKAFVRRDWD--- : 291
D.m. : LPCRDIGLPFKSGDILQIINVKDPNWWQAKNITAESDKIGLIPSQELEERRKAFVAPEADYVH : 301
SH3
H.s. : NSGTLCGSLSGKKKKRMMYLTTKNAEFDRHELIIYEEVARMPPFRRKTLVLIGAQGVGRRSLK : 391
M.m. : NSGPFCGTISNKKKKKMMYLTTRNAEFDRHEIQIYEEVAKMPPFQRKTLVLIGAQGVGRRSLK : 354
D.m. : KIG-ICGTRISKRKRKTMYRSVANCEFDKAELLLYEEVTRMPPFRRKTLVLIGVSGVGRRTLK : 363
H.s. : NKLIMWDPDRYGTTVPYTSRRPKDSEREGQGYSFVSRGEMEADVRAGRYLEHGEYEGNLYGTR : 454
M.m. : NRFIVLNEARFGTTVPFTSRKPREDEKDGQAYKFVSRSEMEADIKAGKYLEHGEYEGNLYGTK : 417
D.m. : NRLINSDVDKFGAVIPHTSRPKRALEENGSSYWFMDREEMEEAVRNNEFLEYGEHNGNLYGTH : 426
GUK
H.s. : IDSIRGVVAAGKVCVLDVNPQAVKVLRTA-EFVPYVVFIEAPDFETL-------RAM--NR-- : 505
M.m. : IDSILEVVQTGRTCILDVNPQALKVLRTS-EFMPYVVFIAAPELETL-------RAM--HK-- : 468
D.m. : LQSIKDVINSGRMCILDCAPNALKILHNSQELMPFVIFVAAPGMEQLKTIYADRRATGSNRNL : 489
H.s. : -----AALKSGISTKQL--T---------EADLRRTVEESSRIQRGYGHYFDLCLVNSNLERT : 552
M.m. : -----AAVDSGTTKQL--T---------DSDLKKTVDESARIQRAYNHYFDLIIVNDNLDKA : 515
D.m. : SATLVALLPLCLNTQTLLNTFAFYDFSEQDDLVATVEESSFVQRKYEKYFDMVIVNEDFDET : 552
H.s. : FRELQTAMEKLRTEPQWVPVSWVY---- : 576
M.m. : FEKLQTAIEKLRMEPQWVPISWVYDL-- : 541
D.m. : FRQVVETLDQMSHEEQWVPVNWIY---- : 576

Chapter 7 : Final Discussion

7-1 Introduction

The research described in this thesis was undertaken to examine the regulation of DmcycE during development of a multicellular animal. The specific aims were to examine the expression of DmcycEII during development, to compare the properties of DmcycEI with DmcycEII *in vivo* and to investigate a mechanism by which DmcycEI is inhibited in the MF during eye development. The relative properties of DmcycEI and DmcycEII in S phase induction was investigated by ectopic expression analysis in the eye imaginal disc and assessing the effects of DmcycE truncations on the ability of the proteins to induce S phase. To identify a DmcycEI specific inhibitor, a genetic interaction screen and a yeast 2-hybrid screen were undertaken. The genetic interaction screen made use of overexpression of DmcycEI in the eye to produce a dose-sensitive rough eye. This phenotype was then used to screen a collection of *P*-element mutations on the 3rd chromosome for dominant enhancers. Six enhancers were isolated and further characterised, with one of these appearing to be specific for DmcycEI. The yeast 2-hybrid screen was carried out using *Drosophila* embryonic and 3rd instar larval libraries to isolate proteins that are capable of binding to the N-terminal region of DmcycEI. These proteins were shown to bind to the N-terminus of DmcycEI, and one may be specific for DmcycEI

7-2 Summary of results

7-2.1 Distribution of DmcycEII during development

To assess the properties and roles of DmcycEII during development, the distribution of DmcycEII was examined. This required the generation of an antibody to the unique N-terminal region of DmcycEII, which then enabled the localisation of DmcycEII during development to be determined. During embryogenesis, DmcycEII is nuclear localised during interphase, as is DmcycEI, and becomes distributed in the cytoplasm during mitosis. DmcycEII protein, which is maternally-deposited, is most abundant during the early rapid nuclear divisions of embryogenesis. During later stages of development, DmcycEII is present during third larval instar eye-antennal and wing imaginal disc development. DmcycEII was also detected during oogenesis, during the early germ cell divisions and in the germinal vesicle. Although it remains unclear as to the precise role of DmcycEII in these tissues, DmcycEII may function in specific cells, for example, in overcoming an inhibitor or to drive entry into S phase.

7-2.2 Functional analysis of DmcycEI and DmcycEII

Functional studies were undertaken to characterise the relative properties of DmcycEI and DmcycEII. This required analysis of the effects of ectopically expressing both full-length DmcycE proteins as well as N- and C-terminal deletions of DmcycEI on S phases in the eye imaginal disc. Ectopic expression of DmcycEII and N-terminal deletions of DmcycEI were able to drive all G1 cells within the morphogenetic furrow (MF) into S phase, while a C-terminal deletion of DmcycEI could not. These results show that DmcycEII is more potent than DmcycEI in driving cells into S phase and that the unique 12 N-terminal amino acids of DmcycEI contains a negative regulatory domain. These observations suggested a model whereby the unique N-terminal region of DmcycEI may be the target region for an inhibitor, present within the MF, that bind to and inhibits DmcycEI function.

Several approaches were undertaken to identify the putative inhibitor, including the examination of candidate inhibitors, Dap and Rux. The p21 homologue, Dap, was shown by yeast 2-hybrid, co-immunolocalisation and *in vivo* functional studies, not to be the mediator of the DmcycEI inhibition in posterior part of the MF. The inhibitor Rux was also shown not to specifically bind to or inhibit DmcycEI in yeast or to act in a dose sensitive manner in restraining DmcycEI function. Taken together, these results do not support a role for Dap or Rux in inhibiting DmcycEI in the posterior MF cells, suggesting that an unknown inhibitory mechanism acts in these posterior MF cells to inhibit DmcycEI.

To identify DmcycEI specific inhibitors, two different approaches that would identify negative regulators of DmcycE were undertaken: a genetic interaction screen, and a yeast 2-hybrid screen.

7-2.3 Genetic interactor screen using *GMR>gcycEI*

A genetic interaction screen was undertaken making use of overexpression of DmcycE in the eye. Characterisation of the tissue-specific ectopic expression of DmcycEI using *GMR>gcycEI* showed this to produce a rough eye phenotype that was due to an increase in S phases posterior to the MF in the eye imaginal disc. In addition to being sensitive to the gene dosage of *DmcycE*, the *GMR>gcycEI* rough eye phenotype was found to be sensitive to the dosage of the negative G1 to S phase regulators *dap* and *Rbf*. Thus, as the *GMR>gcycEI* phenotype is sensitive to a reduction in the dosage of known negative regulators of the G1 to S phase transition, it provided the basis for a sensitised genetic screening system. This phenotype was then used to screen a collection of *P*-element mutations to identify dominant enhancers in an attempt to identify the putative DmcycEI inhibitor present in the posterior region of the MF.

P-element mutations identified as enhancers of *GMR>gcycEI* are likely to disrupt genes involved in negatively-regulating entry into S phase, acting downstream of *DmcycEI*

transcription, and may include a DmcycEI-specific inhibitor. The screen was successful in the identification of novel *DmcycEI* interactors. Two interactors identified are the novel gene *CG7394,* encoding a DnaJ domain protein, and the known previously identified gene *orb,* encoding a cytoplasmic polyadenylation element binding protein. Further characterization of *CG7394* and *orb* is required to elucidate the role for these proteins in novel negative regulation of DmcycEI or downstream negative regulation of entry into S phase.

7-2.4 Yeast two-hybrid screen using the N-terminus of DmcycEI

Another approach to identify the putative DmcycEI specific inhibitor was the use of the yeast 2-hybrid screen to identify proteins that can interact directly with the N-terminal region of DmcycEI. The yeast 2-hybrid analyses screened 3.638 x 10^7 library cDNAs, and identified Caz, Su(var)2-10, and Dcmaguk as interactors of DmcycEI N-terminus. However, these interactors were not specific to the unique N-terminal 12 amino acids of DmcycEI, as they bound relatively similarly to both DmcycEI and DmcycEII. The interactors were further characterised to determine if the interaction with DmcycE was inhibitory. This revealed that neither the Su(var)2-10, Caz nor Dcmaguk interaction with DmcycEI and DmcycEII was inhibitory to DmcycE activity, at least not affecting DmcycE to the same degree as the characterised inhibitor Dap. To verify and investigate the function of these interactors *in vivo* studies were undertaken.

cabeza encodes a RNA binding protein containing a RNA recognition motif (RRM), and appears to be the homologue of human $TAF_{II}68$, a component of RNA polymerase II transcription machinery. The interaction between *caz* and *DmcycE* was verified *in vivo* by examination of genetic interactions, where reducing the dose of *caz* suppressed the $DmcycE^{JP}$ rough eye phenotype. Therefore, from the yeast 2-hybrid interaction and genetic interaction with *DmcycE*, Caz appears to play a negative role in cell cycle regulation during development and perhaps by analogy with Cyclin E regulation of Rb or the androgen receptor, DmcycE binding to Caz may inactivate it.

Su(var)2-10 encodes a protein with homology to the PIAS family of proteins, regulators of JAK-STAT signalling, and recently a member has also been shown to play a role in the SUMO modification of proteins. The interaction between *Su(var)2-10* and *DmcycE* was verified *in vivo* by examination of genetic interactions. Together, these analyses have implicated a role for *Su(var)2-10* as a negative regulator of entry into S phase by directly interacting with DmcycE. This may occur by decreasing DmcycE activity or targeting DmcycE to a specific subcellular location.

dcmaguk (*CG9326*) encodes an uncharacterised protein of the membrane-associated guanylate kinase family (MAGUK). The MAGUK family of proteins have been shown to have a variety of functions, the best characterised in *Drosophila* being a role in control of apical-basal

cell polarity and maintenance of correct cell proliferation patterns. It is unknown how they act to prevent uncontrolled proliferation, but it is evident that cell polarity and proliferation are tightly connected. The interaction between Dcmaguk and DmcycE was confirmed by co-immunoprecipitation from *Drosophila* S2 cell extracts, and this may be specific for DmcycEI Further analysis of the function of Dcmaguk is required to elucidate such a role and the significance of the interaction with DmcycE.

The *P*-element screen and yeast 2-hybrid screen identified candidate DmcycEI specific inhibitors, *CG7394DnaJ* and *dcmaguk*. The yeast 2-hybrid screen was also successful in identifying proteins that directly interacted with DmcycE and these included *cabeza* and *Su(var)2-10* that may act to negatively regulate cell proliferation. Further characterisation of the interactors is required to demonstrate a role for these proteins, in addition to their previously described roles, as regulators of DmcycE and cell proliferation. The identification of such proteins as interactors of DmcycE highlights the importance of the use of the yeast 2-hybrid screen to identify novel genes involved in DmcycE-mediated cell cycle regulation.

7-3 Conclusion

7-3.1 What is the function of DmcycEII during development?

During embryogenesis, DmcycEII is present at high levels in the early embryo when cell cycles are very rapid and essentially have no G1 or G2 phases. It is possible that DmcycEII has a role here in allowing the very rapid S phases to occur in these early embryonic cycles. The demonstration that ectopically-expressed DmcycEII is largely resistant to an inhibitor in the eye disc that targets DmcycEI suggests one way in which the specific properties of DmcycEII may be promoting the rapid embryonic cycles. For example, a maternally-supplied inhibitor may be unable to effectively inhibit DmcycEII/DmCdk2 function *in vivo*, allowing for immediate entry into S phase after the completion of mitosis in these early cycles. In contrast, once DmcycEI protein starts to predominate after post-blastoderm cycle 14, expression of the potential inhibitor may more readily inhibit DmcycEI/DmCdk2 function and this leads to G1 arrest.

It is possible that similar mechanisms exist in mammalian cells to allow different types of cell cycles to occur. Interestingly, three different splice variants of human Cyclin E have been reported (Sewing *et al.*, 1994; Ohtsubo *et al.*, 1995; Mumberg *et al.*, 1997). Two of these variants, Es and Et, are unable to activate Cdk2 activity, suggesting that they may act in a dominant-negative manner in the G1 to S phase transition (Sewing *et al.*, 1994; Mumberg *et al.*, 1997). In contrast, protease-cleaved N-terminal truncated forms (deleting ~45 or ~69 N-terminal amino acids) of human Cyclin E have been identified in tumor cells, and have higher activity and greater S phase inducing potential than full-length Cyclin E (Porter and Keyomarski, 2000;

Porter *et al.*, 2001). These data suggest that human Cyclin E may also be subject to an inhibitory mechanism that acts at the N-terminal region. Interestingly, a second mammalian *cyclin E, E2*, encoding a protein differing significantly in its N-terminal region to Cyclin E1 has been identified, suggesting a role for functionally distinct Cyclin E proteins during development (Lauper *et al.*, 1998; Zariwala *et al.*, 1998; Gudas *et al.*, 1999). It is possible that a similar mechanism may exist in *Drosophila* and mammalian cells to allow tissue specific cell cycle regulation during development. The significance of this study may extend to the understanding of different CyclinE proteins in the mammalian cell cycle during development.

The results of this study have revealed the existence of a novel inhibitory domain at the N-terminus of DmcycEI that prevents ectopic DmcycEI from inducing G1 cells within the posterior region of the MF into S phase. Although DmcycE is normally not expressed at detectable levels within the MF, it is possible that such a mechanism prevents low levels of DmcycE protein from functioning inappropriately during eye development. The results described here have also demonstrated that DmcycEII is largely resistant to the inhibitory mechanism that acts on DmcycEI, highlighting the complexity of G1-S regulation and exposing a novel cell cycle regulatory mechanism that acts during development.

7-3.2 Identification of novel *DmcycE* interactors

The genetic interactor and yeast 2-hybrid screens were successful in the identification of novel DmcycEI interactors and further analysis may elucidate a role for these proteins as novel regulators of DmcycE or downstream regulators of entry into S phase. Due to high level of conservation in the mechanism of cell cycle control, regulators of the G1 to S phase transition identified in *Drosophila* are likely to have comparable functions in mammalian systems. Further analysis of the interactors identified will potentially reveal novel mechanisms for the role of DmcycE in regulation of cell proliferation. Together, this will increase our knowledge of DmcycE regulation in different developmental contexts.

Appendices

Appendix 4.A: LacZ assays for interactions with Dap and Rux

Bait + Prey	OD600	t (min)	vol (ml)	OD420	Miller U	Average	Std Dev
pGildaDmEI+pJGdap	0.791	45	0.5	0.414	23.267	19.124	5.859
pGildaDmEI+pJGdap	0.979	45	0.5	0.330	14.981		
pGildaDmEI+pJGrux	0.893	45	0.5	0.339	16.847	22.815	10.502
pGildaDmEI+pJGrux	0.766	45	0.5	0.602	34.941		
pGildaDmEI+pJGrux	0.741	45	0.5	0.278	16.656		
pGildaDmEI+pJG4-5	0.782	45	0.5	0.031	1.745	1.207	0.690
pGildaDmEI+pJG4-5	0.799	45	0.5	0.008	0.428		
pGildaDmEI+pJG4-5	0.697	45	0.5	0.023	1.447		
pGildaDmEII+pJGdap	0.709	45	0.5	0.583	36.521	30.944	7.887
pGildaDmEII+pJGdap	0.701	45	0.5	0.400	25.367		
pGildaDmEII+pJGrux	0.74	45	0.5	0.513	30.787	29.240	2.188
pGildaDmEII+pJGrux	0.745	45	0.5	0.464	27.693		
pGildaDmEII+pJG4-5	0.721	45	0.5	0.024	1.455	1.514	0.084
pGildaDmEII+pJG4-5	0.737	45	0.5	0.026	1.574		

Appendix 5.A : Analysis of *DmcycE^{JP}* suppressors for modification of *GMR>gcycEI*.

Comparison of the rough eye phenotype of *GMR>gcycEI/DmcycE^{JP}, S(DmcycE^{JP})II* to that of *GMR>gcycEI/DmcycE^{JP}*.

Screen cross: *GMR>gcycEI* X $\frac{DmcycE^{JP}\ S(DmcycE^{JP})}{CyO}$

↓

$\frac{DmcycE^{JP}\ S(DmcycE^{JP})}{GMR>gcycEI}$

Control cross: *GMR>gcycEI* X *DmcycE^{JP}*

↓

$\frac{DmcycE^{JP}}{GMR>gcycEI}$

S(DmcycE^{JP})II examined:

27S3 II.1	39S2 II.2	59S3 II.4	42S11 II.5	67S7 II.6	22S9 II.12
64S9 II.7	E6S4 II.8	E1E4 II.9	**65S13 II.10**	**62S9 II.11**	

Alleles in bold enhanced *GMR>gcycEI.*

Comparison of the rough eye phenotype of *GMR>gcycEI/DmcycE^{JP}; S(DmcycE^{JP})III* to that of *GMR>gcycEI/DmcycE^{JP}*.

Screen cross: *GMR>gcycEI* ; + X *DmcycE^{JP}* ; $\frac{S(DmcycE^{JP})}{TM6B}$

↓

$\frac{DmcycE^{JP}}{GMR>gcycEI}$; $\frac{S(DmcycE^{JP})}{+}$

Control cross: *GMR>gcycEI* ; + X *DmcycE^{JP}* ; +

↓

$\frac{DmcycE^{JP}}{GMR>gcycEI}$; +

S(DmcycE^{JP})III examined:

65S1	E6S25	65S55	1S2	2S1	22S8	47S8	68S10	**moira**
20S1	42S12	42S33	43S2	59S18	1S3	43S1	**brahma**	

Alleles in bold enhanced GMR>gcycEI.
The presence of DmcycEJP did not significantly modify the GMR>gcycEI rough eye phenotype.

Appendix 5.B : Regions of the third chromosome that suppress *DmcycE^{JP}*.

A summary of third chromosome regions that suppress the DmcycEJP rough eye phenotype and candidate genes in there regions (from Secombe, 1999; H. Richardson pers. com.).

Deficiency	Cytology	Candidate genes
Df(3L)HR232 and *Df(3L)HR119*	63C6; 63D3	*sprouty*
Df(3L)GN24	63F4-7; 64C13-15	*cdc4 (ago) (S)*
Df(3L)vin2 and *Df(3L)vin5*	68A2-3; 68D6	none
Df(3L)81K19	73A3; 74F	*argos, dAbl, sina(S), sinah*
Df(3R)p712	84D4-6; 85B6	*pyd*
Df(3R)by10	85D8-12; 85F1	*hyd (NE)*
Df(3R)ChaM7	91A; 91F5	none
Df(3R)XS	96A1-7; 96A21-25	none
Df(3R)TI^{P}	97A; 98A1-2	*l(3)mbt(NE), scribble (S)*
Df(3R)awd^{KRB}	100C6-7; 100D3-4	*tramtrack (NE)*

Gene abbreviations used are *hyperplastic discs* (*hyd*), and *lethal(3)malignant brain tumour* (*l(3)mbt*). Candidate genes that are underlined have been tested for their effect on the *DmcycE^{JP}* phenotype and results are indicated as (S) suppressed, or (NE) no effect.

Appendix 5.C: Analysis of *Sev-cycE* enhancers for modification of *GMR>gcycEI*, *DmcycE^{JP}*, *and GMR-p21.*

Sev-cycE Enhancer	Affect on *GMR>gcycEI*	Affect on *DmcycE^{JP}*	Affect on *GMR-p21*
E(Esev-CycE)^{a14} (2nd)	No effect	Not Tested	Suppressed
E(Esev-CycE)^{e93} (2nd)	Enhanced	Not Tested	Suppressed
E(Esev-CycE)^{g66} (2nd)	No effect	Not Tested	Suppressed
E(Esev-CycE)^{d45} (3rd)	No effect	Suppressed	Suppressed
E(Esev-CycE)^{d50} (3rd)	No effect	Suppressed	Mild Suppression
E(Esev-CycE)^{e19} (3rd)	Enhanced	Not Tested	Enhanced
E(Esev-CycE)^{e44} (3rd)	No effect	Mild suppression	Mild Suppression

Affect of *Sev-cycE* enhancers for modification of *DmcycE^{JP}*, and *GMR-p21* (H. Richardson pers. com.).

E(Esev-CycE)^{e19} appears to be a general enhancer not specific for *DmcycE,* as it also enhancers *GMR-p21*. *E(Esev-CycE)^{e93}* has been shown to be allelic to *scab*, which was also identified as a suppressor of *DmcycE^{JP}*.

Appendix 5.D : Analysis of *GMR-p21* suppressors for modification of *GMR>gcycEI*.

GMR-p21 Suppressors	Affect of *GMR>gcycEI*
AS5-9	No effect
DS2-3	No effect
AS2-5	No effect
MS2-1	No effect

Appendix 5.E : Analysis of *GMR-dE2FdDPp35* enhancers for modification of *GMR>gcycEI*.

GMR-dE2FdDPp35 Enhancer	Affect of *GMR>gcycEI*
E(E2F,Dp) rpd^{16}	Enhancer
E(E2F,Dp) 2B^{janeaway}, 2B^{seattle}	Enhanced
E(E2F,Dp) pnt^{kirk}	Enhanced
E(E2F,Dp) osa^{kry}	No effect
E(E2F,Dp) poc$^{361-6}$, poc$^{231-18}$	No effect

Appendix 5.F : Third chromosome *P*-elements screened against *GMR>gcycEI.*

Genotype	Insertion Site	Gene
y^1w^{1118}; $P\{w^{+mC}=lacW\}l(3)L5150^{L5150}/TM3, Ser^1$	61A1-3	
$P\{ry^{+t7.2}=PZ\}$ $l(3)06240$ $ry^{506}/TM3, ry^{RK}$ Sb^1 Ser^1	61B1-2	*l(3)rH321*
$P\{hsneo\}l(3)neo1^1mwh^1red^1e^1$ /TM3, ry^{RK} Sb^1Ser^1	61C	
$P\{ry^{+t7.2}=PZ\}l(3)10512$ $ry^{506}/TM3, ry^{RK}$ Sb^1 Ser^1	61C1-2	*trh*
$P\{ry^{+t7.2}=PZ\}l(3)05967$ $ry^{506}/TM3, ry^{RK}$ Sb^1 Ser^1	61C7-8	*l(3)06318*
$P\{ry^{+t7.2}=PZ\}l(3)06318$ $ry^{506}/TM3, ry^{RK}$ Sb^1 Ser^1	61C7-8	
$P\{ry^{+t7.2}=PZ\}l(3)00315$ $ry^{506}/TM3, ry^{RK}$ Sb^1 Ser^1	61C7-8, 86C2-3	*l(3)06318?*
y^1w^{1118}; $P\{w^{+mC}=lacW\}l(3)L1170^{L1170}/TM3, Ser^1$	61C7-8	
y^1w^{1118}; $P\{w^{+mC}=lacW\}l(3)L3130^{L3130}/TM3, Ser^1$	61C7-8	
$P\{ry^{+t7.2}=PZ\}l(3)00835^{00835}$ $ry^{506}/TM3, ry^{RK}$ Sb^1Ser^1	61D1-2	
$P\{ry^{+t7.2}=PZ\}l(3)04322$ $ry^{506}/TM3, ry^{RK}$ Sb^1 Ser^1	61D1-2	*emc*
$P\{ry^{+t7.2}=PZ\}l(3)07237$ $ry^{506}/TM3, ry^{RK}$ Sb^1 Ser^1	61D1-2	*emc*
$P\{ry^{+t7.2}=PZ\}l(3)05592$ $ry^{506}/TM3, ry^{RK}$ Sb^1 Ser^1	61D1-2	
y^1w^{1118}; $P\{w^{+mC}=lacW\}l(3)L2049^{L2049}/TM3, Ser^1$	61F3-4	
$P\{ry^{+t7.2}=PZ\}l(3)06345$ $ry^{506}/TM3, ry^{RK}$ Sb^1 Ser^1	61F5-6	*Klp61F*
$P\{ry^{+t7.2}=PZ\}l(3)06836$ $ry^{506}/TM3, ry^{RK}$ Sb^1 Ser^1	61F5-6	*Klp61F*
$P\{ry^{+t7.2}=PZ\}l(3)07012$ $ry^{506}/TM3, ry^{RK}$ Sb^1 Ser^1	61F5-6	*Klp61F*
y^1w^*; $P\{w^{+mC}=lacW\}mtacp1^{f4A6}/TM6B, Tb^+$	61F6-7	*ND-AcC*
$P\{ry^{+t7.2}=PZ\}l(3)02640$ $ry^{506}/TM3, ry^{RK}$ Sb^1 Ser^1	61F7	*l(3)04808?*
$P\{ry^{+t7.2}=PZ\}l(3)04808$ $ry^{506}/TM3, ry^{RK}$ Sb^1 Ser^1	61F7-8	
$P\{ry^{+t7.2}=PZ\}l(3)06465$ $ry^{506}/TM3, ry^{RK}$ Sb^1 Ser^1	61F7-8	
$mwh^1P\{hsneo\}l(3)neo5^1ry^{506}$ red^1e^1 /TM3, Sb^1	62A1-12	
$P\{ry^{+t7.2}=PZ\}l(3)06226$ $ry^{506}/TM3, ry^{RK}$ Sb^1 Ser^1	62A3-4	
$P\{ry^{+t7.2}=PZ\}l(3)02104$ $ry^{506}/TM3, ry^{RK}$ Sb^1 Ser^1	62A4-5	
$mwh^1P\{hsneo\}l(3)62Be^1red^1e^1$ /TM3, ry^{RK} Sb^1Ser^1	62B	
$P\{ry^{+t7.2}=PZ\}l(3)04276^{04276}$ $ry^{506}/TM3, ry^{RK}$ Sb^1Ser^1	62B4-5	
y^1w^{1118}; $P\{w^{+mC}=lacW\}l(3)L1910^{L1910}/TM3, Ser^1$	62C1-3	
$P\{ry^{+t7.2}=PZ\}l(3)rL182^{rL182}/TM3, Sb^1$! viable	62C3-4	
$P\{ry^{+t7.2}=PZ\}l(3)04860$ $ry^{506}/TM3, ry^{RK}$ Sb^1 Ser^1	62C1-2	
y^1w^{1118}; $P\{w^{+mC}=lacW\}l(3)j1E2^{j1E2}/TM3, Sb^1$	62E5-8	*Nik*
$P\{ry^{+t7.2}=PZ\}l(3)06286$ $ry^{506}/TM3, ry^{RK}$ Sb^1 Ser^1	62E6-7	*msn*
$P\{ry^{+t7.2}=PZ\}l(3)06946$ $ry^{506}/TM3, ry^{RK}$ Sb^1 Ser^1	62E6-7	*msn*
$P\{ry^{+t7.2}=PZ\}l(3)01604$ $ry^{506}/TM3, ry^{RK}$ Sb^1 Ser^1	62E7-8, 87D1-2	
$mwh^1P\{hsneo\}l(3)neo8^1red^1e^1$ /TM3, ry^{RK} Sb^1Ser^1	62F	
$P\{ry^{+t7.2}=PZ\}l(3)06803$ $ry^{506}/TM3, ry^{RK}$ Sb^1 Ser^1	63A3-4	
$P\{ry^{+t7.2}=PZ\}Hsp83^{08445}$ $ry^{506}/TM3, ry^{RK}$ Sb^1Ser^1	63AB	*Hsp83*
y^1w^*; $P\{w^{+mC}=lacW\}l(3)j5C2^{j5C2}/TM3, Sb^1$	63B7-8	*Hsp83*
$P\{ry^{+t7.2}=PZ\}l(3)01029$ $ry^{506}/TM3, ry^{RK}$ Sb^1 Ser^1	63B10-11	
y^1w^{1118}; $P\{w^{+mC}=lacW\}l(3)L3659^{L3659}/TM3, Ser^1$	63D1-2	
$P\{ry^{+t7.2}=PZ\}l(3)01318$ $ry^{506}/TM3, ry^{RK}$ Sb^1 Ser^1	63D1	
$P\{ry^{+t7.2}=PZ\}l(3)09143$ $ry^{506}/TM3, ry^{RK}$ Sb^1 Ser^1	63D1-2	
$P\{ry^{+t7.2}=PZ\}l(3)05634$ $ry^{506}/TM3, ry^{RK}$ Sb^1 Ser^1	63F5-6	*Ubi-p63E*
y^1w^{1118}; $P\{w^{+mC}=lacW\}l(3)L1459^{L1459}/TM3, Ser^1$	64A4-5	
$P\{ry^{+t7.2}=PZ\}l(3)rG166^{rG166}$ $ry^{506}/TM3, Sb^1$	64A4-5	
$P\{ry^{+t7.2}=PZ\}l(3)09291$ $ry^{506}/TM3, ry^{RK}$ Sb^1 Ser^1	64B5-6	
$P\{ry^{+t7.2}=PZ\}l(3)02333$ $ry^{506}/TM3, ry^{RK}$ Sb^1 Ser^1	64B16-17	
$P\{ry^{+t7.2}=PZ\}Rpd3^{04556}$ $ry^{506}/TM3, ry^{RK}$ Sb^1Ser^1	64C1-2	*Rpd3*
$P\{ry^{+t7.2}=PZ\}l(3)01418$ $ry^{506}/TM3, ry^{RK}$ Sb^1 Ser^1	64C9-10	*Srp54*
$P\{ry^{+t7.2}=PZ\}l(3)00403$ $ry^{506}/TM3, ry^{RK}$ Sb^1 Ser^1	64C11-12	
$P\{ry^{+t7.2}=PZ\}l(3)06524$ $ry^{506}/TM3, ry^{RK}$ Sb^1 Ser^1	64D3-4	
$P\{ry^{+t7.2}=PZ\}fs(3)07084^{07084}$ $ry^{506}/TM3, ry^{RK}$ Sb^1Ser^1	64E8-12	*p70s6k*
$P\{ry^{+t7.2}=PZ\}l(3)05143$ $ry^{506}/TM3, ry^{RK}$ Sb^1 Ser^1	64E5-6	
$P\{ry^{+t7.2}=PZ\}l(3)02331$ $ry^{506}/TM3, ry^{RK}$ Sb^1 Ser^1	64E8-12	
$P\{ry^{+t7.2}=PZ\}l(3)01640$ $ry^{506}/TM3, ry^{RK}$ Sb^1 Ser^1	64E8-9	
$P\{ry^{+t7.2}=PZ\}l(3)10567$ $ry^{506}/TM3, ry^{RK}$ Sb^1 Ser^1	64F1-2	*vn*
y^1w^{1118}; $P\{w^{+mC}=lacW\}l(3)L3999^{L3999}/TM3, Ser^1$	65A10-11	
$P\{ry^{+t7.2}=PZ\}l(3)06811^{06811}$ $ry^{506}/TM3, ry^{RK}$ Sb^1Ser^1	65A10-11	
$P\{ry^{+t7.2}=PZ\}l(3)rP047^{rP047}$ $ry^{506}/TM3, Sb^1$	65A10-11	
$P\{ry^{+t7.2}=PZ\}l(3)02094$ $ry^{506}/TM3, ry^{RK}$ Sb^1 Ser^1	65A10-12	*U1snRNPA*

Third chromosome *P*-elements screened against *GMR>gcycEI cont.*

Genotype	Insertion Site	Gene
P{ry$^{+t7.2}$=PZ}l(3)03042 ry^{506}/TM3, ry^{RK} Sb^{1} Ser^{1}	65A10-12	*U1snRNPA*
P{ry$^{+t7.2}$=PZ}l(3)04026 ry^{506}/TM3, ry^{RK} Sb^{1} Ser^{1}	65A5-6	
P{ry$^{+t7.2}$=PZ}sfl^{03844} ry^{506}/TM3, ry^{RK} Sb^{1}Ser^{1}	65C1-2	
y^{1}w^{1118}; P{w^{+mC}=lacW}l(3)L4060^{L4060}/TM3, Ser^{1}	65D3-4	
P{ry$^{+t7.2}$=PZ}sgl^{08310} ry^{506}/TM3, ry^{RK} Sb^{1}Ser^{1}	65D4-5	*sgl*
P{ry$^{+t7.2}$=PZ}sgl^{05007} ry^{506}/TM3, ry^{RK} Sb^{1}Ser^{1}	65D4-6	*sgl*
P{ry$^{+t7.2}$=PZ}l(3)10503 ry^{506}/TM3, ry^{RK} Sb^{1} Ser^{1}	65D4-6	*sgl?*
y^{1}w^{1118}; P{w^{+mC}=lacW}l(3)L2249^{L2249}/TM3, Ser^{1}	65E10-11	*Neos*
y^{1}w^{1118}; P{w^{+mC}=lacW}l(3)L7123^{L7123}/TM3, Ser^{1}	65F1-2	*Cdc27*
y^{1}w*; P{w^{+mC}=lacW}l(3)j1D5^{j1D5}/TM3, Sb^{1}	65F5-8	
P{ry$^{+t7.2}$=PZ}l(3)08034 ry^{506}/TM3, ry^{RK} Sb^{1} Ser^{1}	65F1-2	
y^{1}w*; P{w^{+mC}=lacW}l(3)j6B8^{j6B8}/TM3, Sb^{1}	66A1-2	*smid*
P{ry$^{+t7.2}$=PZ}l(3)02067 ry^{506}/TM3, ry^{RK} Sb^{1} Ser^{1}	66A1-2	*l(3)07217*
P{ry$^{+t7.2}$=PZ}l(3)07217 ry^{506}/TM3, ry^{RK} Sb^{1} Ser^{1}	66A1-2	*l(3)02067*
P{ry$^{+t7.2}$=PZ}l(3)09645 ry^{506}/TM3, ry^{RK} Sb^{1} Ser^{1}	66A17-18	
y^{1}w*; P{w^{+mC}=lacW}l(3)j1C7^{j1C7}/TM3, Sb^{1}	66B10-11	*Nmt1*
y^{1}w^{1118}; P{w^{+mC}=lacW}l(3)L0139^{L0139}/TM3, Ser^{1}	66C1-2	
P{ry$^{+t7.2}$=PZ}l(3)03928 ry^{506}/TM3, ry^{RK} Sb^{1} Ser^{1}	66D1-2	*l(3)01323?*
P{ry$^{+t7.2}$=PZ}l(3)01323 ry^{506}/TM3, ry^{RK} Sb^{1} Ser^{1}	66D1-2, 91F11	*l(3)03928?*
y^{1}w^{1118}; P{w^{+mC}=lacW}l(3)L4111^{L4111}/TM3, Ser^{1}	66C1-4	
y^{1}w^{1118}; P{w^{+mC}=lacW}l(3)L3852^{L3852}/TM3, Ser^{1}	66C8-9	
y^{1}w^{1118}; P{w^{+mC}=lacW}l(3)j8E8^{j8E8}/TM3, Sb^{1}	66D5-6	
P{ry$^{+t7.2}$=PZ}l(3)02537 ry^{506}/TM3, ry^{RK} Sb^{1} Ser^{1}	66D10-11	*h*
P{ry$^{+t7.2}$=PZ}l(3)08247 ry^{506}/TM3, ry^{RK} Sb^{1} Ser^{1}	66D10-12	*h*
P{ry$^{+t7.2}$=PZ}l(3)00682 ry^{506}/TM3, ry^{RK} Sb^{1} Ser^{1}	66D10-12	*h?*
P{ry$^{+t7.2}$=PZ}l(3)rK561^{rK561} ry^{506}/TM3, Sb^{1}	66D10-13	*SrpR&bgr*
y^{1}w*; P{w^{+mC}=lacW}l(3)j5B6^{j5B6}/TM3, Sb^{1}	66D13-14	
P{ry$^{+t7.2}$=PZ}l(3)10631 ry^{506}/TM3, ry^{RK} Sb^{1} Ser^{1}	66D14-15	*Prm*
P{ry$^{+t7.2}$=PZ}dally^{06464} ry^{506}/TM3, ry^{RK} Sb^{1}Ser^{1}	66E1-2	*dally*
P{ry$^{+t7.2}$=PZ}l(3)01629 ry^{506}/TM3, ry^{RK} Sb^{1} Ser^{1}	66E1-2	
P{ry$^{+t7.2}$=PZ}l(3)06264 ry^{506}/TM3, ry^{RK} Sb^{1} Ser^{1}	66E1-2	
P{ry$^{+t7.2}$=PZ}l(3)03349 ry^{506}/TM3, ry^{RK} Sb^{1} Ser^{1}	66E6	
P{ry$^{+t7.2}$=PZ}bol^{1}ry^{506}/TM3, ry^{RK} Sb^{1}Ser^{1}	66F	*bol*
P{ry$^{+t7.2}$=PZ}l(3)10534 ry^{506}/TM3, ry^{RK} Sb^{1} Ser^{1}	66F4	*Mrp17*
y^{1}w*; P{w^{+mC}=lacW}l(3)j2B9^{j2B9}/TM3, Sb^{1}	67B4-5	
P{ry$^{+t7.2}$=PZ}l(3)07238 ry^{506}/TM3, ry^{RK} Sb^{1} Ser^{1}	67B1-2	*eIF-4E*
y^{1}w*; P{w^{+mC}=lacW}l(3)j2B8^{j2B8}/TM3, Sb^{1}	67B10-11	*Uch-L3*
P{ry$^{+t7.2}$=PZ}l(3)02240 ry^{506}/TM3, ry^{RK} Sb^{1} Ser^{1}	67C4-5	
y^{1}; P{ry$^{+t7.2}$=PZ}l(3)01859 ry^{506}/TM3, ry^{RK} Sb^{1}Ser^{1}	67C5-8	
y^{1}w^{1118}; P{w^{+mC}=lacW}l(3)L0539^{L0539}/TM3, Ser^{1}	67E1-2	
P{ry$^{+t7.2}$=PZ}l(3)rL562^{rL562} ry^{506}/TM3, Sb^{1}	67E1-4	*Dhh1*
P{ry$^{+t7.2}$=PZ}l(3)rl075^{rl075} ry^{506}/TM3, Sb^{1}	67F1-2	
P{ry$^{+t7.2}$=PZ}l(3)01814 ry^{506}/TM3, ry^{RK} Sb^{1} Ser^{1}	67F1-2	
P{ry$^{+t7.2}$=PZ}l(3)03691 ry^{506}/TM3, ry^{RK} Sb^{1} Ser^{1}	68A1-2	
P{ry$^{+t7.2}$=PZ}l(3)09036 ry^{506}/TM3, ry^{RK} Sb^{1} Ser^{1}	68A1-2	*klu*
P{ry$^{+t7.2}$=PZ}l(3)10052 ry^{506}/TM3, ry^{RK} Sb^{1} Ser^{1}	68A1-2	*klu*
P{ry$^{+t7.2}$=PZ}l(3)02727 ry^{506}/TM3, ry^{RK} Sb^{1} Ser^{1}	68A1-2, 94A1-2	
P{ry$^{+t7.2}$=PZ}l(3)01239 ry^{506}/TM3, ry^{RK} Sb^{1} Ser^{1}	68A4-5	
mwh^{1}P{hsneo}rt^{P}red^{1}e^{1} /TM3, Sb^{1}Ser^{1}	68C	*rt*
P{ry$^{+t7.2}$=PZ}l(3)06477 ry^{506}/TM3, ry^{RK} Sb^{1} Ser^{1}	68C1-4, 93D6-7	
P{ry$^{+t7.2}$=PZ}l(3)01005 ry^{506}/TM3, ry^{RK} Sb^{1} Ser^{1}	68C9-10	
P{ry$^{+t7.2}$=PZ}l(3)00707 ry^{506}/TM3, ry^{RK} Sb^{1} Ser^{1}	68C12-13	
P{ry$^{+t7.2}$=PZ}l(3)05408 ry^{506}/TM3, ry^{RK} Sb^{1} Ser^{1}	68C12-13	
P{ry$^{+t7.2}$=PZ}l(3)01558 ry^{506}/TM3, ry^{RK} Sb^{1} Ser^{1}	68E1-2	*CycA*
P{ry$^{+t7.2}$=PZ}l(3)02461 ry^{506}/TM3, ry^{RK} Sb^{1} Ser^{1}	68E1-2	*CycA*
P{ry$^{+t7.2}$=PZ}l(3)03946 ry^{506}/TM3, ry^{RK} Sb^{1} Ser^{1}	68E1-2	*CycA*
P{ry$^{+t7.2}$=PZ}l(3)04335 ry^{506}/TM3, ry^{RK} Sb^{1} Ser^{1}	68E1-3	*CycA*
P{ry$^{+t7.2}$=PZ}l(3)08232 ry^{506}/TM3, ry^{RK} Sb^{1} Ser^{1}	68F1-3	
mwh^{1}P{hsneo}l(3)neo18^{1}red^{1}e^{1} /TM3, ry^{RK} Sb^{1}Ser^{1}	68F1-8	
y^{1}w*; P{w^{+mC}=lacW}l(3)j2D3^{j2D3}/TM3, Sb^{1}	68F2-3	
P{ry$^{+t7.2}$=PZ}l(3)05088 ry^{506}/TM3, ry^{RK} Sb^{1} Ser^{1}	69A1-3	
P{ry$^{+t7.2}$=PZ}l(3)08483 ry^{506}/TM3, ry^{RK} Sb^{1} Ser^{1}	69C8-9	

Third chromosome *P*-elements screened against *GMR>gcycEI cont.*

Genotype	Insertion Site	Gene
$P\{ry^{+t7.2}=PZ\}l(3)06924^{06924}ry^{506}/CxD, ry^{BW}$	69E3-4	
$P\{ry^{+t7.2}=PZ\}l(3)00305\ ry^{506}/TM3, ry^{RK}\ Sb^{1}\ Ser^{1}$	69E3-5	*l(3)01413*
$w^{1118};\ P\{w^{+mC}=lacW\}l(3)s2783^{s2783}/TM3, Sb^{1}Ser^{1}$	69F5-6	*RpS12*
$y^{1}w^{1118};\ P\{w^{+mC}=lacW\}l(3)j10B6^{j10B6}/TM3, Sb^{1}$	70A1-2	
$P\{ry^{+t7.2}=PZ\}l(3)01470\ ry^{506}/TM3, ry^{RK}\ Sb^{1}\ Ser^{1}$	70A1-2	
$P\{ry^{+t7.2}=PZ\}l(3)04220\ ry^{506}/TM3, ry^{RK}\ Sb^{1}\ Ser^{1}$	70A1-2	
$P\{ry^{+t7.2}=PZ\}l(3)02937^{02937}ry^{506}/TM3, ry^{RK}Sb^{1}Ser^{1}$	70A1-5	*l(3)05121*
$P\{ry^{+t7.2}=PZ\}l(3)05121\ ry^{506}/TM3, ry^{RK}\ Sb^{1}\ Ser^{1}$	70A1-5	*l(3)02937*
$mwh^{1}P\{hsneo\}l(3)neo19^{1}red^{1}e^{1}/TM3, ry^{RK}Sb^{1}Ser^{1}$	70A1-8	
$P\{ry^{+t7.2}=PZ\}l(3)00543\ ry^{506}/TM3, ry^{RK}\ Sb^{1}\ Ser^{1}$	70B1-3	*stv*
$y^{1}w^{1118};\ P\{w^{+mC}=lacW\}l(3)L5212^{L5212}/TM3, Ser^{1}$	70B7-C1	
$P\{ry^{+t7.2}=PZ\}l(3)03699\ ry^{506}/TM3, ry^{RK}\ Sb^{1}\ Ser^{1}$	70B3-4	
$P\{ry^{+t7.2}=PZ\}l(3)05871^{05871}ry^{506}/TM3, ry^{RK}\ Sb^{1}\ Ser^{1}$	70C1-2	
$w^{1118};\ P\{w^{+mC}=lacW\}l(3)s363/TM6C, Antp^{Hu}\ Sb^{1}\ Tb^{1}$	70C4-6	
$P\{ry^{+t7.2}=PZ\}Hsc70Cb^{00082}ry^{506}/TM3, ry^{RK}\ Sb^{1}\ Ser^{1}$	70C12-13	*l(3)06704*
$P\{ry^{+t7.2}=PZ\}l(3)06704\ ry^{506}/TM3, ry^{RK}\ Sb^{1}\ Ser^{1}$	70C12-13	*l(3)00082*
$P\{ry^{+t7.2}=PZ\}stwl^{02024}ry^{506}/TM3, ry^{RK}\ Sb^{1}\ Ser^{1}$	70D-E	*stwl*
$y^{1}w^{1118};\ P\{w^{+mC}=lacW\}l(3)L0499^{L0499}/TM3, Ser^{1}$	70D1-2	
$P\{ry^{+t7.2}=PZ\}Hsc70Cb^{07621}ry^{506}/TM3, ry^{RK}\ Sb^{1}\ Ser^{1}$	70D1-2	
$P\{ry^{+t7.2}=PZ\}l(3)00208\ ry^{506}/TM3, ry^{RK}\ Sb^{1}\ Ser^{1}$	70D1-2	*dev*
$P\{ry^{+t7.2}=PZ\}l(3)04727\ ry^{506}/TM3, ry^{RK}\ Sb^{1}\ Ser^{1}$	70D1-2	*dev*
$P\{ry^{+t7.2}=PZ\}l(3)02402\ ry^{506}/TM3, ry^{RK}\ Sb^{1}\ Ser^{1}$	70D1-2	*l(3)70Da*
$P\{ry^{+t7.2}=PZ\}l(3)00421\ ry^{506}/TM3, ry^{RK}\ Sb^{1}\ Ser^{1}$	70E1-2	
$P\{ry^{+t7.2}=PZ\}l(3)00514\ ry^{506}/TM3, ry^{RK}\ Sb^{1}\ Ser^{1}$	70E1-2	
$P\{ry^{+t7.2}=PZ\}l(3)00564\ ry^{506}/TM3, ry^{RK}\ Sb^{1}\ Ser^{1}$	70E1-2	*PpsM*
$P\{ry^{+t7.2}=PZ\}l(3)04680\ ry^{506}/TM3, ry^{RK}\ Sb^{1}\ Ser^{1}$	70E1-2	*PpsM*
$P\{ry^{+t7.2}=PZ\}l(3)00603\ ry^{506}/TM3, ry^{RK}\ Sb^{1}\ Ser^{1}$	70E2-3	
$w^{1118};\ P\{w^{+mC}=lacW\}Trl^{s2325}/TM3, Sb^{1}$	70F1-4	*Trl*
$w^{1118};\ P\{w^{+mC}=lacW\}l(3)s2172^{s2172}/TM3, Sb^{1}$	71B4-5	
$y^{1}w^{*};\ P\{w^{+mC}=lacW\}l(3)j2A2^{j2A2}/TM3, Sb^{1}$	71B4-5	
$w^{1118};\ P\{w^{+mC}=lacW\}l(3)s1754^{s1754}/TM3, Sb^{1}$	71D1-2	
$P\{ry^{+t7.2}=PZ\}l(3)03576\ ry^{506}/TM3, ry^{RK}\ Sb^{1}\ Ser^{1}$	71D1-2	*Creb*
$y^{1}w^{*};\ P\{w^{+mC}=lacW\}l(3)j6B9^{j6B9}/TM3, Sb^{1}$	71E1-2	
$P\{ry^{+t7.2}=PZ\}l(3)06315\ ry^{506}/TM3, ry^{RK}\ Sb^{1}\ Ser^{1}$	72A-2, 98B1-2	
$P\{ry^{+t7.2}=PZ\}l(3)72Dd^{03802}ry^{506}/TM3, ry^{RK}\ Sb^{1}\ Ser^{1}$	72D1-2	*l(3)72Dd*
$y^{1}w^{*};\ P\{w^{+mC}=lacW\}th^{j5C8}/TM3, Sb^{1}$	72D1-2	*th*
$w^{1118};\ P\{w^{+mC}=lacW\}l(3)s1939^{s1939}/TM3, Sb^{1}$	72D8-9	*SsR&bgr*
$y^{1}w^{*};\ P\{w^{+mC}=lacW\}l(3)72Dn^{j5A4}/TM3, Sb^{1}$	72D10-11	*l(3)72Dn*
$P\{ry^{+t7.2}=PZ\}ms(3)72D^{03957}ry^{506}/MKRS$	72D1-12	
$w^{1118};\ P\{w^{+mC}=lacW\}l(3)s3123^{s3123}/TM3, Sb^{1}$	72E1-2	
$y^{1}w^{*};\ P\{w^{+mC}=lacW\}l(3)j10E8^{j10E8}/TM3, Sb^{1}$	73A1-2	
$P\{ry^{+t7.2}=PZ\}l(3)03639\ ry^{506}/TM3, ry^{RK}\ Sb^{1}\ Ser^{1}$	73A1-2	*gil ?*
$P\{ry^{+t7.2}=PZ\}l(3)05845\ ry^{506}/TM3, ry^{RK}\ Sb^{1}\ Ser^{1}$	73A1-2	*gil*
$P\{ry^{+t7.2}=PZ\}l(3)02540\ ry^{506}/TM3, ry^{RK}\ Sb^{1}\ Ser^{1}$	73A9-10	*l(3)73Ah*
$mwh^{1}P\{hsneo\}l(3)neo20^{1}red^{1}e^{1}/TM3, ry^{RK}Sb^{1}Ser^{1}$	73B1-7	
$P\{ry^{+t7.2}=PZ\}l(3)00274\ ry^{506}/TM3, ry^{RK}\ Sb^{1}\ Ser^{1}$	73B1-2	*Mo25*
$P\{ry^{+t7.2}=PZ\}l(3)04674\ ry^{506}/TM3, ry^{RK}\ Sb^{1}\ Ser^{1}$	73B1-2	
$P\{ry^{+t7.2}=PZ\}l(3)02281\ ry^{506}/TM3, ry^{RK}\ Sb^{1}\ Ser^{1}$	73B5-6	*l(3)01895*
$P\{ry^{+t7.2}=PZ\}l(3)01895\ ry^{506}/TM3, ry^{RK}\ Sb^{1}\ Ser^{1}$	73B5-6	*l(3)02281*
$P\{ry^{+t7.2}=PZ\}l(3)10547\ ry^{506}/TM3, ry^{RK}\ Sb^{1}\ Ser^{1}$	73D1-2	*Int6*
$P\{ry^{+t7.2}=PZ\}l(3)04069\ ry^{506}/TM3, ry^{RK}\ Sb^{1}\ Ser^{1}$	73D3-4	
$w^{1118};\ P\{w^{+mC}=lacW\}l(3)s1629^{s1629}/TM3, Sb^{1}$	73D3-6	
$P\{ry^{+t7.2}=PZ\}l(3)06846\ ry^{506}/TM3, ry^{RK}\ Sb^{1}\ Ser^{1}$	73E1-6	
$P\{ry^{+t7.2}=PZ\}l(3)01658\ ry^{506}/TM3, ry^{RK}\ Sb^{1}\ Ser^{1}$	74B1-2	
$P\{ry^{+t7.2}=PZ\}l(3)00073\ ry^{506}/TM3, ry^{RK}\ Sb^{1}\ Ser^{1}$	74C1-2	*ttv*
$y^{1}w^{*};\ P\{w^{+mC}=lacW\}l(3)j11B2^{j11B2}/TM3, Sb^{1}$	74D3-5	
$mwh^{1}P\{hsneo\}Eip74EF^{neo24}red^{1}e^{1}/TM3, ry^{RK}\ Sb^{1}\ Ser^{1}$	74F1-75A10	*Eip74EF*
$P\{ry^{+t7.2}=PZ\}l(3)02634\ ry^{506}/TM3, ry^{RK}\ Sb^{1}\ Ser^{1}$	75A8-9	
$P\{ry^{+t7.2}=PZ\}l(3)rL061^{rL061}ry^{506}/TM3, Sb^{1}$	75B1-2	
$P\{ry^{+t7.2}=PZ\}l(3)03247\ ry^{506}/TM3, ry^{RK}\ Sb^{1}\ Ser^{1}$	75B1-2	*Eip75B*
$P\{ry^{+t7.2}=PZ\}l(3)07041\ ry^{506}/TM3, ry^{RK}\ Sb^{1}\ Ser^{1}$	75B1-2	*Eip75B*
$P\{ry^{+t7.2}=PZ\}l(3)05014\ ry^{506}/TM3, ry^{RK}\ Sb^{1}\ Ser^{1}$	75C1-2	*W (hid)*

Third chromosome *P*-elements screened against *GMR>gcycEI cont.*

Genotype	Insertion Site	Gene
mwh^{1}*P{hsneo}l(3)neo26*^{1}*red*^{1}*e*^{1} */TM3, ry*^{RK}*Sb*^{1}*Ser*^{1}	75C1-7	*Cat*
P{ry$^{+t7.2}$*=PZ}l(3)02069*^{02069}*ry*^{506} */TM6B, ry*^{CB}	75C3-4	*l(3)06806?*
P{ry$^{+t7.2}$*=PZ}l(3)06806 ry*^{506}*/TM3, ry*^{RK} *Sb*^{1} *Ser*^{1}	75C3-4	*l(3)02069?*
P{ry$^{+t7.2}$ *=PZ}ftz-f1*^{03649}*ry*^{506} */TM3, ry*^{RK}*Sb*^{1}*Ser*^{1}	75D4-5	*ftz-f1*
P{ry$^{+t7.2}$*=PZ}l(3)00864 ry*^{506}*/TM3, ry*^{RK} *Sb*^{1} *Ser*^{1}	75E1-2	
y^{1}*w***; P{w*$^{+mC}$ *=lacW}l(3)j4E6*^{j4E6} */TM3, Sb*^{1}	75E3-5	
P{ry$^{+t7.2}$*=PZ}l(3)04869 ry*^{506}*/TM3, ry*^{RK} *Sb*^{1} *Ser*^{1}	75F6-7, 100F1-5	
mwh^{1}*P{hsneo}l(3)neo27*^{1} *red*^{1} *e*^{1} */TM3, ry*^{RK}*Sb*^{1}*Ser*^{1}	76A1-10	
P{ry$^{+t7.2}$*=PZ}l(3)06945 ry*^{506}*/TM3, ry*^{RK} *Sb*^{1} *Ser*^{1}	76A3-4	
y^{1}*w*^{1118}*; P{w*$^{+mC}$ *=lacW}l(3)L3809*^{L3809} */TM3, Ser*^{1}	76B9-10	
y^{1}*w*^{1118}*; P{w*$^{+mC}$ *=lacW}l(3)L1243*^{L1243} */TM3, Ser*^{1}	76D3-4	
P{ry$^{+t7.2}$*=PZ}l(3)01058 ry*^{506}*/TM3, ry*^{RK} *Sb*^{1} *Ser*^{1}	76D3-4	*Pha*
P{ry$^{+t7.2}$*=PZ}l(3)01673 ry*^{506}*/TM3, ry*^{RK} *Sb*^{1} *Ser*^{1}	77B1-2	
P{ry$^{+t7.2}$ *=PZ}fbl*^{1} *ry*^{506} */TM3, ry*^{RK} *Sb*^{1} *Ser*^{1}	77B1-9	*fbl*
P{ry$^{+t7.2}$*=PZ}l(3)00103 ry*^{506}*/TM3, ry*^{RK} *Sb*^{1} *Ser*^{1}	77B4-7	*l(3)05637*
P{ry$^{+t7.2}$*=PZ}l(3)05637 ry*^{506}*/TM3, ry*^{RK} *Sb*^{1} *Ser*^{1}	77B6-7	*l(3)00103*
y^{1}*w***; P{w*$^{+mC}$ *=lacW}l(3)j10B2*^{j10B2} */TM3, Sb*^{1}	77B6-7	*DNAprim*
P{ry$^{+t7.2}$*=PZ}l(3)04521 ry*^{506}*/TM3, ry*^{RK} *Sb*^{1} *Ser*^{1}	77D4-5	
P{ry$^{+t7.2}$ *=PZ}l(3)rK760*^{rK760} *ry*^{506} */TM3, ry*^{RK} *Sb*^{1} *Ser*^{1}	78A1-2	
P{ry$^{+t7.2}$ *=PZ}l(3)rG554*^{rG554}*ry*^{506} */TM3, Sb*^{1}	78A1-2	
y^{1}*w*^{1118}*; P{w*$^{+mC}$ *=lacW}l(3)L7062*^{L7062} */TM3, Ser*^{1}	78A2-3	
y^{1}*w*^{1118}*; P{w*$^{+mC}$ *=lacW}l(3)L5541*^{L5541} */TM3, Ser*^{1}	78A5-6	
P{ry$^{+t7.2}$*=PZ}l(3)07615 ry*^{506}*/TM3, ry*^{RK} *Sb*^{1} *Ser*^{1}	78C1-2	
P{ry$^{+t7.2}$*=PZ}l(3)00217 ry*^{506}*/TM3, ry*^{RK} *Sb*^{1} *Ser*^{1}	78C3-4	*l(3)78Cb*
P{ry$^{+t7.2}$*=PZ}l(3)02241 ry*^{506}*/TM3, ry*^{RK} *Sb*^{1} *Ser*^{1}	78C3-6	
P{ry$^{+t7.2}$ *=PZ}l(3)04063*^{04063}*ry*^{506} */TM3, ry*^{RK}*Sb*^{1}*Ser*^{1}	78D1-2	*l(3)00534?*
P{ry$^{+t7.2}$*=PZ}l(3)00534 ry*^{506}*/TM3, ry*^{RK} *Sb*^{1} *Ser*^{1}	78D1-2	*l(3)04063?*
P{ry$^{+t7.2}$ *=PZ}bet*^{1} *ry*^{506} */TM3, ry*^{RK} *Sb*^{1} *Ser*^{1}	78D	*bet*
P{ry$^{+t7.2}$*=PZ}l(3)00836 ry*^{506}*/TM3, ry*^{RK} *Sb*^{1} *Ser*^{1}	79B1-2	
P{ry$^{+t7.2}$*=PZ}l(3)04093 ry*^{506}*/TM3, ry*^{RK} *Sb*^{1} *Ser*^{1}	79B1-3	*mub*
P{ry$^{+t7.2}$*=PZ}l(3)01544 ry*^{506}*/TM3, ry*^{RK} *Sb*^{1} *Ser*^{1}	79D1-2	*RpP0*
mwh^{1}*P{hsneo}l(3)neo30*^{1} *red*^{1} *e*^{1}*/TM3, ry*^{RK} *Sb*^{1} *Ser*^{1}	79D1-4	
P{ry$^{+t7.2}$ *=PZ}Hem*^{03335} *ry*^{506} */TM3, ry*^{RK}*Sb*^{1} *Ser*^{1}	79E1-2	*Hem*
P{ry$^{+t7.2}$*=PZ}l(3)00827 ry*^{506}*/TM3, ry*^{RK} *Sb*^{1} *Ser*^{1}	79E1-2	*Aats-ile*
P{ry$^{+t7.2}$*=PZ}l(3)03988 ry*^{506}*/TM3, ry*^{RK} *Sb*^{1} *Ser*^{1}	79E1-2	*Csp*
P{ry$^{+t7.2}$*=PZ}l(3)02017 ry*^{506}*/TM3, ry*^{RK} *Sb*^{1} *Ser*^{1}	79E1-2	*Ten-m*
P{ry$^{+t7.2}$*=PZ}l(3)05309 ry*^{506}*/TM3, ry*^{RK} *Sb*^{1} *Ser*^{1}	79E1-2	*Ten-m*
P{ry$^{+t7.2}$*=PZ}l(3)09070 ry*^{506}*/TM3, ry*^{RK} *Sb*^{1} *Ser*^{1}	79E1-2	
P{ry$^{+t7.2}$ *=PZ}l(3)04053*^{04053} *ry*^{506} */TM3, ry*^{RK} *Sb*^{1} *Ser*^{1}	79E6-7	
y^{1}*w*^{1118}*; P{w*$^{+mC}$ *=lacW}l(3)L7251*^{L7251} */TM3, Ser*^{1}	79F1-2	
P{ry$^{+t7.2}$ *=PZ}l(3)00506*^{00506} *ry*^{506} */TM3, ry*^{RK} *Sb*^{1} *Ser*^{1}	79F1-2	
P{ry$^{+t7.2}$*=PZ}l(3)04281 ry*^{506}*/TM3, ry*^{RK} *Sb*^{1} *Ser*^{1}	79F1-2	
P{ry$^{+t7.2}$ *=PZ}ms(3)80*^{03817} *ry*^{506} */TM3, ry*^{RK} *Sb*^{1} *Ser*^{1}	80	
P{ry$^{+t7.2}$*=PZ}l(3)07310 ry*^{506}*/TM3, ry*^{RK} *Sb*^{1} *Ser*^{1}	80D1-2	
P{ry$^{+t7.2}$*=PZ}l(3)06713*^{06713} *ry*^{506}*/TM3, ry*^{RK} *Sb*^{1} *Ser*^{1}	81F	
y^{1} *w*^{1118}*; P{w*$^{+mC}$*=lacW}l(3)j1E6*^{j1E6}*/TM3, Sb*^{1}	82A3-5	
P{ry$^{+t7.2}$*=PZ}l(3)00620 ry*^{506}*/TM3, ry*^{RK} *Sb*^{1} *Ser*^{1}	82A1-2	*abs*
P{ry$^{+t7.2}$*=PZ}l(3)03407 ry*^{506}*/TM3, ry*^{RK} *Sb*^{1} *Ser*^{1}	82A1-2	
P{ry$^{+t7.2}$*=PZ}l(3)00945 ry*^{506}*/TM3, ry*^{RK} *Sb*^{1} *Ser*^{1}	82A1-4	
P{ry$^{+t7.2}$*=PZ}l(3)02423 ry*^{506}*/TM3, ry*^{RK} *Sb*^{1} *Ser*^{1}	82A4-5, 72D11	
y^{1} *w*^{1118}*; P{w*$^{+mC}$*=lacW}l(3)L1233*^{L1233}*/TM3, Ser*^{1}	82B1-2	
y^{1} *w*^{1118}*; P{w*$^{+mC}$*=lacW}l(3)L0021*^{L0021}*/TM3, Ser*^{1}	82C1-2	
P{ry$^{+t7.2}$*=PZ}shk*^{1} *ry*^{506}*/TM3, ry*^{RK} *Sb*^{1} *Ser*^{1}	82C1-5	*shank*
y^{1} *w***; P{w*$^{+mC}$*=lacW}l(3)j3A4*^{j3A4}*/TM3, Sb*^{1}	82D1-2	*Kary&bgr*
y^{1} *w***; P{w*$^{+mC}$*=lacW}l(3)j4D1*^{j4D1}*/TM3, Sb*^{1}	82D1-2	
P{ry$^{+t7.2}$*=PZ}l(3)10112 ry*^{506}*/TM3, ry*^{RK} *Sb*^{1} *Ser*^{1}	82D1-2	
P{ry$^{+t7.2}$*=PZ}bob*^{06208} *ry*^{506}*/TM3, ry*^{RK} *Sb*^{1} *Ser*^{1}	82D1-8	*bob*
P{ry$^{+t7.2}$*=PZ}l(3)02733 ry*^{506}*/TM3, ry*^{RK} *Sb*^{1} *Ser*^{1}	82D4-5	
P{ry$^{+t7.2}$*=PZ}l(3)01456 ry*^{506}*/TM3, ry*^{RK} *Sb*^{1} *Ser*^{1}	82D6-7	*l(3)02466*
P{ry$^{+t7.2}$*=PZ}l(3)02466 ry*^{506}*/TM3, ry*^{RK} *Sb*^{1} *Ser*^{1}	82D6-7	*l(3)01456*
P{ry$^{+t7.2}$*=PZ}l(3)01010*^{01010} *ry*^{506}*/TM3, ry*^{RK} *Sb*^{1} *Ser*^{1}	82E1-2	
y^{1} *w***; P{w*$^{+mC}$*=lacW}l(3)j4B9*^{j4B9}*/TM3, Sb*^{1}	82E4-5	

Third chromosome *P*-elements screened against *GMR>gcycEI cont.*

Genotype	Insertion Site	Gene
P{ry$^{+t7.2}$=PZ}corto^{07128} ry^{506}/TM3, ry^{RK} Sb^{1} Ser^{1}	82E5-7	*l(3)05259*
P{ry$^{+t7.2}$=PZ}l(3)05259 ry^{506}/TM3, ry^{RK} Sb^{1} Ser^{1}	82E6-7	*l(3)07128*
P{ry$^{+t7.2}$=PZ}l(3)01107 ry^{506}/TM3, ry^{RK} Sb^{1} Ser^{1}	82E1-2	
P{ry$^{+t7.2}$=PZ}l(3)00144 ry^{506}/TM3, ry^{RK} Sb^{1} Ser^{1}	82E6-7	*corto?*
P{ry$^{+t7.2}$=PZ}l(3)00714 ry^{506}/TM3, ry^{RK} Sb^{1} Ser^{1}	82E6-7	
mwh^{1} P{hsneo}corto^{neo32} red^{1} e^{1}/TM3, ry^{RK} Sb^{1} Ser^{1}	82F1-8	*corto*
P{ry$^{+t7.2}$=PZ}l(3)02255^{02255} ry^{506}/TM3, ry^{RK} Sb^{1} Ser^{1}	82F4-7	
P{ry$^{+t7.2}$=PZ}l(3)09904 ry^{506}/TM3, ry^{RK} Sb^{1} Ser^{1}	82F8-9	
P{ry$^{+t7.2}$=PZ}l(3)03644^{03644} ry^{506}/TM3, ry^{RK} Sb^{1} Ser^{1}	83A5-6	
y^{1} w^{1118}; P{w^{+mC}=lacW}l(3)j5E2^{j5E2}/TM3, Sb^{1}	83A5-6	*KSR*
P{ry$^{+t7.2}$=PZ}l(3)01319 ry^{506}/TM3, ry^{RK} Sb^{1} Ser^{1}	83A5-6	*Snr1*
P{ry$^{+t7.2}$=PZ}l(3)05616 ry^{506}/TM3, ry^{RK} Sb^{1} Ser^{1}	83A5-6	*Itp-r83A*
P{ry$^{+t7.2}$=PZ}l(3)03022 ry^{506}/TM3, ry^{RK} Sb^{1} Ser^{1}	83B1-2	
y^{1} w^{1118}; P{w^{+mC}=lacW}l(3)j3E7^{j3E7}/TM3, Sb^{1}	83B1-2	*noi*
y^{1} w^{1118}; P{w^{+mC}=lacW}l(3)j5E7^{j5E7}/TM3, Sb^{1}	83B1-2	
P{ry$^{+t7.2}$=PZ}l(3)03834 ry^{506}/TM3, ry^{RK} Sb^{1} Ser^{1}	83B4-5	*Rga*
y^{1} w^{1118}; P{w^{+mC}=lacW}l(3)j9B6^{j9B6}/TM3, Sb^{1}	83B4-5	
w^{1118}; P{w^{+mC}=lacW}l(3)s1938^{s1938}/TM3, Sb^{1}	83B4-7	*Atu*
y^{1} w^{1118}; P{w^{+mC}=lacW}l(3)j13C8^{j13C8}/TM3, Sb^{1}	83B6-7	
P{ry$^{+t7.2}$=PZ}l(3)02248 ry^{506}/TM3, ry^{RK} Sb^{1} Ser^{1}	83B6-7	*Xe7*
y^{1} w*; P{w^{+mC}=lacW}l(3)neo33^{j1C2}/TM3, Sb^{1}	83C1-2	*cas*
P{ry$^{+t7.2}$=PZ}l(3)04696 ry^{506}/TM3, ry^{RK} Sb^{1} Ser^{1}	83C1-2	
P{ry$^{+t7.2}$=PZ}l(3)03423 ry^{506}/TM3, ry^{RK} Sb^{1} Ser^{1}	83C1-2, 77A1-2	
P{ry$^{+t7.2}$=PZ}l(3)02279 ry^{506}/TM3, ry^{RK} Sb^{1} Ser^{1}	83D3-5	*Lip?*
P{ry$^{+t7.2}$=PZ}l(3)01086 ry^{506}/TM3, ry^{RK} Sb^{1} Ser^{1}	83D4-4	*Lip*
P{ry$^{+t7.2}$=PZ}l(3)03076 ry^{506}/TM3, ry^{RK} Sb^{1} Ser^{1}	83F1-2	
P{ry$^{+t7.2}$=PZ}l(3)03342 ry^{506}/TM3, ry^{RK} Sb^{1} Ser^{1}	83F1-2	*l(3)09312?*
P{ry$^{+t7.2}$=PZ}l(3)09312 ry^{506}/TM3, ry^{RK} Sb^{1} Ser^{1}	83F1-2	*l(3)03342?*
P{ry$^{+t7.2}$=PZ}l(3)01241 ry^{506}/TM3, ry^{RK} Sb^{1} Ser^{1}	84A1-2	*lab*
P{ry$^{+t7.2}$=PZ}twr^{05614} ry^{506}/TM3, ry^{RK} Sb^{1} Ser^{1}	84A4-5	*twr*
P{ry$^{+t7.2}$=PZ}l(3)04498 ry^{506}/TM3, ry^{RK} Sb^{1} Ser^{1}	84A4-5	*pb*
y^{1} w*; P{w^{+mC}=lacW}l(3)j7A6^{j7A6}/TM6B, Tb^{1}	84B1-2	
y^{1} w^{1118}; P{w^{+mC}=lacW}l(3)L2100^{L2100}/TM3, Ser^{1}	84B2-3	
y^{1} w*; P{w^{+mC}=lacW}l(3)j8C8^{j8C8}/TM3, Sb^{1}	84C1-2	
P{ry$^{+t7.2}$=PZ}l(3)02267 ry^{506}/TM3, ry^{RK} Sb^{1} Ser^{1}	84C1-2	*Aly*
w^{1118}; P{w^{+mC}=lacW}l(3)s2214^{s2214}/TM3, Sb^{1}	84C4-6	
P{ry$^{+t7.2}$=PZ}l(3)01773 ry^{506}/TM3, ry^{RK} Sb^{1} Ser^{1}	84C1-2, 100C7	
mwh^{1} P{hsneo}l(3)neo35^{1} red^{1} e^{1}/TM3, ry^{RK} Sb^{1} Ser^{1}	84D-E	
P{ry$^{+t7.2}$=PZ}l(3)02732 ry^{506}/TM3, ry^{RK} Sb^{1} Ser^{1}	84D11-12	
y^{1} w*; P{w^{+mC}=lacW}l(3)j4E1^{j4E1}/TM3, Sb^{1}	84E10-11	
P{ry$^{+t7.2}$=PZ}l(3)03692 ry^{506}/TM3, ry^{RK} Sb^{1} Ser^{1}	84E10-11	*Tom34*
P{ry$^{+t7.2}$=PZ}l(3)05930 ry^{506}/TM3, ry^{RK} Sb^{1} Ser^{1}	84F1-2	*Gata-c*
ry^{506} P{ry$^{+t7.2}$=PZ}Mcm2$^{rl.074}$/TM3, Sb^{1}	84F6-7	*Mcm2*
P{ry$^{+t7.2}$=PZ}cap^{1} ry^{506}/TM3, ry^{RK} Sb^{1} Ser^{1}	85A4-5	*cap*
y^{1} w^{1118}; P{w^{+mC}=lacW}l(3)L4740^{L4740}/TM3, Ser^{1}	85A5-6	
w^{1118}; P{w^{+mC}=lacW}l(3)s3512^{s3512}/TM3, Sb^{1}	85A5-7	*dhod*
y^{1} w^{1118}; P{w^{+mC}=lacW}l(3)j1B9^{j1B9}/TM3, Sb^{1}	85A9-10	*tRNA:y1*
P{ry$^{+t7.2}$=PZ}l(3)00822 ry^{506}/TM3, ry^{RK} Sb^{1} Ser^{1}	85A9-10, 85B2	
P{ry$^{+t7.2}$=PZ}l(3)00281^{00281} ry^{506}/TM3, ry^{RK} Sb^{1} Ser^{1}	85B8-9	
P{ry$^{+t7.2}$=PZ}l(3)04055 ry^{506}/TM3, ry^{RK} Sb^{1} Ser^{1}	85B2-3, 86A4-5	
P{ry$^{+t7.2}$=PZ}l(3)02693 ry^{506}/TM3, ry^{RK} Sb^{1} Ser^{1}	85B4-5	
mwh^{1} P{hsneo}l(3)neo36^{1} red^{1} e^{1}/TM3, ry^{RK} Sb^{1} Ser^{1}	85C1-13	*Rel*
y^{1} w^{1118}; P{w^{+mC}=lacW}l(3)L6332^{L6332}/TM3, Ser^{1}	85C1-2	
P{ry$^{+t7.2}$=PZ}l(3)05652^{05652} ry^{506}/TM3, ry^{RK} Sb^{1} Ser^{1}	85C3-5	
P{ry$^{+t7.2}$=PZ}l(3)05652 ry^{506}/TM3, ry^{RK} Sb^{1} Ser^{1}	85C3-5	
y^{1} w*; P{w^{+mC}=lacW}neur^{j6B12}/TM3, Sb^{1}	85C9-10	*neur*
P{ry$^{+t7.2}$=PZ}l(3)06537 ry^{506}/TM3, ry^{RK} Sb^{1} Ser^{1}	85D1-2, 94F1-2	
P{ry$^{+t7.2}$=PZ}l(3)03203 ry^{506}/TM3, ry^{RK} Sb^{1} Ser^{1}	85D1-2	*pum?*
P{ry$^{+t7.2}$=PZ}l(3)01688 ry^{506}/TM3, ry^{RK} Sb^{1} Ser^{1}	85D2-3	*pum*
P{ry$^{+t7.2}$=PZ}l(3)04837 ry^{506}/TM3, ry^{RK} Sb^{1} Ser^{1}	85D5-6	
P{ry$^{+t7.2}$=PZ}l(3)10467 ry^{506}/TM3, ry^{RK} Sb^{1} Ser^{1}	85D2-3, 70D4-5	
P{ry$^{+t7.2}$=PZ}l(3)01728 ry^{506}/TM3, ry^{RK} Sb^{1} Ser^{1}	85D7-8	

Third chromosome *P*-elements screened against *GMR>gcycEI cont.*

Genotype	Insertion Site	Gene
P{ry$^{+t7.2}$=PZ}l(3)04410 ry^{506}/TM3, ry^{RK} Sb^{1} Ser^{1}	85D7-8	*Aats-trp*
P{ry$^{+t7.2}$=PZ}l(3)05430 ry^{506}/TM3, ry^{RK} Sb^{1} Ser^{1}	85D8	
y^{1} w^{1118}; P{w^{+mC}=lacW}l(3)L4092^{L4092}/TM3, Ser^{1}	85D11-12	
P{ry$^{+t7.2}$=PZ}l(3)10615 ry^{506}/TM3, ry^{RK} Sb^{1} Ser^{1}	85D15-17	
P{ry$^{+t7.2}$=PZ}l(3)03511 ry^{506}/TM3, ry^{RK} Sb^{1} Ser^{1}	85D17-18	
P{ry$^{+t7.2}$=PZ}l(3)06677 ry^{506}/TM3, ry^{RK} Sb^{1} Ser^{1}	85D18-19	*Ras85D*
P{ry$^{+t7.2}$=PZ}l(3)01436 ry^{506}/TM3, ry^{RK} Sb^{1} Ser^{1}	85E12-13	*Pp2A*
P{ry$^{+t7.2}$=PZ}l(3)10477 ry^{506}/TM3, ry^{RK} Sb^{1} Ser^{1}	85F1-2	
w^{1118}; P{w^{+mC}=lacW}l(3)s2681^{s2681}/TM3, Sb^{1}	85F7-8	
P{ry$^{+t7.2}$=PZ}l(3)02414 ry^{506}/TM3, ry^{RK} Sb^{1} Ser^{1}	85F12-13	*tws*
y^{1} w*; P{w^{+mC}=lacW}l(3)j9A5^{j9A5}/TM6B, Tb^{1}	85F15-16	
P{ry$^{+t7.2}$=PZ}l(3)06439^{06439} ry^{506}/TM3, ry^{RK} Sb^{1} Ser^{1}	86B1-2	*l(3)03676*
P{ry$^{+t7.2}$=PZ}l(3)03676 ry^{506}/TM3, ry^{RK} Sb^{1} Ser^{1}	86B1-2	*l(3)06439*
y^{1} w^{1118}; P{w^{+mC}=lacW}l(3)j8B6^{j8B6}/TM3, Sb^{1}	86B1-2	
P{ry$^{+t7.2}$=PZ}l(3)06142 ry^{506}/TM3, ry^{RK} Sb^{1} Ser^{1}	86B1-2	
P{ry$^{+t7.2}$=PZ}l(3)06762 ry^{506}/TM3, ry^{RK} Sb^{1} Ser^{1}	86C1-2	*hth*
y^{1} w^{1118}; P{w^{+mC}=lacW}l(3)j3C1^{j3C1}/TM3, Sb^{1}	86C3-4	*TfIIFbeta*
P{ry$^{+t7.2}$=PZ}tho^{1} ry^{506}/MKRS	86E1-20	*tho*
P{ry$^{+t7.2}$=PZ}l(3)09656^{09656} ry^{506}/TM3, ry^{RK} Sb^{1} Ser^{1}	86E1-2	
P{ry$^{+t7.2}$=PZ}l(3)10419 ry^{506}/TM3, ry^{RK} Sb^{1} Ser^{1}	86E1-2	*pros*
P{ry$^{+t7.2}$=PZ}l(3)00609 ry^{506}/TM3, ry^{RK} Sb^{1} Ser^{1}	86E2-4	*pros?*
P{ry$^{+t7.2}$=PZ}l(3)04629^{04629} ry^{506}/TM3, ry^{RK} Sb^{1} Ser^{1}	86E16-19	
y^{1} w^{1118}; P{w^{+mC}=lacW}l(3)j1D8^{j1D8}/TM3, Sb^{1}	86E16-19	
mwh^{1} P{hsneo}l(3)neo38^{1} red^{1} e^{1}/TM3, ry^{RK} Sb^{1} Ser^{1}	86F1-11	
P{ry$^{+t7.2}$=PZ}l(3)10621^{10621} ry^{506}/TM3, ry^{RK} Sb^{1} Ser^{1}	86F6-7	
P{ry$^{+t7.2}$=PZ}l(3)10586 ry^{506}/TM3, ry^{RK} Sb^{1} Ser^{1}	86F4-5, 91D1-2	
P{ry$^{+t7.2}$=PZ}l(3)07842 ry^{506}/TM3, ry^{RK} Sb^{1} Ser^{1}	87B4-6	*svp*
y^{1} w*; P{w^{+mC}=lacW}Vha55^{l2E9}/TM3, Sb^{1}	87C2-3	*Vha55*
P{ry$^{+t7.2}$=PZ}l(3)05043^{05043} ry^{506}/TM3, ry^{RK} Sb^{1} Ser^{1}	87C6-8	
P{ry$^{+t7.2}$=PZ}l(3)05043 ry^{506}/TM3, ry^{RK} Sb^{1} Ser^{1}	87C6-8	
y^{1} w*; P{w^{+mC}=lacW}l(3)j6E7^{j6E7}/TM3, Sb^{1}	87C11-13	*Ppl-87B*
mwh^{1} P{hsneo}l(3)neo39^{1} red^{1} e^{1}/TM3, ry^{RK} Sb^{1} Ser^{1}	87D1-E12	
P{ry$^{+t7.2}$=PZ}CtBP^{03463} ry^{506}/TM3, ry^{RK} Sb^{1} Ser^{1}	87D7-9	*CtBP*
y^{1} w^{1118}; P{w^{+mC}=lacW}l(3)j5A1^{j5A1}/TM3, Sb^{1}	87E5-6	
w^{1118}; P{w^{+mC}=lacW}l(3)87Eg^{s2149}/TM3, Sb^{1}	87E10-11	*l(3)87Eg*
P{ry$^{+t7.2}$=PZ}l(3)05137 ry^{506}/TM3, ry^{RK} Sb^{1} Ser^{1}	87E7-8	
y^{1} w*; P{w^{+mC}=lacW}sqd^{j6E3}, l(3)j6E3^{j6E3}/TM3, Sb^{1}	87F2-3	*sqd*
y^{1} w*; P{w^{+mC}=lacW}l(3)j4B4^{j4B4}/TM3, Sb^{1}	87F3-4	
y^{1} w^{1118}; P{w^{+mC}=lacW}l(3)L4179^{L4179}/TM3, Ser^{1}	87F7-8	
w^{1118}; P{w^{+mC}=lacW}l(3)s2249^{s2249}/TM3, Sb^{1}	87F7-8	*B52*
ry^{506} P{ry$^{+t7.2}$=PZ}l(3)01949^{01949}/TM3, ry^{RK} Sb^{1} Ser^{1}	87F10-11	
P{ry$^{+t7.2}$=PZ}l(3)04449, ry^{506}/TM3, ry^{RK} Sb^{1} Ser^{1}	87F10-11	
ry^{506} P{ry$^{+t7.2}$=PZ}mei-P19^{03477}/TM3, ry^{RK} Sb^{1} Ser^{1}	88A4-5	*mei-P19*
P{ry$^{+t7.2}$=PZ}l(3)02731, ry^{506}/TM3, ry^{RK} Sb^{1} Ser^{1}	88A4-5	*mei-P19?*
Y^{1} w*; P{w^{+mC}=lacW}l(3)j1E7^{j1E7}/TM3, Sb^{1}	88A4-5	
P{ry$^{+t7.2}$=PZ}l(3)03477, ry^{506}/TM3, ry^{RK} Sb^{1} Ser^{1}	88A4-5	
y^{1} w^{1118}; P{w^{+mC}=lacW}l(3)L5340^{L5340}/TM3, Ser^{1}	88B1-2	
P{ry$^{+t7.2}$=PZ}l(3)00700, ry^{506}/TM3, ry^{RK} Sb^{1} Ser^{1}	88B1-2	*trx?*
P{ry$^{+t7.2}$=PZ}l(3)00347, ry^{506}/TM3, ry^{RK} Sb^{1} Ser^{1}	88B1-3	*trx*
ry^{506} P{ry$^{+t7.2}$=PZ}l(3)06951^{06951}/TM3, ry^{RK} Sb^{1} Ser^{1}	88C1-4	
mwh^{1} red^{1} P{hsneo}l(3)neo41^{1} e^{1}/TM3, ry^{RK} Sb^{1} Ser^{1}	88C1-10	
P{ry$^{+t7.2}$=PZ}l(3)03608 ry^{506}/TM3, ry^{RK} Sb^{1} Ser^{1}	88C6-7	
P{ry$^{+t7.2}$=PZ}l(3)10460 ry^{506}/TM3, ry^{RK} Sb^{1} Ser^{1}	88C9-10	*put*
y^{1} w^{1118}; P{w^{+mC}=lacW}l(3)L1231^{L1231}/TM3, Ser^{1}	88C9-11	
ry^{506} P{ry$^{+t7.2}$=PZ}l(3)03719^{03719}/TM3, ry^{RK} Sb^{1} Ser^{1}	88D1-2	
P{ry$^{+t7.2}$=PZ}l(3)02404, ry^{506}/TM3, ry^{RK} Sb^{1} Ser^{1}	88D1-2	
P{ry$^{+t7.2}$=PZ}l(3)05628, ry^{506}/TM3, ry^{RK} Sb^{1} Ser^{1}	88D1-2	
P{ry$^{+t7.2}$=PZ}l(3)01462, ry^{506}/TM3, ry^{RK} Sb^{1} Ser^{1}	88D5-6	*eff*
P{ry$^{+t7.2}$=PZ}l(3)0653,5 ry^{506}/TM3, ry^{RK} Sb^{1} Ser^{1}	88D2-3	*eff*
P{ry$^{+t7.2}$=PZ}l(3)10418, ry^{506}/TM3, ry^{RK} Sb^{1} Ser^{1}	88D5-6	
P{ry$^{+t7.2}$=PZ}l(3)04713, ry^{506}/TM3, ry^{RK} Sb^{1} Ser^{1}	88E1-2	
P{ry$^{+t7.2}$=PZ}l(3)03550, ry^{506}/TM3, ry^{RK} Sb^{1} Ser^{1}	88E8-9	*Hsc70-4*

Third chromosome *P*-elements screened against *GMR>gcycEI cont.*

Genotype	Insertion Site	Gene
mwh^{1} red^{1} P{hsneo}l(3)neo43$^{1\ e1}$/TM3, ry^{RK} Sb^{1} Ser^{1}	88E9-10	
y^{1} w^{1118}; P{w^{+mC}=lacW}l(3)j6A3^{j6A3}/TM3, Sb^{1}	88E11-12	
ry^{506} P{ry$^{+t7.2}$=PZ}Tm1^{02299}/TM3, ry^{RK} Sb^{1} Ser^{1}	88F1-2	*Tm1*
y^{1} w^{1118}; P{w^{+mC}=lacW}l(3)j6A6^{j6A6}/TM6B	88F7-8	
P{ry$^{+t7.2}$=PZ}l(3)09965, ry^{506}/TM3, ry^{RK} Sb^{1} Ser^{1}	88F1-2	
P{ry$^{+t7.2}$=PZ}l(3)06490, ry^{506}/TM3, ry^{RK} Sb^{1} Ser^{1}	88F7-8	
ry^{506} P{ry$^{+t7.2}$=PZ}l(3)04210^{04210}/TM3, ry^{RK} Sb^{1} Ser^{1}	89A1-2	*Pros26S*
ry^{506} P{ry$^{+t7.2}$=PZ}l(3)rN346^{rN346}/TM3, ry^{RK} Sb^{1} Ser^{1}	89A1-2	
P{ry$^{+t7.2}$=PZ}l(3)05057, ry^{506}/TM3, ry^{RK} Sb^{1} Ser^{1}	89A1-2	
P{ry$^{+t7.2}$=PZ}l(3)06536, ry^{506}/TM3, ry^{RK} Sb^{1} Ser^{1}	89A4-5	
P{ry$^{+t7.2}$=PZ}l(3)01618, ry^{506}/TM3, ry^{RK} Sb^{1} Ser^{1}	89A8-9	
ry^{506} P{ry$^{+t7.2}$=PZ}spn-E^{03987}/TM3, ry^{RK} Sb^{1} Ser^{1}	89B1-2	*spn-E*
P{ry$^{+t7.2}$=PZ}l(3)01549, ry^{506}/TM3, ry^{RK} Sb^{1} Ser^{1}	89B1-3	*srp*
P{ry$^{+t7.2}$=PZ}l(3)08724, ry^{506}/TM3, ry^{RK} Sb^{1} Ser^{1}	89B1-3	
P{ry$^{+t7.2}$=PZ}l(3)04226, ry^{506}/TM3, ry^{RK} Sb^{1} Ser^{1}	89B6	*Akt1*
ry^{506} P{ry$^{+t7.2}$=PZ}ms(3)89B^{04895}/MKRS	89B1-22	*Hrr25*
y^{1} w^{1118}; P{w^{+mC}=lacW}l(3)L1820^{L1820}/TM3, Ser^{1}	89B11-13	
P{ry$^{+t7.2}$=PZ}l(3)08235, ry^{506}/TM3, ry^{RK} Sb^{1} Ser^{1}	89B9-13	*l(3)05203?*
P{ry$^{+t7.2}$=PZ}l(3)05203, ry^{506}/TM3, ry^{RK} Sb^{1} Ser^{1}	89B12-13	*l(3)07636*
P{ry$^{+t7.2}$=PZ}l(3)07636, ry^{506}/TM3, ry^{RK} Sb^{1} Ser^{1}	89B12-13	*l(3)05203*
P{ry$^{+t7.2}$=PZ}l(3)03881, ry^{506}/TM3, ry^{RK} Sb^{1} Ser^{1}	89B12-13	*l(3)05117?*
P{ry$^{+t7.2}$=PZ}l(3)05117, ry^{506}/TM3, ry^{RK} Sb^{1} Ser^{1}	89B12-13	*l(3)03881?*
Y^{1} w^{1118}; P{w^{+mC}=lacW}l(3)L4032^{L4032}/TM3, Ser^{1}	89D1-2	*JadBp*
ry^{506} P{ry$^{+t7.2}$=PZ}l(3)06664^{06664}/TM3, ry^{RK} Sb^{1} Ser^{1}	89D6-7	
ry^{506} P{ry$^{+t7.2}$=PZ}Abd-B^{05649}/CxD, ry^{RK}	89E1-8	*AbdB*
y^{1} w^{1118}; P{w^{+mC}=lacW}EfTuM^{L4569}/CyO	89E7-9	*EfTuM*
y^{1} w^{1118}; P{w^{+mC}=lacW}Dad^{1E4}/TM3, Sb^{1}	89E10-11	*Dad*
P{ry$^{+t7.2}$=PZ}l(3)06658, ry^{506}/TM3, ry^{RK} Sb^{1} Ser^{1}	89E10-11	
P{ry$^{+t7.2}$=PZ}l(3)07882, ry^{506}/TM3, ry^{RK} Sb^{1} Ser^{1}	90B3-4	
ry^{506} P{ry$^{+t7.2}$=PZ}osa^{00090}/TM3, ry^{RK} Sb^{1} Ser^{1}	90C5-8	*osa*
P{ry$^{+t7.2}$=PZ}l(3)04539, ry^{506}/TM3, ry^{RK} Sb^{1} Ser^{1}	90C7-8	*osa*
P{ry$^{+t7.2}$=PZ}l(3)04662, ry^{506}/TM3, ry^{RK} Sb^{1} Ser^{1}	90C7-8	*osa?/eld?*
P{ry$^{+t7.2}$=PZ}l(3)00023, ry^{506}/TM3, ry^{RK} Sb^{1} Ser^{1}	90D1-2	*cpo?*
P{ry$^{+t7.2}$=PZ}l(3)01432, ry^{506}/TM3, ry^{RK} Sb^{1} Ser^{1}	90D1-2	*cpo*
P{ry$^{+t7.2}$=PZ}l(3)04704, ry^{506}/TM3, ry^{RK} Sb^{1} Ser^{1}	90D1-2, 97E5-6	
ry^{506} P{ry$^{+t7.2}$=PZ}l(3)00643^{00643}/TM3, ry^{RK} Sb^{1} Ser^{1}	90E1-2	
P{ry$^{+t7.2}$=PZ}l(3)00643, ry^{506}/TM3, ry^{RK} Sb^{1} Ser^{1}	90E1-2	
ry^{506} P{ry$^{+t7.2}$=PZ}sr^{03999}/TM3, ry^{RK} Sb^{1} Ser^{1}	90E1-2	*sr*
P{ry$^{+t7.2}$=PZ}l(3)06948, ry^{506}/TM3, ry^{RK} Sb^{1} Ser^{1}	90E1-2, 84F6-7	*sr?*
P{ry$^{+t7.2}$=PZ}l(3)05697 ry^{506}/TM3, ry^{RK} Sb^{1} Ser^{1}	90E1-2	
mwh^{1} red^{1} P{hsneo}l(3)neo48$^{1\ e1}$/TM3, ry^{RK} Sb^{1} Ser^{1}	90E1-7	
w^{1118}; P{w^{+mC}=lacW}l(3)s2956^{s2956}/TM3, Sb^{1}	90F1-2	
y$^{1\ w*}$; P{w^{+mC}=lacW}14-3-3epsilon^{j2B10}/TM3, Sb^{1}	90F6-7	*14-3-3 epsilon*
P{ry$^{+t7.2}$=PZ}l(3)03702, ry^{506}/TM3, ry^{RK} Sb^{1} Ser^{1}	90F1-2	*repo*
P{ry$^{+t7.2}$=PZ}l(3)05822, ry^{506}/TM3, ry^{RK} Sb^{1} Ser^{1}	90F9-10	
P{ry$^{+t7.2}$=PZ}l(3)05089, ry^{506}/TM3, ry^{RK} Sb^{1} Ser^{1}	91A1-2	
P{ry$^{+t7.2}$=PZ}l(3)05284, ry^{506}/TM3, ry^{RK} Sb^{1} Ser^{1}	91A4-6	*sprd*
P{ry$^{+t7.2}$=PZ}l(3)07551, ry^{506}/TM3, ry^{RK} Sb^{1} Ser^{1}	91B5-6	*fray*
P{ry$^{+t7.2}$=PZ}l(3)08126, ry^{506}/TM3, ry^{RK} Sb^{1} Ser^{1}	91B5-6	
P{ry$^{+t7.2}$=PZ}l(3)02515, ry^{506}/TM3, ry^{RK} Sb^{1} Ser^{1}	91D3-5	
ry^{506} P{ry$^{+t7.2}$=PZ}l(3)07013^{07013}/TM3, ry^{RK} Sb^{1} Ser^{1}	91F1-5	
P{ry$^{+t7.2}$=PZ}l(3)01536, ry^{506}/TM3, ry^{RK} Sb^{1} Ser^{1}	91F4-5	*nos*
P{ry$^{+t7.2}$=PZ}l(3)07117, ry^{506}/TM3, ry^{RK} Sb^{1} Ser^{1}	91F4-5	*nos*
P{ry$^{+t7.2}$=PZ}l(3)03346, ry^{506}/TM3, ry^{RK} Sb^{1} Ser^{1}	91F6-9	
P{ry$^{+t7.2}$=PZ}l(3)03675, ry^{506}/TM3, ry^{RK} Sb^{1} Ser^{1}	91F7-9	*l(3)03750?*
P{ry$^{+t7.2}$=PZ}l(3)03750, ry^{506}/TM3, ry^{RK} Sb^{1} Ser^{1}	91F7-9	*l(3)03675*
ry^{506} P{ry$^{+t7.2}$=PZ}l(3)02102^{02102}/TM3, ry^{RK} Sb^{1} Ser^{1}	91F10-11	
y$^{1\ w*}$; P{w^{+mC}=lacW}l(3)j5A6^{j5A6}/TM6B, Tb^{1}	91F10-11	
P{ry$^{+t7.2}$=PZ}l(3)06404, ry^{506}/TM3, ry^{RK} Sb^{1} Ser^{1}	91F10-11	
P{ry$^{+t7.2}$=PZ}l(3)05151, ry^{506}/TM3, ry^{RK} Sb^{1} Ser^{1}	92A1-2	*Dl*
P{ry$^{+t7.2}$=PZ}l(3)03745, ry^{506}/TM3, ry^{RK} Sb^{1} Ser^{1}	92A1-2, 85F13	*Dl*
P{ry$^{+t7.2}$=PZ}l(3)06606, ry^{506}/TM3, ry^{RK} Sb^{1} Ser^{1}	92A1-2	*Dl*

Third chromosome *P*-elements screened against *GMR>gcycEI cont.*

Genotype	Insertion Site	Gene
$P\{ry^{+t7.2}=PZ\}l(3)05820$, ry^{506}/*TM3*, ry^{RK} Sb^{1} Ser^{1}	92A1-2	
$P\{ry^{+t7.2}=PZ\}l(3)05113$, ry^{506}/*TM3*, ry^{RK} Sb^{1} Ser^{1}	92A13-14	*VhaG*
$P\{ry^{+t7.2}=PZ\}l(3)06916$, ry^{506}/*TM3*, ry^{RK} Sb^{1} Ser^{1}	92B2-3	
$P\{ry^{+t7.2}=PZ\}l(3)01344$, ry^{506}/*TM3*, ry^{RK} Sb^{1} Ser^{1}	92B3-4	
$P\{ry^{+t7.2}=PZ\}l(3)10585$, ry^{506}/*TM3*, ry^{RK} Sb^{1} Ser^{1}	92B3-5	
ry^{506} $P\{ry^{+t7.2}=PZ\}bwk^{08482}$/*TM3*, ry^{RK} Sb^{1} Ser^{1}	92D1-2	*bwk*
$P\{ry^{+t7.2}=PZ\}l(3)10619$, ry^{506}/*TM3*, ry^{RK} Sb^{1} Ser^{1}	92D4-5	
$P\{ry^{+t7.2}=PZ\}l(3)06346$, ry^{506}/*TM3*, ry^{RK} Sb^{1} Ser^{1}	92E2-4	*Stat92E*
$P\{ry^{+t7.2}=PZ\}l(3)03806$, ry^{506}/*TM3*, ry^{RK} Sb^{1} Ser^{1}	92F1-2	
$P\{ry^{+t7.2}=PZ\}l(3)10575$, ry^{506}/*TM3*, ry^{RK} Sb^{1} Ser^{1}	92F1-2,91F11	
y^{1} w^{*}; $P\{w^{+mC}=lacW\}l(3)j5C7^{j5C7}$/*TM6B*, Tb^{1}	93A4-5	
mwh^{1} red^{1} $P\{hsneo\}l(3)neo54^{1\ e1}$/*TM3*, ry^{RK} Sb^{1} Ser^{1}	93B1-13	
$P\{ry^{+t7.2}=PZ\}l(3)00462$, ry^{506}/*TM3*, ry^{RK} Sb^{1} Ser^{1}	93B1-2	*Atpalpha?*
$P\{ry^{+t7.2}=PZ\}l(3)04492$, ry^{506}/*TM3*, ry^{RK} Sb^{1} Ser^{1}	93B1-2	*Atpalpha?*
$P\{ry^{+t7.2}=PZ\}l(3)01453$, ry^{506}/*TM3*, ry^{RK} Sb^{1} Ser^{1}	93B2	*Atpalpha*
$P\{ry^{+t7.2}=PZ\}l(3)07086$, ry^{506}/*TM3*, ry^{RK} Sb^{1} Ser^{1}	93B8-11	
ry^{506} $P\{ry^{+t7.2}=PZ\}ppan^{02231}$/*TM3*, ry^{RK} Sb^{1} Ser^{1}	93B10-11	*ppan*
$P\{ry^{+t7.2}=PZ\}l(3)02231$, ry^{506}/*TM3*, ry^{RK} Sb^{1} Ser^{1}	93B10-11	
$P\{ry^{+t7.2}=PZ\}l(3)00295$, ry^{506}/*TM3*, ry^{RK} Sb^{1} Ser^{1}	93B10-11	
ry^{506} $P\{ry^{+t7.2}=PZ\}l(3)03773^{03773}$/*TM3*, ry^{RK} Sb^{1} Ser^{1}	93C1-2	
y^{1} w^{*}; $P\{w^{+mC}=lacW\}l(3)j2D1^{j2D1}$/*TM3*, Sb^{1}	93C1-2	
$P\{ry^{+t7.2}=PZ\}l(3)05241$, ry^{506}/*TM3*, ry^{RK} Sb^{1} Ser^{1}	93D4-7	
$P\{ry^{+t7.2}=PZ\}l(3)03852$, ry^{506}/*TM3*, ry^{RK} Sb^{1} Ser^{1}	93E1-2	*mod*
$P\{ry^{+t7.2}=PZ\}l(3)05545$, ry^{506}/*TM3*, ry^{RK} Sb^{1} Ser^{1}	93E4-5	*InR*
ry^{506} $P\{ry^{+t7.2}=PZ\}E2f^{07172}$/*TM3*, ry^{RK} Sb^{1} Ser^{1}	93E8-9	*E2f*
$P\{ry^{+t7.2}=PZ\}l(3)07172$, ry^{506}/*TM3*, ry^{RK} Sb^{1} Ser^{1}	93E8-9	
$P\{ry^{+t7.2}=PZ\}l(3)08072$, ry^{506}/*TM3*, ry^{RK} Sb^{1} Ser^{1}	93E8-9	
ry^{506} $P\{ry^{+t7.2}=PZ\}tsl^{00617}$/*TM3*, ry^{RK} Sb^{1} Ser^{1}	93F6-14	*tsl*
y^{1} w^{*}; $P\{w^{+mC}=lacW\}l(3)j5B5^{j5B5}$/*TM3*, Sb^{1}	94A1-2	*how*
$P\{ry^{+t7.2}=PZ\}l(3)05712$, ry^{506}/*TM3*, ry^{RK} Sb^{1} Ser^{1}	94A3-4	
y^{1} w^{1118}; $P\{w^{+mC}=lacW\}l(3)L3560^{L3560}$/*TM3*, Ser^{1}	94A5-7	
ry^{506} $P\{ry^{+t7.2}=PZ\}l(3)03685^{03685}$/*TM3*, ry^{RK} Sb^{1} Ser^{1}	94A8-12	
ry^{506} $P\{ry^{+t7.2}=PZ\}l(3)rQ178^{rQ178}$/*TM3*, Sb^{1}	94A9-10	
y^{1} w^{1118}; $P\{w^{+mC}=lacW\}l(3)L4910^{L4910}$/*TM3*, Ser^{1}	94B4-5	*Dph5*
y^{1} w^{1118}; $P\{w^{+mC}=lacW\}l(3)L0580^{L0580}$/*TM3*, Ser^{1}	94C1-2	
ry^{506} $P\{ry^{+t7.2}=PZ\}l(3)rN712^{rN712}$/*TM3*, Sb^{1}	94D1-4	*klg*
ry^{506} $P\{ry^{+t7.2}=PZ\}hh^{rJ413}$/*TM3*, ry^{RK} Sb^{1} Ser^{1}	94E1-4	*hh*
ry^{506} $P\{ry^{+t7.2}=PZ\}orb^{dec}$/*TM3*, ry^{RK} Sb^{1}	94E1-10	*orb*
$P\{ry^{+t7.2}=PZ\}l(3)03969$, ry^{506}/*TM3*, ry^{RK} Sb^{1} Ser^{1}	94E1-2, 91F1-2	
$P\{ry^{+t7.2}=PZ\}l(3)03921$, ry^{506}/*TM3*, ry^{RK} Sb^{1} Ser^{1}	94E3-7	*cnc*
ry^{506} $P\{ry^{+t7.2}=PZ\}l(3)01031^{01031}$/*TM3*, ry^{RK} Sb^{1} Ser^{1}	94F1-2	*sec13*
ry^{506} $P\{ry^{+t7.2}=PZ\}l(3)rF149^{rF149}$/*TM3*, ry^{RK} Sb^{1} Ser^{1}	94F1-2	
$P\{ry^{+t7.2}=PZ\}l(3)04263$, ry^{506}/*TM3*, ry^{RK} Sb^{1} Ser^{1}	94F1-2	*pnt*
$P\{ry^{+t7.2}=PZ\}l(3)07825$, ry^{506}/*TM3*, ry^{RK} Sb^{1} Ser^{1}	94F1-2	*pnt*
ry^{506} $P\{ry^{+t7.2}=PZ\}l(3)06906^{06906}$/*TM3*, ry^{RK} Sb^{1} Ser^{1}	95A7-8	
$P\{ry^{+t7.2}=PZ\}l(3)04684$, ry^{506}/*TM3*, ry^{RK} Sb^{1} Ser^{1}	95B1-3	
ry^{506} $P\{ry^{+t7.2}=PZ\}Hmgcr^{01152}$/*TM3*, ry^{RK} Sb^{1} Ser^{1}	95B5-6	*HmG-CoAR*
$P\{ry^{+t7.2}=PZ\}l(3)04295$, ry^{506}/*TM3*, ry^{RK} Sb^{1} Ser^{1}	95B10-12	
$P\{ry^{+t7.2}=PZ\}l(3)06624$, ry^{506}/*TM3*, ry^{RK} Sb^{1} Ser^{1}	95C7-8	
ry^{506} $P\{ry^{+t7.2}=PZ\}l(3)rQ303^{rQ303}$/*TM3*, Sb^{1}	95D1-2	
ry^{506} $P\{ry^{+t7.2}=PZ\}syx1A^{06737}$/*TM3*, ry^{RK} Sb^{1} Ser^{1}	95E1-2	*syx1A*
$P\{ry^{+t7.2}=PZ\}l(3)06737$, ry^{506}/*TM3*, ry^{RK} Sb^{1} Ser^{1}	95E1-2	*syx1A*
$P\{ry^{+t7.2}=PZ\}l(3)10660$, ry^{506}/*TM3*, ry^{RK} Sb^{1} Ser^{1}	95E1-2	*syx1A?*
ry^{506} $P\{ry^{+t7.2}=PZ\}jar^{1}$/*TM3*, ry^{RK} Sb^{1} Ser^{1}	95F	*jar*
ry^{506} $P\{ry^{+t7.2}=PZ\}l(3)05842^{05842}$/*TM3*, Sb^{1}	95F11-12	*l(3)06656?*
$P\{ry^{+t7.2}=PZ\}l(3)06656$ ry^{506}/*TM3*, ry^{RK} Sb^{1} Ser^{1}	95F14-15	
y^{1} w^{1118}; $P\{w^{+mC}=lacW\}l(3)j1B5^{j1B5}$/*TM3*, Sb^{1}	95F11-12	
$P\{ry^{+t7.2}=PZ\}l(3)07207$, ry^{506}/*TM3*, ry^{RK} Sb^{1} Ser^{1}	95F11-12	*l(3)07883*
$P\{ry^{+t7.2}=PZ\}l(3)07883$, ry^{506}/*TM3*, ry^{RK} Sb^{1} Ser^{1}	95F11-12	*l(3)07207*
y^{1} w^{1118}; $P\{w^{+mC}=lacW\}l(3)L6710^{L6710}$/*TM3*, Ser^{1}	95F14-A1	
y^{1} w^{1118}; $P\{w^{+mC}=lacW\}CycB3^{L6540}$/*TM3*, Ser^{1}	96B3-5	*CycB3*
$P\{ry^{+t7.2}=PZ\}l(3)01207$, ry^{506}/*TM3*, ry^{RK} Sb^{1} Ser^{1}	96B10-11	

Third chromosome *P*-elements screened against *GMR>gcycEI cont.*

Genotype	Insertion Site	Gene
$y^1\ w^{1118}$; $P\{w^{+mC}=lacW\}l(3)j2D9^{j2D9}$/TM3, Sb^1	96B19-20	*OstStt3*
ry^{506} $P\{ry^{+t7.2}=PZ\}l(3)rL205^{rL205}$/TM3, ry^{RK} Sb^1 Ser^1	96C1-2	*Fur1*
$P\{ry^{+t7.2}=PZ\}l(3)01969$, ry^{506}/TM3, ry^{RK} Sb^1 Ser^1	96C7-8	
ry^{506} $P\{ry^{+t7.2}=PZ\}l(3)05461^{05461}$/TM3, ry^{RK} Sb^1 Ser^1	96C8-9	*Aats-gln*
$y^1\ w^{1118}$; $P\{w^{+mC}=lacW\}l(3)j12B4^{j12B4}$/TM3, Sb^1	96C8-9	
ry^{506} $P\{ry^{+t7.2}=PZ\}l(3)rJ880^{rJ880}$/TM3, Sb^1	96D1-2	
ry^{506} $P\{ry^{+t7.2}=PZ\}l(3)rQ197^{rQ197}$/TM3, Sb^1	96F1-2	
$y^1\ w^*$; $P\{w^{+mC}=lacW\}l(3)j7B3^{j7B3}$/TM3, Sb^1	97B8-9	
ry^{506} $P\{ry^{+t7.2}=PZ\}Rb97D^1$/TM3, ry^{RK} Sb^1 Ser^1	97D	*Rb97D*
ry^{506} $P\{ry^{+t7.2}=PZ\}l(3)rK344^{rK344}$/TM3, ry^{RK} Sb^1 Ser^1	97D1-2	
$P\{ry^{+t7.2}=PZ\}l(3)05146$, ry^{506}/TM3, ry^{RK} Sb^1 Ser^1	97D3-6	*H2AvD*
$P\{ry^{+t7.2}=PZ\}l(3)03884$, ry^{506}/TM3, ry^{RK} Sb^1 Ser^1	97D6-9	
ry^{506} $P\{ry^{+t7.2}=PZ\}ms(3)98B^{06302}$/CxD, ry^{HW}	98B	
ry^{506} $P\{ry^{+t7.2}=PZ\}l(3)rL203^{rL203}$/TM3, ry^{RK} Sb^1 Ser^1	98B1-2	
ry^{506} $P\{ry^{+t7.2}=PZ\}l(3)06487^{06487}$/TM3, ry^{RK} Sb^1 Ser^1	98C3-4	
w^{1118}; $P\{w^{+mC}=lacW\}l(3)s2976^{s2976}$/TM3, Sb^1	98E1-2	
w^{1118}; $P\{w^{+mC}=lacW\}l(3)s2784^{s2784}$/TM3, Sb^1	98F1-2	
$P\{ry^{+t7.2}=PZ\}l(3)04743$, ry^{506}/TM3, ry^{RK} Sb^1 Ser^1	98F1-2	*Doa*
$P\{ry^{+t7.2}=PZ\}l(3)01705$, ry^{506}/TM3, ry^{RK} Sb^1 Ser^1	98F4-5	*Doa*
$P\{ry^{+t7.2}=PZ\}l(3)04708$, ry^{506}/TM3, ry^{RK} Sb^1 Ser^1	99A1-2	
$P\{ry^{+t7.2}=PZ\}l(3)06743$, ry^{506}/TM3, ry^{RK} Sb^1 Ser^1	99A4-5	
$y^1\ w^{1118}$; $P\{w^{+mC}=lacW\}l(3)L6241^{L6241}$/TM3, Ser^1	99A5-6	
$P\{ry^{+t7.2}=PZ\}l(3)01235$, ry^{506}/TM3, ry^{RK} Sb^1 Ser^1	99A5-6	*stg*
$P\{ry^{+t7.2}=PZ\}l(3)05473$, ry^{506}/TM3, ry^{RK} Sb^1 Ser^1	99A5-7	*stg*
$P\{ry^{+t7.2}=PZ\}l(3)02521$, ry^{506}/TM3, ry^{RK} Sb^1 Ser^1	99A6	
$P\{ry^{+t7.2}=PZ\}l(3)06734$, ry^{506}/TM3, ry^{RK} Sb^1 Ser^1	99B8-10	
ry^{506} $P\{ry^{+t7.2}=PZ\}l(3)05884^{05884}$/TM3, ry^{RK} Sb^1 Ser^1	99C1-2	*ncd*
w^{1118}; $P\{w^{+mC}=lacW\}l(3)s2222^{s2222}$/TM3, Sb^1	99D1-2	
$y^1\ w^*$; $P\{w^{+mC}=lacW\}l(3)j11B7^{j11B7}$/TM3, Sb^1	99E1-2	
$y^1\ w^{1118}$; $P\{w^{+mC}=lacW\}l(3)j2D5^{j2D5}$/TM3, Sb^1	99F1-2	
$P\{ry^{+t7.2}=PZ\}l(3)00451$, ry^{506}/TM3, ry^{RK} Sb^1 Ser^1	99F1-2	*Fer1HCH*
$P\{ry^{+t7.2}=PZ\}l(3)00035$, ry^{506}/TM3, ry^{RK} Sb^1 Ser^1	99F1-2	*l(3)00823?*
$P\{ry^{+t7.2}=PZ\}l(3)00823$, ry^{506}/TM3, ry^{RK} Sb^1 Ser^1	99F1-2	*l(3)00035?*
$P\{ry^{+t7.2}=PZ\}l(3)05950$, ry^{506}/TM3, ry^{RK} Sb^1 Ser^1	99F1-2	
$y^1\ w^{1118}$; $P\{w^{+mC}=lacW\}l(3)j8B9^{j8B9}$/TM3, Sb^1	99F8-9	
ry^{506} $P\{ry^{+t7.2}=PZ\}l(3)00848^{00848}$/TM3, ry^{RK} Sb^1 Ser^1	99F10-11	
$P\{ry^{+t7.2}=PZ\}l(3)00848$, ry^{506}/TM3, ry^{RK} Sb^1 Ser^1	99F10-11	*Trm*
$P\{ry^{+t7.2}=PZ\}l(3)02288$, ry^{506}/TM3, ry^{RK} Sb^1 Ser^1	99F10-11	*Trm*
ry^{506} $P\{ry^{+t7.2}=PZ\}zfh1^{00865}$/TM3, ry^{RK} Sb^1 Ser^1	100A1-2	*zfh1*
w^{1118}; $P\{w^{+mC}=lacW\}l(3)s2500^{s2500}$/TM3, Sb^1	100A5-6	
$P\{ry^{+t7.2}=PZ\}l(3)07028^{07028}$, ry^{506}	100B1-2	
$P\{ry^{+t7.2}=PZ\}l(3)03670$, ry^{506}/TM3, ry^{RK} Sb^1 Ser^1	100B1-2	
$P\{ry^{+t7.2}=PZ\}l(3)07028$, ry^{506}/TM3, ry^{RK} Sb^1 Ser^1	100B1-2	
$y^1\ w^*$; $P\{w^{+mC}=lacW\}dbt^{j3B9}$/TM3, Sb^1	100B2-4	*dbt*
ry^{506} $P\{ry^{+t7.2}=PZ\}l(3)00720^{00720}$/TM3, ry^{RK} Sb^1 Ser^1	100B5-7	
ry^{506} $P\{ry^{+t7.2}=PZ\}Gprk2^{06936}$/TM3, ry^{RK} Sb^1 Ser^1	100C	*Gprk2*
ry^{506} $P\{ry^{+t7.2}=PZ\}l(3)rM731^{rM731}$/TM3, Sb^1	100C1-2	
$P\{ry^{+t7.2}=PZ\}l(3)02667$, ry^{506}/TM3, ry^{RK} Sb^1 Ser^1	100D1-2	*Ttk*
w^{1118}; $P\{w^{+mC}=lacW\}l(3)s1921^{s1921}$/TM3, Sb^1	100E1-2	
$y^1\ w^*$; $P\{w^{+mC}=lacW\}l(3)j2A4^{j2A4}$/TM3, Sb^1	100E1-2	*awd*
ry^{506} $P\{ry^{+t7.2}=PZ\}ms(3)100EF^{07570}$/TM3,$ry^{RK}$ Sb^1 Ser^1	100E1-F5	*mod*
$y^1\ w^{1118}$; $P\{w^{+mC}=lacW\}l(3)L1022^{L1022}$/TM3, Ser^1	100F1-2	
$y^1\ w^{1118}$; $P\{w^{+mC}=lacW\}l(3)L7321^{L7321}$/TM3, Ser^1	100F1-2	
$P\{ry^{+t7.2}=PZ\}l(3)03429$, ry^{506}/TM3, ry^{RK} Sb^1 Ser^1	100F1-2	
ry^{506} $P\{ry^{+t7.2}=PZ\}l(3)03847^{03847}$/TM3, ry^{RK} Sb^1 Ser^1	100F4-5	*M102*
$P\{ry^{+t7.2}=PZ\}l(3)06886$, ry^{506}/TM3, ry^{RK} Sb^1 Ser^1	100F4-5	
$P\{ry^{+t7.2}=PZ\}l(3)06497$, ry^{506}/TM3, ry^{RK} Sb^1 Ser^1	100F5	
$P\{ry^{+t7.2}=PZ\}l(3)04679$ ry^{506}/TM3, ry^{RK} Sb^1 Ser^1	61-100	
$P\{ry^{+t7.2}=PZ\}l(3)01215$ ry^{506}/TM3, ry^{RK} Sb^1 Ser^1		
$P\{ry^{+t7.2}=PZ\}l(3)05668$ ry^{506}/TM3, ry^{RK} Sb^1 Ser^1		

Appendix 6.A : LacZ assays with N- and C-terminal DmcycEI

Bait + Prey	OD600	t (min)	vol (ml)	OD420	Miller U	Average	St Dev
pEG46N+pJG4-5	0.795	170	0.5	0.111	1.638	1.619	0.317
pEG46N+pJG4-5	0.944	122	0.5	0.074	1.292		
pEG46N+pJG4-5	0.841	122	0.5	0.099	1.926		
pEGCterm+pJG4-5	0.712	122	0.5	0.032	0.744	1.074	0.354
pEGCterm+pJG4-5	0.865	122	0.5	0.054	1.031		
pEGCterm+pJG4-5	0.801	122	0.5	0.071	1.447		
pEG46N+pJGcaz	0.928	71	1	0.330	5.015	3.197	2.570
pEG46N+pJGcaz	0.778	175	1	0.188	1.380		
pEGCterm+pJGcaz	0.795	175	1	0.020	0.146	0.113	0.031
pEGCterm+pJGcaz	1.04	175	1	0.015	0.084		
pEGCterm+pJGcaz	1.026	175	1	0.020	0.109		
pEG46N+pJGeif5a	0.949	175	1	0.056	0.335	0.349	0.156
pEG46N+pJGeif5a	1.117	175	1	0.100	0.511		
pEG46N+pJGeif5a	0.976	175	1	0.034	0.201		
pEGCterm+pJGeif5a	0.876	175	1	0.096	0.629	0.718	0.115
pEGCterm+pJGeif5a	1.004	175	1	0.149	0.848		
pEGCterm+pJGeif5a	0.834	175	1	0.099	0.678		
pEG46N+pACT	0.8895	164	0.1	0.006	0.377	0.396	0.027
pEG46N+pACT	0.5437	164	0.1	0.004	0.415		
pEG46N+pACTBip2	0.9535	33	0.1	0.506	160.652	157.800	4.034
pEG46N+pACTBip2	0.463	54	0.1	0.387	154.948		
pEG46N+pACTSu(var)2-10	0.8265	164	0.1	0.100	7.400	8.475	1.521
pEG46N+pACTSu(var)2-10	0.3007	164	0.1	0.047	9.551		

Appendix 6.B : LacZ assays with full-length DmcycEI, II and PCL-C

Bait + Prey	OD600	t (min)	vol (ml)	OD420	Miller U	Average	Std Dev
pGildaDmEI+pACT	0.982	60	0.5	0.352	11.952	13.265	3.304
pGildaDmEI+pACT	2.067	60	0.5	0.631	10.173		
pGildaDmEI+pACT	1.198	60	0.5	0.417	11.603		
pGildaDmEI+pACT	0.898	50	0.5	0.400	17.800		
pGildaDmEI+pACT	1.058	50	0.5	0.452	17.096		
pGildaDmEI+pACT	1.27	50	0.5	0.348	10.967		
pGildaDmEII+pACT	1.378	60	0.5	0.368	8.890	10.539	2.296
pGildaDmEII+pACT	1.458	60	0.5	0.311	7.117		
pGildaDmEII+pACT	1.562	60	0.5	0.494	10.542		
pGildaDmEII+pACT	1.227	50	0.5	0.413	13.454		
pGildaDmEII+pACT	0.856	50	0.5	0.233	10.864		
pGildaDmEII+pACT	1.029	50	0.5	0.318	12.365		
pGildaDmEI+pACTBip2	1.227	17	0.5	2.126	203.816	228.928	29.554
pGildaDmEI+pACTBip2	1.142	17	0.5	2.672	275.214		
pGildaDmEI+pACTBip2	1.124	17	0.5	2.133	223.299		
pGildaDmEI+pACTBip2	1.041	18	0.5	1.977	210.972		
pGildaDmEI+pACTBip2	1.027	18	0.5	2.357	255.004		
pGildaDmEI+pACTBip2	0.965	18	0.5	1.783	205.262		
pGildaDmEII+pACTBip2	1.141	17	0.5	2.014	207.620	189.010	35.770
pGildaDmEII+pACTBip2	1.164	17	0.5	1.713	173.145		
pGildaDmEII+pACTBip2	1.305	17	0.5	2.257	203.453		
pGildaDmEII+pACTBip2	1.08	18	0.5	2.368	243.601		
pGildaDmEII+pACTBip2	0.977	18	0.5	1.310	148.971		
pGildaDmEII+pACTBip2	0.837	18	0.5	1.185	157.268		
pGildaDmEI+pACTSu(var)2-10	1.236	60	0.5	1.119	30.165	36.784	6.906
pGildaDmEI+pACTSu(var)2-10	1.35	60	0.5	1.534	37.874		
pGildaDmEI+pACTSu(var)2-10	1.119	60	0.5	0.967	28.803		
pGildaDmEI+pACTSu(var)2-10	0.813	50	0.5	0.971	47.793		
pGildaDmEI+pACTSu(var)2-10	0.783	50	0.5	0.712	36.388		
pGildaDmEI+pACTSu(var)2-10	0.843	50	0.5	0.836	39.682		
pGildaDmEII+pACTSu(var)2-10	1.074	60	0.5	0.717	22.250	26.492	6.039
pGildaDmEII+pACTSu(var)2-10	1.314	60	0.5	0.737	18.691		
pGildaDmEII+pACTSu(var)2-10	1.073	60	0.5	1.108	34.405		
pGildaDmEII+pACTSu(var)2-10	0.606	50	0.5	0.490	32.323		
pGildaDmEII+pACTSu(var)2-10	0.997	50	0.5	0.680	27.290		
pGildaDmEII+pACTSu(var)2-10	0.639	50	0.5	0.383	23.994		

LacZ assays with full-length DmcycEI, II and PCL-C cont.

Bait + Prey	OD600	t (min)	vol (ml)	OD420	Miller U	Average	Std Dev
pGildaDmEI+pACT	1.023	20	0.5	0.08	7.820	9.474	2.820
pGildaDmEI+pACT	1.149	20	0.5	0.1078	9.382		
pGildaDmEI+pACT	1.115	20	0.5	0.0739	6.628		
pGildaDmEI+pACT	1.323	23	0.5	0.1805	11.864		
pGildaDmEI+pACT	1.687	23	0.5	0.2677	13.799		
pGildaDmEI+pACT	1.572	23	0.5	0.1329	7.351		
pGildaDmEII+pACT	1.276	20	0.5	0.1267	9.929	8.304	2.015
pGildaDmEII+pACT	1.237	20	0.5	0.1024	8.278		
pGildaDmEII+pACT	1.431	20	0.5	0.1012	7.072		
pGildaDmEII+pACT	1.615	23	0.5	0.1061	5.713		
pGildaDmEII+pACT	0.955	23	0.5	0.1239	11.282		
pGildaDmEII+pACT	1.856	23	0.5	0.1612	7.552		
pGildaDmEI+pACTFbp1	1.562	20	0.5	1.2429	79.571	129.717	41.690
pGildaDmEI+pACTFbp1	1.407	20	0.5	1.7956	127.619		
pGildaDmEI+pACTFbp1	0.907	23	0.5	1.2977	124.414		
pGildaDmEI+pACTFbp1	1.626	23	0.5	2.2703	121.413		
pGildaDmEI+pACTFbp1	1.265	23	0.5	2.845	195.566		
pGildaDmEII+pACTFbp1	1.496	20	0.5	1.3868	92.701	90.916	15.524
pGildaDmEII+pACTFbp1	1.537	20	0.5	1.6296	106.025		
pGildaDmEII+pACTFbp1	1.581	20	0.5	1.0211	64.586		
pGildaDmEII+pACTFbp1	1.343	23	0.5	1.3413	86.846		
pGildaDmEII+pACTFbp1	1.21	23	0.5	1.4883	106.957		
pGildaDmEII+pACTFbp1	1.194	23	0.5	1.2136	88.384		
pGildaDmEI+pACTdcmaguk	1.492	20	0.5	0.6389	42.822	49.599	11.153
pGildaDmEI+pACTdcmaguk	1.585	20	0.5	0.5985	37.760		
pGildaDmEI+pACTdcmaguk	1.281	20	0.5	0.6988	54.551		
pGildaDmEI+pACTdcmaguk	1.267	23	0.5	1.0025	68.803		
pGildaDmEI+pACTdcmaguk	0.988	23	0.5	0.4902	43.144		
pGildaDmEI+pACTdcmaguk	1.064	23	0.5	0.6181	50.515		
pGildaDmEII+pACTdcmaguk	1.565	20	0.5	0.3141	20.070	28.427	9.389
pGildaDmEII+pACTdcmaguk	1.351	20	0.5	0.6	44.412		
pGildaDmEII+pACTdcmaguk	1.622	20	0.5	0.3441	21.215		
pGildaDmEII+pACTdcmaguk	1.013	23	0.5	0.2604	22.353		
pGildaDmEII+pACTdcmaguk	1.165	23	0.5	0.4494	33.544		
pGildaDmEII+pACTdcmaguk	1.426	23	0.5	0.4751	28.971		

LacZ assays with full-length DmcycEI, II and PCL-C cont.

Bait + Prey	OD600	t (min)	vol (ml)	OD420	Miller U	Average	Std Dev
pGildaDmEI+pJG4-5	0.747	110	0.5	0	0.000	-	
pGildaDmEI+pJG4-5	1.146	110	0.5	0.2168	3.440	3.746	0.433
pGildaDmEI+pJG4-5	0.935	110	0.5	0.2084	4.053		
pGildaDmEII+pJG4-5	0.922	110	0.5	0.09	1.775	1.788	0.377
pGildaDmEII+pJG4-5	1.015	110	0.5	0.1212	2.171		
pGildaDmEII+pJG4-5	1.215	110	0.5	0.0947	1.417		
pGildaDmEI+pJGcaz	1.031	110	0.5	0.4467	7.878	7.082	0.749
pGildaDmEI+pJGcaz	1.219	110	0.5	0.4285	6.391		
pGildaDmEI+pJGcaz	0.725	110	0.5	0.2782	6.977		
pGildaDmEII+pJGcaz	0.874	110	0.5	0.2608	5.425	5.561	0.433
pGildaDmEII+pJGcaz	0.966	110	0.5	0.3212	6.046		
pGildaDmEII+pJGcaz	1.195	110	0.5	0.3425	5.211		
pEG-Pcl+pJG4-5	1.35	110	0.5	0	0.000		0.000
pEG-Pcl+pJG4-5	1.191	110	0.5	0	0.000	0.000	
pEG-Pcl+pJG4-5	1.446	110	0.5	0	0.000		
pEG-Pcl+pJGcaz	1.171	110	0.5	0	0.000	0.000	0.000
pEG-Pcl+pJGcaz	1.378	110	0.5	0	0.000		
pEG-Pcl+pJGcaz	1.004	110	0.5	0	0.000		
pEG-Pcl+pACT	0.73	110	0.5	0	0.000	0.000	0.000
pEG-Pcl+pACT	1	110	0.5	0	0.000		
pEG-Pcl pACT	1.112	110	0.5	0	0.000		
pEG-Pcl+pACTBip2	1.726	125	0.5	0.4693	4.350	5.163	0.737
pEG-Pcl+pACTBip2	1.461	125	0.5	0.4887	5.352		
pEG-Pcl+pACTBip2	1.328	125	0.5	0.4803	5.787		
pEG-Pcl+pACTSu(var)2-10	1.458	125	0.5	0	0.000	0.000	0.000
pEG-Pcl+pACTSu(var)2-10	1.48	125	0.5	0	0.000		
pEG-Pcl+pACTSu(var)2-10	1.468	125	0.5	0	0.000		
pEG-Pcl+pACTFbp1	0.829	110	0.5	0	0.000	0.000	0.000
pEG-Pcl+pACTFbp1	1.097	110	0.5	0	0.000		
pEG-Pcl+pACTFbp1	0.98	110	0.5	0	0.000		
pEG-Pcl+pACTdcmaguk	0.992	110	0.5	0	0.000	0.000	0.000
pEG-Pcl+pACTdcmaguk	0.992	110	0.5	0	0.000		
pEG-Pcl+pACTdcmaguk	0.99	110	0.5	0	0.000		

References

Alevizopoulos, A. and Mermod, N. (1997). Transforming growth factor-b: the breaking open of a black box. *BioEssays* **19**: 581-591.

Anderson, J.M. (1996). Cell signalling: MAGUK magic. *Curr. Biol.* **6**: 382-384.

Ausubel, S. F., Brent, R., Kingston, R. E., Moore, D., Seideman, J. G., Smith, J. A., and Struhl, K. (1994). *In*, Current Protocols In Molecular Biology. Wiley, New York.

Avedisov, S. N., Krasnoselskaya, I., Mortin, M. and Thomas, B. J. (2000). Roughex mediates G(1) arrest through a physical association with cyclin A. *Mol Cell Biol.* **20**: 8220-9.

Baldin, V., Lukas, J., Marcote, M. J., Pagano, M. and Draetta, G. (1993). Cyclin D1 is a nuclear protein required for cell cycle progression in G1. *Genes Dev.* **7**: 812-821.

Betz, A., Lampen, N., Martinek, S., Young, M. W., and Darnell, J. E., Jr. A *Drosophila* PIAS homologue negatively regulates *stat92E. Proc. Natl. Acad. Sci. USA* **98**: 9563-9568.

Bilder, D. and Perrimon, N. (2000). Localisation of the apical epithelial determinants by the basolateral PDZ protein Scribble. *Nature* **403**: 676-680.

Bilder, D., Li, M. and Perrimon, N. (2000). Cooperative regulation of cell polarity and growth by Drosophila tumor suppressors. *Science* **289**: 113-116.

Bottazzi, M. E. and Assoin, R. K. (1997). The extracellular matrix and mitogenic growth factors control G1 phase cyclins and cyclin-dependent kinase inhibitors. *Trends Cell Biol.* **7**: 348-352.

Brand, A., and Perrimon, N. (1993). Targeted gene expression as a means of altering cell fates and generating dominant phenotypes. *Development* **118**: 401-415.

Brumby, A., Zraly, C., Horsfield, J., Secombe, J., Saint, R., Dingwell, A., and Richardson, H. (2002). *Drosophila* cyclin E interacts with components of the SWI/SNF complex. Submitted to *EMBO J.*

Bryant, P.J. and Huwe, A. (2000). LAP proteins: what's up with epithelia? *Nature Cell Biol.* **2**: E141-143.

Burley, S. K. and Roeder, R. G. (1996). Biochemistry and structural biology of transcription factor IID (TFIID). *Annu. Rev. Biochem.* **65**: 769-799.

Caplan, A. J., Langley, E., Wilson, E. M. and Vidal, J. (1995). Hormone-dependent transactivation by the human androgen receptor is regulated by a DnaJ protein. *J. Biol. Chem.* **270**: 5251-5257.

Carnero, A. and Hannon, G. (1998). The INK4 family of CDK inhibitors. *Curr. Top. Microbiol. Immunol.* **227**: 43-55.

Chang, J. S., Tan, L., and Schedl, P. (1999). The *Drosophila* CPEB homolog, *orb*, is required for oskar protein expression in oocytes. *Dev Biol.* **215**: 91-106.

Chang, J. S., Tan, L., Wolf, M. R., and Schedl, P. (2001). Functioning of the *Drosophila orb* gene in *gurken* mRNA localization and translation. *Development* **128**: 3169-77.

Chung, C. D., Liao, J., Liu, B., Rao, X., Jay, P., Berta, P. and Shuai, K. (1997). Specific inhibition of Stat3 signal transduction by PIAS3. *Science* **278**:1803-5.

Clurman, B. E., Sheaff, R. J., Thress, K., Groudine, M. and Roberts, J. M. (1996). Turnover of cyclin E by the ubiquitin-proteosome pathway is regulated by cdk2 binding and cyclin phosphorylation. *Genes Dev.* **10**: 1979-1990.

Crack, D. M. (1996). Investigation of the properties of *Drosophila melanogaster* type II *cyclinE*. Hon. Thesis. University of Adelaide, Adelaide.

Crack, D., Secombe, J., Coombe, M., Brumby, A., Saint, R. and Richardson, H. (2002). Analysis of *Drosophila* Cyclin EI and EII function during development: Identification of an inhibitory zone within the morphogenetic furrow of the eye imaginal disc that blocks the function of Cyclin EI but not Cyclin EII. *Dev. Biol.* **241**: 157-171.

Datar, S. A., Jacobs, H. W., de la Cruz, A. F., Lehner, C. F. and Edgar, B. A. (2000). The Drosophila cyclin D-Cdk4 complex promotes cellular growth. *EMBO J.* **19**: 4543-4554.

Deng, C., Zhang, P., Harper, J. W. Elledge, S. J. and Leder, P. (1995). Mice lacking p21Cip1/WAF1 undergo normal development, but are defective in G1 checkpoint control. *Cell* **82**: 675-684.

de Nooij, J. (1998). Regulation of cell proliferation during the development of *Drosophila melanogaster*. PhD thesis, Harvard medical school, Boston, U.S.A

de Nooij, J. C., Graber, K.H. and Hariharan, I. K. (2000). Expression of the cyclin-dependent kinase inhibitor Dacapo is regulated by Cyclin E. *Mech. Devel.* **97**: 73-83.

de Nooij, J. C., Letendre, M. A. and Hariharan, I. K. (1996). A cyclin-dependent kinase inhibitor, Dacapo, is necessary for timely exit from the cell cycle during *Drosophila* embryogenesis. *Cell* **87**: 1237-1247.

de Nooij J. C. and Hariharan I. K. (1995). Uncoupling cell fate determination from patterned cell division in the *Drosophila* eye. *Science* **270**: 983-5.

Desdouets, C., Sobczak-Thepot, J., Murphy, M. and Brechot, C. (1995). Cyclin A: function and expression during cell proliferation. Progress in Cell Cycle Research. L. Meijer, Guidet, S. and Vogel, L. New York, Plenum Press. **1:** 115-123.

Dong, X., Zavitz, K. H., Thomas, B. J., Lin, M., Campbell, S. and Zipursky, S. L. (1997). Control of G1 in the developing *Drosophila* eye: Rca1 regulates Cyclin A. *Genes Dev.* **11**: 94-105.

Du, W., and N. Dyson. (1999) The role of RBF in the introduction of G1 regulation during *Drosophila* embryogenesis. *EMBO J.* **18:** 916-925

Du, W., Vidal, M., Xie, J.-E. and Dyson, N. (1996). *RBF*, a novel RB-related gene that regulates E2F activity and interacts with cyclin E in *Drosophila*. *Genes Dev.* **10**: 1206-1218.

Dulic, V., Kaufmann, W. K., Wilson, S. J., Tlsty, T. D., Lees, E., Harper, W. J., Elledge, S. J. and Reed, S. I. (1994). p53-dependent inhibition of cyclin-dependent kinase activities in human fibroblasts during radiation-induced G1 arrest. *Cell* **76**: 1013-1023.

Durand, B., Fero, M. L., Roberts, J. M. and Raff, M. C. (1998). P27Kip1 alters the response of cells to mitogen and is part of a cell-intrinsic timer that arrests the cell cycle and initiates differentiation. *Curr. Biol.* **8**: 431-440.

D'Urso, G., Marraccino, R. L., Marshak, D. R. and Roberts, J. M. (1990). Cell cycle control of DNA replication by a homolog from human cells of the $p34^{cdc2}$ protein kinase. *Science* **250**: 786.

Dyson, N. (1998). The regulation of E2F by pRB-family proteins. *Genes Dev.* **12**: 2245-2262.

Edgar, B. (1995). Diversification of cell cycle controls in developing embryos. *Curr. Opin. Cell Biol.* **7**: 815-824.

Edgar, B. A. and Lehner, C. F. (1996). Developmental control of cell cycle regulators: a fly's perspective. *Science* **274**: 1646-1652.

Edgar, B. A. and O'Farrell, P. H. (1990). The three postblastoderm cell cycles of *Drosophila* embryogenesis are regulated in G2 by *string*. *Cell* **57**: 177-187.

Ekholm, S. V. and Reed, S. I. (2000). Regulation of G1 cyclin dependent kinases in the mammalian cell cycle. *Curr. Opin. Cell Biol.* **12**, 676-684.

El-Deiry, W. S., Tokino, T., Velculescu, V. E., Levy, D. B., Parsons, R., Trent, J. M., Lin, D., Mercer, W. E., Kinzler, K. W. and Vogelstein, B. (1993). WAF1, a potential mediator of p53 tumour suppression. *Cell* **75**: 817-825.

Elledge, S. J. (1996). Cell cycle checkpoints: preventing an identity crisis. *Science* **274**: 1664-1672.

Estojak, J., Brent, R. and Gloemis, E.A. (1995). Correlation of two-hybrid affinity data with in vitro measurements. *Mol Cell Biol.* **15**: 5820-9.

Fantl, V., Stamp, G., Andrews, A., Rosewell, I. and Dickson, C. (1995). Mice lacking cyclin D1 are small and show defects in eye and mammary gland development. *Genes Dev.* **9**: 2364-2372.

Fehon, R. G., Kooh, P. J., Rebay, I., Regan, C. L., Xu, T., Muskavitch, M. A. and Artavanis-Tsakonas, S. (1990). Molecular interactions between the protein products of the neurogenic loci Notch and Delta, two EGF-homologous genes in *Drosophila*. *Cell* **61**: 523-534.

Fero, M. L., Rivkin, M., Tasch, M., Porter, P., Carow, C. E., Firpo, E., Polyak, K., Tsai, L.-H., Broudy, V., Perlmutter, R. M., Kaushansky, K. and Roberts, J. M. (1996). A syndrome of multiorgan hyperplasis with features of gigantism, tumorigenesis, and female sterility in p27kip1-deficient mice. *Cell* **85**: 733-744.

Finley, R. L. Jr., and Brent, R. (1994). Interaction mating reveals binary and ternary connections between *Drosophila* cell cycle regulators. *Proc. Natl. Acad. Sci. USA* **91**: 12980-12984.

FlyBase (1999). The FlyBase database of the Drosophila genome projects and community literature. *Nucleic Acids Research* **27**: 85-88. http://flybase.bio.indiana.edu/

Foe, V. E. (1989). Mitotic domains reveal early commitment of cells in *Drosophila* embryos. *Development* **107**: 1-22.

Foe, V. E. and Alberts, B. A. (1983). Studies of nuclear and cytoplasmic behaviour during the five mitotic cycles that precede gastrulation in Drosophila embryogenesis. *J. Cell Sci.* **61**: 31-70.

Furstenthal, L., Kaiser, B. N., Swanson, C. and Jackson, P. K. (2001). Cyclin E uses Cdc6 as a chromatin-associated receptor required for DNA replication. *J. Cell Biol.* **152**: 1267-1278.

Garcia-Bustos, J., Heitman, J. and Hall, M. N. (1991). Nuclear protein localization. *Biochim. Biophys. Acta.* **1071**: 83-101.

Geng, Y., Whoriskey, W., Park, M. Y., Bronson, R. T., Medema, R. H., Li, T., Weinberg, R. A. and Sicinski, P. (1999). Rescue of *cyclin D1* deficiency by knockin *cyclin E*. *Cell* **97**: 767-777.

Gietz, R. D. and Schiestl, R. H. (1996). Transforming yeast with DNA. (Invited chapter) Methods in Molecular and Cellular Biology.

Girard (1991). Cyclin A is required for the onset of DNA replication in mammalian fibroblasts. *Cell* **67**: 1169-1179.

Glotzer, M. (1995). Cell cycle. The only way out of mitosis. *Curr. Biol.* **5**: 970-972.

Green, M. R. (2000). TBP-associated factors ($TAF_{II}s$): multiple, selective transcriptional mediators in common complexes. *TiBS* **25**: 59-63.

Groisman I., Jung, M. Y., Sarkissian, M., Cao, Q. and Richter, J. D. (2002). Translational control of the embryonic cell cycle. *Cell* **109**: 473-83.

Gross, M., Liu B., Tan, J., French, F. S. Carey, M. and Shuai, K. (2001). Distinct effects of PIAS proteins on androgen-mediated gene activation in prostate cancer cells. *Oncogene* **20**: 3880-7.

Gudas, J. M., Payton, M., Thukral, S., Chen, E., Bass, M., Robinson, M. O., and Coats, S. (1999). Cyclin E2, a novel G1 cyclin that binds Cdk2 and is aberrantly expressed in human cancers. *Mol. Cell. Biol.* **19**, 612-622.

Gyuirs, J., Golemis, E. A., Chertkov, H., and Brent, R. (1993). Cdi1, a human G1- and S-phase protein phosphatase associates with Cdk2. *Cell* **75**: 791-803.

Hadwiger, J. A., Witenberg, C., Richardson, H., De Barros Lopes, M. and Reed, S. I. (1989). A family of cyclin homologs that control the G1 phase in yeast. *Proc. Natl. Acad. Sci.* **86**: 6255-6259.

Halevy, O., Novitch, B. G., Spicer, D. B., Skapek, S. X., Rhee, J., Hannon, G. J., Beach, D. and Lassar, A. B. (1995). Correlation of terminal cell cycle arrest of skeletal muscle with induction of p21 by MyoD. *Science* **267**: 1018-1021.

Hannon, G. J. and Beach, D. (1994). $p15^{INK4b}$ is a potent effector of cell cycle arrest mediated by TGF-b. *Nature* **371**: 257-261.

Hari, K. L., Cook, K. R. and Karpen, G. H. (2001). The *Drosophila Su(var)2-10* locus regulates chromosome structure and function and encodes a member of the PIAS protein family. *Genes Dev.* **15**: 1334-1348.

Harrison, D. A., Binari, R., Nahreini, T. S., Gilman, M., and Perrimon, N. (1995). Activation of a *Drosophila* Janus kinase (JAK) causes hematopoietic neoplasia and developmental defects. *EMBO J.* **14**: 2857-2865.

Hay, B.A., Wolff, T and Rubin, G. M. (1994). Expression of the baculovirus p35 prevents cell death in *Drosophila*. *Development* **120**: 2121-2129.

Hendrick, J. P., Langer, T., Davis, T. A., Hartl, F. U. and Wiedmann, M. (1993). Control of folding and membrane translocation by binding of the chaperone DnaJ to nascent polypeptides. *Proc. Natl. Acad. Sci. USA* **90**: 10216-10220.

Hengat, L. and Reed, S. (1998). Inhibitors of the Cip/Kip family. *Curr. Top. Microbiol. Immunol.* **227**: 25-41.

Hinchcliffe, E. H., Li, C., Thompson, E. A., Maller, J. L. and Sluder, G. (1999). Requirement of Cdk2-cyclin E activity for repeated centrosome reproduction in Xenopus egg extracts. *Science* **283**: 851-854.

Hoffman, I., Draetta, G. and Karsenti, E. (1994). Activation of the phosphatase activity of human cdc25A by a cdk2-cyclin E dependent phosphorylation at the G1/S transition. *EMBO J.* **13**: 4302-4310.

Horsfield, J., Penton, A., Secombe, J., Hoffman, F. M. and Richardson, H. (1998). *decapentaplegic* is required for arrest in G_1 phase during *Drosophila* eye development. *Development* **125**: 5069-5078.

Immanuel, D., Zinszner, H., and Ron, D. (1995). Association of SARFH (Sarcoma-Associated RNA-Binding Fly Homolog) with regions of chromatin transcribed by RNA polymerase II. *Mol. Cell. Biol.* **15**: 4562-4571.

Ishidate, T., Matsumine, A., Toyoshima, K., and Akiyama, T. (2000). The APC-hDlg complex negatively regulates cell cycle progression from the G0/G1 to S phase. *Oncogene* **19**: 365-372.

Jackson, P. K. (2001). A new RING for SUMO: wrestling transcriptional responses into nuclear bodies with PIAS family E3 SUMO ligases. *Genes Dev.* **15**:

James, P., Halladay, J., and Craig, E. A. (1996). Genomic libraries and a host strain designed for highly efficient two-hybrid selection in yeast. *Genetics* **144**: 1425-1436.

Jinno, S., Suto, K., Nagata, M., Igarashi, M., Kanaoka, Y., Nojima, H. and Okayama, H. (1994). Cdc25A is a novel phosphatase functioning early in the cell cycle. *EMBO J.* **13**: 1549-1566.

Johnson, L. A. and Edgar, B. A. (1998). Wingless and Notch regulate cell cycle arrest in the developing Drosophila wing. *Nature* **394**: 82-84.

Kamberov, E., Makarova, O., Roh, M., Liu, A., Karnak, D., Straight, S. and Margolis, B. (2000). Molecular cloning and characterization of Pals, proteins associated with mLin-7. *J. Biol. Chem.* **275**: 11425-11431.

Kelley, W. L. (1998). The J-domain family and the recruitment of chaperone power. *Trends Biochem. Sci.* **23**: 222-227.

King, R. W., Deshaies, R. J., Peters, J.-M. and Kirschner, M. W. (1996). How proteolysis drives the cell cycle. *Science* **274**: 1652-1659.

Kiyokawa, H., Kineman, R. D., Manova-Todorova, K. O., Soares, V. C., Hoffman, E. S., Ono, M., Khanam, D., Hayday, A. C., Frohman, L. A. and Koff, A. (1996). Enhanced growth of mice lacking the cyclin-dependent kinase inhibitor function of p21kip1. *Cell* **85**: 721-732.

Kiyono T., Hiraiwa A., Fujita M., Hayashi Y., Akiyama T. and Ishibashi M. (1997). Binding of high-risk human papillomavirus E6 oncoproteins to the human homologue of the Drosophila discs large tumor suppressor protein. *Proc Natl Acad Sci U S A.* **94**: 11612-6.

Knoblich, J., Sauer, K., Jones, L., Richardson, H. E. and Saint, R. B. (1994). Cyclin E controls progression through S phase and its downregulation during *Drosophila* embryogenesis is required for the arrest of cell proliferation. *Cell* **77**: 107-120.

Koff, A., Ohtsuki, M., Polyak, K., Roberts, J. and Massague, J. (1993). Negative regulation of G1 in mammalina cells: Inhibition of cyclin E-dependent kinase by TGF-beta. *Science* **260**: 536-539.

Kotaja, N., Aittomaki, S., Silvennoinen, O., Palvimo, J. J. and Janne, O. A. (2000). ARIP3 (androgen receptor-interacting protein 3) and other PIAS (protein inhibitor of activated STAT) proteins differ in their ability to modulate steroid receptor-dependent transcriptional activation. *Mol Endocrinol.* **14**: 1986-2000.

Krek, W. (1998). Proteolysis and the G1-S transition: the SCF connection. *Curr. Opin. Genet. Dev.* **8**: 36-42.

Kurzik-Dumke, U., Gundacker, D., Rentrop, M. and Gateff, E. (1995). Tumor suppression in *Drosophila* is causally related to the function of the *lethal(2)tumorous* imaginal discs gene, a dnaJ homolog. *Dev. Genet.* **16**: 64-76.

Lane, M. E., Elend, M., Heidmann, D., Herr, A., Marzodko, S., Herzig, A., and Lehner, C. F. (2000). A screen for modifiers of *Cyclin E* function in *Drosophila melanogaster* identifies *Cdk2* mutations, revealing the insignificance of putative phosphorylation sites in Cdk2. *Genetics* **155**: 233-244.

Lane, M. E., Sauer, K., Wallace, K., Jan, Y. N., Lehner, C. F. and Vaessin, H. (1996). *Dacapo*, a cyclin-dependent kinase inhibitor, stops cell proliferation during *Drosophila* development. *Cell* **87**: 1225-1235.

Lantz, V., Chang, J. S., Horabin, J. I., Bopp, D. and Schedl, P. (1994). The *Drosophila* orb RNA-binding protein is required for the formation of the egg chamber and establishment of polarity. *Genes Dev.* **8**: 598-613.

Lauper, N., Beck, A. R., Cariou, S., Richman, L., Hofmann, K., Reith, W., Slingerland, J. M., and Amati, B. (1998). Cyclin E2, a novel Cdk2 partner in the late G1 and S phases of the mammalian cell cycle. *Oncogene* **17**, 2637-2643.

Lees, E. M. and Harlow, E. (1993). Sequences within the conserved cyclin box of human cyclin A are sufficient for binding to and activation of cdc2 kinase. *Mol. Cell. Biol.* **13**: 1194-1201.

Lee S.S., Weiss R.S. and Javier R.T. (1997). Binding of human virus oncoproteins to hDlg/SAP97, a mammalian homolog of the Drosophila discs large tumor suppressor protein. *Proc Natl Acad Sci U S A.* **94**: 6670-5.

Lehner, C. F. and O'Farrell, P. H. (1990). *Drosophila* Cdc2 homologs: A functional homolog is co-expressed with a cognate variant. *EMBO J.* **9**, 3573-3581.

Lew, D. J., Dulic, V. and Reed, S. I. (1991). Isolation of three novel human cyclins by rescue of G1 cyclin (Cln) function in yeast. *Cell* **66**: 1197-1206.

Lew, D. J. and Kornbluth, S. (1996). Regulatory roles of cyclin dependent kinase phosphorylation in cell cycle control. *Curr. Opin. Cell Biol.* **8**: 795-804.

Lilly, M. and Spradling, A. (1996). The *Drosophila* endocycle is controlled by cyclin E and lacks a checkpoint ensuring S-phase completion. *Genes Dev.* **10**: 2514-2526.

Lindsay, D. L., and Zimm, G. G. (1992) *In*, The genome of *Drosophila melanogaster*. Academic Press, San Diego.

Liu, B., Liao, J., Rao, X., Kushner, S. A., Chung, C. D., Chang, D. D and Shuai, K. (1998). Inhibition of Stat1-mediated gene activation by PIAS1. *Proc Natl Acad Sci U S A.* **95**:10626-31.

Long, X. and Griffith, L. C. (2000). Identification and characterisation of a SUMO-1 conjugation system that modifies neuronal calcium/calmodulin-dependent protein kinase in *Drosophila melanogaster. J. Biol. Chem.* **275**: 40765-40776.

Lukas, J., Bartkova, J., Rohde, M., Strauss, M. and Bartek, J. (1995). Cyclin D is dispensible for G1 control in retinoblastoma gene-deficient cells independently of Cdk4 activity. *Mol. Cell. Biol.* **15**: 2600-2611.

Lukas, J., Herzinger, T., Hansen, K., Moroni, M. C., Resnitzky, D., Helin, K., Reed, S. I. and Bartek, J. (1997). Cyclin E-induced S phase without activation of the pRB/E2F pathway. *Genes Dev.* **11**: 1479-1492.

Lundberg, A. S. and Weinberg, R. A. (1998). Functional inactivation of the retinoblastoma protein requires sequential modification by at least two distinct Cyclin-Cdk complexes. *Mol. Cell. Biol.* **18**: 753-761.

Luo, H. and Dearolf, C. R. (2001). The JAK/STAT pathway and *Drosophila* development. *BioEssays* **23**: 1138-1147.

Ma, T., Van Tine, B. A., Wei, Y., Garrett, M. D., Nelson, D., Adams, P. D., Wang, J., Qin, J., Chow, L. T. and Harper, J. W. (2000). Cell cycle-regulated phosphorylation of p220(NPAT) by cyclin E/Cdk2 in Cajal bodies promotes histone gene transcription. *Genes Dev.* **14**: 2298-2313.

Masucci, J. D., Miltenberger, R. J. and Hoffmann, F. M. (1990). Pattern-specific expression of the Drosophila decapentaplegic gene in imaginal disks is regulated by 3' cis-regulatory sequences. *Genes Dev.* **4**: 2011-2023.

Matsumoto, Y., Hayashi, K. and Nishida, E. (1999). Cyclin-dependent kinase 2 (Cdk2) is required for centrosome duplication in mammalian cells. *Curr Biol.* **9**: 429-432.

Matsushime, H., Roussel, M. F., Ashmun, R. A. and Sherr, C. J. (1991). Colony-stimulating factor 1 regulates novel cyclins during the G1 phase of the cell cycle. *Cell* **65**: 701-713.

Maixner, A., Hecker, T. P., Phan, Q. N., and Wassarman, D., A. (1998). A screen for mutations that prevent lethality caused by expression of activated Sevenless and Ras1 in the *Drosophila* embryo. *Dev. Genet.* **23**: 347-361.

Mayer, M. P. and Bukau, B. (1998). Hsp70 chaperone systems: diversity of cellular functions and mechanism of action. *Biol. Chem.* **379**; 261-268.

Mazoyer, S., Gayther, S. A., Nagai, M. A., Smith, S. A., Dunning, A., van Rensburg, E. J., Albertsen, H., White, R. and Ponder, B. A. (1995). A gene (DLG2) located at 17q12-q21 encodes a new homologue of the *Drosophila* tumor suppressor dIg-A. *Genomics* **28**: 25-31.

Mendenhall, M. D., Richardson, H. E. and Reed, S. I. (1988). Dominant negative protein kinase mutations that confer a G1 arrest phenotype. *Proc. Natl. Acad. Sci. USA* **85**: 4426-30.

Mendez, R. and Richter, J. D. (2001). Translational control by CPEB: A means to the end. *Nature Reviews Molecular Cell Biology* **2**: 521 –529.

Melchior, F. (2000). SUMO: Nonclassical ubiquitin. *Annu. Rev. Cell Dev. Biol.* **16**: 591-626.

Meyer, C. A., Jacobs, H. W., Datar, S. A., Du, W., Edgar, B. A. and Lehner, C. F. (2000). Drosophila Cdk4 is required for normal growth and is dispensable for cell cycle progression. *EMBO J.* **19**: 4533-4542.

Mohr, S. E. and Boswell, R. E. (1999). *Zimp* encodes a homologue of mouse Miz1 and PIAS3 and is an essential gene in *Drosophila melanogaster. Gene* **229**: 109-188.

Motokura, T., Bloom, T., Kim, H. G., Juppner, H., Ruderman, J. V., Kronenberg, H. M. and Arnold, A. (1991). A novel cyclin encoded by a Bcl1-linked candidate oncogene. *Nature* **350**: 512-515.

Mumberg, D., Wick, M., Burger, C., Haas, K., Funk, M., and Muller, R. (1997). Cyclin ET, a new splice variant of human cyclin E with a unique expression pattern during cell cycle progression and differentiation. *Nuc. Acids Res.* **25**, 2098-2105.

Nakayama, K., Ishida, N., Shirane, M., Inomata, A., Inoue, T., Shishido, N., Horii, I., Loh, D. Y. and Nakayama K. (1996). Mice lacking p27Kip1 display increased body size, multiple organ hyperplasia, retinal dysplasia and pituitary tumors. *Cell* **85**: 707-720.

Nurse, P. (1990). Universal control mechanisms regulating onset of M-phase. *Nature* **344**: 503-507.

Ohtsubo, M. and Roberts, J. M. (1993). Cyclin-dependent regulation of G1 in mammalian fibroblasts. *Science* **259**: 1908-1912.

Ohtsubo, M., Theodoras, A. M., Schumacher, J. and Roberts, J. M. (1995). Human cyclin E, a nuclear protein essential for the G1 to S phase transition. *Mol. Cell. Biol.* **15**: 2612-2624.

Okuda, M., Horn, H. F., Tarapore, P., Tokuyama, Y., Smulian, A. G., Chan, P. K., Knudsen, E. S., Hofmann, I. A., Snyder, J. D., Bove, K. E., *et. al.*, (2000). Nucleophosmin/B23 is a target of CDK2/cyclin E in centrosome duplication. *Cell* **103**: 127-140.

Pagano, M., Pepperkok, R., Verde, F., Ansorge, W. and Draetta, G. (1992). Cyclin A is required at two points in the human cell cycle. *EMBO J.* **11**: 961-971.

Pardee, A. B. (1974). A restriction point for control of normal animal cell proliferation. *Proc. Natl. Acad. Sci.* **71**: 1286-1290.

Pardee, A. B. (1989). G1 events and regulation of cell proliferation. *Science* **246**: 603-608.

Parker, S. B., Eichele, G., Zhang, P., Rawls, A., sands, A. T., Bradley, A., Olson, E. N., Harper, J. W. and Elledge, S. J. (1995). p53-independent expression of $p21^{Cip1}$ in muscle and other terminally differentiating cells. *Science* **267**: 1024-1027.

Parry, D., Bates, S., Mann, D. J. and Peters, G. (1995). LAck of cyclin D-Cdk complexes in Rb-negative cells correlates with high levels of $p16^{INK4/MTS1}$ tumour suppressor gene product. *EMBO J.* **14**: 503-511.

Penton, A., Selleck, S. B. and Hoffman, F. M. (1997). Regulation of cell cycle synchronization by decapentaplegic during Drosophila eye development. *Science* **275**: 203-206.

Phelps, C. B. and Brand, A. H. (1998). Ectopic gene expression in *Drosophila* using GAL4 system. *Methods* **14** (4): 367-379.

Pines, J. (1992). Cell proliferation and control. *Curr. Opin. Cell Biol.* **4**: 144-148.

Planas-Silva, M. D. and Weinberg, R. A. (1997). The restriction point and control of cell proliferation. *Curr. Opin. Cell Biol.* **9**: 768-772.

Polyak, K., Kato, J., Solomon, M., Sherr, C., Massague, J., Roberts, J. and Koff, A. (1994). $p27^{Kip1}$, a cyclin-Cdk inhibitor, links transforming growth factor b and contact inhibition to cell cycle arrest. *Genes Dev.* **8**: 9-22.

Poon, R. Y., Yamashita, K., Adamczewski, P., Hunt, T. and Shuttleworth, J. (1993). The cdc2-related protein p40MO15 is the catalytic subunit of a protein kinase that can activate p33cdk2 and p34cdc3. *EMBO J.* **12**: 3123-3132.

Porter, D. C., and Keyomarsi, K. (2000). Novel splice variants of cyclin E with altered substrate specificity. *Nucl. Acids Res.* **28**, E101.

Porter, D.C. Zhang, N., Danes, C., McGahren, M.J., Harwell, R.M., Faruki, S., and Keyomarsi, K. (2001). Tumor-specific proteolytic processing of cyclin E generates hyperactive lower-molecular-weight forms. *Mol Cell Biol.* **21**, 6254-6269.

Prober, D. A. and Edgar, B. A. (2000). Ras1 promotes cellular growth in the *Drosophila* wing. *Cell* **100**: 435-46.

Prober, D. A. and Edgar, B. A. (2001). Growth regulation by oncogenes-new insights from model organisms. *Curr. Opin. Genet. Dev.* **11**:19-26.

Reed, S. I., Ed. (1996). *G1/S regulatory mechanisms from yeast to man*. Progress in cell cycle research. New York, Plenum Press.

Raftery, L. H., Twombly, V., Wharton, K., and Gelbart, W. M. (1995). Genetic screen to identify elements of the *decapentaplegic* signaling pathway in *Drosophila*. *Genetics* **139**: 241-254.

Rempel R. E., Sleight, S. B. and Maller, J. L. (1995). Maternal *Xenopus* Cdk2-cyclinE complexes function during meiotic and early embryonic cell cycles that lack a G1 phase. *J. Biol. Chem.* **270**: 6843-6855.

Resnitzky, D., Gossen, M., Bujard, H. and Reed, S. I. (1994). Acceleration of the G1/S transition by expression of cyclins D1 and E using an inducible system. *Mol. Cell. Biol.* **14**: 1669-1679.

Resnitzky, D., Hengst, L. and Reed, S. I. (1995). Cyclin A-associated kinase activity is rate limiting for entrance into S phase and is negatively regulated in G1 by $p27^{Kip1}$. *Mol. Cell. Biol.* **15**: 4347-4352.

Resnitzky, D. and Reed, S. I. (1995). Different roles for cyclins D1 and E in regulation of the G1-to-S transition. *Mol. Cell. Biol.* **15**: 3463-3469.

Richardson, H., O'Keefe, L. V., Marty, T. and Saint, R. (1995). Ectopic cyclin E expression induces premature entry into S phase and disrupts pattern formation in the *Drosophila* eye imaginal disc. *Development* **121**: 3371-3379.

Richardson, H. L., O'Keefe, L. V., Reed, S. I. and Saint, R. (1993). A *Drosophila* G1-specific cyclin E homolog exhibits different modes of expression during embryogenesis. *Development* **119**: 673-690.

Robles, A. I., Larcher, F., Whalin, R. B., Murillas, R., Richie, E., Gimenez-Conti, I. B., Jorcano, J. L. and Conti, C. J. (1996). Expression of cyclin D1 in epithelial tissues of transgenic mice results in epidermal hyperproliferation and severe thymic hyperplasia. *Proc Natl Acad Sci USA* **93**: 7634-7638.

Rodriguez-Puebla, M. L., LaCava, M.and Conti, C. J. (1999). Cyclin D1 overexpression in mouse epidermis increases cyclin-dependent kinase activity and cell proliferation *in vivo* but does not affect skin tumor development. *Cell Growth Differ* **10**: 467-472.

Sachdev, S., Bruhn, L., Sieber, H., Pichler, A., Melchior, F. and Grosschedl, R. (2001). PIASy, a nuclear matrix-associated SUMO E3 ligase, represses LEF1 activity by sequestration into nuclear bodies. *Genes Dev.* **15**:

Sambrook J., Fritsch, E. F. and Maniatis, T. (1989). *Molecular cloning: a laboratory manual.* Cold Spring Harbour Laboratory Press, Cold Spring Harbour, New York.

Sarkar, S., Pollack, B. P., Lin, K.-T., Kontenko, S. V., Cook, J. R., Lewis, A and Pestka, S. (2001). hTid-1. a human DnaJ protein, modulates the interferon signaling pathway. *Proc. Natl. Acad. Sci. USA* **276**: 49034-49042.

Sauer, K., Knoblich, J. A., Richardson, H. and Lehner, C. F. (1995). Distinct modes of cyclin E/cdc2c kinase regulation and S-phase control in mitotic and endoreduplication cycles of Drosophila embryogenesis. *Genes Dev.* **9**: 1327-1339.

Schilling, B., De-Medina, T., Syken, J., Vidal, M. and Munger, K. (1998). A novel human DnaJ protein, hTid-1, a homolog of the *Drosophila* tumor suppressor protein Tid56, can interact with the human papillomavirus type 16 E7 oncoprotein. *Virology* **247**: 74-85.

Schneider, I. (1972). Cell lines derived from late embryonic stages of *Drosophila* melanogaster. *J. Embryol. Exp. Morphol.* **27**: 353-365.

Secombe, J. (1995). The significance of PEST sequences in the G1 specific DmcycE of *Drosophila melanogaster.* Hon. Thesis, University of Adelaide, Adelaide.

Secombe, J. (1999). Identification of novel G1 to S phase regulators in *Drosophila.* Ph.D. Thesis, The University of Adelaide, Adelaide

Secombe, J., Pispa, J., Saint, R. and Richardson, H. (1998). Analysis of a *Drosophila cyclin E* hypomorphic mutation suggests a novel role for Cyclin E in cell proliferation control during eye imaginal disc development. *Genetics* **149**: 1867-1882.

Seghezzi, W., Chua, K., Shanahan, F., Gozani, O., Reed, R. and Lees, E. (1998). Cyclin E associates with components of the pre-mRNA splicing machinery in mammalian cells. *Mol. Cell. Biol.* **18**: 4526-4536.

Sewing, A., Ronicke, V., Burger, C., Funk, M., and Muller, R. (1994). Alternative splicing of human cyclin E. *J. Cell Sci.* **107**, 581-588.

Sherr, C. J. and Roberts, J. M. (1999). CDK inhibitors: positive and negative regulators of G1-phase progeression.. *Genes Dev.* **13**: 1501-1512.

Shridhar, V., Bible, K. C., Staub, J., Avula, R., Lee, Y. K., Kalli K, Huang, H., Hartmann, L. C., Kaufmann, S. H. and Smith, D. I. (2001). Loss of expression of a new member of the DNAJ protein family confers resistance to chemotherapeutic agents used in the treatment of ovarian cancer. *Cancer Res.* **61**: 4258-4265.

Sicinski, P., Donaher, J. L., Parker, S. B., Li, T., Fazeli, A., Gardner, H., Haslam, S. Z., Bronson, R. T., Elledge, S. J. and Weinberg, R. A. (1995). Cyclin D1 provides a link between development and oncogenesis in the retina and breast. *Cell* **82**: 621-630.

Simon, M. A., Bowtell, D., Dodson, G. S. Laverty, T. R., and Rubin G. M. (1991). Ras1 and a putative guanine nucleotide exchange factor perform crucial steps in the signaling by the sevenless protein tyrosine kinase. *Cell* **67**: 701-716.

Slingerland, J., Hengst, L., Pan, C., Alexander, D., Stampfer, M. R. and Reed, S. I. (1994). A novel inhibitor of cyclin-Cdk activity detected in transforming growth factor beta-arrested epithelial cells. *Mol. Cell. Biol.* **14**: 3683-3694.

Smith, A. V. and Orr-Weaver, T. L. (1991). The regulation of the cell cycle during *Drosophila* embryogenesis: the transition to polyteny. *Development* **112**: 997-1008.

Smith, A. V., King, J. A. and Orr-weaver, T. L. (1994). Identification of genomic regions required for DNA replication during *Drosophila* embryogenesis. *Genetics* **135**:817-29.

Smith, D B. and Johnson K. S. (1988). Single-step purification of polypeptides expressed in *Escherichia coli* as fusions with glutathione S-transferase. *Gene* **67**: 31-40.

Solomon, M. J., Harper, J. W. and Shuttleworth, J. (1993). CAK, the p34cdc2 activating kinase, contains a protein identical or closely related to p40MO15. *EMBO J.* **12**: 3133-3142.

Spradling, A. C. (1993). Developmental genetics of oogenesis. In The development of *Drosophila melanogaster* Vol.1 (de. M Bates and A Martinez Arias), pp1-70. New York: Cold Spring Harbour Laboratory Press.

Spradling, A. C., Stern, D. M., Kiss, I., Roote, J., Laverty, T., and Rubin, G. M. (1995). Gene disruptions using P transposable elements: an integral component of the *Drosophila* genome project. *Proc. Natl. Acad. Sci.* **92**: 10824-30.

Spradling, A. C., Stern, D., Beaton, A., Rhem, E. J., Laverty, T., Mozden, N., Misra, S., and Rubin, G. M. (1999). The BDGP gene disruption project: single P element insertions mutating 25% of vital *Drosophila* genes. *Genetics* **153**: 135-77.

Sprenger, F., Yakubovich, N. and O'Farrell, P. H. (1997). S-phase function of *Drosophila* cyclinA and its downregulation in G1 phase. *Curr. Biol.* **7**: 488-499.

Spruck, C.H., Won, K.A. and Reed, S.I. (1999). Deregulated cyclin E induces chromosome instability. *Nature* **410**: 297-300.

Staehling-Hampton, K., Ciampa, P. J., Brook, A, and Dyson, N. (1999). A genetic screen for modifiers of E2F in *Drosophila melanogaster. Genetics* **153**: 275-287.

Stolow, D. T. and Haynes, S. R. (1995). Cabeza, a *Drosophila* gene encoding a novel RNA binding protein, shares homology with EWS and TLS, two genes involved in human sarcoma formation. *Nucl. Acid. Res.* **23**: 835-843.

Su, T. T., Campbell, S. D. and O'Farrell, P. H. (1998). The cell cycle program in germ cells of the *Drosophila* embryo. *Dev. Biol.* **196**: 160-70.

Sumerel, J. L., Moore, J. C, Schnackenberg, B. J., Nichols, J. A., Canman, J. C., Wessel, G. M. and Marzluff, W. F. (2001). Cyclin E and its associated cdk activity do not cycle during early embryogenesis of the sea urchin. *Dev. Bio.* **234**: 425-440.

Suzuki, T., Ohsugi, Y. Uchida-Toita M., Akiyama, T. and Yoshida, M. (1999). Tax oncoprotien of HTLV-1 binds to the human homolog of Drosophila discs large tumor suppresor protein, hDlg, and perturbs its function in cell growth control. *Oncogene* **18**: 5967-72

Swanson, C., Ross, J. and Jackson, P. K. (2000). Nuclear accumulation of cyclin E/Cdk2 triggers a concentration-dependent switch for destruction of $p27^{xic1}$. *Proc. Natl. Acad. Sci.* **97**: 7796-7801.

Tam, S. W., Theodoras, A. M., Shay, J. W., Draetta, G. F. and Pagano, M. (1994). Differential expression and regulation of Cyclin D1 protein in normal and tumor human cells: association with Cdk4 is required for Cyclin D1 function in G1 progression. *Oncogene* **9**: 2663-2674.

Thomas, B. J., Gunning, D. A., Cho, J. and Zipursky, S. L. (1994). Cell cycle progression in the developing *Drosophila* eye: *roughex* encodes a novel protein required for the establishment of G1. *Cell* **77**: 1003-1014.

Thomas, B. J., Zavits, K. H., Dong, X., Lane, M. E., Weigmann, K., Finley Jr., R. L., Brent, R., Lehner, C. F. and Zipursky, S. L. (1997). *Roughex* downregulates G2 cyclins in G1. *Genes Dev.* **11**: 1289-1298.

Tokuyama, Y., Horn, H. F., Kawamura, K., Tarapore, P. and Fukasawa, K. (2001). Specific Phosphorylation of Nucleophosmin on Thr199 by Cyclin- dependent Kinase 2-Cyclin E and Its Role in Centrosome Duplication. *J Biol Chem.* **276**: 21529-21537.

Tseng, T. C., Marfatia, S. M., Bryant, P. J., Pack, S., Zhuang, Z., O'Brien, J. E., Lin, L., Hanada, T. and Chishti, A. H. (2001). VAM-1: a new member of the MAGUK family binds to human Veli-1 through a conserved domain. *Biochim. Biophys. Acta* **1518**: 249-259.

Tyers, M., Tokiwa, G., Nash, R. and Futcher, B. (1992). The Cln3-Cdc28 kinase complex of S. cerevisiae is regulated by proteolysis and phosphorylation. *EMBO J.* **11**: 1773-1784.

Vidwans, S. J. and Su, T. T. (2001). Cycling through development in Drosophila and other metazoa. *Nat. Cell Biol.* **3**: E35-E39.

Wang, T. C., Cardiff, R. D., Zukerberg, L., Lees, E., Arnold, A. and Schmidt, E. V. (1994). Mammary hyperplasia and carcinoma in MMTV-cyclin D1 transgenic mice. *Nature* **369**: 669-671.

Watson, K. L., Johnson, T. K., and Dennell, R. E. (1991). *Lethal (1) aberrant immune response* mutations leading to melanotic tumour formation in *Drosophila melanogaster. Dev. Genet.* **12**: 173-187.

Wolff, T. and Ready, D. F., Eds. (1993). *Pattern formation in the Drosophila retina*. The Development of *Drosophila melanogaster*. New York, Cold Spring Harbor Press.

Won, K.-A. and Reed, S. I. (1996). Activation of cyclin E/Cdk2 is coupled to site-specific autophosphorylation and ubiquitin-dependent degradation of cyclin E. *EMBO J.* **15**: 4182-4193.

Wuarin, J. and Nurse, P. (1996). Regulating S phase: CDKs, licencing and proteolysis. *Cell* **85**: 785-787.

Yaglom J. A., Goldberg A. L., Finley D. and Sherman M. Y. (1996). The molecular chaperone Ydj1 is required for the p34CDC28-dependent phosphorylation of the cyclin Cln3 that signals its degradation. *Mol. Cell. Biol.* **16**: 3679-3684.

Yamamoto, A., Hashimoto, Y., Kohri, K., Ogata, E., Kato, S., Ikeda, K. and Nakanishi, M. (2000). Cyclin E as a coactivator of the androgen receptor. *J. Cell. Biol.* **150**: 873-80.

Yan, Y., Frisen, J., Lee, M.-H., Massague, J and Barbacid, M. (1997). Ablation of the CDK inhibitor p57kip2 results in increased apoptosis and delayed differentiation during mouse development. *Genes Dev.* **11**: 973-983.

Zalvide, J., Stubdal, H. and DeCaprio, J. A. (1998). The J domain of simian virus 40 large T antigen is required to functionally inactivate RB family proteins. *Mol. Cell. Biol* **3**: 1408-1415.

Zariwala, M., Liu, J., and Xiong, Y. (1998). Cyclin E2, a novel human G1 cyclin and activating partner of Cdk2 and Cdk3, is induced by viral oncoproteins. *Oncogene* **17**, 2787-2798.

Zhang, P., Liegeois, N. J., Wong, C., Finegold, M., Hou, H., Thompson, J. C., Silverman, A., Harper, J. W., DePinho, R. A. and Elledge, S. J. (1997). Altered cell differentiation and proliferation in mice lacking p57KIP2 indicates a role in Beckwith-Wiedemann syndrome. *Nature* **387**: 151-158.

Zhao, J., Kennedy, B. K., Lawrence, B. D., Barbie, D. A., Matera, A. G., Fletcher, J. A. and Harlow, E. (2000). NPAT links cyclin E-Cdk2 to the regulation of replication-dependent histone gene transcription. *Genes Dev.* **14**: 2283-2297.

Zhu, L. and Skoultchi, A. I. (2001). Coordinating cell proliferation and differentiation. *Curr Opin Genet Dev.* **11**: 91-97.

Addendum

Chapter 1:

Figure 1.3 modified from Richardson *et al.* (1995).

Chapter 3:

Section 3-2.2: In early syncytial embryos, DmcycEII protein was detected at high levels in interphase nuclei but upon entry into mitosis became distributed throughout the cell (Figure 3.2A and data not shown).

Section 3-2.4: enodreplication should read endoreplication

Chapter 4:

In all experiment appropriate controls were carried out and the control shown in Figures 4.2 and 4.5 is a representative example.

Magnification of Figure 4.5A is 40X and 4.5B is 100X.

Chapter 5:

Enhancers identified by testing genes identified in screen carried out in other labs are the intellectual property of these labs and as such were not at my liberty to pursue.

In all experiment appropriate controls were carried out and the control shown is a representative example.

The levels of alteration to the number of S phase were determined by counting BrdU labelled cells across a given area of the eye disc (data not shown).